REFERENCE ONLY

UNIVERSITY OF LONDON THESIS

Degree PhD Year 2006 Name of Author LANGMEAD, C.J

Structural and functional characterisation of neuronal G_q protein coupled receptors

Christopher J. Langmead

Department of Pharmacology

University College London

Supervisors:

Dr Hugh J. Herdon

Professor Steve Moss

Thesis submitted for the degree of Doctor of Philosophy (Ph.D.)

University of London

January 2006

ProQuest LLC
789 East Eisenhower Parkway
P.O. Box 1346
Ann Arbor, MI 48106-1346

Abstract

Both G protein coupled receptor 10 (GPR10) and the muscarinic M_1 receptor are members of family A of the G protein coupled receptor superfamily. GPR10 is the human orthologue of a former orphan receptor for which prolactin releasing peptides (PrRP) have been identified as the cognate ligands. In contrast, the M_1 receptor represents a well-established receptor for which up until the discovery of AC-42 (4-(4-butyl-1-piperidinyl)-1-(2-methylphenyl)-1-butanone) it has been difficult to identify a selective agonist.

Little is known of the pharmacology of PrRPs and AC-42 at GPR10 and the human M_1 (hM_1) receptor, respectively. Similarly, the molecular nature of their respective binding sites is as yet unknown. In the studies in this thesis, the interaction of PrRPs with GPR10 and of AC-42 (and other ectopic agonists) with the hM_1 receptor have been extensively characterised using a range of pharmacological techniques in both recombinant cell lines stably and transiently expressing the receptor(s) of interest and native tissue preparations. Furthermore, the molecular interactions between ligand and receptor have been probed using homology modelling, site-directed mutagenesis (SDM) and pharmacological evaluation.

The results generated reveal that PrRPs are high affinity, potent agonists at GPR10 that cause the receptor to activate effector systems that are known to couple to $G_{q/11}$ proteins. Radioligand binding studies suggest both high and low affinity sites for binding. In addition, homology modelling and SDM have been used to reveal key interactions of the C-terminal region of PrRP with transmembrane domain (TM) 6 (D302) and TM7 (Q317) and extracellular loop (ECL) 2 (E213).

Selective activation of the M_1 receptor can be achieved using AC-42 and other novel ligands. Using functional calcium mobilisation assays, inositol phosphate assays and

radioligand binding studies it has been possible to demonstrate that this class of compounds interacts with the receptor in an allosteric manner. SDM studies also suggest that residues distinct from the orthosteric binding site form part of the binding site for AC-42 and related compounds.

These studies provide the first extensive pharmacological analysis characterising the interaction of PrRP and GPR10 and identify the signal transduction cascade activated by this former orphan receptor. Furthermore, SDM studies have partly elucidated the molecular nature of the PrRP binding site. Both pharmacological and SDM based examination of the muscarinic M_1 receptor have revealed a unique allosteric method of activation by AC-42 and a novel class of allosteric agonists.

Declaration

I declare that all work presented in this thesis is entirely my own, with the exception of the homology modelling and ligand docking, which was performed by Ben Tehan and Frank Blaney, the construction of the mutant GPR10 and muscarinic M_1 receptors, which was performed by Angela Bridges, Abby Sukman and Jim Fornwald and the GPR10 cAMP assay, which was performed by Jon Chambers. The electrophysiology studies were performed whilst on a collaborative placement with Prof. Miles Whittington and Anita Roopun in the Department of Biomedical Sciences, University of Leeds.

Christopher Langmead

Acknowledgements

I would like to thank my supervisor, Dr Hugh Herdon, for the huge amount of support, input and advice that he has provided throughout the past 4 years. Thanks must also go to Dr Ceri Davies for his support of and enthusiasm for this project in its latter years and to Professor Derek Middlemiss for giving me the opportunity to carry out my PhD studies whilst working at SmithKline Beecham and latterly GlaxoSmithKline.

I would also like to acknowledge the valuable advice and insight of of Drs Mene Pangalos, Andy Calver, Martyn Wood and Arthur Christopoulos at various points through the past 4 years and also Professor Miles Whittington and Anita Roopun for their time and help during an interesting week at the University of Leeds. I would also like to gratefully acknowledge others at GlaxoSmithKline who have kindly provided technical support for parts of this thesis, including Angela Bridges, Jon Chambers, Frank Blaney, Ben Tehan, Abby Sukman and Jim Fornwald.

Thanks to all the girls in the lab for making it such a fun place to work and for my continuing education on shopping and accessorising!

Finally I must thank Lorraine for all her love, support and understanding in a relationship that has almost entirely coincided with this work. Thank you so much for being so patient.

Table of contents

List of Figures and Tables

Abbreviations

77-LH-28-1	1-[3-(4-butyl-1-piperidinyl)propyl]-3,4-dihydro-2(1H)-quinolinone
aa	amino acids
ABNR	adopted basis Newton Raphson
AC-42	4-(4-butyl-1-piperidinyl)-1-(2-methylphenyl)-1-butanone
ACh	acetylcholine
AC	adenylyl cyclase
ACSF	artificial cerebrospinal fluid
2-APB	2-aminoethoxydiphenyl borate
BSA	bovine serum albumin
BST	bed nucleus of the stria terminalis
C_7/3-phth	heptane-1,7-bis(dimethyl-3'-phthalimidopropyl)ammonium bromide
cAMP	cyclic adenosine monophosphate
CCh	carbamylcholine (carbachol)
CHARMm	Chemistry at HARvard Molecular Mechanics
CHO	Chinese hamster ovary
CPCCOEt	7-hydroxyiminocyclopropan[b]chromen-1a-carboxylic acid ethyl ester
cGMP	cyclic guanosine monophosphate
CNS	central nervous system
CR	concentration ratio
CREB	cAMP response element binding protein
CRH	corticotropin releasing hormone
DAG	diacyglycerol
DMEM	Dulbecco's modified Eagle medium
DMH	dorsomedial hypothalamus
EC_{50}	effective concentration$_{50}$
ECL	extracellular loop
EDTA	ethylene diammine tetraacetic acid
EMEM	Eagle's minimum essential medium
ERK	extracellular signal-regulated kinase
FBS	foetal bovine serum
FFT	fast Fourier transformation
FLIPR	fluorometric imaging plate reader
GABA	γ-amino butyric acid
GDP	guanosine diphosphate
GPCR	G protein coupled receptor
GPR10	G protein coupled receptor 10
GppNHp	5'-guanosyl-β,γ-imidotriphosphate
GRK	G protein coupled receptor kinase

GTP	guanosine 5' triphosphate
GTPγS	guanosine 5,-O-(3-thiotriphosphate)
HEK293	human embryonic kidney 293
HEPES	4-2-hydroxyethyl-1-piperazineethanesulphonic acid
IBMX	3-isobutyl-1-methylxanthine
IC_{50}	inhibitory concentration$_{50}$
i.c.v.	intracerebroventricular
IF	inositol-free
IP	inositol phosphate
IP_3	inositol trisphosphate
LGIC	ligand gated ion channel
mAChR	muscarinic acetylcholine receptor
MAP	mitogen activated protein
nAChR	nicotinic acetylcholine receptor
NCMB	*N*-chloromethyl brucine
NMR	nuclear magnetic resonance
NMS	*N*-methyl scopolamine
NOE	Newton Overhauser effect
NPAF	neuropeptide-AF
NPFF	neuropeptide-FF
NPY	neuropeptide-Y
NTS	nucleus of the tractus solitarius
Oxo-M	oxotremorine-M
PBS	phosphate buffered saline
PCR	polymerase chain reaction
PDE	phosphodiesterase
PEI	polyethyleneimine
pfu	plaque-forming units
PIP_2	phosphatidyl inositol 4,5 bisphosphate
PIP_3	phosphatidyl inositol 3,4,5, trisphosphate
PKC	protein kinase C
PLC	phospholipase C
PMSF	phenylmethylsulphonyl fluoride
PrRP	prolactin releasing peptide
PTX	pertussis toxin
PVN	paraventricular nucleus
QNB	quinuclidinylbenzilate
sACSF	sucrose artificial cerebrospinal fluid
SB-213698	(-)-trans-4a-(3-hydroxyphenyl)-2-methyl-1,2,3,4,4a,5,12,12a-octahydropyrido[3,4-b]acridine
SCG	superior cervical ganglion

SD	steepest descent
SDM	site-directed mutagenesis
s.e.m.	standard error of mean
SPA	scintillation proximity assay
tetra-W84	hexane-1,6-bis[methyl-bis~3'-phthalimidopropyl] ammonium bromide
TM	transmembrane
TRH	thyrotropin releasing hormone
U2OS	U2 osteosarcoma
U-50488	(1R,2R)-3,4-dichloro-N-methyl-N-[2-(1-pyrrolidinyl)cyclohexyl]-benzeneacetamide
U73122	1-[6-[[(17 β)-3-methoxyestra-1,3,5(10)-trien-17-yl]amino]hexyl]-1H-pyrrole-2,5-dione
UHR-1	Unknown Hypothalamic Receptor-1
VLRN	ventral and lateral reticular nuclei

Chapter 1

Introduction

1. G protein coupled receptors

(i) Ligand gated ion channels and G protein coupled receptors.

Neuronal communication within the CNS is largely by means of chemical neurotransmission. This process involves the release of a chemical neurotransmitter from the nerve terminal of one neurone, diffusion across the synapse and interaction with a receptor protein on the cell surface of one or more post-synaptic neurones to instigate a physiological response in that neurone. Receptor proteins can mediate the actions of hormones, neurotransmitters, growth factors and cytokines. Receptors can be subdivided into four superfamilies, based on their molecular structure and mechanism of signal transduction (Rang *et al.*, 1999). The four families are ligand gated ion channels (LGIC), G protein coupled receptors (GPCR), kinase linked receptors and nuclear receptors. LGICs are plasma membrane bound receptors that couple directly to an ion channel to mediate fast, millisecond neurotransmission in the CNS e.g. nicotinic acetylcholine receptors (Rang *et al.*, 1999). GPCRs are also plasma membrane bound receptors, but they couple to intracellular effector systems *via* guanine nucleotide binding (G) proteins (Rang *et al.*, 1999). Typically, GPCRs mediate slower neurotransmission than ligand gated ion channels, over a time frame of seconds rather than milliseconds, and include receptors for noradrenaline, acetylcholine, 5-HT and dopamine. Kinase linked receptors, that are also membrane bound, incorporate an intracellular protein kinase domain in their structure. They include receptors for insulin as well as cytokines and growth factors (Rang *et al.*, 1999). The final family are the nuclear receptors. Unlike the other three, nuclear receptors are not membrane bound and are usually found, as their name suggests, in the nuclear compartment (though are also present in the cytosol), where they regulate gene transcription. This family includes receptors for steroid hormones, thyroid hormone and vitamin D (Rang *et al.*, 1999). Responses mediated *via* kinase

linked receptors and nuclear receptors occur over the timeframe of minutes and hours.

(ii) The G protein coupled receptor superfamily

The GPCR superfamily is characterised by proteins which contain seven distinct hydrophobic regions, each 20-30 amino acids in length and each of which forms an α-helical transmembrane domain (Figure 1; Schoneberg *et al.,* 1999). These are connected by intracellular and extracellular loops and the receptor is completed by an extracellular N-terminus and an intracellular C-terminal tail (Kristiansen, 2004). The sequence of the human genome revealed 616 putative GPCRs (Venter *et al.*, 2001), many of which have been discovered recently with the development of genome and cDNA research (Gether, 2000). In 1994, mammalian GPCRs were classified into 3 families, A, B and C, by sequence homology and predicted structure (Kolakowski, 1994). Since that time the classification has been widened to include newly discovered GPCRs and the mammalian superfamily now encompasses 7 families, namely A, B, large N-terminal family B, C, Frizzled/Smoothened, taste 2 and vomeronasal 1 (Kristiansen, 2004).

By far the largest and best studied of the families is family A, i.e. those receptors showing close relation to the light receptor, rhodopsin (Gether, 2000). The majority of family A receptors are olfactory GPCRs, although nearly 200 non-olfactory GPCRs, recognising over 80 ligands, have also been characterised (Pierce *et al.*, 2002). Phylogenetically, family A can be further subdivided into six major groups, as shown in Table 1. The overall homology between members of family A is low and restricted to several highly conserved key residues. Most notable is the arginine residue that is part of the Asp-Arg-Tyr (DRY) motif at the interface of TM3 and intracellular loop 2 and which is conserved in almost all family A receptors (Gether, 2000; Figure 1).

Family A GPCRs	Biogenic amine receptors
	CCK, endothelin, tachykinin, NPY, bombesin, TRH, vertebrate opsin receptors
	Invertebrate opsins & bradykinin receptors
	Adenosine, cannabinoid, melanocortin and olfactory receptors
	Chemokine, gonadotropin-releasing hormone, eicosanoid, leukotriene, follicle-stimulating hormone, lutenising hormone, thyroid-stimulating hormone, galanin, nucleotide, opioid, oxytocin, vasopressin, somatostatin, protease-activated receptors.
	Melatonin receptors and other non-classified.

Table 1. Six phylogentically defined subgroups of family A GPCRs (adapted from Gether *et al.*, 2002).

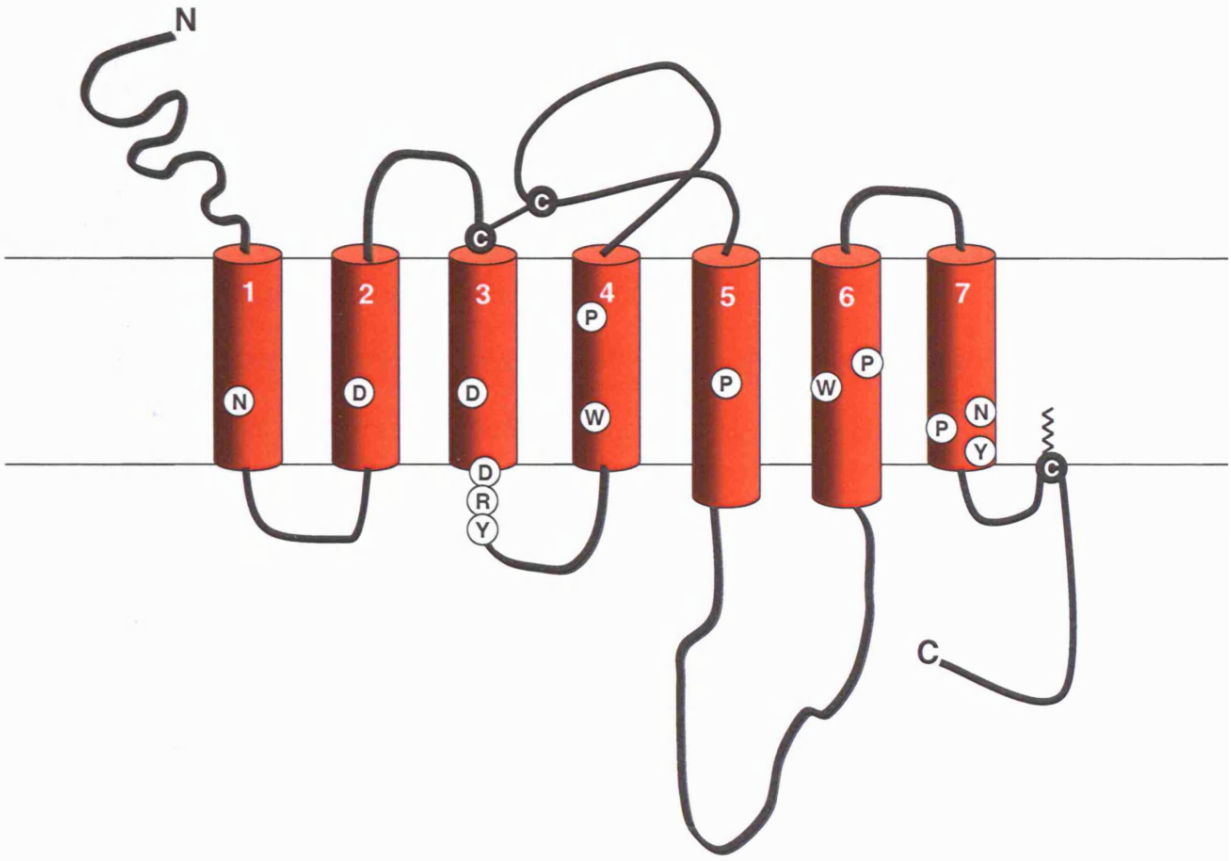

Figure 1. Membrane topology of the β_2 adrenoceptor, a typical member of family A GPCRs. This subfamily of receptors is characterised by a series of highly conserved key residues (black letter in white circles). In most family A receptors, a disulphide bridge connects ECL2 and ECL3 (white letters in black circles). Additionally, the majority of the receptors have a palmitoylated cysteine in the carboxy-terminal tail causing formation of a putative fourth intracellular loop.

Family B consists of approximately 25 members, including receptors for gastrointestinal peptides (eg. secretin, glucagon, vasoactive intestinal peptide), corticotrophin-releasing hormone and parathyroid hormone (Pierce *et al.*, 2002; Gether, 2000). The most prominent characteristic of family B GPCRs is the large extracellular N-terminus of approximately 100 aa, which contains a number of cysteine residues thought to form a network of disulphide bridges (Ulrich *et al.*, 1998). The DRY motif, found in family A receptors, is notably absent in receptors in family B (Gether, 2000).

Family C is also small and contains the metabotropic glutamate receptors, the $GABA_B$ receptor and the calcium sensing receptor (Schoneberg, 2002; Pierce *et al.*, 2002). These receptors are characterised by an extremely large N-terminal domain (500 – 600 aa) that shows homology with bacterial periplasmic binding proteins and which is thought to be involved in ligand binding and receptor activation (Pin *et al.*, 2003).

The remaining families are those that have been created to better classify new GPCRs as they are discovered and now also include some receptors that were previously classified in family B (large N-terminal family B 7TM receptors, Frizzled/Smoothened) or family C (taste 2 and vomeronasal 1 receptors). Large N-terminal family B 7TM receptors share some similarities with family B receptors in their TM domains (Fredriksson *et al.*, 2003) and include brain specific angiogenesis inhibitor receptor (BAI 1-3) and calcium independent receptor of α-latrotoxin (CIRL 1-3; Kristiansen, 2004). Similarly, Frizzled and Smoothened receptors show low but significant homology with family B receptors (Foord *et al.*, 2002), but are sufficiently different in their N-termini to warrant a separate subfamily. Vomeronasal 1 receptors are a family of 12 weakly homologous receptors for pheromones that have short N-terminal domains, suggesting that their ligands bind within the TM bundle

(Kristiansen, 2004). Their significant differences from family C receptors led to their re-classification into a novel family, along with the bitter-sensing taste 2 receptor.

(iii) Structure of GPCRs

A possible development in the understanding of the structure of GPCRs, particularly those belonging to family A, was the determination of the crystal structure of the photoreceptor, rhodopsin (Palczewski *et al.*, 2000). The crystal structure of rhodopsin has confirmed the molecular architecture of an extracellular N-terminus, an intracellular C-terminus and seven TM domains connected by alternating intracellular and extracellular loops (Palczewski *et al.*, 2000). GPCRs are also often subject to a number of post-translational modifications, including N-glycosylation and palmitoylation (Schoneberg, 2002). Glycosylation sites are usually found in the N-terminal domain, but can also be found in the extracellular loops. Some GPCRs, such as the adenosine A_2 receptor and human α_{2B} adrenergic receptor, lack consensus sites for glycosylation, yet are fully functional in the absence of this modification (Schoneberg, 2002). For others, such as the parathyroid hormone receptor and human calcium sensing receptor, glycosylation is a pre-requisite for correct function or cell surface expression (Schoneberg, 2002). Another post-translational modification is palmitoylation and the best example of this is found in several family A GPCRs where the so-called fourth intracellular loop is formed by a palmitoylated cysteine in the C-terminus. This 'loop' adopts an α-helical formation running parallel to the plasma membrane and as such has been termed helix VIII (Palczewski *et al.*, 2000). Furthermore, the majority of family A and family B GPCRs are characterised by pair of conserved cysteine residues linking the first and second extracellular loops via a disulphide bond (Schoneberg, 2002). Mutation of these cysteine residues for a number of GPCRs has resulted in a loss of high affinity ligand binding (Perlman *et al.*, 1995; Schoneberg, 2002), suggesting that this disulphide

bond may be critical to the formation of the ligand binding site for some GPCRs. In support of this hypothesis, in the crystal structure of rhodopsin the second extracellular loop actually dips down into the TM bundle (Palczewski *et al.*, 2000).

Whilst rhodopsin remains the only GPCR for which the crystal structure has been determined, the strong conservation of key amino acid residues amongst family A receptors has allowed researchers to construct homology models of the transmembrane domains of other receptors (Lu *et al.*, 2002). These residues include the asparagine in TM1 (Asn 1.50), the aspartate in TM2 (Asp 2.50), the Asp-Arg-Tyr triad at the cytoplasmic face of TM3 (Asp 3.49, Arg 3.50, Tyr 3.51; Glu-Arg-Tyr in bovine rhodopsin), the tryptophan in TM4 (Trp 4.50) and the conserved prolines in TM5 (Pro 5.50), TM6 (Pro 6.50) and TM7 (Pro 7.50; Gether, 2000; Kristiansen, 2004). Iterative modelling of the docking of ligands into such homology models can identify key ligand contact points on the receptor. The most common method to assess whether residues are involved in the binding of ligand involves mutating either single residues or regions of a receptor protein to alter the amino acid sequence, a technique known as site-directed mutagenesis (SDM). The effect of different mutations on ligand binding and receptor signalling can then be assessed. A common mutation that is used for pharmacological analysis is the conversion of residues to alanine to remove any side chain beyond the β-carbon, yet preserve the integrity of the receptor structure. More investigative mutations are often used to probe specific side-chain function e.g. mutation of Y82 and Y85 to both phenylalanine and alanine has been used to determine whether either the hydroxyl or aromatic moiety of these tyrosine residues is involved in the binding of [^{3}H]NMS in the muscarinic M_1 receptor (Lee *et al.*, 1996). SDM is now a common technique that has been useful to determine the key residues for both ligand binding (Berkhout *et al.*, 2003; Bikker *et al.*, 1998; Hirst *et al.*, 2003) and receptor activation (Fanelli *et al.*, 1998; Greasley *et al.*, 2002) for a number of GPCRs.

(iv) GPCR ligand diversity

Despite the similar molecular architecture of seven TM domains which characterises the entire superfamily, GPCRs have evolved to be activated by a vast array of different stimuli. These include small biogenic amines (eg. acetylcholine, dopamine), amino acids (eg. glutamate), photons, ions (eg. Ca^{2+}), peptides (eg. neurokinins, orexins), large glycoproteins (eg. human immunodeficiency virus coat protein) and proteases (which can cleave the N-terminus of GPCRs leaving a truncated N-terminus that can interact with the TM bundle to activate the receptor; Schoneberg, 2002). These ligands can be extremely small, such as photons and calcium ions, which activate rhodopsin and the calcium-sensing receptor, respectively. Alternatively, the ligands can be very large, such as orexin-A peptide (molecular weight = 3561; Sakurai *et al.*, 1998) or viral coat proteins such as gp120 (molecular weight ~ 100,000; Kenakin, 2004).

The GPCR binding site for small endogenous agonists, such as biogenic amines, is located deep in the receptor in the TM bundle and formed by residues in TM3 (Asp 3.32, Ser 3.36), TM5 (Ser/Thr 5.42, Ser 5.43, Ser/Thr 5.46), TM6 (Asn 6.55) and TM7 (Asp 7.36, Trp 7.40, Tyr 7.43; Gether, 2000; Kristiansen, 2004). This has been demonstrated for a number of aminergic GPCRs, including the β_2 adrenoceptor (Strader *et al.*, 1987, 1989) and the muscarinic M_1 receptor (Lu *et al.*, 2002). An important interaction is thought to be between the carboxylate side chain of a highly conserved Asp in TM3 (18 residues N-terminal of the invariant Arg of TM3) and the charged amine group of biogenic amines such as noradrenaline (Gether, 2000), acetylcholine (Spalding *et al.*, 1994), serotonin (Wang *et al.*, 1993), dopamine (Mansour *et al.*, 1992) and histamine (Gantz *et al.*, 1992).

In addition to these findings, it has also been demonstrated that residues in the ECL2 are involved in the binding of some small molecules, such as phentolamine at the α_{1A} adrenoceptor (Zhao *et al.*, 1996) and ligands at the adenosine receptor (Kim *et al.*, 1996). It has been suggested that the loop may dip down into the binding crevice in the TM bundle due to the formation of a disulphide bridge between cysteine residues in ECL2 and top of TM3, (Kim *et al.*, 1996).

In contrast to aminergic receptors, the binding sites for peptide receptors in family A are generally considered to be more extracellular, incorporating residues in the extracellular loops and N-terminus, as has been demonstrated for the receptors for angiotensin II, neuropeptide Y, oxytocin, bradykinin and neurotensin (Gether, 2000). However, due to their size, some peptides may have additional points of interaction in the transmembrane bundle and may actually enter the TM binding crevice (Gether, 2000). This has been shown for longer peptides, including angiotensin (Yamano *et al.*, 1995) and opiates (Befort *et al.*, 1996), but also for small tripeptides such as thyrotropin-releasing hormone (Perlman *et al.*, 1994). Despite the proximity of peptide binding sites to the binding site for biogenic amines, the residues in the TM bundle recognised by these peptides are largely distinct from those involved in the binding of biogenic amines (Gether, 2000).

(v) Activation of GPCRs

An agonist is a ligand capable of binding to a specific recognition site on a receptor and causing that receptor to adopt an active state (Kenakin, 1997). For a GPCR, as has been discussed, a wide array of different ligands are capable of acting as agonists. Wherever their binding site on the receptor, they cause a change in the conformation of the receptor such that it is able to bind and activate G protein(s) to propagate the signal to the intracellular compartment (Rasmussen & Gether, 2002).

In contrast, a competitive antagonist is able to bind to the receptor, but does not make the necessary contacts to trigger receptor activation. However, its presence in the binding site is capable of blocking agonist mediated receptor activation.

In practice, it is likely that most 'antagonists' are actually inverse agonists. These ligands act to stabilise the receptor in its inactive conformation and therefore reduce any constitutive activity of the receptor (activity in the absence of bound agonist; Kenakin, 1997). Atropine and *N*-methylscopolamine (NMS) have been reported to display inverse agonist at muscarinic acetylcholine receptors (Hulme *et al.*, 2003). Both of these ligands contain a phenyl group which is thought to further stabilise the hydrophobic intramolecular interactions in the endofacial region of the TM domains which hold the receptor in an inactive conformation (Hulme *et al.*, 2003).

GPCR activation is accompanied by movement of the TM domains in order to allow the receptor to bind G protein(s). Studies to determine the active conformations of both rhodopsin and the β_2 adrenoceptor suggest that agonist binding triggers an outward tilting of TM6, an anticlockwise rotation of TM5 and an increased flexibility of the lower half of TM7 as well as movements of TM1, TM2 and TM3 (Gouldson *et al.*, 2004). These movements break the intramolecular bonds that hold the receptor in the inactive state; in turn, new intramolecular bonds that hold the receptor in an active conformation are formed (Rasmussen & Gether, 2002).

Varying intracellular portions of GPCRs have been implicated in mediating interactions with G proteins. The first (formyl peptide and cholecystekinin CCK_A receptors), second ($GABA_B$ receptor) and third (endothelin ET_B receptor) intracellular loops have all been shown to participate in G protein activation (Schoneberg, 2002). Furthermore, studies suggest that it is residues close to the TM helix – intracellular loop interface that are responsible for mediating interactions with G proteins. In both

the muscarinic M_3 receptor and the neurokinin NK-1 receptor, deletion of large portions of the third intracellular loop has little or no effect on ligand binding and receptor function (Schoneberg *et al.*, 1995; Nielsen *et al.*, 1998).

(vi) G protein coupled receptor signalling

When an extracellular agonist ligand such as a biogenic amine or a peptide interacts with its GPCR, the ligand induces a conformational change in the receptor that activates a heterotrimeric guanine nucleotide binding protein (G protein; Cabrera-Vera *et al.*, 2003). G proteins are composed of α-, β- and γ- subunits and are found on the inner membrane surface of the cell - Gα subunits are often post-translationally lipidated (eg. N-terminal myristoylation of $G\alpha_i$) to allow the protein to anchor to the plasma membrane (Ho & Wong, 2002). Prior to receptor activation, the Gα subunit of the heterotrimeric G protein has a molecule of guanine diphosphate (GDP) bound. Upon agonist binding and receptor activation, the Gα subunit binds to the receptor. Various regions of Gα contribute to the association with GPCRs, most notably the extreme C-terminal region (Ho & Wong, 2002). Indeed, replacement of the five C-terminal amino acids of $G\alpha_q$ with those of $G\alpha_{i2}$, $G\alpha_o$, $G\alpha_z$ or $G\alpha_s$ alters the profile of receptor coupling (Conklin *et al.*, 1993, 1996).

Upon Gα binding to the GPCR a molecule of GDP is released and exchanged for a molecule of guanine triphosphate (GTP). This transition precipitates the dissociation of the Gα from both the Gβγ subunit and the receptor. Both Gα–GTP and Gβγ are then accessible to activate downstream effector systems (Cabrera-Vera *et al.*, 2003). The duration of action is determined by the rate of the intrinsic GTPase hydrolysis rate of the Gα subunit, which, once it has hydrolysed GTP to GDP, re-associates with Gβγ. Both Gα and Gβγ are capable of modulating different intracellular effector systems and multiple subtypes of heterotrimeric G proteins provide an extremely

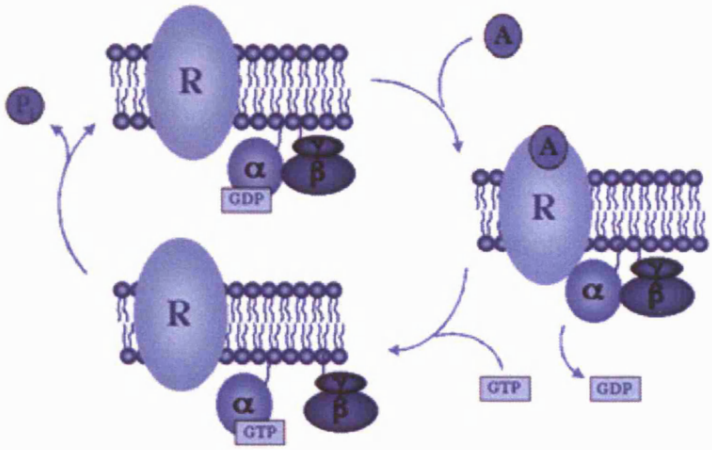

Figure 2. Agonist mediated activation of a GPCR induces a conformational change in the receptor that activates a heterotrimeric guanine nucleotide binding protein (G protein; Cabrera-Vera *et al.*, 2003). G proteins are composed of α-, β- and γ- subunits and are found on the inner membrane surface of the cell. Prior to receptor activation, the Gα subunit of the heterotrimeric G protein has a molecule of guanine diphosphate (GDP) bound. Upon agonist binding and receptor activation, the molecule of GDP is released and exchanged for a molecule of guanine triphosphate (GTP). This transition precipitates the dissociation of the Gα from both the Gβγ subunit and the receptor. The duration of action is determined by the rate of the intrinsic GTPase hydrolysis rate of the Gα subunit, which, once it has hydrolysed GTP to GDP, re-associates with Gβγ.

diverse range of signal transduction pathways that can be modulated by GPCRs. The G protein cycle is shown in Figure 2.

Whilst there are five different Gβ subunits and thirteen different Gγ subunits that have been identified to date (Carera-Vera *et al.*, 2003), G proteins are usually referred to by their Gα subunit. There are four families of Gα subunit, namely $G\alpha_s$, $G\alpha_i$, $G\alpha_q$ and $G\alpha_{12}$. The G_s family consists of $G\alpha_s$ and $G\alpha_{olf}$ and activation of G_s coupled receptors is generally associated with stimulation of adenylyl cyclase (AC) and a subsequent increase the intracellular concentration of cAMP (Ho & Wong, 2002; Cabrera-Vera *et al.*, 2003).

The G_i family of Gα proteins consists of $G\alpha_{i1}$, $G\alpha_{i2}$, $G\alpha_{i3}$, $G\alpha_o$, $G\alpha_z$, $G\alpha_{t1}$, $G\alpha_{t2}$ and $G\alpha_g$. In contrast to the G_s family, $G\alpha_{i1}$, $G\alpha_{i2}$ $G\alpha_{i3}$, $G\alpha_o$ and $G\alpha_z$ proteins inhibit adenylyl cyclase to lower the intracellular levels of cAMP, although $G\alpha_o$ can stimulate phosphoinositide 3-kinase and $G\alpha_{t1}$ and $G\alpha_{t2}$ regulate cGMP phosphodiesterases (Ho & Wong, 2002). The G_q family consists of $G\alpha_q$, $G\alpha_{11}$, $G\alpha_{14}$ and $G\alpha_{16}$, all of which act to stimulate phospholipase-Cβ to convert phosphatidyl inositol bisphosphate (PIP_2) into inositol triphosphate (IP_3) and diacylglycerol (DAG). IP_3 then is able to activate its receptor in the membrane of the smooth endoplasmic reticulum to cause the release of intracellular calcium (Ho & Wong, 2002). Finally, the G_{12} family consists of $G\alpha_{12}$ and $G\alpha_{13}$. Both are known to stimulate the Btk tyrosine kinase receptor and $G\alpha_{12}$ is known to simulate phospholipase-Cε (Ho & Wong, 2002).

In addition to this wide variety of effectors, Gα subunits are known regulate a plethora of ion channels, monomeric G proteins, transcription co-factors, G protein receptor kinases and tyrosine kinases (Cabrera-Vera *et al.*, 2003; Ho & Wong, 2002). With almost as many regulatory roles for the Gβγ subunits as for Gα subunits, the variety and control of signal transduction pathways mediated by GPCRs is extensive.

Such signal transduction pathways have been extensively studied and there are a number of pharmacological tools available with which to probe signal transduction mechanisms *in vitro*. The G_i family of G proteins (except $G\alpha_z$) is unique in their sensitivity to the bacterial pertussis toxin (PTX) which inactivates the $G\alpha$ subunit by ADP ribosylation. The G_s family is similarly sensitive to permanent activation by the bacterial cholera toxin which inhibits GTP hydrolysis (Cassel & Selinger, 1977). Of greatest interest in these studies are GPCRs linked to the mobilisation of intracellular calcium and there are a number of tools available with which to monitor the signal transduction of G_q / G_{11} coupled receptors. U73122 is a well characterised PLC inhibitor (Marshall *et al.*, 2003; Thompson *et al.*, 1991), 2-APB is a non-competitive inhibitor of the IP_3 receptor (Maruyama *et al.*, 1997; Ma *et al.*, 2001; Gregory & Barritt, 2003) and thapsigargin is an inhibitor of the smooth endoplasmic reticulum Ca^{2+}-ATPase that causes depletion of intracellular calcium stores (Marshall *et al.*, 2003). Very recently, Takasaki *et al.* (2004) have described a novel specific peptide inhibitor of the $G\alpha_q$ subunit, YM-254890, although it is not currently commercially available.

(vii) Second messengers and effector systems

The coupling of GPCRs to such a wide array of different $G\alpha$ and $G\beta\gamma$ subunits as described above leads to control of a highly divergent range of effector systems (Pierce *et al.*, 2002; Rang *et al.*, 1999). Broadly these comprise (i) activation or inhibition of AC and cAMP-dependent pathways, (ii) activation or inhibition of cyclic nucleotide phosphodiesterase and cGMP-dependent pathways, (iii) activation of phospholipase-Cβ, DAG, IP_3 and Ca^{2+} dependent pathways, (iv) inhibition of voltage gated calcium channels, (v) stimulation of inwardly rectifying potassium channels and (vi) activation of guanine nucleotide exchange factors of small G proteins eg. Ras (Rang *et al.*, 1999; Landry *et al.*, 2006).

Ten isoforms of adenylyl cyclases have been cloned, nine of which are membrane bound and are regulated by G proteins (AC1 – AC9). $G\alpha_s$ activates all nine membrane bound adenylyl cyclases, whereas $G\alpha_i$ selectively inhibits AC5 and AC6 and $G\alpha_o$ is thought to inhibit AC1 (Landry *et al.*, 2006). Interestingly, $G\beta\gamma$ subunits, probably from G_i and G_o inhibit AC1, AC5 and AC6 but activate AC2, AC4 and AC7. Activation of adenylyl cyclases increases cAMP which activates protein kinase A (Rang *et al.*, 1999). This kinase phosphorylates serine and threonine residues on a number of target proteins, including voltage sensitive calcium channels (eg. after activation of β_1 adrenergic receptors in the heart; Landry *et al.*, 2006). Increases in cAMP and cGMP activate cyclic nucleotide phosphodiesterases (PDEs) which catalyse their breakdown to 5'-AMP and 5'-GMP, respectively. There are eleven different PDE families which show varying selectivity for cAMP and cGMP.

Of the three common mammalian PLC subtypes, β, γ and δ, only PLCβ is thought to regulated by G proteins (Landry *et al.*, 2006), although $G\alpha_{12}$ does activate PLCε (Ho & Wong, 2002). Activation of PLCβ is predominantly *via* $G\alpha_q$ and results in the conversion of PIP_2 into IP_3 and DAG. However, $G\beta\gamma$ subunits of various G proteins are also capable of activating PLCβ (Landry *et al.*, 2006). IP_3 usually activates its own receptor in the membrane of the smooth endoplasmic reticulum to cause the release of intracellular calcium (Ho & Wong, 2002). DAG participates in the activation of various isoforms of protein kinase C, a process which also requires membrane lipids or cytosolic calcium (Landry *et al.*, 2006).

$G\beta\gamma$ subunits play an important role in the control of ion channels by GPCRs. $G\beta\gamma$ dimers from PTX sensitive GPCRs inhibit P/Q-type, N-type and R-type calcium channels, all of which are found pre-synaptically and control the calcium entry into the nerve terminal governing neurotransmitter release (Landry *et al.*, 2006). Inwardly

rectifying K^+ channels are also subject to modulation by $G\beta\gamma$ subunits – activation of muscarinic M_2 receptors in the heart stimulates G_{i2} and $G_{i3,}$ which, in turn, activates K^+ currents Kir3.1 and Kir3.4 (Landry *et al.*, 2006). Additionally, L-type calcium channels can be activated by phosphorylation by protein kinase A and protein kinase C in response to activation of receptors coupled to G_s, G_i and G_q (Landry *et al.*, 2006).

GPCR mediated signalling can also influence signal cascades that modulate transcription factors in the nucleus (Challiss & Nahorski, 2002; Landry *et al.*, 2006). $G\alpha_{12/13}$, $G\beta\gamma$ subunits and PIP_3 are all capable of stimulate guanine nucleotide exchange factors which can activate small G proteins such as Ras, Rho, Rab, Arf/Sar and Ran (Landry *et al.*, 2006). Activated Ras, Rho and others are capable of interacting with their own cytosolic effectors, such as MAP kinase kinase kinase. This in turn phosphorylates MAP kinase kinase, which phosphorylates MAP kinase (Challiss and Nahorski, 2002). MAP kinases include the extracellular signal-regulated kinases-1 and -2 (ERK1/2), c-Jun N-terminal protein kinases and p38 MAP kinases (Challiss and Nahorski, 2002). ERK1/2 activation can lead to nuclear translocation where it can directly affect transcription through phosphorylation of ternary complex factors such as Elk-1, or indirectly through activation of other protein kinases such as $p90^{RSK}$ which phosphorylates the cAMP response element binding protein which regulates transcription factor activity (Challiss and Nahorski, 2002).

(viii) Role of GPCRs in disease

Given their extensive role in neurotransmission and other essential physiology it is unsurprising that naturally occurring mutations in GPCRs should be the cause of a number of pathologies. Mutations can arise from either the germline (i.e. inherited) or can occur postzygotically. Disease-causing mutations of GPCRs can be classified

into two broad groups. Firstly, they can cause a loss of receptor function which can occur at any number of levels from precluding normal formation of stable mRNA or protein to abnormal membrane trafficking or impaired high affinity agonist binding (Spiegel *et al.*, 1995). Alternatively, mutations can result in a gain of function by causing GPCRs to become stabilised in an active conformation – this includes mutations of residues which take part in intramolecular interactions to hold a GPCR in the inactive, uncoupled state (Spiegel *et al.*, 1995). A vast range of diseases result from loss of function mutations in GPCRs, including colour blindness (cone opsins), retinitis pigmentosa (rhodopsin), nephrogenic diabetes insipidus (vasopressin V_2 receptor), familial hypothyroidism (thyroid stimulating hormone receptor) and congenital bleeding (thromboxane A_2 receptor; Spiegel *et al.*, 1995). Interestingly, at least 27 different mutations that cause nephrogenic diabetes insipidus have been identified in the vasopressin V_2 receptor, a number of which result in truncated receptors which are thought to be non-functional (Spiegel *et al.*, 1995). Diseases that are associated with gain of function mutations include congenital night blindness (rhodopsin), sporadic hyperfunctional thyroid nodules (thyroid stimulating hormone receptor) and familial hyperparathyroidism (calcium sensing receptor; Spiegel *et al.*, 1995). In the latter disease, mutation of either of two acidic residues in the large N-terminal domain of the calcium sensing receptor appears to increase the sensitivity of the receptor to calcium itself (Spiegel *et al.*, 1995).

(ix) Life-cycle of GPCRs

GPCRs are subject to extensive regulation. It is now known that there are systems in place to desensitise and traffic GPCRs after activation in order to regulate their signalling and expression (Hepler & Saugstad, 2002). Desensitisation of GPCRs can occur very rapidly after agonist activation and can be either homologous (where only the response of the activated receptor is affected) or heterologous (whereby

activation of one receptor causes desensitisation of others that are utilising similar effector cascades; Hepler & Saugstad, 2002). For the β_2 adrenoceptor, homologous desensitisation is caused by phosphorylation of serine and threonine residues in the third intracellular loop by G protein coupled receptor kinases (GRKs). However, heterologous desensitisation is caused by phosphorylation of serine residues in both the third intracellular loop and the C-terminal tail by protein kinase A (Bunemann & Hosey, 1999).

Following GRK phosphorylation, arrestin proteins are recruited from the cytosol to bind to the phosphorylated residues, forming an arrestin-GPCR complex that prevents further G protein binding (Pierce *et al.*, 2002; Hepler & Saugstad, 2002). There are seven different GRK isoforms and four different arrestin isoforms, which allow a complex array of differential of GPCR regulation (Pierce *et al.*, 2002).

The arrestin-GPCR complex is then targeted to microdomains of the plasma membrane to aid endocytosis. It has been suggested that arrestins and GRKs may also bind to other proteins to facilitate the internalisation of GPCRs. These include caveolin and actin for GRKs and clathrin for arrestins (Hepler & Saugstad, 2002). Interestingly clathrin is the protein coating the plasma membrane pits which pinch off to precipitate receptor internalisation (Hepler & Saugstad, 2002). Endocytosis can lead to recycling of the receptor, eventually returning it to the plasma membrane, or receptor degradation in lysosomal compartments. Longer term desensitisation can be achieved through changes in expression or stability of receptor mRNA and subsequent changes in receptor expression levels. This can often be a result of chronic drug treatment or progressive pathological states (Hepler & Saugstad, 2002).

2. GPR10 and prolactin-releasing peptide

(i) RF amide peptides and their receptors

RF-amides are peptides characterised by an amidated arginine-phenylalanine motif at their C-terminus. There are multiple non-mammalian RF-amide peptides, many found in annelids and molluscs, including FMRF-amide, Pol-RF-amide, ACEP-1 and Antho-RF-amide (Hinuma *et al.*, 1999; Table 2). With the discovery of these peptides many groups sought to identify potential mammalian RF-amide peptides. The most well characterised mammalian RF-amides are neuropeptide-FF (NPFF) and neuropeptide-AF (NPAF; Yang *et al.*, 1985), which are thought to modulate the central opioid system (Yang *et al.*, 1985; Roumy & Zajac, 1998) and possibly stimulate prolactin secretion (Aarnisalo *et al.*, 1997). NPFF and NPAF are thought to be the cognate ligands of an orphan receptor identified as HLWAR77 (Elshourbagy *et al.*, 2000; Kotani *et al.*, 2001a) that is thought to signal through the G_i family of G proteins as it both stimulates the binding of the radiolabelled, non-hydrolysable form of GTP, [^{35}S]GTPγS, and inhibits forskolin induced increases in intracellular cAMP levels in CHO cells stably expressing HLWAR77 (Kotani *et al.*, 2001a).

More recently, Hinuma and co-workers have searched for novel RF-amide peptide genes in the GenBank/EMBL database (Hinuma *et al.*, 2000). Using this method, they cloned 3 possible RF-amide peptide genes and isolated human, bovine, rat and mouse cDNAs for the peptides, designated RFRP-1 (12 aa), RFRP-2 (12 aa) and RFRP-3 (8 aa). Unlike RFRP-1 and –3, RFRP-2 contains a serine residue in place of the C-terminal phenylalanine. The C-terminus of hRFRP-1 is identical to that of the chicken RF-amide peptide, LPLRF-amide (Dockray *et al.*, 1983) and the C-terminal 4 amino acids of hRFRR-3 identical to those in NPFF (Yang *et al.*, 1985), suggesting that these peptides all originate from a common evolutionary ancestor. By using

Peptide	Sequence
AnthoRF- amide	pEGRF-$CONH_2$
AF-2	KHEYLRF-$CONH_2$
ACEP-1	SGQSWRPQGRF-$CONH_2$
FLRF-amide	FLRF-$CONH_2$
FMRF-amide	FMRF-$CONH_2$
PrRP-20	TPDINPAWYTGRGIRPVGRF-$CONH_2$
Kiss(107–121)	KDLPNYNWNSFGLRF-$CONH_2$
Kiss(112–121)	YNWNSFGLRF-$CONH_2$
PQRF-amide	PQRF-$CONH_2$
Neuropeptide FF	FLFQPQRF-$CONH_2$
Neuropeptide AF	AGEGLNSQFWSLAAPQRF-$CONH_2$
RFRP-1	MPHSFANLPLRF-$CONH_2$
RFRP-3	VPNLPQRF-$CONH_2$
Neuropeptide Y	YPSKPEDMARYYSALRHYINLITRQRY-$CONH_2$

Table 2. Peptide sequences for a range of RF-amides. Adapted from Han *et al.* (2002).

synthetic RFRP peptides as 'bait' to 'fish' against a variety of recombinantly expressed orphan GPCRs, the authors suggested that RFRP-1 and RFRP-3 may be cognate ligands of the rat orphan GPCR, OT7T022 (Hinuma *et al.*, 2000). RFRP-1 and -3, but not RFRP-2, activate OT7T022 when expressed in CHO cells and act to inhibit forskolin stimulated levels of intracellular cAMP, suggesting coupling through the G_i family of G proteins. The lack of activity of RFRP-2 suggests that the presence of the C-terminal phenylalanine in the RF-amide peptide may be crucial to activity.

KiSS-1 is a human metastasis suppresser gene (Lee *et al.*, 1996) that has been shown to encode an RF-amide peptide of 54 aa, termed metastin (Ohtaki *et al.*, 2001). In a similar 'reverse pharmacology' approach, this peptide was purified from human placental tissue and shown to potently stimulate intracellular calcium mobilisation in CHO cells stably transfected with the orphan GPCR, hOT7T175 (Ohtaki *et al.*, 2001). The non-amidated acid form (with C-terminal –COOH group as opposed to $–CONH_2$) was approximately 1000-fold less potent at stimulating calcium mobilisation. These data also suggest that the amide group is key to normal metastin function at hOT7T175 and that this receptor may signal through the $G_{q/11}$ pathway. Concurrent studies also identified the same 54 aa peptide from human placenta along with two other N-terminally truncated variants of 14 aa and 13 aa (Kotani *et al.*, 2001b). These peptides were termed kisspeptin-54, kisspeptin-14 and kisspeptin-13, respectively. In this study, the kisspeptins were shown to be equipotent agonists at both the human and rat orphan receptor GPR54 when stably co-expressed with $G_{\alpha 16}$ in CHO cells (Kotani *et al.*, 2001b). Consistent with the studies of Ohtaki *et al.*, (2001), the non-amidated peptides were inactive. This same family of kisspeptins have also been shown to be potent agonists at another orphan receptor, AXOR12 (Muir *et al.*, 2001). These combined data suggest another subfamily of mammalian RF-amide peptides with a potential family of related kisspeptin receptors.

Similar 'reverse pharmacology' studies have also shown that a number of RF-amide peptides can act as moderate potency surrogate agonists at the orphan GPCRs, MrgA1 and MrgC11, and that these receptors are likely to couple through the $G_{q/11}$ pathway (Han *et al.*, 2002). Further studies may help identify more potent, likely cognate, ligands for these receptors.

The RF-amide family of peptides and their receptors are clearly an expanding field and the popularity of the novel 'reverse pharmacology' approach will undoubtedly reveal further ligand-receptor pairings in the future.

(ii) Identification of GPR10 - PrRP ligand pair

The RF-amide peptide receptors are an excellent example of the modern 'reverse pharmacology' approach, where ligands are identified from native tissue extracts or synthesised based on genetic sequences. These are then screened against a variety of orphan receptor targets, often co-expressed with a promiscuous G protein that can couple to any GPCR to allow signalling through the PLC-calcium pathway eg. $G\alpha_{16}$ (Wilson *et al.*, 1998).

This technique, often referred to as 'ligand fishing', was used to identify the RF-amide peptide, prolactin-releasing peptide (PrRP), as the cognate ligand of the orphan receptor, GPR10.

GPR10 is a novel 370 aa GPCR identified by polymerase chain reaction and genomic DNA library screening (Marchese *et al.*, 1995). It is the human orthologue of rat Unknown Hypothalamic Receptor-1 (UHR-1; Welch *et al.*, 1995) and shares the highest level of homology with the neuropeptide Y receptor family (31% overall, 46% in the transmembrane domains; Marchese *et al.*, 1995). A receptor termed hGR3 (Hinuma *et al.*, 1998) is identical at the amino acid level to GPR10. The same

authors used a similar 'ligand fishing' approach as above to identify potential ligands for hGR3 / GPR10.

Ligand identification for the receptor was carried out utilising an arachidonic acid release assay using Chinese hamster ovary (CHO) cells stably transfected with hGR3 / GPR10, in which bovine hypothalamic extracts were positive. Chromatographic purification of the extracts led to the identification of a human preproprotein cDNA encoding 87 aa and rat and bovine orthologues. The N-terminal portion of the cDNA displayed the typical profile of a secretory signal peptide, which left two peptide sequences with identical C-terminal regions, one of which appears to be a truncated form of the other (Hinuma *et al.*, 1998). Studies showed that the PrRP preproprotein can be cleaved at two different positions to give rise to two forms of 31 or 20 aa; PrRP-31 and PrRP-20 respectively. Rat and bovine PrRPs have also been identified and occur as 31 or 20 aa forms; these peptides are highly conserved between species (Figure 3; Hinuma *et al.*, 1998).

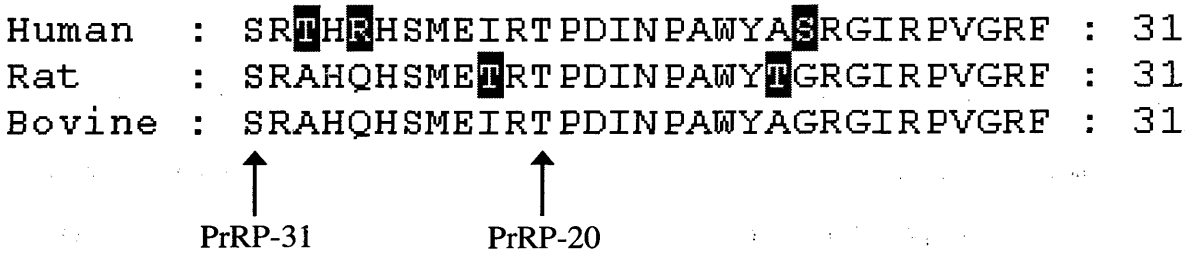

Figure 3. Alignment of the amino acid sequences of human, rat and bovine prolactin releasing peptide. Arrows indicate the N-termini of the two isoforms of the peptides, PrRP-31 and PrRP-20. Amino acid residues that differ from the consensus sequence are shaded. Sequence homology with human PrRP-31 is 84% (rat) and 90% (bovine).

(iii) Expression profile of PrRP and GPR10

Studies using reverse transcriptase PCR in rat brain tissue have detected PrRP mRNA in the medulla oblongata, with moderate levels in the hypothalamus (Table 3; Hinuma *et al.*, 1998; Fujii *et al.*, 1999). *In situ* hybridisation studies in rat brain have also detected PrRP mRNA in neurones of the nucleus of the tractus solitarius (NTS), the ventral and lateral reticular nuclei (VLRN) of the medulla and the dorsomedial hypothalamus (DMH). The strongest hybridisation was observed in the NTS (Lee *et al.*, 2000; Maruyama *et al.*, 1999; Minami *et al.*, 1999; Roland *et al.*, 1999; Ibata *et al.*, 2000). Peripherally, PrRP mRNA has been detected in the adrenal gland, pancreas, placenta and testis (Fujii *et al.*, 1999; Nieminen *et al.*, 2000).

PrRP immunoreactivity has been detected by enzyme immunoassay, in rank order of high to low expression levels, in rat hypothalamus, midbrain, pituitary, medulla, adrenal gland and plasma (Table 3; Matsumoto *et al.*, 1999). Studies using radioimmunoassay also detected PrRP in the human hypothalamus and to a lesser extent in the medulla (Takahashi *et al.*, 2000). These assay methodologies detect bioactive PrRP and, in agreement with studies determining arachidonic acid release with tissue extracts (Hinuma *et al.*, 1998), suggest that the hypothalamus contains the highest levels of PrRP, despite the greater amount of mRNA being found in the medulla.

Immunohistochemical studies have also detected PrRP in the NTS, VLRN, DMH and pituitary of the rat brain (Chen *et al.*, 1999; Maruyama *et al.*, 1999; Yamakawa *et al.*, 1999; Matsumoto *et al.*, 1999). The distribution of PrRP in the NTS and VLRN was also shown to be co-localised with tyrosine hydroxylase, suggesting that PrRP was present in noradrenergic neurones (Chen *et al.*, 1999). Given that the hypothalamus contains the highest reported levels of bioactive PrRP, it is possible that PrRPs

PrRP		GPR10 / UHR-1	
mRNA	**Protein**	**mRNA**	**Protein**
Medulla	Hypothalamus	Pituitary	Thalamus
Hypothalamus	Midbrain	Cerebellum	Hypothalamus
NTS	Pituitary	Hypothalamus	NTS
DMH	Medulla	Thalamus	Area postrema
VLRN	PVN	Spinal cord	
	BST	Adrenal gland	

Table 3. Summary of distribution of PrRP and GPR10 / UHR-1 mRNA and protein. Data are taken from Hinuma *et al.*, 1998; Fujii *et al.*, 1999; Lee *et al.*, 2000; Maruyama *et al.*, 1999; Minami *et al.*, 1999; Roland *et al.*, 1999; Ibata *et al.*, 200; Nieminen *et al.*, 2000; Matsumoto *et al.*, 1999; Takahashi *et al.*, 2000; Chen *et al.*, 1999; Maruyama *et al.*, 1999; Yamakawa *et al.*, 1999; Welch *et al.*, 1995; Ellacott *et al.*, 2005.

produced in the cell bodies of the NTS (where PrRP mRNA is most prominent) are transported to the hypothalamus. PrRP has also been detected in the paraventricular nucleus (PVN) and the bed nucleus of the stria terminalis (BST), suggesting more varied CNS roles for PrRPs.

The literature on distribution of GPR10 or UHR-1 is scarcer than that for PrRP. The mRNA for the UHR-1, as determined by RT-PCR, is expressed in rat pituitary, cerebellum and hypothalamus (Table 3; Welch *et al.,* 1995), although other studies have also observed mRNA in thalamus, spinal cord, and adrenal gland (Hinuma *et al.,* 1998; Roland *et al.*, 1999). In contrast, early autoradiographic studies with [^{125}I]-hPrRP-31 have shown receptor binding only in thalamus and hypothalamus in the rat brain (Table 3; Roland *et al.*, 1999), with more recent studies showing specific binding of [^{125}I]-hPrRP-20 in the NTS and area postrema (Ellacott *et al.*, 2005). Other studies have detected levels of specific binding of [^{125}I]-hPrRP-31 in membranes prepared from rat hypothalamus, medulla, pituitary and cerebellum and also heart, soleus muscle, adipose tissue, kidney, adrenal gland, testis and small intestine (Satoh *et al.*, 2000). These data suggest that binding sites for PrRP may be widely expressed in both the brain and the periphery, in common with a number of suggested roles for PrRP including stress responses, cardiovascular regulation and food intake.

Interestingly, analysis of the binding sites of [^{125}I]-hPrRP-31 by chemical cross-linking suggested a binding site of M_W = 69,000 in hypothalamus, but of only 41,000 in heart and soleus muscle (Satoh *et al.*, 2000). The size of the binding site in hypothalamus is far in excess of that predicted from the sequence of UHR-1 (M_W = 41,165) and is probably due to differences in receptor glycosylation (Satoh *et al.*, 2000). The size of the binding site in heart and soleus muscle suggests either a non-glycosylated form of UHR-1, or more likely a truncated or cleaved form of UHR-1. This phenomenon

has been suggested in a recent publication on the anorectic effect of PrRP-31 in rats, where a polymorphism in the putative translational initiation site of UHR-1 results in an ATG to ATA change, potentially resulting in a truncated receptor with translation starting at a later in-frame start codon (Ellacott *et al.*, 2005). In rats expressing the polymorphism, PrRP-31 still evoked an anorectic response (see below), although there was no specific binding of [^{125}I]-hPrRP-20 in brain slices from these animals, unlike in slices from rats expressing non-polymorphic UHR-1 (Ellacott *et al.*, 2005). It is possible that an alternative receptor for PrRP exists (data from Welch *et al.* (1995) suggested that UHR-1 may one of a family of receptors). However, PrRP may simply be binding elsewhere in the brain with its detection being missed due to low cell surface expression or because it is beyond the limits of film autoradiography.

(iv) Physiological function of PrRP and GPR10

Hinuma *et al.* (1998) demonstrated that bovine PrRP-31, in a rat pituitary adenoma derived cell line which had been shown to express UHR-1 mRNA, caused prolactin secretion in a concentration-dependent manner. Similarly, PrRP-31 stimulated prolactin secretion from anterior pituitary cells harvested from lactating female rats with a similar potency to that of thyrotropin releasing hormone (TRH), a hormone that is already known to stimulate prolactin secretion (Lamberts & Macleod, 1990). PrRP-31 did not alter the release of other anterior pituitary hormones (growth hormone, follicle stimulating hormone, lutenising hormone, thyroid stimulating hormone and adrenocorticotropin) and stimulated prolactin secretion in a perifusion assay protocol within 15 min to 1 h of application. These data suggested that the effect of PrRP-31 on prolactin release was both selective and direct and led to the naming of the peptides as 'prolactin releasing peptides' or PrRP. Subsequently, the same group demonstrated the prolactin-releasing effects of PrRPs *in vivo* (Matusmoto *et al.*, 1999). However, many recent studies have questioned the role of PrRPs as

physiological prolactin releasing agents, suggesting stimulation of prolactin release with PrRP only occurs, if at all, at pharmacological concentrations (Samson *et al.*, 1998; Jarry *et al.*, 2000; Curlewis *et al.*, 2002). Morphological studies further question the role of PrRPs in prolactin release, suggesting the absence of PrRP in the external lamina of the median eminence, an area of the hypothalamus where recognised releasing and inhibiting factors of hypothalamic origin gain access to the hypophysial portal vasculature and the anterior lobe (Taylor & Samson, 2001).

Since the initial claim of prolactin releasing effects, a large number of alternative functions for PrRP have been suggested, largely based on the varied CNS distribution of the peptide. Based on the expression of PrRP in the DMH, one of the suggested roles for PrRP is in food intake and body weight regulation. Lawrence *et al.* (2000) provided evidence to suggest that the number of PrRP mRNA containing neurones was dramatically reduced in the DMH and NTS of both fasting and lactating rats, both states of negative energy balance. This effect was coupled by a reduction in food, but not water, intake in rats dosed with intracerebroventricular (i.c.v.) PrRP (Lawrence *et al.*, 2000). This effect was independently verified (Seal *et al.*, 2001), but also shown to diminish after repeated dosing with PrRP (Ellacott *et al.*, 2003), suggesting a short term effect on energy balance. Furthermore, the GPR10 knockout mouse displays a hyperphagic and obese phenotype (Gu *et al.*, 2004). These data strongly suggest that PrRP acts centrally to inhibit food intake.

In common with a number of other neuropeptides, PrRP has also been shown to interact with leptin to regulate energy homeostasis, as i.c.v. injection of PrRP with leptin produces an additive anorectic effect (Ellacott *et al.*, 2002). PrRP has also been shown to increase the release of neurotensin and α-melanocyte-stimulating hormone from a hypothalamic explant culture (Seal *et al.*, 2001). Both of these transmitters are known inhibitors of food intake, suggesting a possible indirect effect

of PrRP on food intake. However, the effects of PrRP on food intake are not blocked by the melanocortin receptor-3/4 antagonist, SHU-9119, but are blocked by the corticotropin-releasing hormone (CRH) receptor antagonist astressin (Lawrence *et al.*, 2004). Finally, studies in humans found no significant association between a GPR10 coding polymorphism (P305L) and obesity parameters, although the same study suggested that the polymorphism has only a small effect on receptor function *in vitro* (Bhattacharyya *et al.*, 2003). Taken as whole, these data strongly suggest that PrRP inhibits food intake in rodents, although the precise mechanism of action remains to be fully determined.

There is also evidence that PrRP modulates the hypothalamic-pituitary-adrenal axis as a stimulator of CRH neurones in the PVN (Matsumoto *et al.*, 2000). Administration of PrRP into the PVN results in increased plasma adrenocorticotropic hormone (Seal *et al.*, 2002) and centrally administered PrRP-31 causes increased plasma corticosterone levels (Samson *et al.*, 2003). This effect was blocked with anti-serum to CRH, but not by α-helical CRH(9-41), suggesting PrRP acts not only on CRH-producing neurones, but also on other adrenocorticotropic hormone secretagogues such as oxytocin or vasopressin, as proposed previously (Maruyama *et al.*, 1999). These data suggest a role for PrRP in mediating responses to stressors. Additionally, noradrenergic fibres in the medulla have been shown to mediate stress responses in the CNS and PrRP has been shown to co-localise with tyrosine hydroxylase in these neurones (Chen *et al.*, 1999). Foot-shock, haemorrhage and conditioned fear stimuli have also been shown to activate PrRP neurones in the medulla (Morales & Sawchenko, 2003; Zhu & Onaka, 2003), further implicating PrRP as playing a role in mediating stress responses.

The localisation of PrRPs in regions of the brainstem such as the NTS, the ventrolateral medulla and the area postrema suggest a possible involvement in

cardiovascular regulation. Central administration of PrRP-31 in the rat has been shown to produce a profound increase in mean arterial blood pressure (Samson *et al.*, 2000), an effect that was independently verified and also shown to be dose-dependent (Horiuchi *et al.*, 2002). Furthermore, in genetic studies in humans, the GPR10 polymorphism, P305L, was shown to be associated with significantly lower blood pressure (Bhattacharyya *et al.*, 2003). Additionally, other roles have been suggested for PrRPs including regulation of sleep (Zhang *et al.*, 2000), the lutenising hormone surge (Hizume *et al.*, 2000; Watanobe, 2001) and growth hormone regulation (Iijima *et al.*, 2001; Rubinek *et al.*, 2001).

In summary, the varied expression profiles described for PrRPs and their receptor has led to a wide range of investigations into the physiological roles of PrRPs beyond the initial description of them as prolactin releasing factors. There now seems to be substantial evidence to implicate PrRPs as having roles in food intake, stress responses and possibly cardiovascular regulation.

3. Muscarinic M_1 acetylcholine receptors

(i) Nicotinic and muscarinic acetylcholine receptors

In 1914, Henry Dale classified two types of pharmacological activity mediated by the chemical transmitter, acetylcholine (ACh), as muscarinic and nicotinic. Muscarinic activity was the activity of ACh that could be replicated by muscarine, the active agent found in the poisonous mushroom *Amanita muscaria* and could then be blocked by low concentrations of atropine. Muscarinic activity corresponds closely to that of ACh released at postganglionic parasympathetic nerve endings (except ACh-mediated generalised vasodilatation and secretion from sweat glands; Rang *et al.*, 1999). After blockade of muscarinic receptor activity with atropine, large doses of ACh mediate effects similar to those observed with nicotine, including stimulation of autonomic ganglia and voluntary muscle and secretion of adrenaline from the adrenal medulla. These nicotinic effects correspond to ACh acting on autonomic ganglia of the sympathetic and parasympathetic nervous systems, the neuromuscular junction and secretory cells of the adrenal medulla (Rang *et al.*, 1999).

Acetylcholine receptors are now broadly defined along the divide established pharmacologically by Dale. Nicotinic ACh receptors are ligand gated ion channels, whereas muscarinic ACh receptors are GPCRs.

Nicotinic ACh receptors (nAChR) consist of two broad subtypes, the neuromuscular and neuronal nAChRs (Colquhoun *et al.*, 1987). The neuromuscular receptor is a pentameric structure made up of four subunits ($\alpha\alpha\beta\gamma\varepsilon$ in human; Rang *et al.*, 1999), whereas the neuronal nAChR is more varied, especially in the brain, consisting of various permutations of eight different α-subunits and four β-subunits (McGehee & Role, 1995). Neuromuscular and neuronal nAChRs can be distinguished pharmacologically – decamethonium and epibatidine are potent and subtype selective neuromuscular and neuronal nAChR agonists, respectively, whereas

α-bungarotoxin and mecamylamine are respective selective nAChR receptor antagonists (Rang *et al.*, 1999).

In the periphery, muscarinic receptor agonists mediate smooth muscle contraction, glandular secretions and the modulation of heart rate and force of contraction (Caulfield & Birdsall., 1998). In the CNS, muscarinic receptor agonists are thought to be involved in motor control, temperature regulation, cardiovascular regulation and memory (Caulfield & Birdsall, 1998).

(ii) Characterisation of muscarinic receptor subtypes

The first evidence of the existence of more than one muscarinic ACh receptor subtype was the relatively selective actions of gallamine on the heart (Riker & Wescoe, 1951). Subsequently Barlow *et al.* (1976) demonstrated that there were significant differences in the pharmacology of muscarinic receptors in atrial and ileal tissue. Together with the development of pirenzepine, a muscarinic receptor antagonist which shows a limited degree of selectivity for the M_1 receptor subtype (Hammer *et al.*, 1980; Brown *et al.*, 1980), researchers concluded that there were at least three pharmacologically defined muscarinic receptor subtypes (Birdsall & Hulme, 1983). These receptor subtypes, now known as M_1, M_2 and M_3, are sometimes still referred to by the tissue type in which they are predominantly expressed, namely 'neural', 'cardiac' and 'glandular' muscarinic receptors. Given that the most pronounced pharmacological differences were seen between the muscarinic receptor population in the forebrain and the heart, it was from porcine receptors in these tissues that the first partial amino acid sequences for the muscarinic receptors were derived (Haga & Haga, 1983; Peterson *et al.*, 1984). This led to full length cloning of the respective cDNAs for the M_1 and M_2 muscarinic receptors (Kubo *et al.*, 1986a; Kubo *et al.*, 1986b), which was rapidly followed by the cloning of a further three muscarinic receptor subtypes, namely M_3, M_4 and M_5

(Bonner *et al.*, 1987; Bonner *et al.*, 1988). All five genes encode proteins that have similar structural features suggesting they are members of the seven transmembrane domain GPCR superfamily. There is a significant degree of homology between muscarinic receptor subtypes (Hulme *et al.*, 1990) and sequences are highly conserved across mammalian species (Ellis, 2002).

(iii) Expression profile and physiological role of muscarinic M_1 receptors

Subsequent to the cloning of the muscarinic receptor family, the distribution of the five members has been extensively characterised. Indeed, it was the pharmacological differences between muscarinic receptors found in brain, heart and ileum that first suggested the presence of more than one muscarinic receptor subtype. All five subtypes are expressed in the brain (Ellis, 2002), although the M_1 receptor subtype predominates in the forebrain regions (cortex, hippocampus, striatum and thalamus) with higher levels of M_2 receptor in the brainstem and cerebellum. The M_4 receptor is found in many brain regions, but mostly in the striatum, whereas the M_3 and M_5 receptor subtypes are only expressed at very low levels, although the M_5 receptor subtype does have a very discrete localisation in the substantia nigra (Ellis, 2002). Peripherally, the M_1 receptor is also localised in glandular tissues. The M_2 receptor subtype is strongly expressed in the heart, but also in smooth muscle and lung, whereas the M_3 receptor subtype is localised mainly to smooth muscle and glandular tissues (Ellis, 2002). The M_4 and M_5 receptor subtypes appear to be only expressed peripherally at very low levels, if at all, although the M_4 receptor subtype is highly expressed in rabbit lung (Lazareno *et al.*, 1990), although not in the lung tissue of other species (Zaagsma *et al.*, 1997).

	Receptor subtype				
	M_1	**M_2**	**M_3**	**M_4**	**M_5**
Preferred G protein(s)	$G_{q/11}$	$G_{i/o}$	$G_{q/11}$	$G_{i/o}$	$G_{q/11}$
Second messenger(s)	PLC; IP_3/ DAG; Ca^{2+} / PKC	Adenylyl cyclase (inhibition)	PLC; IP_3/ DAG; Ca^{2+} / PKC	Adenylyl cyclase (inhibition)	PLC; IP_3/ DAG; Ca^{2+} / PKC
Expression profile	Cortex, hippocampus Glands Sympathetic ganglia	Heart Hindbrain Smooth muscle	Smooth muscle Glands Brain	Basal forebrain Striatum	Substantia nigra
Functional Response(s)	M-current inhibition	K^+ channels ($\beta\gamma$ activates) Inhibit Ca^{2+} channels ↓ Heart rate and force ↓ Neuro-transmitter release (presynaptic)	Smooth muscle contraction Gland secretion ↓ Neuro-transmitter release (presynaptic)	Inhibit Ca^{2+} channels	

Table 4. Signal transduction, distribution and physiological function of muscarinic acetylcholine receptor subtypes.

The physiological functions of the M_1 receptor tie in well with its localisation. M_1 receptors are thought to generate slow excitatory post-synaptic potentials in the forebrain regions by inhibition of a K^+ current, termed the M-current (I_M) due to its control by muscarinic receptor agonists. Hence, mice lacking the M_1 receptor gene display loss of inhibition of I_M (Hamilton *et al.*, 1997). Other notable phenotypes include reductions in long term potentiation in the hippocampus (Ellis, 2002), impaired performance in spatial memory tasks (Anagnostaras *et al.*, 2003) and a loss of muscarinic receptor agonist induced mitogen-activated protein (MAP) kinase activity in the cortex (Veinbergs *et al.*, 2003). These observations strongly suggest that the M_1 receptor plays a role in learning and memory processes within the CNS. Indeed, the selective loss of cholinergic neurones in the basal forebrain seen in Alzheimer's disease is accompanied by severe cognitive deficits (Ellis, 2002).

(iv) Muscarinic M_1 receptor signalling & pharmacology

The signal transduction mechanisms of muscarinic receptors have been extensively studied. In general, the 'odd-numbered' receptors, namely M_1, M_3 and M_5, have been shown to couple via the Gα subunits of the $G_{q/11}$ family to stimulate phospholipase-Cβ (PLCβ) mediated conversion of phosphatidyl inositol 4,5-bisphosphate (PIP_2) into inositol trisphosphate (IP_3) and diacylglycerol (DAG). IP_3 then binds to its cognate receptor in the membrane of the smooth endoplasmic reticulum to cause the release of intracellular calcium (Caulfield, 1993; Caulfield & Birdsall, 1998; Ellis, 2002). In contrast, the 'even-numbered' receptors, M_2 and M_4, preferentially couple via the G_i family to inhibit adenylyl cyclase (AC) and reduce the intracellular concentration of cAMP (Caulfield, 1993; Caulfield & Birdsall, 1998; Ellis, 2002). This coupling of the M_2 and M_4 receptors is sensitive to PTX treatment, which ADP ribosylates both $G\alpha_i$ and $G\alpha_o$.

However, with the discovery of more complex signal transduction pathways, signalling *via* Gβγ subunits, cross-talk between receptor subtypes and even G protein independent signalling, the transduction pathways mediated *via* muscarinic receptors are now known to be diverse (Ellis, 2002). In addition to its release of calcium from intracellular stores, the M_1 receptor has been shown to stimulate a range of other effector systems, including arachidonic acid release (Conklin *et al.*, 1988), phospholipase-D (Ellis, 2002) and the MAP kinase cascade (Berkeley *et al.*, 2001).

Additionally, muscarinic receptors have been shown to modulate a variety of ion channel conductances in the CNS. In fact a neuronal potassium current has been termed the M-current (I_M), because it was inhibited by muscarinic receptor agonists (Brown & Adams, 1980). In recombinant cell studies, $G_{q/11}$ coupled receptors reduce I_M in a manner that suggests a diffusible second messenger mediated inhibition (Robbins *et al.*, 1993); recent studies suggest that depletion of membrane phosphatidylinositol bisphosphate (PIP_2) may be involved (Suh & Hille, 2002). Pharmacological studies on I_M in the superior cervical ganglion (SCG) suggest that the current may be inhibited *via* the M_1 receptor (Bernheim *et al.*, 1992); this observation was seemingly confirmed by studies which showed the absence of muscarinic receptor agonist induced inhibition of I_M in the M_1 receptor knockout mouse (Hamilton *et al.*, 1997). The M_1 receptor has also been shown to inhibit N-type and L-type calcium currents in the SCG, an effect that is insensitive to PTX and has a slow time course consistent with a diffusible second messenger mediated inhibition (Ellis, 2002). These effects were also shown to be absent the M_1 receptor knockout mouse (Shapiro *et al.*, 2001). Muscarinic receptors also mediate fast inhibition of N- and P/Q-type calcium channels, but this effect has been shown to be PTX sensitive and is absent in the SCG of M_2 knockout mice (Shapiro *et al.*, 2001), suggesting that it is this subtype that mediates the inhibition.

There is a wide array of pharmacological tools with which to study populations of muscarinic receptors. *N*-methyl scopolamine (NMS), quinuclidinylbenzilate (QNB), pirenzepine and darifenacin amongst muscarinic receptor antagonists and ACh and oxotremorine-M amongst muscarinic receptor agonists have been radiolabelled and extensively used to characterise muscarinic receptors. Unfortunately, most of the pharmacological tools available show low levels of selectivity (often 10-fold or less) between the muscarinic receptor subtypes (Caulfield & Birdsall, 1998; Ellis, 2002). This is primarily due to the high level of conservation amongst the residues forming the orthosteric binding site of muscarinic receptors, which prevents the design of subtype selective agonists and antagonists. Given the mixed muscarinic receptor population in most tissues and the relative lack of selectivity amongst radioligands and other reagents, a large amount of pharmacology has been carried out in recombinant cell lines stably expressing single subtypes of muscarinic receptors.

(v) Characterisation of the muscarinic M_1 orthosteric binding site

As discussed earlier, the elucidation of the crystal structure of rhodopsin has increased the understanding of the structure of family A GPCRs (Section 1, iv). One of the best studied in this regard has been the muscarinic M_1 receptor. The orthosteric binding site of aminergic family A receptors comprises a network of residues in the TM bundle including residues from TM3, TM4, TM5, TM6 and TM7 (Gether, 2000; Kristiansen, 2004).

Studies using [^{3}H]ACh mustard (an analogue of ACh that both activates and covalently binds to muscarinic receptors) have shown that the conserved Asp residue in TM3 (D105 in both rat and human M_1 receptors) is the primary site of interaction for the amine group of ACh (Spalding *et al.*, 1994). Further studies using both point and scanning mutagenesis have comprehensively identified the residues that are

involved in the binding of ACh and atropine-like muscarinic receptor antagonists such as NMS. The amine headgroup of ACh interacts with D105; even the conservative D105E mutation reduces ACh potency 1000-fold (Hulme *et al.*, 1995) and strongly reduces the high agonist affinity component of agonist binding (Page *et al.*, 1995). This interaction is thought to be stabilised by contacts with Y404, C407 and Y408 in TM7 of the rat M_1 receptor. The mutations Y404A and Y404F both reduce ACh binding affinity, but only Y404A reduces the maximal phosphoinositide response (Lu *et al.*, 2001). Similar results were seen for Y408 (Lu *et al.*, 2001). These data suggest it is the hydroxyl group that is involved in the binding of agonist, but it is the aromatic moiety that is involved in receptor activation. Two tyrosine residues in TM2, Y82 and Y85 in the rat M_1 receptor, are close to D105, Y404 and Y408 and have been implicated in agonist binding and receptor activation. Loss of the hydroxyl group alone, or in combination with the aromatic ring, reduces the affinity of the ACh analogue, carbachol and its potency to stimulate phosphoinositide hydrolysis (Lee *et al.*, 1996).

ACh is also thought to interact with residues in TM6, including W378 and Y381. The mutation Y381F reduces ACh potency ~70-fold; Y381A reduces the potency ~3000-fold, suggesting that this tyrosine residue plays a major role in receptor activation (Ward *et al.*, 1999).

The ammonium headgroup of NMS has also been shown to interact with D105, Y381, Y404 and Y408 (Lu *et al.*, 2002), but NMS is a larger molecule than ACh and hence the phenyl ring is thought to plunge deep into the TM bundle between TM3, TM5 and TM6 (Lu *et al.*, 2002). Some studies have suggested that N382 in TM6 is involved in antagonist binding alone (Huang *et al.*, 1999), although loss of this asparagine has been shown to markedly reduce agonist potency (Ward *et al.*, 1999; Spalding *et al.*, 2002).

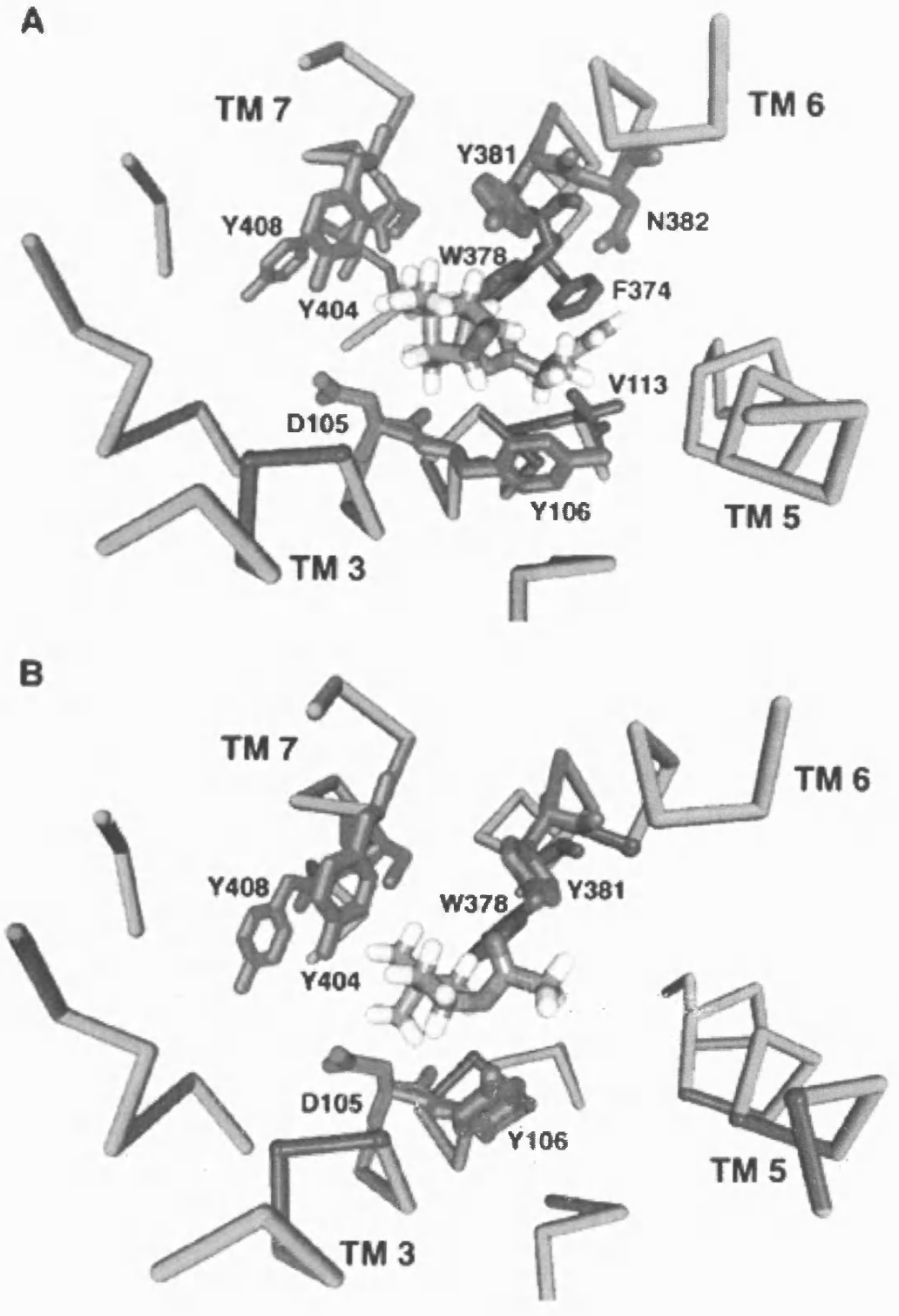

Figure 4. NMS (A) and ACh (B) docked into a homology model of the muscarinic M_1 receptor showing the proximity of the amino acid residues in TM3, TM6 and TM7 that have been implicated in their binding (figure taken from Hulme *et al.*, 2003).

Both NMS and ACh have been docked into a homology model of the muscarinic M_1 receptor (Hulme *et al.*, 2003) which shows their close proximity to amino acids in TM3, TM6 and TM7 (Figure 4). The smaller ACh molecule is also thought to interact with residues towards the top of TM5 and TM6, mutation of which affect ACh, but not NMS binding. Mutation of T192 in TM5 reduces both ACh potency and affinity, with no effect on antagonist binding (Huang *et al.*, 1999). Similarly, loss of L386 in TM6 reduces ACh affinity, potency and efficacy (Huang *et al.*, 1999).

There are also thought to be key residues more extracellular to the main interaction site of ACh and NMS that facilitate the access of these diffusible ligands into the TM bundle. Mutation of W157 in TM4 causes a large decrease in [^{3}H]NMS binding and ACh signalling efficacy (Lu *et al.*, 1999) as well as ACh affinity (Hulme *et al.*, 2003). This residue is very close to the exofacial acidic residue in TM3 that is adjacent to the cysteine residue that forms a disulphide bridge with another cysteine in the second extracellular loop (Lu *et al.* 2002). This configuration is thought to facilitate the access and egress of ligands to the deeper binding site.

The invariant arginine residue (R123) at the base of TM3 found in all family A GPCRs (part of the DRY motif), is key to receptor activation – all mutations which result in a loss or reversal of charge at this position drastically reduce ACh potency in phosphoinositide hydrolysis assays (Hulme *et al.*, 1995). However, a range of other residues have been implicated in activation of the M_1 receptor, including D71 (TM2; Fraser *et al.*, 1989), N414, P415 and Y418 (all TM7; Lu *et al.*, 2001). These latter residues form part of a conserved NSxxNPxxY motif which is thought to form intramolecular interactions to hold the receptor in the ground state; upon agonist binding these interactions are broken and new intramolecular bonds are made to hold the receptor in the active state (Lu *et al.*, 2001).

The residues implicated in the binding of ACh and NMS are highly conserved across the muscarinic receptor family (Figure 5). The consequence of this conservation, as discussed earlier, is difficulty in distinguishing between receptor subtypes with pharmacological tools directed against the orthosteric binding site. It is likely that any pharmacological selectivity is probably achieved through allosteric ligand interactions, such as is observed for the non-competitive selective M_1 receptor peptide antagonist, muscarinic toxin (MT)-7 (Mourier *et al.*, 2003) and the recently described novel M_1 receptor agonist, AC-42 (Spalding *et al.*, 2002; see Chapters 5 and 6).

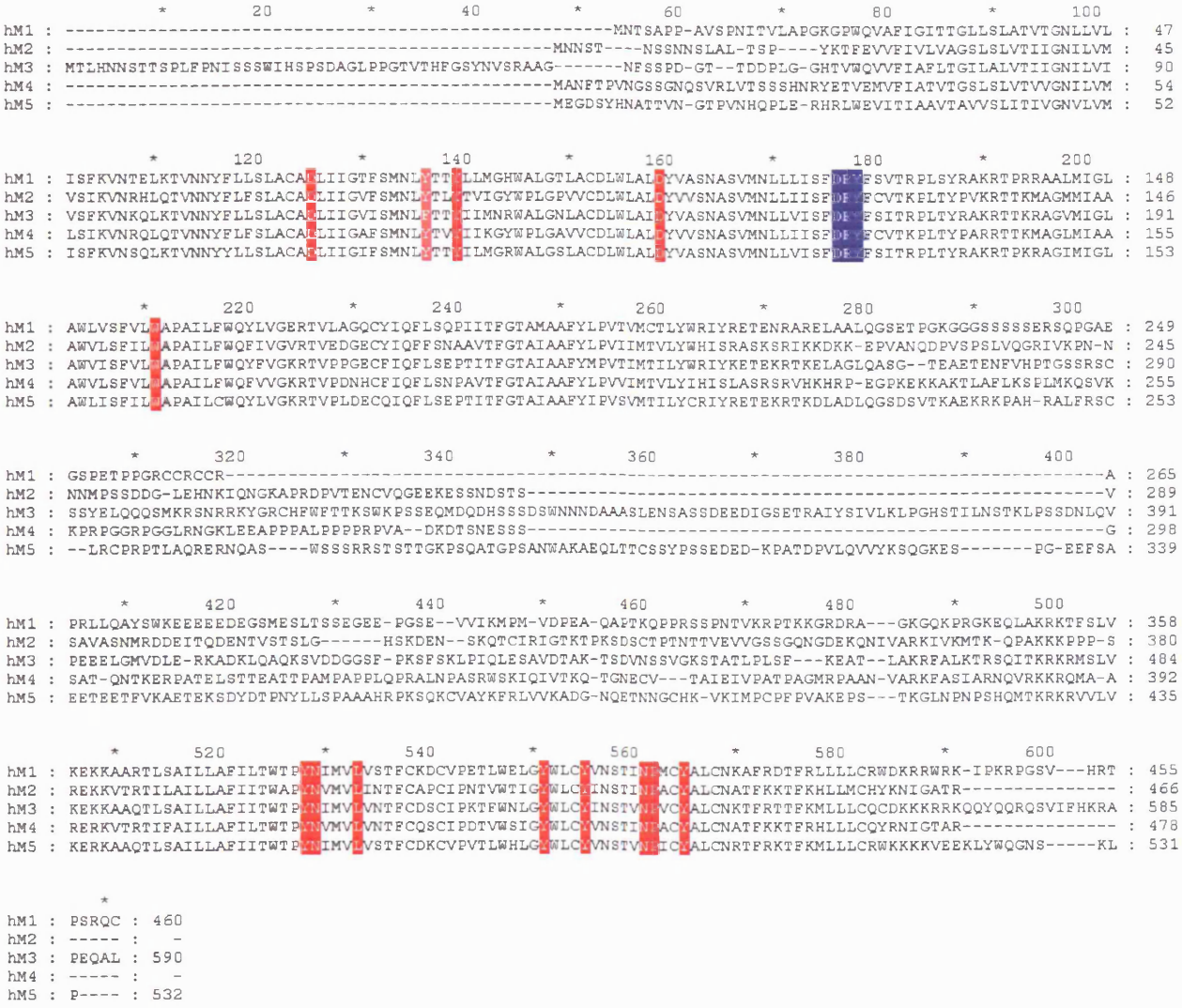

Figure 5. Alignment of the amino acid sequences of the five cloned human muscarinic acetylcholine receptors (hM_1 - M_5). Red shading indicates the residues implicated in the binding of orthosteric ligands that are fully conserved across all five subtypes; lighter shading indicates residues that are conserved in 4 out of 5 subtypes. The invariant DRY motif of family A GPCRs is labelled in blue.

(vi) Allosterism at GPCRs

The concept of allosterism was first introduced into the field of enzymology (Monod *et al.*, 1963) where enzymes were described as containing a number of topographically distinct binding sites in addition to the primary substrate binding site. The site on a GPCR analogous to the substrate binding site of an enzyme is the orthosteric site that binds the endogenous ligand for that receptor (Christopoulos *et al.*, 1998). By definition, an allosteric ligand binds to a site on a GPCR that is topographically distinct from the orthosteric site yet is able to alter orthosteric ligand binding and / or receptor function (Christopoulos & Kenakin, 2002; May *et al.*, 2004). Allosteric ligands can be agonists, antagonists or positive modulators (increasing the affinity of an agonist though lacking intrinsic agonist activity in its own right).

The most obvious allosteric modulators at GPCRs are the G proteins themselves, which bind to the intracellular domains of the receptor and can alter orthosteric ligand binding (May *et al.*, 2004). However, in terms of pharmacological manipulation and drug development, the greatest interest remains in small molecule allosteric ligands which target extracellular allosteric sites on a receptor (May *et al.*, 2004).

The simplest form of allosteric ligand - GPCR interaction involves the ligand altering the confirmation of the receptor such that the affinity of the receptor for an orthosteric ligand is changed (Christopoulos *et al.*, 1998; Christopoulos & Kenakin, 2002). This alteration in affinity can be either positive or negative i.e. the presence of the allosteric ligand can either increase or decrease the receptor affinity for an orthosteric ligand (Avlani *et al.*, 2004). The interaction is a reciprocal one, in so much as the binding at either the allosteric or orthosteric site will affect the binding at the other site in the same way and the same degree (Christopoulos *et al.*, 1998).

At their simplest, these allosteric actions are defined by a model that allows the receptor to be simultaneously occupied by two ligands, known as the allosteric ternary complex model (Figure 6; Ehlert *et al.*, 1988). This model describes the interaction between an orthosteric ligand, A, and an allosteric ligand, B, with a receptor, R. The constants K_A and K_B denote equilibrium dissociation constants for the binding of A and B, respectively, to their binding sites on the unoccupied receptor. However, these constants alone do not fully characterise allosteric interactions. The co-operativity factor, α, is a measure of the degree of co-operativity for the interaction between a given allosteric and orthosteric ligand pair at a receptor (Ehlert *et al.*, 1988; Christopoulos & Kenakin, 2002). Values of $\alpha > 1$ denote positive co-operativity whereas values of $\alpha < 1$ denote negative co-operativity; a value of $\alpha = 1$ denotes an allosteric interaction that does not alter the ligand affinity (Christopoulos & Kenakin, 2002). In contrast, values of α that approach zero are difficult to distinguish from competitive antagonism (Christopoulos *et al.*, 1998). Thermodynamically, α is the ratio of the affinity of a ligand for the occupied receptor versus the affinity of the ligand for the unoccupied receptor (Christopoulos *et al.*, 1998). There is a rapidly increasing literature on allosteric ligands acting at GPCRs, including ligands acting at the dopamine D_2 receptor (Hoare & Strange, 1996), the adenosine A_1 receptor (Bruns & Fergus, 1990) and metabotropic glutamate receptor 5 (Spooren *et al.*, 2001).

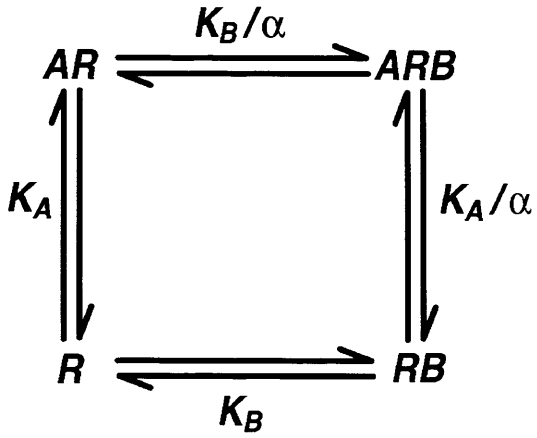

Figure 6. Simple allosteric ternary complex model. *R* denotes the receptor, *A* and *B* denote the orthosteric and allosteric ligand, respectively and K_A and K_B denote the equilibrium dissociation constants of *AR* and *BR*, respectively. The symbol α denotes the co-operativity factor and is a quantitative measure of the maximal, reciprocal alteration of affinity of *A* and *B* for their respective binding sites when both ligands bind simultaneously to form the ternary complex, *ARB*.

Unlike orthosteric ligands, allosteric ligands display some unique properties. Irrespective of its affinity for a receptor, it is theoretically possible for an allosteric ligand to display neutral ($\alpha = 1$), or close to neutral, co-operativity with all subtypes of a given receptor except the subtype of interest (May *et al.*, 2004). This property has been termed 'absolute subtype selectivity' (Lazareno *et al.*, 1998) and is a potentially powerful means of positively or negatively modulating a single subtype of a receptor family while having no net effect on the function of the other subtypes. This may well prove a route to developing novel, selective tools for receptor subtypes within families where targeting the orthosteric site has failed to deliver suitably selective agents. Such an example has been shown recently with the thiamine metabolite, thiochrome, which exerts positive co-operativity with ACh at the M_4 receptor subtype,

while having neutral co-operativity at the M_1, M_2, M_3 and M_5 receptor subtypes (Lazareno *et al.*, 2004).

The effects of allosteric modulators are also saturable; once all the allosteric sites on a receptor population are fully occupied then no further allosteric effect is observed (Christopoulos, 2002). In contrast, orthosteric competitive antagonism is theoretically, if not practically, infinite, depending as it does on the relative concentrations of the two competing molecules (Figure 7; Christopoulos, 2002). This saturation effect has been observed with both positive and negative allosteric modulators at muscarinic acetylcholine receptors. *N*-chloromethylbrucine (NCMB) is a positive allosteric modulator at the M_3 receptor subtype and produces concentration-dependent leftward shifts in concentration response curves to ACh in functional [^{35}S]GTPγS binding assays. However, there is a limit to the degree of leftward shift achievable beyond which further increases in NCMB will have no additive effect (Birdsall *et al.*, 1999). Similarly, gallamine gives a concentration-dependent rightward shift of concentration response curves to ACh evoked contractions of the guinea-pig left atrium (Christopoulos, 2000). However, as with NCMB, the effects of gallamine are saturable and reach a maximal shift beyond which further increases in the gallamine concentration have no effect. This profile results in a shallow, curvilinear Schild plot, which, if the saturation point was reached in the assay, reaches a plateau (Figure 7; Christopoulos, 2000; Christopoulos & Kenakin, 2002).

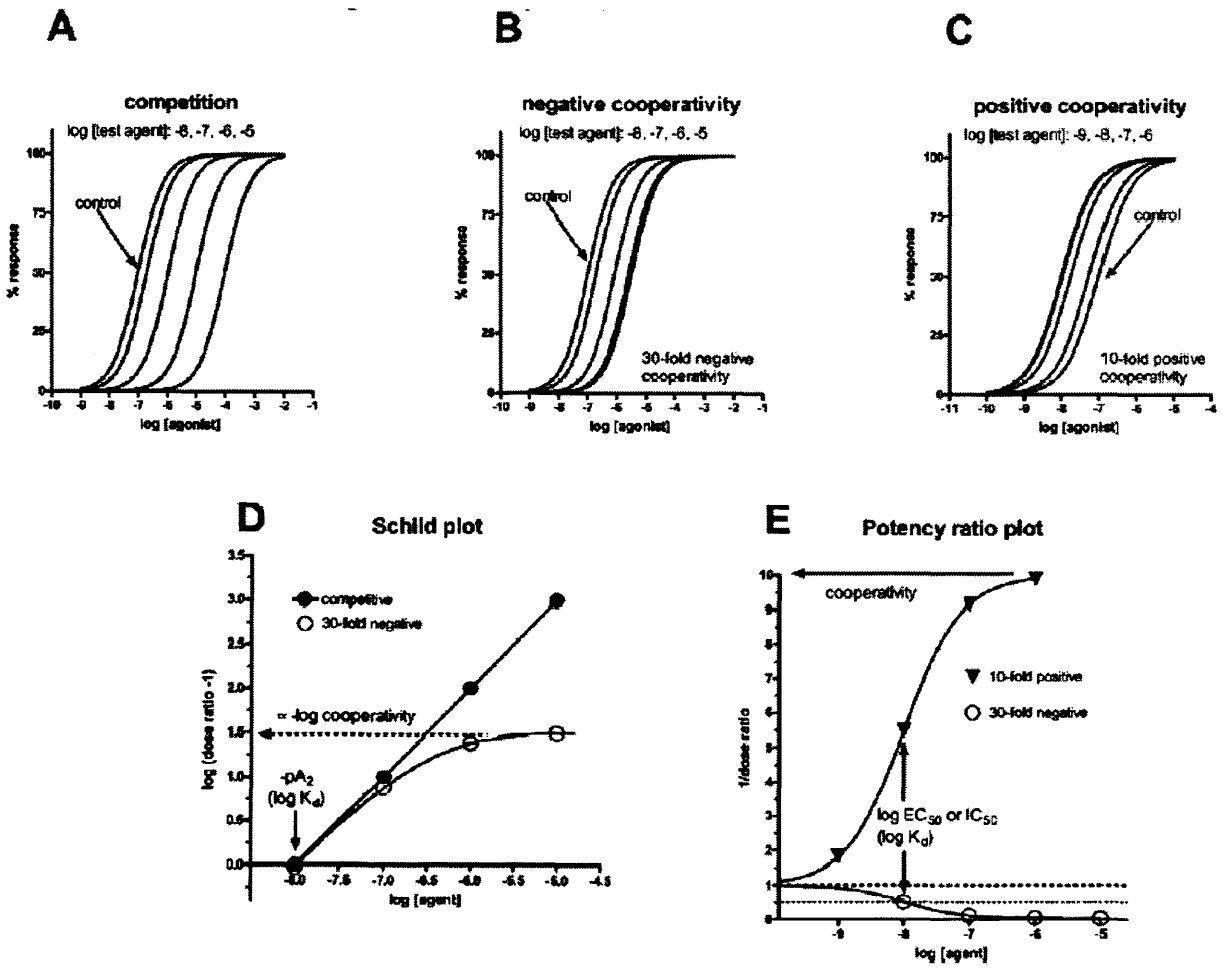

Figure 7. Analysis of concentration-response curves for a competitive inhibitor, a negative allosteric modulator and a positive allosteric modulator. Theoretical dose-response curves are shown for an agonist (EC_{50} = 100 nM) in the presence increasing concentrations of a test agent with a K_D = 10 nM, which is either (A) a competitive inhibitor, (B) a negative allosteric modulator, or (C) a positive allosteric modulator. The parallel rightward shift of the agonist curve in the presence of inhibitor is expressed as a dose-ratio (ratio of equi-effective agonist concentrations in the presence and absence of inhibitor) and the Schild plot (D) shows the log (dose-ratio –1) plotted against the log concentration of inhibitor. The Schild plot of the competitive inhibitor is a straight line with a slope of unity, whereas the Schild plot of the negative allosteric modulator curves and eventually reaches an asymptotic value, which is approximately equal to –log co-operativity (where negative co-operativity has values < 1). For both competitive and allosteric inhibitors the log concentration of

Figure 7 *cont.*

inhibitor associated with zero on the Y axis (i.e. causing a 2-fold increase in the agonist EC_{50}) is the log K_D of the inhibitor. In the affinity ratio (or potency ratio) plot (E) 1/dose-ratio is plotted against the log concentration of allosteric agent: the curves start at 1 and reach an asymptotic value equivalent to the co-operativity. For both positive and negative allosteric agents the log EC_{50} or log IC_{50} values correspond to the log K_D of the allosteric agent. Taken from Birdsall & Lazareno (2005).

In the studies with both NCMB and gallamine, the maximal degree of shift of the agonist concentration response curve seen is governed by the co-operativity factor, α, for the ligand pair. For example, a value of $\alpha = 0.1$ suggests negative co-operativity and would permit a maximal 10-fold rightward shift in the concentration response curve to the orthosteric agonist (Figure 7). Similarly, if the value of α was 10, then this would suggest positive co-operativity and permit a maximal 10-fold leftward shift in the concentration response curve to the orthosteric agonist (Figure 7; Christopoulos & Kenakin, 2002). In the studies by Christopoulos (2000), the value of α for gallamine and ACh was 0.0053, as observed by the maximal ~200-fold rightward shift in the ACh concentration response curve. If the α value cannot be derived from the concentration-response curves because the allosteric effect has not saturated (possible with very low α values) then the log (CR - 1) value on the Y-axis of the estimated plateau of the Schild plot can be taken as an estimate of log α (Figure 7, Christopoulos & Kenakin, 2002).

The saturability of effect makes allosteric ligands and their binding sites attractive drug targets. Having a limit beyond which a drug will no longer 'stimulate' or 'inhibit' a receptor system is an inherent safety device that could prevent the undesirable effects of an overdose (May *et al.*, 2004). This is seen as a clinical advantage of the benzodiazepines, which act allosterically at the $GABA_A$ receptor, compared to ligands acting directly at the GABA binding site.

It is clear that the effects of allosteric modulators can be detected functionally, as demonstrated with the studies using NCMB and gallamine already discussed (Birdsall *et al.*, 1999; Christopoulos, 2000). Visualisation of positive co-operativity is relatively straightforward, displaying a parallel leftward shift of the concentration-response curve to an orthosteric agonist. However, allosteric ligands with a high degree of negative co-operativity can appear indistinguishable from competitive

antagonists (Christopoulos & Kenakin, 2002). In this case a wide range of 'antagonist' concentrations should be used and analysis performed using the Schild equation (Arunlakshana & Schild, 1959):

$$\log (\text{concentration ratio} - 1) = \log [B] - \log K_B$$

where the concentration ratio is the equiactive concentration ratio of agonist concentrations measured alone or in the presence of an antagonist and [B] and K_B are the antagonist concentration and equilibrium dissociation constant for the receptor – antagonist complex.

A competitive interaction would be predicted to give a linear Schild plot with a slope of unity (Figure 7). However, many conditions can result in non-parallel concentration-response curves (eg. irreversible or non-competitive antagonism; Kenakin, 1997) or non-linear Schild regressions (eg. non-equilibrium conditions such as the presence of agonist removal / uptake mechanisms; Kenakin, 1997). Allosteric antagonism, as observed with the gallamine data in the guinea-pig heart (Christopoulos, 2000), can result in non-linear Schild plots. Functional assays can also be used to detect allosteric modulators by combining a second, competitive antagonist along with the 'test antagonist' and the agonist. If both antagonists are competitive then their effects should be additive i.e. the combined concentration ratio for two competitive antagonists, B and C, would be defined as follows (Paton & Rang, 1964):

$$CR_{BC} = CR_B + CR_C - 1$$

However, if one of the antagonists is allosteric, then this can produce marked deviations in this model and result in 'greater than additive' or 'less than additive' combination concentration ratios. The combination of *N*-methyl scopolamine (NMS)

and alcuronium at the muscarinic M_2 receptor produces a much greater than predicted antagonism of the carbachol mediated contractions of the guinea-pig left atrium (Lanzafame *et al.*, 1997). This confirms the allosteric nature of alcuronium and is consistent with its positive co-operativity with respect to NMS and negative co-operativity with respect to carbachol.

Equally well used to detect allosteric interactions are radioligand binding assays with orthosteric site radioligands. The most well characterised effects of allosteric ligands on radioligand binding are alteration of radioligand dissociation rate. It is the alteration of orthosteric ligand kinetics that underlies the effects of allosteric modulators on orthosteric ligand affinity (Christopoulos & Kenakin, 2002). There are a number of examples, particularly with muscarinic receptors, of allosteric ligands that can both increase (eg. amiloride at human α_{1A}-adrenergic receptor; Leppik *et al.*, 2000) and decrease (eg. gallamine at the human muscarinic M_1 receptor; Christopoulos *et al.*, 1999; Avlani *et al.*, 2004) the rate of orthosteric radioligand dissociation.

The same alteration of orthosteric radioligand affinity can be observed in saturation analysis binding studies as an apparent parallel shift in the saturation isotherm (when plotted as % specific binding versus the logarithm of the radioligand concentration; Lanzafame & Christopoulos, 2004). As with the functional studies discussed earlier, the shift is saturable and governed in its extent by the co-operativity factor, α. This change in affinity of the receptor for the orthosteric radioligand allows simple inhibition binding assays to be used to detect allosteric ligands at GPCRs (Christopoulos & Kenakin, 2002). In inhibition binding assays (often referred to as 'competition binding'), a single concentration of radioligand is used, often around 0.5 – 1 x K_D for the radioligand at the target receptor. This represents conditions designed to yield a reasonable signal-to-noise ratio without high receptor occupancy.

The presence of a negative allosteric modulator may increase the K_D of the orthosteric radiolabel and hence place the assay on a different part of the saturation binding curve (Figure 8). In these circumstances, the allosteric ligand may be unable to fully inhibit the orthosteric radioligand binding to non-specific levels (Figure 8; Christopoulos & Kenakin, 2002). Even if the negative allosteric modulator is capable of full inhibition of radioligand binding, a 10 or 100-fold increase in the radioligand concentration shifts the assay to a different part of the saturation curve and often reveals incomplete inhibition and hence the presence of allosterism (Christopoulos & Kenakin, 2002). In contrast, a competitive antagonist should, theoretically, always be able to overcome the specific binding of a radioligand. Incomplete inhibition of specific orthosteric ligand binding has been observed with a number of negative allosteric modulators, including gallamine (Stockton *et al.*, 1983) and C_7/3-phth (heptane-1,7-bis(dimethyl-3'-phthalimidopropyl)ammonium bromide; Christopoulos *et al.*, 1999). However, it must be remembered that not all negative allosteric ligands can be detected using equilibrium inhibition binding assays; neither tetra-W84 (hexane-1,6-bis[methyl-bis~3'-phthalimidopropyl] ammonium bromide) nor CPCCOEt (7-hydroxyiminocyclopropan[b]chromen-1a-carboxylic acid ethyl ester) have any effect on [^{3}H]NMS and [^{3}H]glutamate equilibrium binding at the muscarinic M_2 and metabotropic glutamate 1α receptors, respectively, despite these being receptors at which they are known allosteric ligands (Kostenis & Mohr, 1996; Litschig *et al.*, 1999). In the case of tetra-W84, allosteric effects are only observed when the compound is assessed using the dissociation rate technique described above (Kostenis & Mohr, 1996).

In contrast, the effects of an allosteric ligand with positive co-operativity are relatively easy to assess, often giving concentration-dependent potentiation of orthosteric radioligand binding, as is the case with alcuronium at the muscarinic M_2 receptor (Christopoulos, 2000).

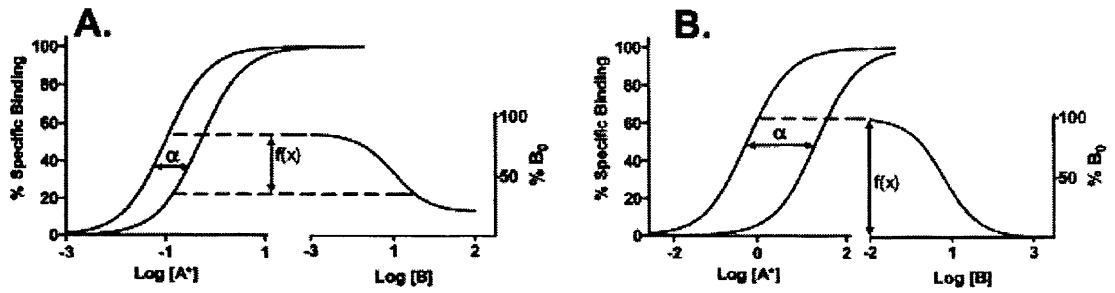

Figure 8. Inhibition of orthosteric radioligand binding by negative allosteric modulators. (A) Saturation binding curve for a radioligand shifted to the right by a maximally effective concentration of negative allosteric modulator with α = 0.2. The curve to the left of the panel shows the displacement of a defined concentration of radioligand by a range of concentrations of allosteric antagonist. Note how the displacement does not reduce the bound counts to non-specific binding levels. (B) As for A but for a more powerful negative allosteric modulator (α = 0.01). In this case, the displacement counts are reduced to non-specific binding levels. Adapted from Christopoulos & Kenakin (2002).

4. Aims of thesis research

The studies on GPR10 reported in this thesis were aimed at (a) characterising the pharmacology of PrRP and GPR10 using radioligand binding and functional assays and (b) probing the interaction between PrRP and GPR10 using site directed mutagenesis.

Whilst the binding of various radiolabelled forms of [^{125}I]-PrRP to cells stably transfected with GPR10 has been previously described (Hinuma *et al.*, 1998; Roland *et al.*, 1999), the binding of these ligands has yet to be fully characterised in terms of affinity and kinetics. The studies in Chapter 3 have fully characterised the binding of [^{125}I]-hPrRP-20 to the GPR10 receptor stably expressed in HEK293 cells (Wilson *et al.,* 1998) using saturation, inhibition and kinetic assays. Similarly, with exception of studies in rat pituitary primary cultured neurons (Kimura *et al.*, 2000), the intracellular biochemistry of GPR10 signalling has not been assessed. Functional aspects of rat and human PrRPs have also been assessed using calcium mobilisation, cAMP Flashplate technology and inositol phosphate accumulation assays in the same cell line to assess the signal transduction pathways involved after activation of GPR10.

Furthermore, several studies have sought to identify the structural components of the PrRP peptides required for binding to and activation of GPR10 (Roland *et al.*, 1999; Danho *et al.*, 2003; Boyle *et al.*, 2005). However, no complementary studies have been attempted to identify the molecular nature of the binding pocket on the GPR10 receptor for PrRP. Chapter 4 describes the construction of a homology model of the receptor based on the published crystal structure of rhodopsin, which, in turn, has allowed prediction of proposed molecular interactions between hPrRP-20 and GPR10. On this basis, site-directed mutagenesis has been carried out and mutant constructs assessed using [^{125}I]-hPrRP-20 binding and functional calcium

mobilisation to determine the validity of the model in predicting the key residues involved in PrRP-20 binding to GPR10.

Due to the lack of pharmacological tools for GPR10, which has prevented a more thorough characterisation of the receptor, the second half of the thesis has focussed on examining the pharmacology of the muscarinic M_1 receptor with particular reference to the novel, selective, 'ectopic' agonist, AC-42. The mechanism of agonist action of AC-42 at the M_1 receptor remain unknown - is the unique selectivity of this compound derived from an allosteric interaction with the receptor? Understanding of the mechanism of this compound may enable the future development of further selective agonists for this receptor subtype. Furthermore, the signal transduction pathway(s) stimulated by M_1 receptor activation with AC-42 are largely unknown. Also, there is currently little or no literature describing the effects of this novel class of agonists in native tissue preparations. In Chapter 5 these points have been addressed through a thorough pharmacological characterisation of AC-42, a closely related analogue, 77-LH-28-1 and two novel, unrelated compounds which also purport to be 'ectopic' agonists, compound A and compound B (structures undisclosed for patent reasons). Radioligand binding, functional calcium mobilisation, inositol phosphate accumulation and electrophysiological assays, in both recombinant cells and native tissue, have been used to characterise the interaction of these compounds with the M_1 receptor.

Having characterised the pharmacology of the allosteric mode of action of these agonists with the M_1 receptor, using a similar approach as with GPR10 in Chapter 4, the studies in Chapter 6 describe the construction of a homology model of the muscarinic M_1 receptor, based on the crystal structure of rhodopsin. Whilst the orthosteric site of the M_1 receptor has been well-characterised, with numerous residues implicated in the binding of ACh, carbachol and other agonists and

antagonists (Hulme *et al.*, 2003), the molecular nature of the binding site for AC-42 and other similar agonists remains unknown. The model of the human M_1 receptor and subsequent docking of AC-42 and compound A has allowed the prediction of the site(s) of interactions of these compounds with the M_1 receptor. These predictions have been assessed by both radioligand binding and functional studies with M_1 receptors containing appropriate point mutations.

Chapter 2

Methods

1. Materials

[^{3}H]NMS (81 Ci / mmol), [^{3}H]QNB (42 Ci / mmol), [^{3}H]-*myo*-inositol (86 Ci / mmol) and [^{125}I]-hPrRP-20 (2000 Ci / mmol) were from Amersham Bioscience (U.K.); [^{3}H]-oxotremorine-M (75.8 Ci / mmol) and cAMP FlashPlate kits were from NEN Life Science (U.S.A.). HEK293, HEK293-GPR10, CHO-K1 and CHO-hM_1 cell lines were cloned / subcloned in house; U2OS cells were obtained from the American Type Culture Collection. All cell culture reagents were from Invitrogen (U.K.); Accutase was obtained from PAA Labs (U.K.). All drugs and reagents were from Sigma-Aldrich (U.K.) except Complete^{TM} tablets (Roche, U.K.), [pGlu^1, Trp^2, Lys^3, Leu^4] hPrRP(25-31), substance P, neurokinin-A, Me-Phe^7-neurokinin-B, neuropeptide-Y, neuropeptide-FF (Bachem, U.K.), rat / human PrRP-20 / PrRP-31 and hPrRP(25-31) (in house), YSi-SPA beads (Amersham Bioscience, U.K.), oxotremorine-M (Tocris, U.K.), Ca^{2+}-plus, Ca^{2+}-3 and Fluo-4AM dyes (Molecular Devices, U.S.A.), NaCl, KCl, $MgCl_2$, NaH_2PO_4, $NaHCO_3$, $CaCl_2$, glucose and sucrose (BDH, U.K.) and all oligonucleotides (Sigma-Genosys Ltd., U.K.).

2. Molecular biology

(i) Plasmid construction and site-directed mutagenesis (SDM)

The construction of the mutant GPR10 and muscarinic hM_1 receptors was performed by Angela Bridges, Abby Sukman and Jim Fornwald (GlaxoSmithKline). Mutations E212A and E213A were introduced into the wild-type GPR10 sequence using the QuikChange PCR-based mutagenesis kit (Stratagene, Netherlands) according to manufacturer's instructions. Mutations Q141A (forward primer CTGGTCTTCTTCCTGGCGCCGGTCACCGTC; reverse primer GACGGTGACCGGAGCCAGGAAGAAGACCAG), E202A (forward primer CACCTATCACGTGGCGCTCAAGCCGCAC; reverse primer

GTGCGGCTTGAGCGCCACGTGATAGGTG), N298A (forward primer CGCTGCACGTCTTCGCCCTGCTGCGGGAC; reverse primer GTCCCGCAGCAGGGCGAAGACGTGCAGCG), D302A (forward primer CAACCTGCTGCGGGCCCTCGACCCCCACGC; reverse primer GCGTGGGGGTCGAGGGCCCGCAGCAGGTTG) and Q317A (forward primer CTTTGGGCTCGTCGCGCTGCTCTGCCACTG; reverse primer CAGTGGCAGAGCAGCGCGACGAGCCCAAAG) were introduced using the modified PCR method of splicing by overlap extension (PCR SOEing; Horton *et al.*, 1990). Both rounds of PCR consisted of 3 min at 95°C followed by 30 cycles of 1 min at 95°C, 1 min at 55°C and 2 min at 72°C. For both methods, the sequence of GPR10 was amplified using primers which incorporate the desired point mutations, using the wild type expression vector, pCDN-GPR10, as the template for mutagenesis.

Mutations E397A (forward primer GCAAGGACTGTGTTCCCGCGACCCTGTGGG AGCTGGG; reverse primer CCCAGCTCCCACAGGGTCGCGGGAACACAGT CCTTGC), E401A (forward primer GTTCCCGAGACCCTGTGGGCGCTGGGCTAC TGGCTGTG; reverse primer CACAGCCAGTAGCCCAGCGCCCACAGGGTCTCG GGAAC), E397A/E401A (forward primer GCAAGGACTGTGTTCCCGCGACCCT GTGGGCGCTGGGCTACTGGCTGGC; reverse primer GCACAGCCAGTA GCCCAGCGCCCACAGGGTCGCGGGAACACAGTCCTTGC) and Y82F (forward primer CCTTCTCCATGAACCTCTTTACCACGTACCTGCTC; reverse primer GAGCAGGTACGTGGTAAAGAGGTTCATGGAGAAGG) were introduced into the human M_1 receptor using the QuikChange PCR-based mutagenesis kit (Stratagene, U.S.A.) according to manufacturer's instructions. The mutation Y381A (forward primers GCCATCGAATTCGCCACCATGAACACTTCAGCCCCA and CCCTGA GTGCCATCCTCCTGGCCTTCATCCTCACCTGGACACCGGCCAACATCATGGTGC TGGTGTCCACCTTCTGCAAGGACTGTGTTCC; reverse primers GAACACAGT CCTTGCAGAAGGTGGACACCAGCACCATGATGTTGGCCGGTGTCCAGGTGAGG

ATGAAGGCCAGGAGGATGGCACTCAGGG and GAGGTGGATATCCTGGTAACC CAGGGTCCTGGGAAG) was introduced using the modified PCR method of splicing by overlap extension (PCR SOEing; Horton *et al.*, 1990). For both methods, the sequence of the human muscarinic M_1 receptor was amplified using primers which incorporate the desired point mutations. Modified baculovirus containing the mammalian cytomegalovirus promoter ('BacMam'; Ames *et al.*, 2004b) was produced using the Bac to Bac Baculovirus Expression System (Invitrogen, U.S.A.). The accuracy of all PCR-derived sequences was confirmed by dideoxy sequencing of the mutant plasmids.

3. Cell culture and transfection

(i) HEK293 and HEK293-GPR10

Human embryonic kidney 293 (HEK293) cells were routinely maintained in T80 or T175 flasks in Eagle's Modified Essential medium (EMEM) containing 10% foetal bovine serum (FBS) and 1% L-glutamine (2 mM final) at 37°C in humidified 95% air / 5% CO_2. Cells were passaged twice weekly by harvesting with either PBS or Accutase (PAA Labs) followed by centrifugation (200 x g, 5 min) and resuspension in fresh media.

HEK293 cells were passaged at 1:2 one day prior to transfection. Cells were transiently transfected with plasmids coding for the various GPR10 constructs using Lipofectamine 2000 as follows. For each T80 flask to be transfected, Optimem (2.25 ml) was mixed with 90 µl Lipofectamine 2000. In a second tube, Optimem (2.25 ml) was mixed with 15 µg cDNA. Mixtures were allowed to equilibrate for 5 minutes and then the Optimem-Lipofectamine and Optimem-cDNA mixtures combined and incubated at room temperature for 20 minutes before addition to the flask. Cells were harvested and assayed 48 h post-transfection.

(ii) CHO-hM$_1$, CHO-K1 and U2OS

CHO-hM$_1$ cells were routinely cultured in T175 flasks in Alpha MEM with ribonucleosides plus 10% foetal bovine serum (FBS). CHO-K1 wild type cells were routinely cultured in T175 flasks in Alpha MEM with ribonucleosides plus 10% FBS and 0.45 mg / ml hygromycin-B. U2OS cells (Ames *et al.*, 2004a) were routinely cultured in T175 flasks in DMEM / F12 plus 10% FBS. All cells lines were kept in humidified atmosphere at 37°C in 95% air / 5% CO_2 and passaged twice weekly by scraping in media, centrifugation (200 x g, 5 min) followed by resuspension of the pellet in fresh media.

For muscarinic M$_1$ receptor SDM constructs, recombinant BacMam virus (Ames *et al.*, 2004b) expressing the sequence of wild-type and mutated M$_1$ receptor constructs was added to cell suspensions of CHO-K1 or U2OS cells to give a final viral titre of 30 - 50 and 8 pfu. / cell, respectively. For functional calcium mobilisation assays CHO-K1 or U2OS virus-cell mixtures were then seeded into clear bottomed black walled 96-well microtitre plates (100 µl / well; Costar, U.K.) at a density of 50,000 or 25,000 cells / well, respectively. For CHO-K1 membrane preparations, virus-cell mixtures were seeded into T175 flasks at 2 x 10^8 cells per flask. Cells were assayed or harvested, as appropriate, 24h later.

4. Membrane preparation

(i) HEK293-GPR10 cell membrane preparation

Human embryonic kidney 293 (HEK293) cells either stably or transiently transfected with GPR10 were harvested with phosphate buffered saline (PBS), pelleted and stored at –80°C until further use. Membranes were prepared using a modification of the method of Miyamoto *et al.* (1994); all procedures were carried out at 4°C. Cells

were washed in 30 vols (w/v) of PBS with 0.2 mM EDTA. The suspension was homogenised using an Ultra-Turrax homogeniser and the subsequent homogenates centrifuged at 39,000 x *g* for 15 min. The resultant pellets were resuspended in 30 volumes of buffer containing 10 mM Na_2CO_3, 1 mM EDTA, 0.5 mM phenylmethylsulphonyl fluoride (PMSF), 1 μg / ml pepstatin and 1 x Complete™ serine and cysteine protease inhibitor tablet / 250 ml (pH 7.4). The suspension was then homogenised and centrifuged at 1,000 x *g* for 10 min, the supernatant decanted and centrifuged at 48,000 x *g* for 20 min. The resultant pellets were resuspended in buffer containing 20 mM Tris-HCl, 0.25 M sucrose, 2 mM EDTA, 0.5 mM PMSF, 1 μg / ml pepstatin and 1 x Complete™ serine and cysteine protease inhibitor tablet / 250 ml (pH 7.4) to a volume of approx. 0.5 - 1.2 x 10^7 cells / ml and stored at –80°C until used.

(ii) Rat cortex membrane preparation

Cerebral cortex from male Sprague Dawley rats (Charles River, U.K.) was rapidly dissected on ice; all subsequent procedures were carried out at 4°C. Tissue was homogenised using an Ultra-Turrax homogeniser in 2.5 vols (w/v) Tris-HCl (pH 7.7) and the subsequent homogenate was centrifuged at 24,000 x g for 15 min. The supernatant was discarded and the pellet resuspended in 2.5 vols fresh buffer and washed twice more before being resuspended at a protein concentration of 10 mg / ml and stored at –80°C until further use.

(iii) CHO-hM_1 and CHO-K1 cell membrane preparation

Cell membrane preparation was performed as described in Lanzafame & Christopoulos (2004); all procedures were carried out at 4°C. Stable CHO-hM_1 cells or CHO-K1 cells transiently transduced with muscarinic M_1 receptor constructs were harvested as described above. The cell pellet was resuspended in 5 ml of ice-cold

buffer containing 50 mM Tris-HCl, 3 mM $MgCl_2$ and 0.2 mM EGTA (pH 7.4) and then homogenised using an Ultra-Turrax homogeniser for 30 s. The homogenate was centrifuged at 1000 x *g* for 10 min. The remaining pellet was discarded and the supernatant was re-centrifuged at 39,000 x *g* for 30 min. The resulting cell membrane pellet was resuspended in the same buffer at protein concentrations of 2 mg / ml (CHO-hM_1) or 1 mg / ml (CHO-K1), as determined by the method of Bradford (Bradford, 1976). Aliquots were stored at –80°C until further use.

5. Radioligand binding studies

(i) HEK293-GPR10 [^{125}I]-hPrRP-20 saturation binding assays

HEK293-GPR10 cell membranes (400 µl; 4 µg protein / well) were incubated in a total volume of 0.5 ml with assay buffer (50 µl) containing 20 mM Tris-HCl, 5 mM Mg-acetate, 2 mM EGTA, 0.5 mM PMSF, 1 µg / ml pepstatin and 1 x Complete™ serine and cysteine protease inhibitor tablet 250 / ml and 0.1 % (w/v) BSA (pH 7.4) and varying concentrations of [^{125}I]-hPrRP-20 (50 µl; 10 pM – 20 nM) at 25°C for 90 min. Non-specific binding was defined as that remaining in the presence of 0.1 µM rat PrRP-31. The reaction was terminated by rapid filtration through Whatman GF/B filter mats pre-soaked in 1 % PEI using a 48-well Brandel cell harvester (Semat, U.K.) Filters were washed with 5 x 1 ml ice-cold harvest buffer containing 50 mM Tris-HCl, 10 mM $MgCl_2$ (pH 7.4) and allowed to dry before bound radioactivity was measured by gamma counting. Specific binding data were analysed using the program Radlig (Biosoft, U.K.) to provide estimates of K_D and B_{max} values (Appendix 1). Protein content was assayed using the Bradford method (Bradford, 1976) using bovine serum albumin (BSA) as a standard. Results are presented as means (± s.e.m.) of at least 3 independent experiments.

(ii) HEK293-GPR10 [^{125}I]-hPrRP-20 inhibition binding assays

Inhibition binding studies were performed by incubating HEK293-GPR10 cell membranes (400 µl; 2 µg protein / well) with [^{125}I]-hPrRP-20 (50 µl; 0.2 nM) and a range of concentrations of the test compound (50 µl) at 25°C for 90 min. The final assay volume was 0.5 ml. Compounds were serially diluted in assay buffer (158 µl compound + 342 µl buffer, equivalent to 0.5 log) to give 10 different test concentrations over a 5 log unit range using either the Biomek FX (Beckam Coulter, U.S.A.) or Tecan Genesis (Tecan, U.K.) liquid handling systems. Buffer composition, non-specific binding determination, reaction termination and radioactivity determination were all as for HEK293-GPR10 saturation binding. Inhibition curves were analysed by non-linear least-squares fitting to a four parameter logistic equation (equation 1; Appendix 1) in Microsoft Excel in order to determine IC_{50} values (Bowen & Jerman, 1995).

$$Y = Bottom + \frac{Top - Bottom}{1 + 10^{(\log IC_{50} - X).n_H}}$$

Top and *Bottom* represent the maximal and minimal asymptotes of the curve, IC_{50} is the concentration of compound required to inhibit 50 % of specific radioligand binding and n_H is the Hill slope. K_i values were then derived from the IC_{50} values using a K_D value of 0.1 nM to take into account binding to both high (K_D = 0.03 nM) and low (K_D = 0.6 nM) affinity binding sites (equation 2; Appendix 1; Cheng & Prussoff, 1973):

$$K_i = \frac{IC_{50}}{1 + \frac{[L]}{K_D}}$$

Where K_i is the inhibition constant for the competing ligand, K_D is the dissociation constant for the radioligand (concentration required to occupy 50 % of specific

binding sites) and *[L]* is the radioligand concentration. Protein content was assayed as for saturation binding. Results are presented as means (± s.e.m.) of at least 3 independent experiments.

(iii) [^{125}I]-hPrRP-20 radioligand kinetic binding assays

Association kinetic studies were performed by measuring triplicate determinations total and non-specific binding of [^{125}I]-hPrRP-20 (50 µl; 0.2 nM) at various time points after the addition of HEK293-GPR10 cell membranes (400 µl; 2 µg protein / well). The final assay volume was 0.5 ml. Buffer composition, total and non-specific binding determination, reaction termination and radioactivity determination were all as for HEK293-GPR10 saturation binding.

For dissociation studies, HEK293-GPR10 cell membranes (400 µl; 2 µg protein / well) were pre-incubated with [^{125}I]-hPrRP-20 (50 µl; 0.2 nM) and either assay buffer (50 µl) or rat PrRP-31 (50 µl; 0.1 µM final) for 90 min in a final assay volume was 0.5 ml. Triplicate determinations of total and non-specific binding of [^{125}I]-hPrRP-20 as defined above were then measured at various time points after the addition of 50 µl 1.1 µM rat PrRP-31 (0.1 µM final). Buffer composition, reaction termination and radioactivity determination were all as for HEK293-GPR10 saturation binding. Kinetic data were analysed by GraFit (Erithacus Software) to provide estimates of k_{on} and k_{off} values (Appendix 1). Results are presented as means (± s.e.m.) of at least 3 independent experiments.

(iv) Rat cortex [^{3}H]QNB inhibition binding assays

Inhibition binding studies were performed by incubating rat cortical membranes (400 µl; 8 µg protein / well) with [^{3}H]QNB (50 µl; 0.3 nM) and a range of concentrations of

the test compound (50 µl) at 37°C for 40 min in buffer containing 50 mM Tris-HCl (pH 7.7). The final assay volume was 0.5 ml. Compounds were serially diluted in Tris-HCl buffer (158 µl compound + 342 µl buffer, equivalent to 0.5 log) to generate 10 different test concentrations over a 5 log unit range using either the Biomek FX (Beckam Coulter, U.S.A.) or Tecan Genesis (Tecan, U.K.) liquid handling systems. Non-specific binding was defined as that remaining in the presence of 1 µM atropine. The reaction was terminated by rapid filtration through GF/B filter mates pre-soaked in 0.05 % PEI using a 48-well Brandel cell harvester (Semat, U.K.) Filters were washed with 5 x 1 ml ice-cold 50 mM Tris-HCl (pH 7.7) and allowed to dry before bound radioactivity was measured using liquid scintillation counting with Ultima Gold MV scintillant (Perkin Elmer, U.K.). Inhibition curves were analysed by non-linear least-squares fitting to a four parameter logistic equation by Microsoft Excel in order to determine IC_{50} values (equation 1; Bowen & Jerman, 1995). K_i values were then derived from the IC_{50} values using the K_D value of 0.3 nM (equation 2; Appendix 1; Cheng & Prussoff, 1973). Results are presented as means (± s.e.m.) of at least 3 independent experiments.

(v) Rat cortex [^{3}H]oxotremorine-M inhibition binding assays

Inhibition binding studies were performed by incubating rat cortical membranes (400 µl; 100 µg protein / well) with [^{3}H]oxotremorine-M (50 µl; 1.9 nM) and a range of concentrations of the test compound (50 µl) at 37°C for 40 min in buffer containing 50 mM Tris-HCl and 2 mM $MgCl_2$ (pH 7.7). The final assay volume was 0.5 ml. Compounds were serially diluted in Tris-HCl buffer (158 µl compound + 342 µl buffer, equivalent to 0.5 log) to generate 10 different test concentrations over a 5 log unit range using either the Biomek FX (Beckam Coulter, U.S.A.) or Tecan Genesis (Tecan, U.K.) liquid handling systems. Non-specific binding was defined as that remaining in the presence of 10 µM oxotremorine sesquifumarate. The reaction was

terminated by rapid filtration through GF/B filter mates pre-soaked in 0.05 % PEI using a 48-well Brandel cell harvester (Semat, U.K.) Filters were washed with 5 x 1 ml ice-cold 50 mM Tris-HCl (pH 7.7) and allowed to dry before bound radioactivity was measured using liquid scintillation counting with Ultima Gold MV scintillant. Inhibition curves were analysed by non-linear least-squares fitting to a four parameter logistic equation by Microsoft Excel in order to determine IC_{50} values (equation 1; Bowen & Jerman, 1995). K_i values were then derived from the IC_{50} values using the K_D value of 3 nM (equation 2; Cheng & Prussoff, 1973). Results are presented as means (± s.e.m.) of at least 3 independent experiments.

(vi) CHO-hM$_1$ [^{3}H]NMS saturation binding assays

CHO-hM$_1$ cell membranes (400 µl; 10 µg protein / well) were incubated in a total volume of 0.5 ml with assay buffer (50 µl) containing 50 mM HEPES, 110 mM NaCl, 5.4 mM KCl, 1.8 mM $CaCl_2$, 1 mM $MgSO_4$, 25 mM glucose and 58 mM sucrose (pH 7.4) and varying concentrations of [^{3}H]*N*-methyl-scopolamine (NMS; 50 µl; 5 pM – 10 nM) at 37°C for 1 h. Non-specific binding was defined as that remaining in the presence of 1 µM atropine. The reaction was terminated by rapid filtration through GF/B filter mates pre-soaked in ddH_2O using a 48-well Brandel cell harvester (Semat, U.K.) Filters were washed with 5 x 1 ml ice-cold 0.9 % (w/v) NaCl solution and allowed to dry before bound radioactivity was measured using liquid scintillation counting with Ultima Gold MV scintillant. Specific binding data were analysed using GraphPad Prism (GraphPad, U.S.A.) to provide estimates of K_D and B_{max} values (Appendix 1). Protein content was assayed using the Bradford method (Bradford, 1976) using bovine serum albumin (BSA) as a standard.

(vii) CHO-hM$_1$ [^{3}H]NMS inhibition binding assays

Inhibition binding studies were performed by incubating CHO-hM$_1$ cell membranes (400 µl; 10 µg protein / well) with [^{3}H]NMS (50 µl; 0.2 nM or 2 nM) and a range of concentrations of the test compound (50 µl) at 37°C for 1 h. The final assay volume was 0.5 ml. Compounds were serially diluted in assay buffer (158 µl compound + 342 µl buffer, equivalent to 0.5 log) to give 10 different test concentrations over a 5 log unit range using either the Biomek FX (Beckam Coulter, U.S.A.) or Tecan Genesis (Tecan, U.K.) liquid handling systems. Buffer composition, non-specific binding determination, reaction termination and radioactivity determination were all as for CHO-hM$_1$ saturation binding.

Data for inhibition curves at 0.2 nM and 2 nM radioligand were analysed simultaneously using the following equation (3) in Prism 4 (GraphPad, U.S.A.):

$$\frac{Y}{Y_{max}} = \frac{[A]}{[A] + K_A \cdot \left(\frac{K_B + [B]}{K_B + [B]/\alpha} \right)}$$

where Y/Y_{max} represents fractional receptor occupancy, $[A]$ and $[B]$ represent the concentrations of radioligand and allosteric ligand, K_A and K_B represent equilibrium dissociation constants of the radioligand and allosteric ligand for the unoccupied receptor and α represents the co-operativity factor between the two ligands. For each series of inhibition curves, the negative logarithm of the K_A value for [^{3}H]NMS was fixed at 9.6, and the K_B and α parameters were constrained to be shared across both curves. Results are presented as means (± s.e.m.) of at least 3 independent experiments.

(viii) CHO-K1 [^{3}H]NMS inhibition binding assays

Inhibition binding studies were performed by incubating membranes from CHO-K1 cells transiently expressing muscarinic M_1 receptor SDM constructs (400 µl; 10-20 µg protein / well) with [^{3}H]NMS (50 µl; 0.2 nM) and a range of concentrations of the test compound (50 µl) at 37°C for 1 h. The final assay volume was 0.5 ml. Compounds were serially diluted in assay buffer (100 µl + 900 µl buffer) to give 6 different test concentrations over a 6 log unit. Buffer composition, non-specific binding determination, reaction termination and radioactivity determination were all as for CHO-hM_1 saturation binding. Inhibition curves were analysed by non-linear least-squares fitting to a four parameter logistic equation (equation 1; GraphPad Prism v4, GraphPad) in order to determine IC_{50} values. K_i values were then derived from the IC_{50} values using the K_D value determined from saturation studies (equation 2; Appendix 1; Cheng & Prussoff, 1973). Results are presented as means (± s.e.m.) of at least 3 independent experiments.

(ix) CHO-hM_1 [^{3}H]NMS kinetic binding assays

Association kinetic studies were performed by measuring triplicate determinations of total and non-specific binding of [^{3}H]NMS (50 µl; 0.2 nM) at various time points after addition of CHO-hM_1 cell membranes (400 µl; 10 µg protein / well). The final assay volume was 0.5 ml. Buffer composition, total and non-specific binding determination, reaction termination and radioactivity determination were all as for CHO-hM_1 saturation binding.

For dissociation studies, CHO-hM_1 cell membranes (400 µl; 10 µg protein / well) were pre-incubated with [^{3}H]NMS (50 µl; 0.2 nM) and either assay buffer (50 µl) or atropine (50 µl; 1 µM final) for 60 min in a final assay volume was 0.5 ml. Triplicate

determinations of total and non-specific binding of [^{3}H]NMS as defined above were then measured at various time points after the addition of 50 µl 11 µM atropine (1 µM final) either in the presence or absence of AC-42 (100 µM final), compound A (100 µM final) or gallamine (1 mM final). Buffer composition, reaction termination and radioactivity determination were all as for CHO-hM$_1$ saturation binding.

Dissociation curves were described by a monoexponential function according to the equation (4):

$$B_t = B_o \cdot e^{-k_{off_{obs}} \cdot t}$$

where for allosteric interactions k_{offobs} is described by the following equation (5):

$$k_{off_{obs}} = \frac{[B] \cdot k_{offB} / \alpha \cdot K_B + k_{off}}{1 + [B] / \alpha \cdot K_B}$$

In the above equations, B_t denotes bound radioligand at time t after dissociation has started, B_o denotes bound radioligand at equilibrium, k_{offobs} denotes the observed radioligand dissociation constant, k_{off} denotes the rate constant for dissociation from the free (unoccupied) receptor, k_{offB} is the rate constant from the allosteric ligand occupied receptor, [B] is the concentration of allosteric ligand and αK_B is the dissociation constant of the allosteric ligand for the radioligand occupied receptor. Note that in the absence of allosteric modulator, k_{offobs} is equal to k_{off}.

6. Signal transduction studies

(i) FLIPR calcium mobilisation assays

Intracellular calcium was monitored using the wash-free fluorescent dyes Calcium-Plus (CHO-hM$_1$ cells), Calcium-3 (U2OS and CHO-K1 cells). Calcium-3 was preferred for U2OS and CHO-K1 cells as this dye is more sensitive than Calcium-

Plus to excitation at 488 nm and a lower level of receptor expression was anticipated in transiently transduced cells. The high level of receptor expression and efficiency of coupling in CHO-hM_1 cells allowed use of the less sensitive Calcium-Plus dye. Fluo 4AM, a fluorescent dye that requires a wash step, was used for studies with HEK293-GPR10 cells as previous studies with this cell line had utilised this dye. All calcium studies were carried out using a Fluorometric Imaging Plate Reader (FLIPR, Molecular Devices, U.K.). Calibration of the FLIPR for calcium measurements was carried by measuring fluorescence evoked by the dye with the addition of a calcium ionophore in the presence (F_{max}) and absence (F_{min}) of extracellular calcium (1.8 mM). Changes in fluorescence measured experimentally (F) were directly proportional to the intracellular calcium concentration:

$$[Ca^{2+}] = K_D \cdot (F - F_{min}) / (F_{max} - F)$$

where K_D is the affinity of the dye used for calcium ions. For both Fluo-4AM and Calcium-3, the K_D = 345 nM; for Calcium-Plus the K_D = 390 nM.

HEK293 cells transiently expressing GPR10 (100 µl) were seeded in clear bottomed, black walled poly-D-lysine coated 96-well microtitre plates (Costar, U.K.) 24 hours before use at a density of 52,000 cells / well. Prior to assay on FLIPR, cells were incubated with Fluo 4AM (1 µM) for 60 minutes at 37°C in Hank's buffered saline solution containing 0.1% BSA (w/v) and 2.5 mM probenicid. Extracellular dye was then removed by washing three times with 150 µl Hank's buffered saline solution containing 2.5 mM probenicid without BSA using a Skatron 96-way plate washer.

Where tested, signal transduction inhibitors (25 µl) were incubated with the cells for 30 min at 37°C prior to agonist addition. Compounds were tested for agonist activity in FLIPR by adding 50 µl of test solution to a plate volume of 150 µl at 37°C and the

fluorescence was monitored (λ_{ex} = 488 nm, λ_{EM} = 540 nm) before and after the addition of agonist at 1 s intervals for 60 s and at 5 s intervals for a further 60 s.

CHO-hM_1 and CHO-K1 cells (100 µl) were seeded into clear bottomed black walled 96-well microtitre plates (Costar, U.K.) 24 hours before use at a density of 50,000 cells / well. U2OS cells (100 µl) were seeded at a density of 25,000 cells / well. Prior to assay on FLIPR, medium was removed and cells were incubated with Calcium Plus or Calcium-3 wash-free dye according to manufacturer's instructions for 60 minutes at 37°C in Tyrode's buffer (145 mM NaCl, 2.5 mM KCl, 1.2 mM $MgCl_2$, 10 mM Na-HEPES, 10 mM glucose, 1.5 mM $CaCl_2$; pH 7.4) containing 2.5 mM probenicid. For agonist studies, compounds were tested for activity in FLIPR by adding 50 µl of test solution to a plate volume of 50 µl (final assay volume 100 µl). For antagonist studies, cells were pre-incubated with antagonist / buffer (50 µl), as appropriate, for 30 min prior to agonist addition on the FLIPR (50 µl; final assay volume 150 µl). Fluorescence was monitored as for HEK293-GPR10 cells.

Peak stimulation minus basal was plotted versus concentration of test compound and iteratively curve fitted using a four parameter logistic equation (equation 6; GraphPad Prism v4, GraphPad) to assess agonist potency and maximal response.

$$Y = Bottom + \frac{Top - Bottom}{1 + 10^{(\log EC_{50} - X).n_H}}$$

Where *Top* and *Bottom* represent the maximal and minimal asymptotes of the curve, EC_{50} is the concentration of agonist required to stimulate 50% of the maximal response and n_H is the Hill slope.

Where appropriate concentration-response curves to agonist in the presence and absence of antagonist were analysed using a global allosteric model (Motulsky & Christopoulos, 2004) according to the following equation (7):

$$\log(CR-1) = \log\left(\frac{[B]\cdot(1-\alpha)}{\alpha\cdot[B]+K_B}\right)$$

where *CR* is the concentration ratio (the ratio of equiactive agonist concentrations obtained in the absence or presence of antagonist), [*B*] is the concentration of antagonist, K_B is the dissociation constant of the antagonist for the receptor and α represents the allosteric co-operativity factor between the two ligands.

(ii) Inositol phosphate accumulation scintillation proximity assays (SPA)

Inositol phosphate accumulation scintillation proximity assays (IP-SPA) were carried out as described in Brandish *et al.* (2003) with minor modifications. This assay methodology utilises SPA technology to discriminate between negatively charged inositol phosphates and parental inositol. Cell derived negatively charged [^{3}H] inositol phosphates bind to the positively charged yttrium silicate beads and are in sufficient proximity to the scintlillant contained therein to emit a signal that can be detected by scintillation spectroscopy. Inositol lacks a negative charge and therefore remains free in the solution where it cannot excite the scintillant.

HEK293 cells transiently expressing GPR10 or CHO-hM$_1$ cells (100 µl) were seeded into clear bottomed black walled 96-well microtitre plates (Costar, U.K.; poly-D-lysine coated for HEK293-GPR10 cells) at a density of 50,000 cells / well. After 24 h the cell medium was removed and replaced with 200 µl inositol-free (IF) DMEM containing 5 µCi / ml [^{3}H]-*myo*-inositol (Amersham, U.K.). After 16 h, the [^{3}H]-*myo*-inositol was removed and the cells washed with 2 x 200 µl IF-DMEM. Cells were then incubated with 100 µl agonist (made up in media) and 100 µl antagonist or media in IF-DMEM

containing 5 mM LiCl for 1 h at 37°C. The reaction was terminated by the removal of the medium and the addition of 200 µl 0.1 M formic acid (Sigma Aldrich, U.K.). The cell solubilisation was allowed to continue for 1 h at room temperature after which 20 µl samples of the lysates were removed from each well and combined with 80 µl RNA binding yttrium silicate SPA beads (12.5 mg / ml) in a opaque bottomed 96-well picoplates (Packard, U.K.). Plates were agitated for 1 h at room temperature and then the beads left to settle for 2 h. The accumulation of negatively charged [^{3}H] inositol phosphates (IP_4, IP_3, IP_2 and IP_1) was determined on the TopCount plate counter (Packard, U.K.).

[^{3}H]IP_X accumulation (cpm) was plotted versus concentration of test compound and iteratively curve fitted using a four parameter logistic equation (equation 6; GraphPad Prism v4, GraphPad) to assess agonist potency and maximal response. Where appropriate, data analysis for allosteric interactions was carried out as for calcium mobilisation studies (equation 7).

(iii) Cyclic AMP FlashPlate assays

Cyclic AMP assays were performed by Jon Chambers (GlaxoSmithKline). Intracellular cAMP levels were determined using FlashPlate technology (Watson *et al.*, 1998). This technique is a 96-plate based radioimmunoassay, relying on the competition of tracer [^{125}I]cAMP and cell-derived cAMP for anti-cAMP antibody bound to scintlillant-coated wells in a 96-well microtitre plate. Only cAMP bound to antibody is sufficiently proximal to the scintillant to emit light to be detected by scintillation spectroscopy.

HEK293-GPR10 cells (50 µl) were dispensed into 96-well FlashPlates (50,000 cells / well) at 37°C and incubated with 0.5 mM isobutylmethylxanthene (IBMX) for 15

minutes before human PrRP-20 and / or forskolin (30 μM) were added simultaneously to a final volume of 100 μl. After 15 minutes the incubation was terminated with 100 μl detection buffer containing a cell lysis agent proprietary to Perkin Elmer and tracer [^{125}I]cAMP (16.5 nCi / well). Plates were incubated at 25°C for 2 h and then counted in a TopCount scintillation counter (Packard, U.K.) to determine anti-cAMP bound radioactivity. Cyclic AMP levels were calculated by comparison with a standard cAMP curve.

7. Homology modelling and ligand docking

(i) Nomenclature

Amino acid residues of specific receptor subtypes are described using the single letter amino acid code followed by the number of the residue in the receptor eg. Y381. Where a residue is being described as conserved across a number of GPCRs, the Ballesteros-Weinstein nomenclature is used. This describes residues using the three letter amino acid code, followed by the TM domain in which the residue is found and its position with reference to the most conserved residue in the same helix, this being designated position 50 eg. Arg 3.50.

Amino acid residues in peptides are described using the three letter amino acid code to distinguish from residues in the receptor, followed by the numerical position of the residue in the peptide eg. Arg^{6}.

(ii) Construction of the GPR10 and muscarinic M_1 receptor homology models

Homology modelling was performed by Frank Blaney and Ben Tehan (GSK).
The initial model of the TM domain of the human GPR10 and M_1 receptors was constructed by homology with the published X-ray crystal structure of bovine

rhodopsin (Palczewski *et al.*, 2000). Alignment between the GPR10, hM_1 sequences and bovine rhodopsin was based on the 'classical' motifs found in each TM region. These were the asparagine in TM1 (Asn 1.50, Ballesteros-Weinstein notation), the aspartate in TM2 (Asp 2.50), the 'DRY' motif (ERY in rhodopsin) of TM3 (Asp 3.49, Arg 3.50, Tyr 3.51), the tryptophan in TM4 (Trp 4.50), and the conserved prolines in TM5 (Pro 5.50), TM6 (Pro 6.50) and TM7 (Pro 7.50). These alignments were used, with the standard homology modelling tools in the Quanta program (Accelrys, La Jolla, CA) to construct the seven helical bundle domain of GPR10 and the hM_1 receptor.

The extracellular loop regions of the receptors were subsequently added using a procedure developed at GlaxoSmithKline, which makes use of a combined distance geometry sampling and molecular dynamics simulation (Blaney *et al.*, 2001). The side chains of this model were then refined using the Karplus standard rotamer library (Dunbrack & Karplus, 1993). The final model was optimised fully (500 steps of Steepest Descent (SD) followed by 5000 steps of Adopted Basis Newton Raphson (ABNR)) with the CHARMm force field (Accelrys, La Jolla, CA) using helical distance constraints between the *ith* and *i+4th* residues (except proline) within a range of 1.8Å-2.5Å, to maintain the backbone hydrogen bonds of the helix bundle.

(iii) Ligand docking studies

Human PrRP(25-31) (GPR10) and AC-42 (hM_1 receptor) were docked into the receptor models manually using a variety of low energy starting conformations. Adjustments of the receptor protein side chains were made where necessary, always ensuring that these side chains were only in allowed rotameric states (Dunbrack & Karplus, 1993). Once again, full optimisation of the receptor-ligand complexes was performed using CHARMm, the only constraints used being those which maintained

the hydrogen bonding pattern of the helical bundle. This procedure allows full relaxation of both the ligand and the whole protein, something which is not possible with automated docking procedures. From the initial low energy starting conformations, typically between 4 and 12 docking configurations were found to be possible. Binding orientations were assessed by calculating the approximate free energy of the receptor-ligand complex as a sum of the various electrostatic and van der Waals forces between each residue and the ligand. One docked orientation of hPrRP(25-31) in GPR10 and of AC-42 in the hM_1 receptor was particularly favoured (lowest overall binding energy) and this was used as the basis for [pGlu^1, Trp^2, Lys^3, Leu^4] hPrRP(25-31) docking into GPR10 and compound A in the hM_1 receptor.

8. Electrophysiology

(i) Network oscillations in rat temporal cortex

The studies described below were performed whilst on a collaborative placement with Prof. Miles Whittington and Anita Roopun in the Department of Biomedical Sciences, University of Leeds.

Experiments were performed using slices from young adult male Wistar rats, aged between 42 and 70 days, weighing approximately 150 g. All procedures were in accordance with the regulations stipulated in the UK Animals (Scientific Procedures) Act, 1986. Rats were euthanased with an overdose of isofluorane and the brain rapidly dissected out into ice-cold oxygenated sACSF (containing, in mM, 252 sucrose, 3 KCl, 1.25 NaH_2PO_4, 2 $MgSO_4$, 2 $CaCl_2$, 24 $NaHCO_3$ and 10 glucose). 400 μm thick coronal sections of brain tissue were cut using a Leica VT1000 vibratome and transferred to an interface chamber. Slices were maintained at 34°C at the interface between circulating oxygenated ACSF (flow rate 1-2 ml / min; containing, in mM, 126 NaCl, 3 KCl, 1.25 NaH_2PO_4, 1 $MgSO_4$, 1.2 $CaCl_2$, 24 $NaHCO_3$ and 10

glucose) and humidified 95% O_2 / 5% CO_2. Brain slices were left to equilibrate for 1 h before the onset of recording.

Extracellular recordings from temporal cortex were obtained using glass micropipettes pulled from thin walled borosilicate tubing (1.2mm outer diameter x 0.94 mm inner diameter), (Harvard Apparatus Ltd, Kent, UK) containing an inner filament, using a P-97 Flaming/Brown type horizontal puller (Sutter Instruments Co., U.S.A.). Micropipettes were filled with ACSF (resistance 2 - 5 MΩ).

Data were recorded in current-clamp mode, and amplified by an Axoclamp-2A amplifier (X10 Axon instruments Inc., U.S.A.) and a Neurolog AC-DC preamplifier (Digitimer Ltd.). Extracellular data were band pass filtered at 0.002 - 0.42 kHz. Mains supply noise (50 Hz) was eliminated from the raw signal by Humbugs (Quest Scientific Instruments Inc., Canada). Data were redigitised at 10 kHz by an Instutech ITC-16 A/D board (Instutech Corp., U.S.A.) and stored on an AppleMac Power G4 computer using AxoGraph 4.6 software (Axon Instruments) for off-line analysis.

The behaviour and properties of network oscillations were determined by calculating the power spectra of network activity by performing Fast-Fourier Transforms (FFTs) on 60 s worth of activity. Due to the variation in the peak frequencies between experiments the power of gamma oscillations in the frequency range 30 – 80 Hz was calculated. This quantitative measure of oscillatory strength was generated by using AxoGraph 4.6 to calculate the area under the spectra in this frequency range.

Chapter 3

Pharmacological characterisation of GPR10

(i) Introduction

In the original paper identifying PrRP as the ligand for GPR10, [^{125}I]-bovine PrRP-31 was shown to bind to membranes from CHO cells stably expressing both GPR10 and the rat orthologue, UHR-1 (GPR10 and UHR-1 share 90% homology at the amino acid level). [^{125}I]-bovine PrRP-31 bound with high affinity and almost identical K_D values of 26 and 25 pM to GPR10 and UHR-1, respectively (Hinuma *et al.*, 1998). Binding to both GPR10 and UHR-1 appeared to be monophasic, although the levels of specific binding were only defined by five data points and did not appear to fully saturate at up to approximately 30 nM ligand. A similar radioligand binding study with [^{125}I]-human PrRP-31 in membranes from CHO-K1 cells stably expressing GPR10 suggested that the radioligand bound to GPR10 in a monophasic fashion, although with a substantially higher K_D value of approximately 1 nM (Roland *et al.*, 1999). The same authors also described specific [^{125}I]-human PrRP-31 binding to the reticular thalamic nucleus and to a lesser extent to the periventricular hypothalamus in coronal sections of rat brain. No other regions displayed any specific binding. These data may reflect a very specific localisation of UHR-1 or, more likely, a low level of expression of UHR-1 in regions other than the thalamus and hypothalamus beyond detection in this paradigm. Satoh *et al.* (2000) have also demonstrated [^{125}I]-human PrRP-31 binding in rat native tissue. [^{125}I]-human PrRP-31 displayed specific binding in membranes from hypothalamus, medulla, cerebellum, pituitary, heart, soleus muscle, adipose tissue, kidney, adrenal gland, testis and small intestine. Highest levels of specific binding were observed in hypothalamus (50%), heart (46%), soleus muscle (45%) and pituitary (44%), where inhibition binding studies with [^{125}I]-human PrRP-31 suggested IC_{50} values for unlabelled PrRP-31 of 5.2, 6.6, 9.8 and 1.4 nM, respectively. These data are largely in agreement with the affinity of [^{125}I]-human PrRP-31 for CHO cells stably expressing GPR10 (Roland *et al.*, 1999), although

substantially lower than the affinity of [^{125}I]-bovine PrRP-31 binding to UHR-1 (Hinuma *et al.*, 1998).

Studies in rat heart and hypothalamus also suggested rapid kinetics for the binding of [^{125}I]-human PrRP-31, with equilibrium being reached within 5 minutes at 4°C and stable for up to 90 min, although not for longer than 30 min at room temperature (Satoh *et al.*, 2000). Isotopic dilution induced dissociation at 4°C was initially rapid, though appeared biphasic with a much slower rate resulting in only 90 % and 70 % of [^{125}I]-human PrRP-31 specific dissociation being complete after 60 min in heart and hypothalamic membranes, respectively (Satoh *et al.*, 2000).

The signal transduction pathways for GPR10 have not yet been fully characterised, although there are a number of studies that have suggested signalling pathways through which GPR10 may couple. In the initial report describing PrRP as the ligand for GPR10, PrRP was claimed to induce intracellular calcium influx in cells stably expressing GPR10 (Hinuma *et al.*, 1998). Furthermore, PrRP-31 stimulates calcium mobilisation in both HEK293 and CHO cells expressing GPR10 in the absence of any co-expressed promiscuous G protein with potencies in the 1 – 2 nM range (Wilson *et al.*, 1998; Boyle *et al.*, 2005; Bhattacharyya *et al.*, 2003; Roland *et al.*, 1999). These data suggest that GPR10 may be signalling through the $G_{q/11}$ pathway to stimulate PLC and intracellular calcium mobilisation in these assay systems.

However, in a study in both GH3 rat pituitary cells and primary cultures of rat anterior pituitary, PrRP activated extracellular signal-regulated kinase (ERK) in an almost wholly PTX-sensitive manner (Kimura *et al.*, 2000), presumably *via* activation of endogenously expressed UHR-1. In addition, PrRP has been shown to inhibit cAMP production (Hinuma *et al.*, 1998) and stimulate [^{35}S]GTPγS binding in CHO cells stably expressing GPR10 in a wholly PTX sensitive manner (Engstrom *et al.*, 2003).

In both the Engstrom *et al.* (2003) and Kimura *et al.* (2000) studies the potency of PrRP to activate GPR10 appears to be in line with the potency of PrRP-20 and PrRP-31 to stimulate arachidonic acid metabolism (Hinuma *et al.*, 1998) and calcium mobilisation (Wilson *et al.*, 1998; Roland *et al.*, 1999) in CHO cells stably expressing GPR10. Hinuma *et al.* (1998) do not show any data to support their claim that PrRP inhibits cAMP production. Furthermore, the PrRP-mediated stimulation of [^{35}S]GTPγS binding in CHO cells stably expressing GPR10 (Engstrom *et al.*, 2003) is relatively small. However, these data suggest that at least part of the coupling of GPR10 may be through the G_i/G_o family of G proteins.

Additionally, Kimura *et al.* (2000) demonstrated that PrRP causes activation of c-Jun N-terminal protein kinase (JNK). This response is protein kinase C (PKC) dependent, as it is inhibited by pre-incubation with phorbol esters and insensitive to PTX treatment.

It is apparent from this small data set that the signal transduction cascade mediated by stimulation of GPR10 remains unclear. Given that all data (except that of Kimura *et al.* (2000)) has been generated in recombinant cells likely overexpressing GPR10, it is difficult to draw any firm conclusions on the physiological signal transduction pathway for GPR10 due to the possibility of promiscuous coupling to multiple G proteins. However, given the numerous reports of calcium mobilisation induced by PrRP in cells expressing GPR10, it seems likely that the receptor couples through the $G_{q/11}$ pathway, although the signal transduction pathways for GPR10 clearly warrant further investigation.

More recently, the pharmacology of PrRPs at other RF-amide receptors has been investigated. Most interestingly, both hPrRP-20 and hPrRP-31 display high affinity for both the NPFF2 receptor stably expressed in CHO cells and the rat NPFF receptor in

spinal cord (Engstrom *et al.*, 2003). These data, generated using [^{125}I](1DMe)Y8Famide binding assays, suggested that both hPrRP-20 and hPrRP-31 have nanomolar affinity for both the rat NPFF receptor in rat spinal cord and the NPFF2 receptor stably expressed in CHO cells, with affinities only approximately 30-fold and 5-fold, respectively, lower than the cognate ligand NPFF itself. Furthermore, in [^{35}S]GTPγS binding studies in CHO cells stably expressing the NPFF2 receptor, both hPrRP-20 and hPrRP-31 appeared as full agonists, with EC_{50} values of 170 nM and 240 nM, less than 10-fold lower than that of NPFF (28 nM; Engstrom *et al.*, 2003). Interestingly, this was the first report separating the efficacy of PrRP forms in that hPrRP-31 appeared as a 'super agonist', with substantially higher efficacy than hPrRP-20 and even NPFF and (1DMe)Y8Famide.

Studies conducted by Han *et al.* (2002) have determined PrRP-20 mediated stimulation of the orphan mas-related gene receptor, MrgC11, with an EC_{50} of 144 nM, as measured by calcium mobilisation in HEK293 cells stably expressing MrgC11. PrRP-20 was shown to be inactive at a similar, related receptor, MrgA1. A range of other RF-amide peptides, including NPFF, RFRP-3, antho-RF-amide and FMRF-amide, were also shown to activate MrgC11 with potencies in a similar range to PrRP-20, suggesting that the cognate ligand for this receptor may well be an, as yet, undiscovered member of this peptide family. Similarly, in the studies by Engstrom *et al.* (2003), a number of RF-amide peptides were shown to bind to, and activate, the NPFF2 receptor with affinities and potencies within 10-fold of those displayed by NPFF. These data mark out GPR10 as unusual in displaying such selectivity for PrRPs versus other members of the RF-amide peptide family.

Initial studies have suggested that in contrast to other RF-amide peptide receptors, such as those for NPFF, GPR10 exhibits a high degree of selectivity for PrRPs amongst the RF-amide peptides and a wider range of ligands. Whilst PrRPs have

been shown to activate GPR10 at concentrations of approximately 1 – 2 nM (Wilson *et al.*, 1998; Boyle *et al.*, 2005; Bhattacharyya *et al.*, 2003; Roland *et al.*, 1999) and bind to GPR10 with similarly high affinity (Roland *et al.*, 1999), no other ligands have been shown to bind to, or activate, GPR10 with such high affinity or potency. GPR10 displays no significant affinity for NPFF, NPAF, RFRP-1, RFRP-3 and neuropeptide-Y(18-36) as measured by [^{125}I]-PrRP-20 inhibition binding assays (Engstrom *et al.*, 2003) and neither NPY, NPFF nor NPAF stimulated calcium mobilisation in HEK293 cells stably expressing GPR10 (Wilson *et al.*, 1998). Furthermore, non-PrRP RF-amide peptides (FMRF-amide, antho-RF-amide and pol-RF-amide) only weakly stimulated calcium mobilisation, with EC_{50} values in excess of 10 μM (Wilson *et al.*, 1998). Radioligand binding studies using [^{125}I]-hPrRP-31 in rat hypothalamus, heart, soleus muscle and pituitary also showed that thyrotropin-releasing hormone, lutenising hormone-releasing hormone, growth hormone-releasing hormone, somatostatin, calcitonin, α-calcitonin gene related peptide, amylin, galanin, arginine vasopressin, endothelin-1, substance P, cholecystekinin, glucagon, glucagon like peptide-2, rat pancreatic polypeptide nor neuropeptide-Y display any significant affinity for GPR10 at concentrations up to 1 μM (Satoh *et al.*, 2000). These data further underline the selectivity of GPR10 for the PrRPs.

Despite the studies described above, relatively little is known with regard to the pharmacology of the interaction of PrRP and GPR10 and the subsequent signal pathways involved. The studies on GPR10 reported in this chapter were aimed at characterising the pharmacology of PrRPs and GPR10 using radioligand binding and functional assays. These studies have fully characterised the binding of [^{125}I]-hPrRP-20 to the GPR10 receptor stably expressed in HEK293 cells using saturation, inhibition and kinetic assays. Functions of rat and human PrRPs have also been assessed using calcium mobilisation, cAMP Flashplate technology and inositol phosphate accumulation assays to assess the signal transduction pathways involved

after activation of GPR10. Most functional assays were carried out using HEK293 cells transiently expressing GPR10 due to an intractable infection in the stable cell line.

(ii) HEK293-GPR10 [^{125}I]-hPrRP-20 saturation binding assays

Saturation assays were carried out to determine the affinity and maximal binding capacity of [^{125}I]-hPrRP-20 binding to membranes from HEK293 cells stably expressing GPR10. Specific binding of [^{125}I]-hPrRP-20 represented more than 90% of total binding and was saturable, whereas non-specific binding increased linearly with radioligand concentration (Figure 9a). Non-specific binding was defined using rat PrRP-31 to eliminate the possibility of pseudo-specific binding. Non-linear regression analysis of binding data revealed that [^{125}I]-hPrRP-20 bound to two sites on the HEK293-GPR10 membranes with equilibrium dissociation constant (K_D) values of 0.026 ± 0.006 nM and 0.57 ± 0.14 nM, with respective maximal binding capacity (B_{max}) values of 3010 ± 400 fmol / mg protein and 8570 ± 2240 fmol / mg protein (Figure 9b). This was reflected in the clearly curvilinear nature of the Scatchard regression (Figure 9b). Each individual experiment showed a two site fit to be statistically better than a one site fit ($p < 0.05$, F-test). No specific binding was detected in membranes from wild-type HEK293 cells (data not shown). Specific binding of [^{125}I]-hPrRP-20 to membranes from HEK293 cells transiently transfected with wild-type GPR10 displayed similar high and low affinity K_D and B_{max} values to those of the stable cell line (Langmead *et al.*, 2000). Analysis of binding data revealed that [^{125}I]-hPrRP-20 bound to two sites on membranes from the HEK293 cells transiently expressing GPR10 with K_D values of 0.05 ± 0.01 nM and 1.55 ± 0.52 nM and respective B_{max} values of 2605 ± 1072 fmol mg protein^{-1} and 6275 ± 800 fmol mg protein^{-1}.

A

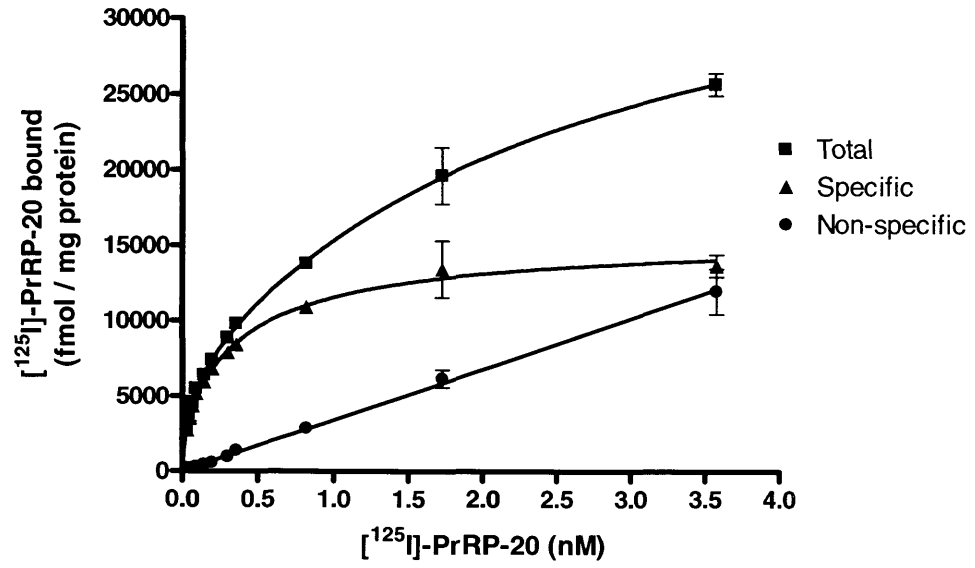

B

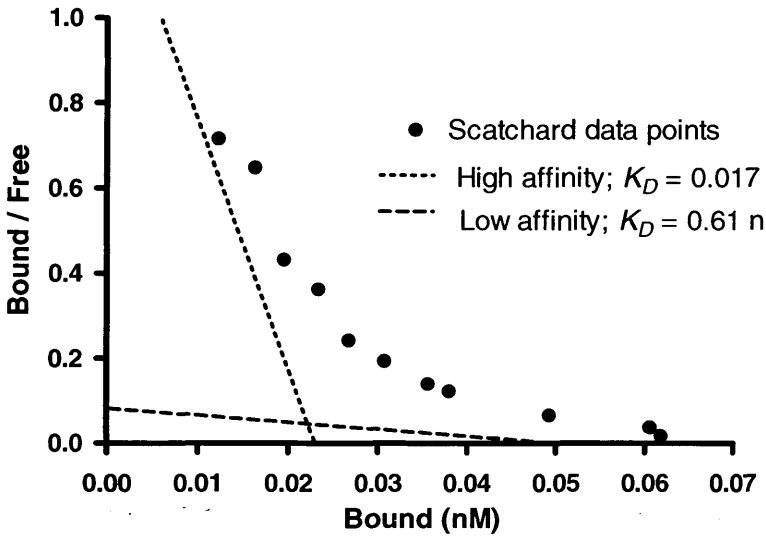

Figure 9. (A) Total, non-specific and specific binding of [^{125}I]-hPrRP-20 binding to membranes from HEK293 cells stably expressing GPR10 with increasing radioligand concentration. Data represents a single, representative experiment, with each point determined in quadruplicate, which was replicated six times with similar results. (B) Scatchard transformation of the data from (A). Dashed lines indicate high and low affinity binding sites.

(iii) HEK293-GPR10 [^{125}I]-hPrRP-20 kinetic binding assays

Kinetic studies of [^{125}I]-hPrRP-20 binding to HEK293-GPR10 cell membranes were performed in order to determine the time course of radioligand association and dissociation. Association studies indicated that [^{125}I]-hPrRP-20 binding to HEK293 cell membranes reached equilibrium within 60 min. Association curves appeared to be biphasic and in 3 out of 5 studies a two-site fit was preferred to a single-site by statistical analysis (F-test). However, estimates of observed association constants for the two site fits were extremely variable and hence all data were analysed based on monophasic exponential association (Figure 10a and inset linear transformation).

Dissociation of [^{125}I]-hPrRP-20 upon addition of excess cold rat PrRP-31 was very slow and appeared monophasic, with 50% of specific binding being dissociated after 120 min (Figure 10b and inset linear transformation).

Single site analysis of these kinetic data yielded a k_{obs} value of 0.077 ± 0.008 min^{-1} and a k_{off} value of 0.0048 ± 0.0002 min^{-1}, leading to a calculated k_{on} value of 396 ± 54 min^{-1} μM^{-1}. The K_D value derived from these data was 0.012 nM, which is similar to the value for the high affinity site derived from the saturation studies.

(iv) HEK293-GPR10 [^{125}I]-hPrRP-20 inhibition binding assays

Human PrRP-20, human PrRP-31, rat PrRP-20 and rat PrRP-31 displayed high affinity for GPR10 receptors, with pK_i values of 9.59 ± 0.18, 9.19 ± 0.31, 9.62 ± 0.08 and 9.68 ± 0.03, respectively (Table 5; Figure 11). All inhibition curves appeared to be monophasic and Hill slopes did not differ significantly from 1 (F-test). These values agree well with previous estimates of affinity for the PrRP isoforms (Hinuma *et al.*, 1998; Roland *et al.*, 1999).

A range of other drugs which are known ligands at receptors which share limited homology with GPR10 were tested against [^{125}I]-hPrRP-20 binding to determine the selectivity of GPR10 for the PrRPs. None of the compounds tested displayed any affinity for GPR10 receptors at concentrations of up to 30 μM (3 μM for SB-213698; Table 6).

A

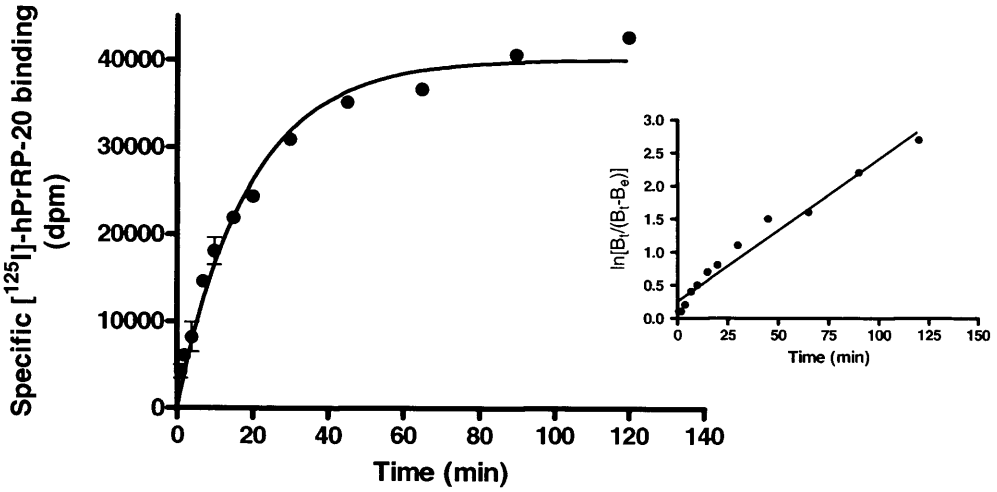

B

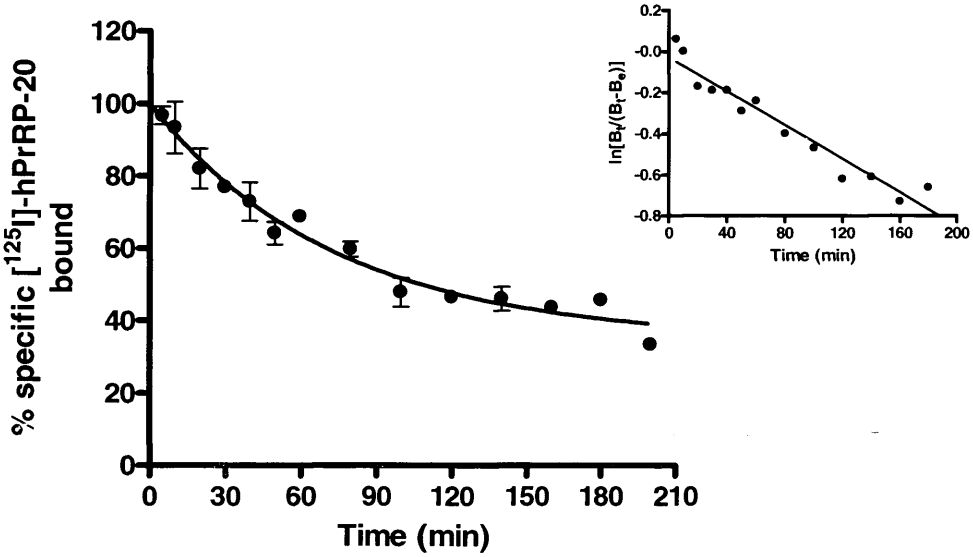

Figure 10. Time course of (A) association and (B) dissociation of [^{125}I]-hPrRP-20 to and from membranes from HEK293 cells stably expressing GPR10. Insets show data transformed as semi-log plots where B_t is specific binding measured at time *t* and B_e is the specific binding at equilibrium. Data represents a single experiment in duplicate that was repeated 5 (association) and 3 (dissociation) times with similar results.

Peptide / Species	Human	Rat
PrRP-20	9.59 ± 0.18	9.62 ± 0.08
PrRP-31	9.19 ± 0.31	9.68 ± 0.03

Table 5. Affinities of PrRP variants for GPR10. Data are the mean of 3 independent experiments (± s.e.m.). Affinity (pK_i) values calculated from IC_{50} values as described in Appendix 1.

A

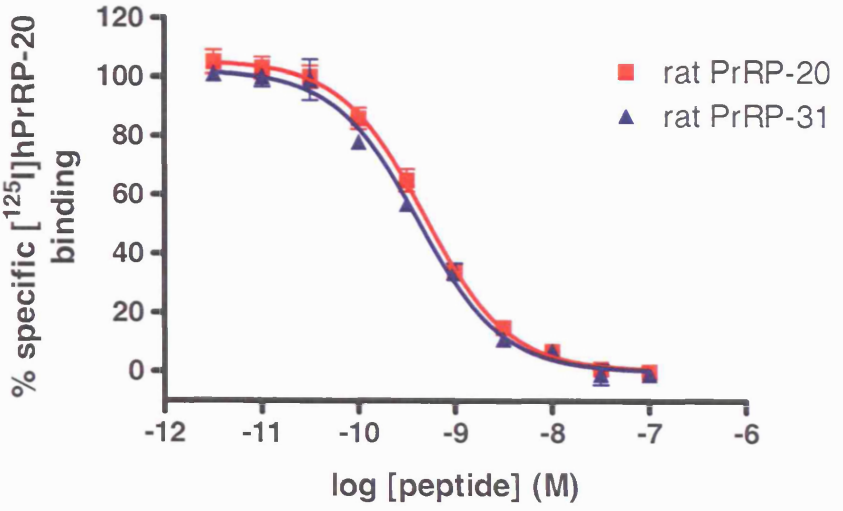

B

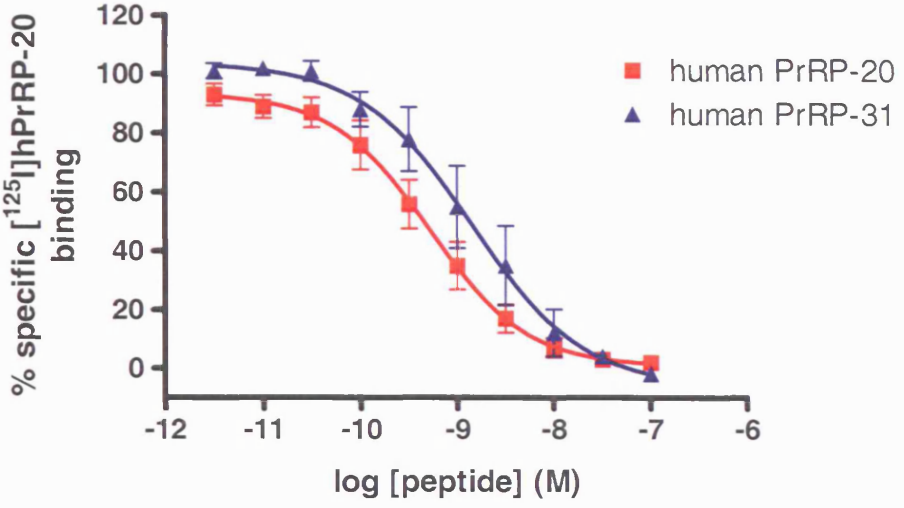

Figure 11. Concentration-dependent inhibition of [^{125}I]-hPrRP-20 binding from membranes of HEK293 cells stably expressing GPR10 by (A) rat PrRP-20 and rat PrRP-31 and (B) human PrRP-20 and human PrRP-31. Data shown are the mean of 3 experiments; error bars show s.e.m..

Compound	Native receptor	pK_i at GPR10
Substance P	NK-1	< 4.5
Neurokinin-A	NK-2	< 4.5
Methyl-Phe^7-Neurokinin-B	NK-3	< 4.5
DAMGO	μ-opioid	< 4.5
U-50488	κ-opioid	< 4.5
SB-213698	δ-opioid	< 5.5
Nociceptin	ORL-1	< 4.5
Naloxone	μ-opioid	< 4.5
Neuropeptide-Y	NP-Y	< 4.5
Neuropeptide-FF	NP-FF	< 4.5
Somatostatin	SST-R	< 4.5

Table 6. Affinities of a range of drugs active at G protein coupled receptors which share limited homology with GPR10. pK_i values are from 2 - 3 determinations.

(v) HEK293-GPR10 calcium mobilisation assays

Previous studies have demonstrated that PrRPs are capable of activating GPR10 to mobilise intracellular calcium in cells recombinantly expressing this receptor (Roland *et al.*, Bhattacharyya *et al.*, 2004; Boyle *et al.*, 2005). Human PrRP-20 stimulates intracellular Ca^{2+} mobilisation in HEK293 cells transiently transfected with the GPR10 receptor; an example trace of the temporal calcium response to 1 μM hPrRP-20 is shown in Figure 12. Furthermore, human PrRP-20, human PrRP-31, rat PrRP-20 and rat PrRP-31 were approximately equipotent in stimulating calcium mobilisation (Figure 13); all four PrRPs appeared as agonists with pEC_{50} values of 9.54 ± 0.09, 9.34 ± 0.12, 9.77 ± 0.14 and 9.46 ± 0.02 respectively, with Hill slopes not significantly different from unity (F-test). Agonist activity was assumed to be full as PrRPs are the cognate ligands for GPR10. PrRPs did not stimulate calcium mobilisation in untransfected HEK293 cells (data not shown).

(vi) HEK293-GPR10 Ca^{2+} mobilisation – signal transduction studies

Signal transduction studies were carried out on the calcium mobilisation response mediated *via* GPR10 to determine whether the response was consistent with coupling to the $G_{q/11}$-phospholipase-C-IP_3 pathway. The effects of a range of signal transduction inhibitors on the calcium mobilisation responses to hPrRP-20 are shown in Figure 14. The phospholipase-C inhibitor, U73122 (Thompson *et al.*, 1991; 10 μM), inhibited hPrRP-20 stimulated calcium mobilisation, reducing the maximal response to approximately 30 % of the maximal control response. The non-competitive inhibitor of the inositol triphosphate (IP_3) receptor, 2-APB (Maruyama *et al.*, 1997; 100 μM), similarly reduced the maximal response to hPrRP-20 to approximately 30 % of the control response. The Ca^{2+}-ATPase inhibitor, thapsigargin (Marshall *et al.*, 2003; 1 μM),

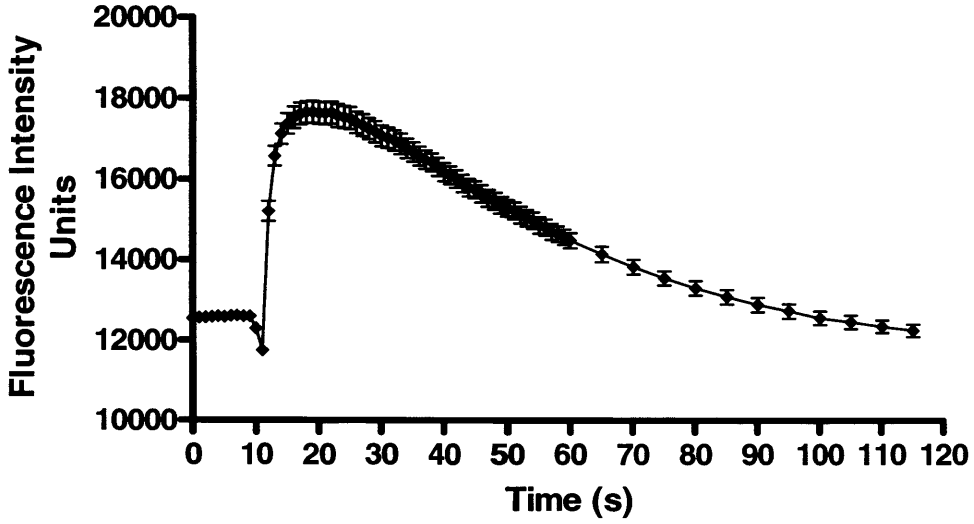

Figure 12. Temporal calcium response to hPrRP-20 (1 μM) in HEK293 cells transiently expressing GPR10. Peptide was added at $t = 10$ s. Data represents the mean of 8 independent calcium measurements; error bars represent s.e.m..

A

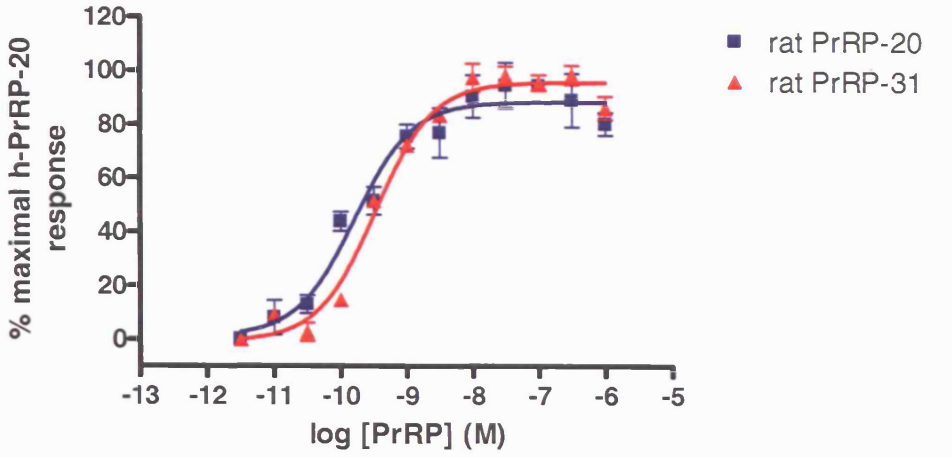

B

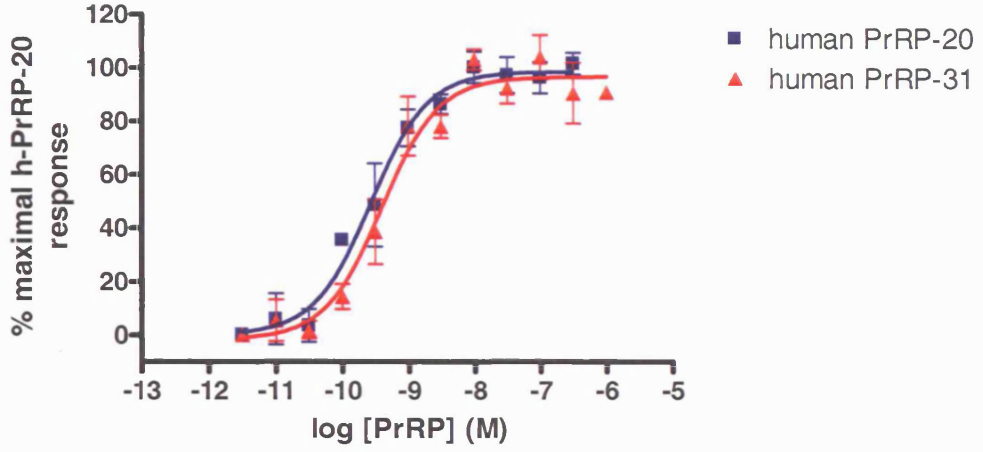

Figure 13. Concentration-dependent stimulation of intracellular Ca^{2+} mobilisation in HEK293 cells transiently expressing GPR10 by (A) rat PrRP-20 and rat PrRP-31 and (B) human PrRP-20 and human PrRP-31. Data are the means of 4 experiments; error bars show s.e.m..

abolished the calcium mobilisation response to hPrRP-20. The phosphoinositide-3-kinase and phospholipase-D inhibitor, wortmannin (1 μM), did not significantly alter the calcium mobilisation response to hPrRP-20 (F-test). No cellular toxicity was observed with any of the inhibitors and the final DMSO concentration was always ≤ 1% (v/v). The effects of U73122, 2-APB and thapsigargin on the hPrRP-20 stimulated calcium response are consistent with GPR10 coupling to the $G_{q/11}$-phospholipase-C-IP_3 pathway.

(vii) HEK293-GPR10 inositol phosphate accumulation

Inositol phosphate accumulation assays were performed to confirm whether PrRP mediated activation of GPR10 led to the hydrolysis of PIP_2 and the production of inositol phosphates. Human PrRP-20 potently stimulated inositol phosphate accumulation in HEK293 cells transiently transfected with GPR10 with a pEC_{50} of 10.21 ± 0.05 and an E_{max} of 435 ± 5 cpm (Figure 15). Carbachol, acting *via* activation of endogenous muscarinic M_3 receptors (Brandish *et al.*, 2003), stimulated inositol phosphate accumulation with a pEC_{50} of 4.95 ± 0.09 and an E_{max} of 534 ± 12 cpm in the same cell line (Figure 15).

(viii) cAMP accumulation studies

Human PrRP-20 (10 μM) did not elevate intracellular cAMP levels in HEK293-GPR10 cells (2.96 ± 0.42 pmol / 10^6 cells compared to basal level of 4.09 ± 0.57 pmol 10^6 / cells; Figure 16). Human PrRP-20 (10 μM) also failed to significantly decrease cAMP levels following stimulation with concomitantly administered forskolin (30 μM; 508 ± 12.6 pmol 10^6 / cells compared to control level of 502 ± 17.8 pmol 10^6 / cells; Figure 16).

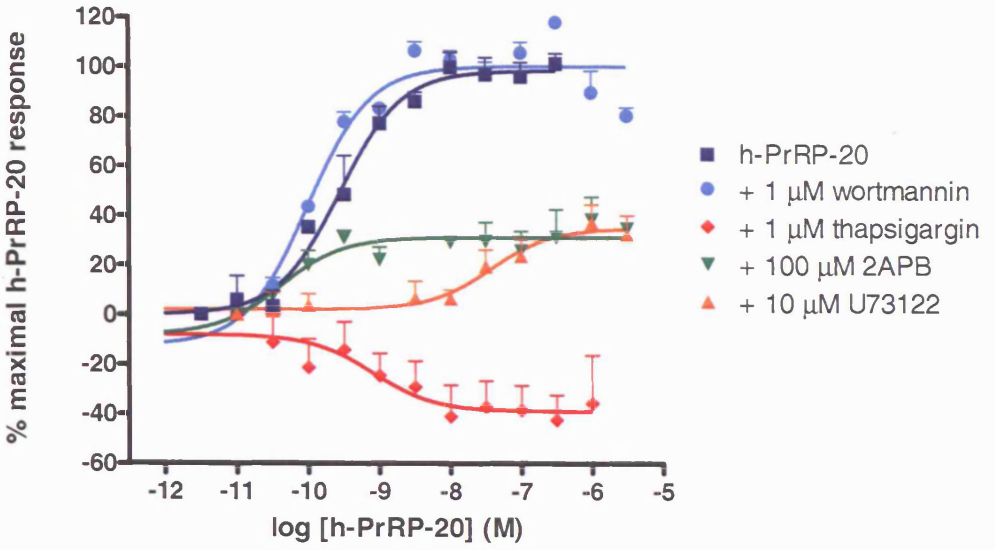

Figure 14. Effect of signal transduction inhibitors on hPrRP-20 stimulated intracellular calcium mobilisation in HEK293 cells transiently expressing GPR10. Data shown are the means of 4 experiments; error bars represent s.e.m.

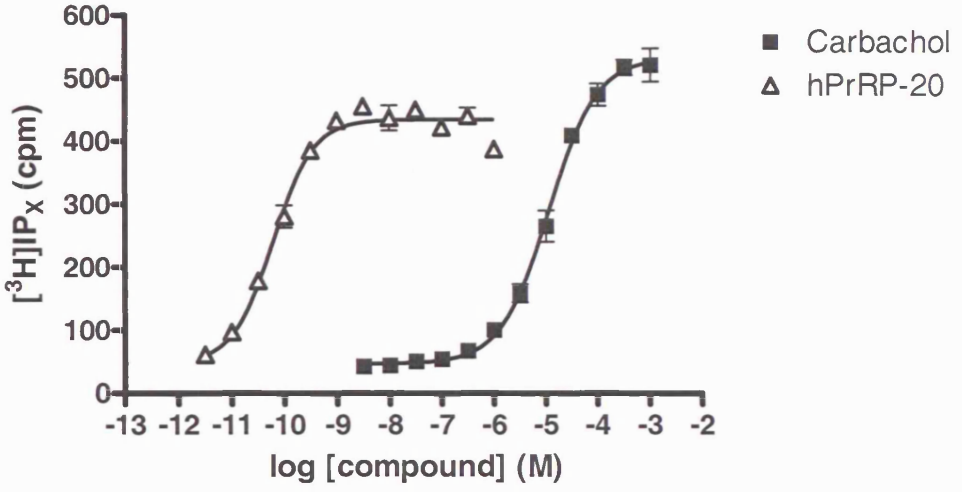

Figure 15. Concentration-dependent stimulation of inositol phosphate accumulation by hPrRP-20 and carbachol in HEK293 cells transiently expressing GPR10. Data shown are the means of 4 experiments; error bars represent s.e.m..

(ix) Discussion

These studies indicate that [^{125}I]-hPrRP-20 is a high affinity radioligand for the GPR10 receptor. Saturation studies clearly suggested the existence of two distinct binding sites for [^{125}I]-hPrRP-20 which bind with sub-nanomolar affinity (K_D values of 0.026 nM and 0.57 nM respectively).

Kinetic studies were unable to accurately discern two distinct binding sites and although a trend towards biphasic association was observed, this was not consistently replicated. Dissociation of [^{125}I]-hPrRP-20 was very slow and apparently monophasic. Single site analysis of the data produced a K_D of 0.012 nM, which is similar to the value for the higher affinity site obtained from saturation studies. The K_D value of the higher affinity site determined by saturation studies is similar to that reported by Hinuma *et al.* (1998) for bovine [^{125}I]-PrRP-31 binding to hGR3 / GPR10 and UHR-1. The K_D of the lower affinity site is similar to the affinities of human and rat PrRP-20 and PrRP-31 determined by inhibition of [^{125}I]-hPrRP-20 binding and also the affinity of [^{125}I]-hPrRP-31 as determined by Roland *et al.* (1999).

The apparently monophasic saturation analysis initially described by Hinuma *et al.* (1998) represents a rather incomplete 5 data point study in which the binding of the radioligand did not saturate. The saturation study by Roland *et al.* (1999) was more extensive, covering 9 data points, yet the higher concentration range tested may have missed any higher affinity binding site at lower radioligand concentrations.

Several different possibilities could result in the observed two-site binding of [^{125}I]-hPrRP-20. Firstly, it may be that there are two physically distinct sites of attachment for different parts of the peptide. Whilst it has been recognised both in these studies (Chapter 4) and in the literature (Roland *et al.*, 1999) that hPrRP(25-31), a truncated

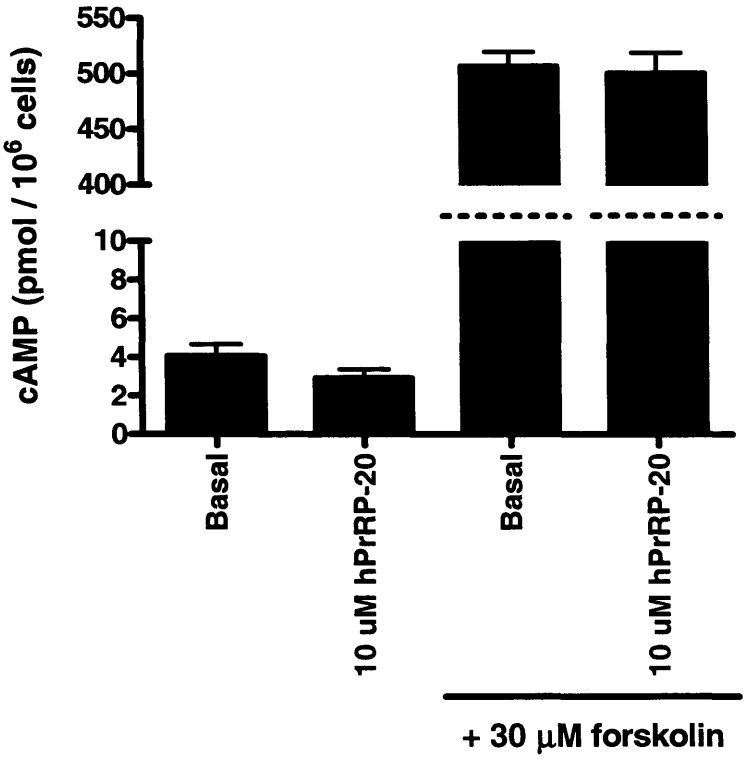

Figure 16. Effect of hPrRP-20 on basal and forskolin-stimulated cAMP levels in HEK293 cells stably expressing GPR10. Data shown are the means of 3 experiments; error bars represent s.e.m..

seven amino acid C-terminal portion of hPrRP-20, retains agonist activity at GPR10, the potency of the truncated peptide is reduced approximately 30 to 100-fold compared to the full length peptide. This implies that the N-terminal region must contribute to the higher potency of PrRP-20 compared to PrRP(25-31), either by stabilising the C-terminal region in the binding pocket or through a direct interaction with the receptor. The possibility of two direct receptor-peptide interactions mediating the observed biphasic binding is discussed further in Chapter 4.

An alternative possibility is that receptors coupled to heterotrimeric G proteins may bind the agonist peptide with higher affinity than uncoupled receptors. The existence of a 'high agonist affinity state' has been extensively described for small molecule agonist G protein coupled receptors, such as 5-HT_{1A} (Newman-Tancredi *et al.*, 1998), muscarinic M_2 (Birdsall *et al.*, 1981) and dopamine D_2 (Lahti *et al.*, 1992) receptors. The availability of non-hydrolysable analogues of GTP, such as GppNHp, permits experimental determination of such states. By carrying out 'GTP-shift' studies, where inhibition or saturation isotherms are carried out in the presence of increasing concentrations of GppNHp, it should be possible to delineate whether the high affinity [^{125}I]-hPrRP-20 binding occurs as a result of G protein coupling. If the high affinity binding site were to represent binding to G protein coupled receptors, the presence of GppNHp should shift the high affinity component into a low affinity state and result in a monophasic profile.

Alternatively, it is possible that PrRP-31 (used in both the studies by Hinuma *et al.* (1998) and Roland *et al.* (1999)), unlike PrRP-20, does not exhibit two site binding. Intuitively it might be expected that PrRP-20, as a truncate of PrRP-31, might exhibit a less, rather than more, complex binding profile than the longer analogue. However, in the absence of a comparative study with [^{125}I]-hPrRP-20 and [^{125}I]-hPrRP-31 this question remains unanswered. Finally, it is possible that the iodination of hPrRP-20

required in order to synthesise the radioligand may alter the conformation of the peptide such that it displays biphasic binding in a manner that the native peptide does not. This is, however, unlikely, as both the Hinuma *et al.* (1998) and Roland *et al.* (1999) studies employed iodinated ligands – in neither of these studies were biphasic binding profiles observed. The data presented herein provide the most extensive characterisation of the binding of [^{125}I]-hPrRP-20 to GPR10 to date and clearly suggest the presence of biphasic binding.

All four forms of PrRP (human 20 and 31 and rat 20 and 31) bound to GPR10 receptors with high and similar affinity (pK_i values ≈ 9) in a competitive manner with Hill slopes not significantly different from unity. In contrast, no other ligand studied exhibited any affinity for the receptor at concentrations up to 3 μM. These observations are in agreement with the low levels of homology between GPR10 and other known G-protein coupled receptors. Indeed, the greatest identity (30% homology) is seen with the neuropeptide Y receptor family and here it has been shown that neuropeptide Y has very low affinity for GPR10 ($pK_i < 4.5$). In addition, the mammalian RF-amide neuropeptide-FF displays similarly low affinity for the receptor ($pK_i < 4.5$). Further supporting this, neuropeptide-FF was also found to be inactive at GPR10 in calcium mobilisation studies (Wilson *et al.*, 1998). These data are in contrast to findings for other RF-amide peptide receptors, which have been shown to be activated by range of members of the RF-amide family, such as MrgA1 and MrgC11 (Han *et al.*, 2002) and NPFF-2 (Engstrom *et al.*, 2003). Interestingly, the latter study demonstrated potent agonist activity of the prolactin-releasing peptides at the NPFF-2 receptor. Despite the apparent promiscuous activity of their cognate ligands, the findings described herein demonstrate the high degree of selectivity of GPR10 for the prolactin releasing peptides.

In calcium mobilisation studies, all four PrRP peptides were shown to be potent, full agonists at the GPR10 receptor. The sub-nanomolar potencies of these peptides agreed with their affinities as determined by inhibition of [^{125}I]-hPrRP-20 binding. Further calcium mobilisation studies showed that the response to hPrRP-20 was completely abolished by pre-incubation for 30 minutes with thapsigargin, an inhibitor of the endoplasmic reticulum Ca^{2+}-ATPase. Furthermore, the response to hPrRP-20 was almost completely blocked by the inhibitor of phospholipase-C, U73122 and the non-competitive inhibitor of the IP_3 receptor, 2-APB. The phosphoinositide-3-kinase and phospholipase-D inhibitor, wortmannin, did not alter the response to hPrRP-20. These results are entirely consistent with GPR10 mediating signalling through the $G_{q/11}$-phospholipase-C-IP_3 pathway to mobilise intracellular calcium, although in the absence of control data (eg. treatment of cells with the inactive isomer of U73122, U73443), non-specific cytotoxic effects of these inhibitors cannot be ruled out. However, in support of this hypothesis, hPrRP-20 potently stimulated IP accumulation in HEK293 cells transiently expressing GPR10, consistent with the phospholipase-C catalysed breakdown of PIP_2 to IP_3 and DAG. These observations are in good agreement with numerous previous studies that, although all employing recombinant systems, have shown GPR10 to couple to the mobilisation of intracellular calcium in the absence of any co-expressed G proteins (Wilson *et al.*, 1998; Roland *et al.*, 1999; Bhattacharyya *et al.*, 2003; Boyle *et al.*, 2005).

In contrast, studies on HEK293-GPR10 cells using Flashplate technology showed that human PrRP-20 had no effect on basal levels of intracellular cAMP. This implies that GPR10 does not couple through G_s, which would activate adenylyl cyclase to increase the cAMP concentration. Additionally, hPrRP-20 failed to decrease cAMP levels after stimulation with forskolin, indicating that GPR10 does not couple *via* G_i (which would inhibit adenylyl cyclase to lower cAMP levels). However, it must be noted that cAMP studies were carried out in the HEK293 cells stably expressing

GPR10, rather than the transient expression systems used for all other functional data. These data are in contrast to that of Kimura *et al.* (2000), which showed that PrRP stimulated extracellular signal-regulated protein kinase (ERK) in both GH3 rat pituitary tumour cells and primary cultures of rat anterior pituitary. They demonstrated that the effect was largely pertussis toxin sensitive, indicating that the greatest coupling contribution was *via* G_i/G_o and likely to mediated *via* $G\beta\gamma$ subunits. Additionally, they showed that ERK activation is independent of intracellular calcium. Furthermore, Engstrom *et al.* (2003) also demonstrated a small, but significant pertussis toxin sensitive stimulation of [^{35}S]GTPγS binding in CHO cells stably expressing GPR10 by PrRPs.

However, Kimura *et al.* (2000) also demonstrate that activation of c-Jun N-terminal protein kinase (JNK) by PrRP is fully dependent on protein kinase C (PKC). This suggests the possibility that GPR10 also signals through a G_q pathway to stimulate PLC to produce diacylglycerol (DAG) and activate PKC. Comparison of the findings of Kimura *et al.* (2000) and Engstrom *et al.* (2003) with the results presented here suggest that the coupling of GPR10 may be dependent on the cell system in which it is expressed and the pathway being monitored.

These studies have confirmed the high affinity binding of [^{125}I]-hPrRP-20 to GPR10 and further suggested the existence of high and low affinity binding sites, although their aetiology remains unknown. Functional studies clearly suggest that GPR10 couples *via* $G_{q/11}$ to the phospholipase C-IP_3 signalling pathway, as hPrRP-20 has been shown to stimulate both calcium mobilisation and inositol phosphate accumulation when expressed in HEK293 cells. Furthermore, at least in this recombinant system, hPrRP-20 has been shown not to alter intracellular cAMP levels, suggesting that GPR10 does not couple *via* G_s or G_i/G_o proteins.

These results represent significant advances in understanding the binding profile of the PrRPs at GPR10 and elucidating the signal transduction pathway(s) of the receptor. [^{125}I]-hPrRP-20 has been shown to be a high affinity, selective radioligand for GPR10 which may prove a very useful tool in future studies into the localisation and function of the receptor. The calcium mobilisation and inositol phosphate accumulation data clearly suggest that GPR10 is capable of robust coupling to the $G_{q/11}$–phospholipase-C-IP_3 signalling pathway, at least in a recombinant system. However, it may be that, as described by Kimura *et al.* (2000), differential G protein coupling occurs in native systems. This, as yet, remains undetermined.

Chapter 4

Characterisation of the PrRP-GPR10 interaction

(i) Introduction

In common with other RF-amide peptide ligands, the amide group distal to the terminal phenylalanine residue of PrRP appears to be key to activity as bovine PrRP-31-COOH (the non-amidated acid) neither binds to GPR10 nor stimulates arachidonic acid metabolism in CHO cells stably expressing GPR10 (Hinuma *et al.*, 1998; Nishimura *et al.*, 1998). Several subsequent studies have examined the structure of the PrRPs and attempted to identify key residues for activity at GPR10. The main structural feature of PrRP-20 as determined by NMR spectroscopy appears to be a flexible N-terminus with no regular secondary structure and an α-helical structure spanning the C-terminal ten amino acids (Danho *et al.*, 2003; D'Ursi *et al.*, 2002). This basic template appears similar to the C-terminal structure of another amidated peptide, NPY (D'Ursi *et al.*, 2002). These structural data provided rationale to support the observation that substantial agonist activity at GPR10 is retained in both C-terminal heptapeptide (Roland *et al.*, 1999) and hexapeptide (Danho *et al.*, 2003) fragments of PrRP-20, albeit with reduced potency. The C-terminal heptapeptide fragment, PrRP(25-31), stimulates calcium mobilisation in CHO cells stably expressing GPR10 with an EC_{50} of approximately 30 nM as compared to ~ 1 nM for PrRP-20 (Roland *et al.*, 1999). Similarly, successive N-terminal deletions from PrRP-20 to PrRP(25-31) resulted in successive reductions in peptide affinity as measured by [^{125}I]-hPrRP-31 binding (Roland *et al.*, 1999). In an elegant study, the same authors performed alanine scanning of the heptapeptide PrRP(25-31) which resulted in reductions in affinity for GPR10 at all positions, but most markedly when Arg^2 (Arg^{26} in PrRP-31) and Arg^6 (Arg^{30} in PrRP-31) were substituted (Roland *et al.*, 1999). Furthermore, alignment of the sequences of NPY and hPrRP-31 revealed significant homology between the two (D'Ursi *et al.*, 2002) and aligns Arg^{30} of hPrRP-31 with Arg^{35} of NPY. This residue has been shown to be crucial for NPY activity, since replacement of Arg^{35} by Ala results in a complete loss of affinity at all cloned

NPY receptor subtypes (Cabrele & Beck-Sickinger, 2000). Most recently, an extensive study has examined a large number of single replacement analogues of a C-terminal tridecapeptide fragment of hPrRP-31, PrRP(19-31) (Boyle *et al.*, 2005). PrRP(19-31) retains significant potency and affinity at GPR10 as measured by calcium mobilisation and Eu-(Lys)PrRP-31 binding to HEK293 cells stably expressing GPR10 (EC_{50} = 20 nM; K_i = 5.3 nM). These studies have focussed mainly on the C-terminal six residues of the peptide, particularly on the Phe^{31} residue. Both methylation of Phe^{31} and substitution of the C-terminal amide with an acid or an alcohol effectively abolished functional agonist activity and affinity. Replacement of the C-terminal amide with a secondary methylamide and to a lesser extent a methyl ester had little effect on potency or affinity. The data suggested that the Phe^{31} residue was key for activity, providing a hydrophobic side-chain in the L-position, a free NH on the backbone and a suitably blocked carboxyl terminus (Boyle *et al.*, 2005). Arg^{30} appeared to be crucial to both potency and affinity at GPR10, as substitution by a range of other polar residues such as Lys, His, Ser or Glu was not tolerated. It is clear from the data that the appropriately located diffuse positive charge in the L-configuration provided by Arg^{30} is essential (Boyle *et al.*, 2005). Substitution of Gly^{29} was also poorly tolerated and the authors speculate that this residue lies in a functionally important position and that as a spacer residue it requires unhindered flexibility to allow the peptide to fold correctly. Replacements of both Val^{28} and Pro^{27} suggested the 'reasonably sized' hydrophobic side chain in the L-configuration, the free NH on the backbone of Val^{28} and the small turn provided by Pro^{27} are the reasons for their being preferred in their respective positions. A similar hydrophobic side chain to that of Val^{28} was preferred when replacements were made for Ile^{25}. Substitution of Arg^{26} for Lys was well tolerated; however, other polar residues in position 26 resulted in inactive analogues. The data suggest that the positively charged side-chain of Arg^{26} is important for activity, but is less crucial than Arg^{30} (Boyle *et al.*, 2005).

These data, together with that of Roland *et al.*, (1999) and D'Ursi *et al.*, (2002) suggest that whilst all seven C-terminal residues of PrRP-31 may have a role to play in binding to GPR10, Arg^{26} and Arg^{30} may have key roles in docking the peptide into the agonist binding site of the receptor.

Despite the extensive structural work that has been carried out on the PrRPs, the precise nature of the molecular interaction between PrRP and GPR10 is unknown. The studies detailed above have identified many of the structural components that are key to the activity of PrRP at GPR10 (Roland *et al.*, 2005; Boyle *et al.*, 2005). However, the cognate binding pocket of GPR10 has not been examined. The studies on GPR10 reported in this chapter were designed to characterise the molecular nature of the interaction between PrRP and GPR10 using site directed mutagenesis, radioligand binding and functional calcium mobilisation assays.

A homology model of the receptor has been constructed based on the published crystal structure of rhodopsin and this in turn has allowed the prediction of proposed molecular interactions between GPR10 and the C-terminal heptapeptide of hPrRP-20, hPrRP(25-31) and another heptapeptide analogue, [$pGlu^1$, Trp^2, Lys^3, Leu^4] hPrRP(25-31). On this basis, site-directed mutagenesis has been carried out and mutant constructs assessed using [^{125}I]-hPrRP-20 binding and functional calcium mobilisation with hPrRP-20, hPrRP(25-31) and [$pGlu^1$, Trp^2, Lys^3, Leu^4] hPrRP(25-31) in order to partially determine the validity of the model in predicting the key residues involved in hPrRP-20 binding to GPR10.

The homology model and ligand docking was performed by Dr Frank Blaney (GSK). SDM constructs were made by Dr Angela Bridges (GSK).

A Thr-Pro-Asp-Ile-Asn-Pro-Ala-Trp-Tyr-Ala-Ser-Arg-Gly-Ile-Arg-Pro-Val-Gly-Arg-Phe-$CONH_2$

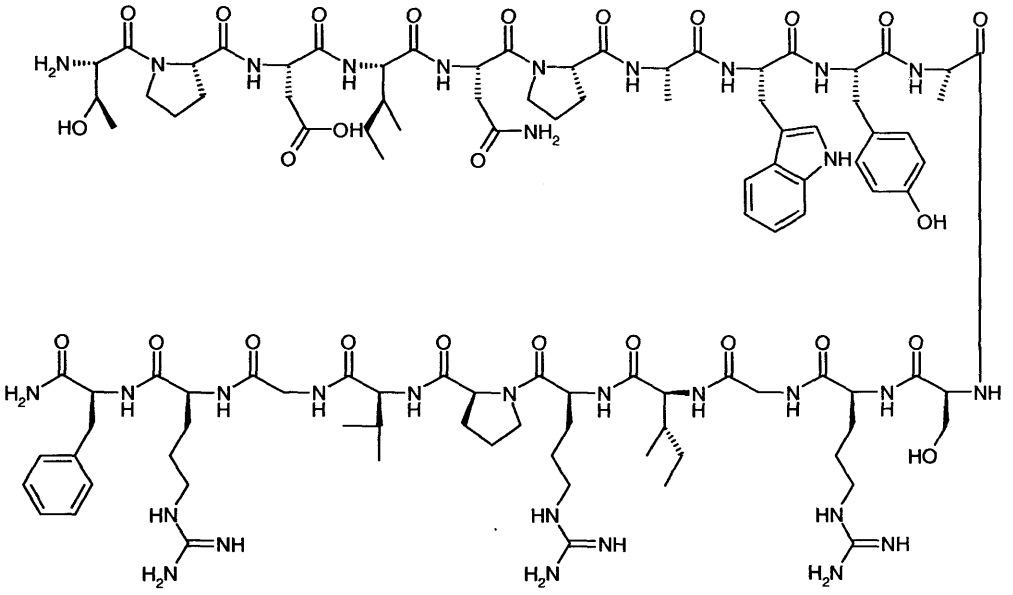

B Ile-Arg-Pro-Val-Gly-Arg-Phe-$CONH_2$

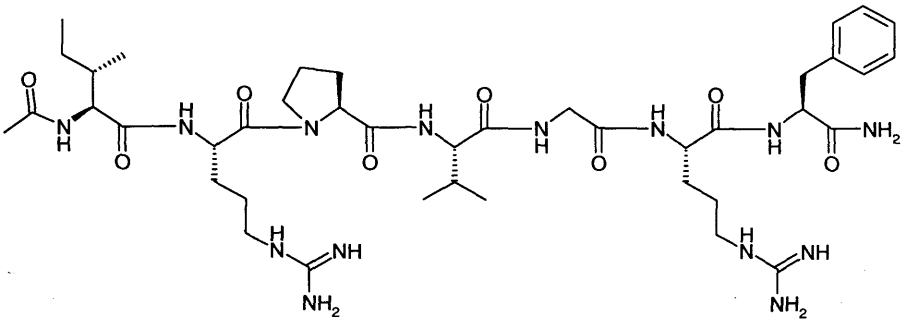

C pGlu-Trp-Lys-Leu-Gly-Arg-Phe-$CONH_2$

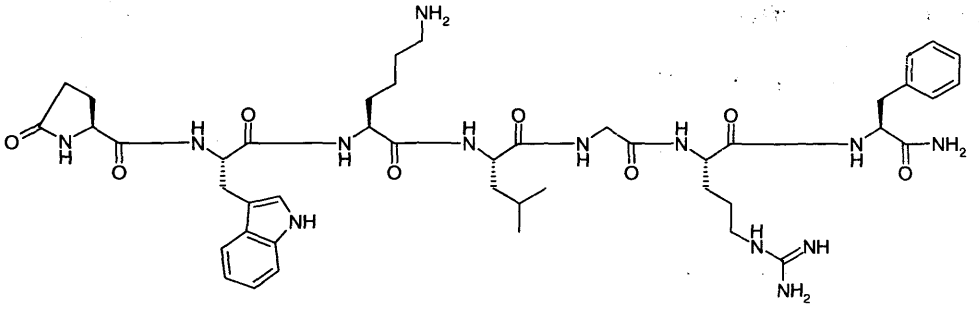

Figure 17. Sequences and structures of (A) hPrRP-20, (B) hPrRP(25-31) and (C) [pGlu^1, Trp^2, Lys^3, Leu^4] hPrRP(25-31).

(ii) Ligand docking and site directed mutagenesis

Structures of hPrRP-20, hPrRP(25-31) and [pGlu^1, Trp^2, Lys^3, Leu^4] hPrRP(25-31) are shown in Figure 17. Manual docking of hPrRP(25-31) was performed by allowing only acceptable Ramachandran ϕ–φ values of the peptide backbone (Ramachandran *et al.*, 1963) and reasonable rotamer states of the side chains. The initial placement was guided by the fact that hPrRP(25-31) contained two essential basic side chains (Arg^2 and Arg^6) for which acidic residues in the receptor that may form salt bridges with the ligand were sought. Following the various initial placements of the ligand, the complex was minimised with CHARMm (using NOE distance helical constraints in the TM bundle, distance dependent dielectric, 2000 steps Steepest Descent (SD) and 5000 steps Adopted Basis Newton Raphson (ABNR)). All the acceptable docked solutions suggested that the penultimate arginine (Arg^6) was able to form a salt bridge with E213, which is two residues along from the disulphide bond in the second extracellular loop (Figure 18a). This placed the terminal phenylalanine in a hydrophobic pocket between the TM6 residues W291 and L294, and L323 in TM7 (Figure 18a). The terminal carboxamide was predicted to form a hydrogen bonding network with Q141 (TM3), E212 (ECL2) and H321 (TM7) as shown in Figure 18a. In an earlier homology model of GPR10 that did not contain the extracellular loops, the Arg^6 residue was believed to interact with the TM6 aspartate, D302. The second arginine residue in position 2 of hPrRP(25-31) (Arg^2) in this older model was predicted to form a salt bridge with E202 at the top of TM4. However, the latest model incorporating the loops instead suggested an ionic interaction of Arg^2 with D302 (Figure 18b). A number of other hydrogen bonding interactions were predicted to occur between the backbone chain of the peptide ligand and the receptor. Thus, N298 (TM6) formed a hydrogen bond between its side chain carbonyl and the backbone NH of Arg^6 of hPrRP(25-31) (Figure 18a). In addition to this the two NH hydrogens of the sidechain formed further hydrogen bonds with the backbone carbonyl of E213 and the carboxylate of D302, respectively, further stabilising

A

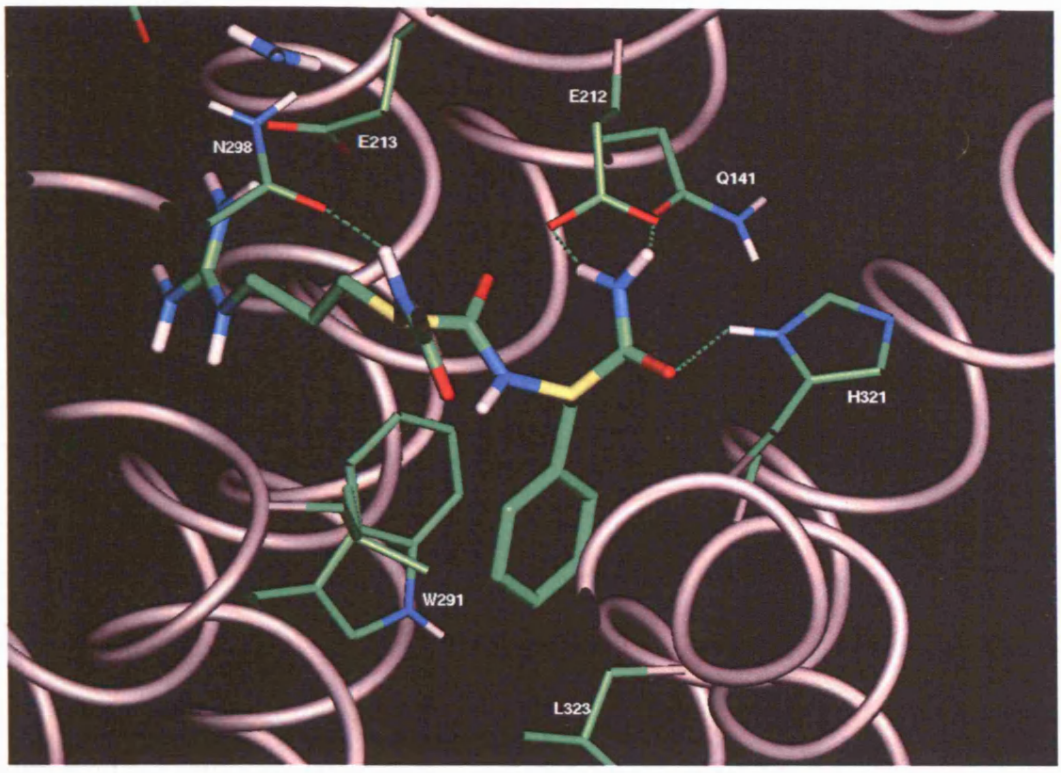

B

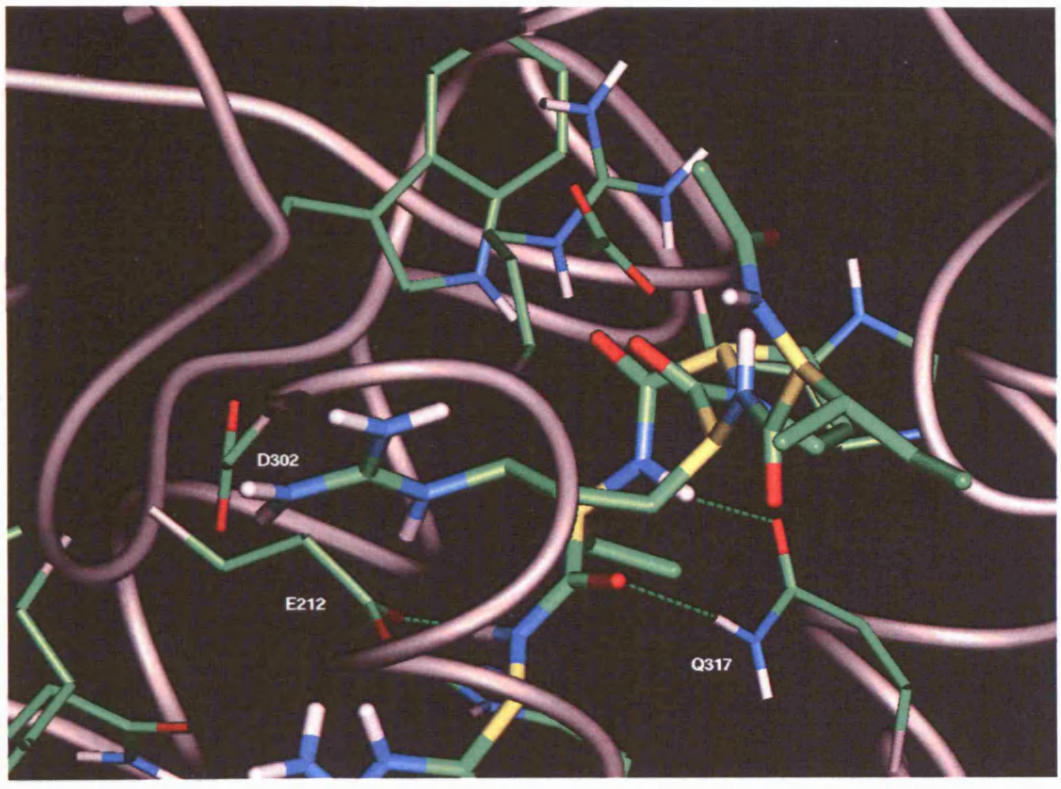

Figure 18. Predicted interactions of hPrRP(25-31) with GPR10; (A) interactions with the C-terminal RF-amide region and (B) Arg^{2} - D302 and Val^{4} - Q317 interactions.

the receptor structure in its binding pocket. Q317 (TM7) formed two hydrogen bonds with the NH and carbonyl of Val^4 of hPrRP(25-31) (Figure 18b) completely locking the orientation of the ligand backbone in this region. The commercially available peptide analogue, [$pGlu^1$, Trp^2, Lys^3, Leu^4] hPrRP(25-31), was also docked into the GPR10 model. It was found that the terminal Arg-Phe-$CONH_2$ formed identical interactions with the receptor as had hPrRP(25-31). [$pGlu^1$, Trp^2, Lys^3, Leu^4] hPrRP(25-31), however, is a heptapeptide with a lysine residue in position 3 (Lys^3; Figure 17). Sequentially, therefore, it cannot align directly with hPrRP(25-31). Despite this, the lysine was able to adopt an acceptable rotameric state where it could still form a salt bridge with D302 of the receptor. This, however, placed the N-terminal pyroglutamate in a different pocket to that of hPrRP(25-31). As shown in Figure 19, the two peptides still overlay very closely in their bound conformations.

On the basis of these docking studies, the acidic and amido residues above were identified as targets for SDM studies. It was very important to carry out complementary SDM studies along with the modelling and docking as without such biological validation the homology model remains simply hypothetical. It was also particularly interesting to gain support for the predicted binding hypotheses because this was the first time that a theoretically derived loop structure for a 7TM receptor has suggested critical binding elements in its sequence. If the hypothesis was correct then this would provide support to the loop construction methodology. The following mutant constructs of GPR10 were made: Q141A, E202A, E212A, E213A, N298A, D302A and Q317A; sites of these residues are shown on the schematic model of GPR10; Figure 20). Mutations to alanine were employed in order to remove the amino acid side-chains beyond the β-carbon whilst maintaining the α-helical structure of the transmembrane domains to minimise any gross changes to receptor conformation.

(iii) HEK293-GPR10 SDM [^{125}I]-hPrRP-20 saturation binding assays

Saturation binding was carried out on membranes prepared from HEK293 cells transiently expressing either wild-type GPR10 (two separate transfections and membrane preparations) or mutant GPR10 constructs (single transfection and membrane preparation) to determine the effects of the point mutations on the K_D and B_{max} of [^{125}I]-hPrRP-20 binding. Specific binding of [^{125}I]-hPrRP-20 to membranes from HEK293 cells transiently transfected with wild-type GPR10 displayed similar high and low affinity K_D and B_{max} values to those of the stable cell line (Chapter 3; Langmead *et al.*, 2000). Specific binding of [^{125}I]-hPrRP-20 to transiently expressed GPR10 represented more than 90% of total binding and was saturable, whereas non-specific binding increased linearly with radioligand concentration. Analysis of binding data revealed that [^{125}I]-hPrRP-20 bound to two sites on the HEK293-GPR10 membranes with K_D values of 0.05 ± 0.01 nM and 1.55 ± 0.52 nM, with respective B_{max} values of 2605 ± 1072 fmol mg protein^{-1} and 6275 ± 800 fmol mg protein^{-1}.

Individual K_D and B_{max} values for each receptor construct are reported in Table 7. GPR10-E213A, GPR10-D302A and GPR10-Q317A displayed no specific binding at radioligand concentrations of up to 6 nM. GPR10-E212A exhibited 2 site binding with ~80% specific binding and a similar B_{max} for the low affinity site (6196 ± 1602 fmol / mg) as for the wild-type receptor (6275 ± 800 fmol / mg). However, the B_{max} for the high affinity site was much reduced (421 ± 90 fmol / mg) and the K_D value for the high affinity site (0.0036 ± 0.0007 nM) was actually lower than the wild-type (0.050 ± 0.012 nM). GPR10-Q141A and GPR10-N298A exhibited relatively unchanged K_D values of 0.050 ± 0.004 and 0.085 ± 0.018 nM, respectively, but lower B_{max} values for the high affinity site (519 ± 43 and 251 ± 25 fmol / mg, respectively). Binding to the lower affinity site in these two mutants was extremely difficult to discern and, despite these saturation isotherms

Figure 19. Overlay of hPrRP(25-31) [pGlu^{1}, Trp^{2}, Lys^{3}, Leu^{4}] hPrRP(25-31) in their receptor bound conformations. The alpha carbons of hPrRP(25-31) are in yellow and those of [pGlu^{1}, Trp^{2}, Lys^{3}, Leu^{4}] hPrRP(25-31) are in silver.

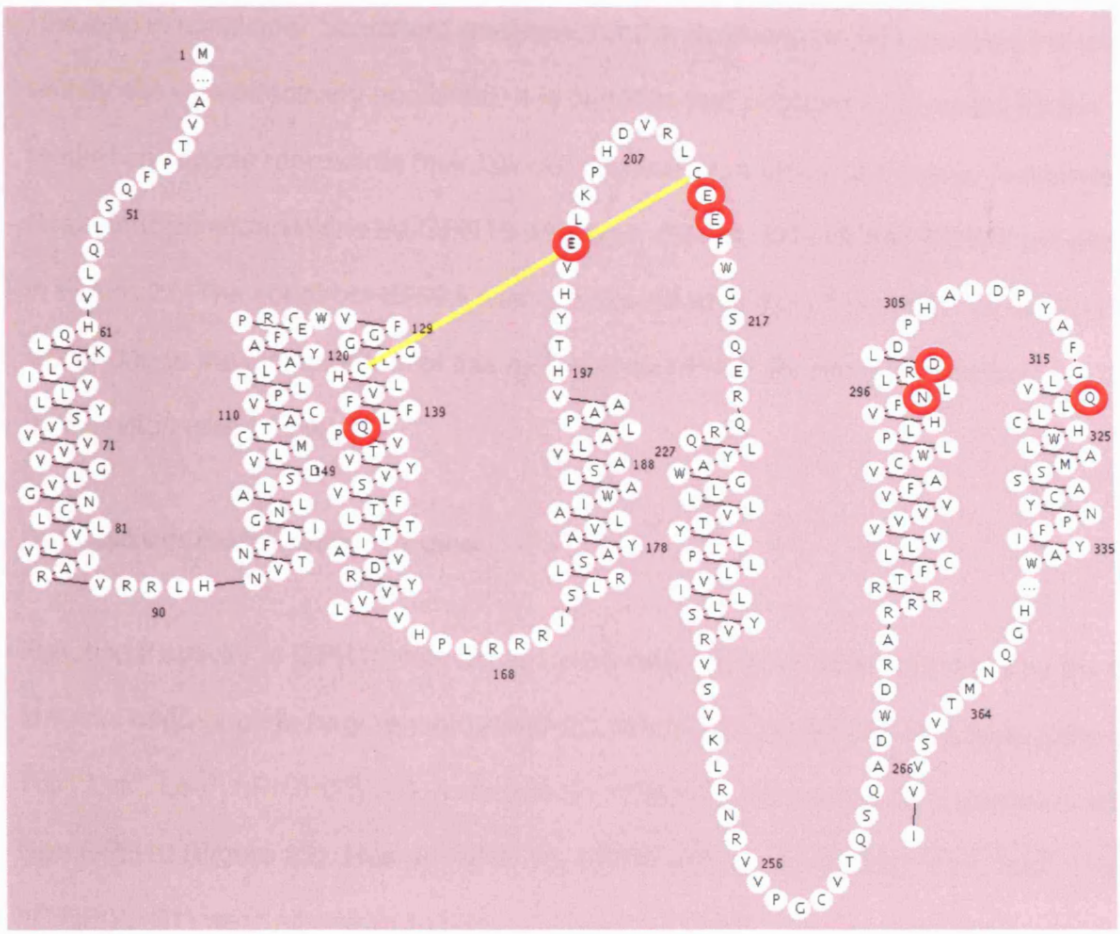

Figure 20. Schematic representation of GPR10 highlighting key residues which were predicted to be involved in interactions with hPrRP(25-31); the residues circled in red were mutated. The yellow bar represents a disulphide bond. For reasons of clarity both the C-terminus and N-terminus have been truncated.

resulting in curvilinear Scatchard analyses, for the purposes of data analysis the low affinity site was effectively abolished. It is possible that reduced B_{max} values for the mutant constructs represents their low cell surface expression. Saturation isotherms and Scatchard transformations for GPR10-wild-type, E212A, Q141A and N298A are shown in Figure 21. The construct E202A was not examined in the [^{125}I]-hPrRP-20 binding assay due to the lack of effect of this mutation on hPrRP-20 stimulated calcium mobilisation (see below).

(iv) Calcium mobilisation studies

Functional activity at GPR10 was shown to be retained even when activated by the C-terminal heptapeptide fragment of hPrRP-20, hPrRP(25-31) and its analogue, [pGlu^1, Trp^2, Lys^3, Leu^4] hPrRP(25-31), as tested on HEK293 cells transiently expressing wild-type GPR10 (Figure 22). Human PrRP-20, hPrRP(25-31) and [pGlu^1, Trp^2, Lys^3, Leu^4] hPrRP(25-31) were all shown to be full agonists, with pEC_{50} values of 9.54 ± 0.12, 7.39 ± 0.08 and 6.55 ± 0.02, respectively. Table 8 reports the potency of hPrRP-20, hPrRP(25-31) and [pGlu^1, Trp^2, Lys^3, Leu^4] hPrRP(25-31) at a range of transiently expressed mutant GPR10 receptors. Structures of hPrRP-20 and other peptide analogues are shown in Figure 17.

The individual mutation Q141A caused a significant 3-fold reduction in the potency of hPrRP-20 to stimulate calcium mobilisation and reduced the potency of hPrRP(25-31) and pGlu^1, Trp^2, Lys^3, Leu^4] hPrRP(25-31) by 10-fold. N298A produced an approximately 10-fold reduction in the potency of all three peptides. E213A, Q317A and D302A had more marked effects on agonist potencies (Figure 23; Table 8). causing greater than 100-fold reductions in the potency of hPrRP-20 and effectively abolishing the agonist activity of hPrRP(25-31) and [pGlu^1, Trp^2, Lys^3, Leu^4] hPrRP(25-31) at GPR10. The point mutation E202A did not significantly affect the potency of hPrRP-20;

Receptor	$K_{D\,1}$ (nM)	$B_{max\,1}$ (fmol/mg)	$K_{D\,2}$ (nM)	$B_{max\,2}$ (fmol/mg)
wild-type	0.050 ± 0.012	2605 ± 1072	1.55 ± 0.52	6275 ± 800
Q141A	0.050 ± 0.004	519 ± 43	n.d.	n.d.
E202A	-	-	-	-
E212A	0.0036 ± 0.0007	421 ± 90	0.75 ± 0.14	6196 ± 1602
E213A	n.d.	n.d.	n.d.	n.d.
N298A	0.085 ± 0.018	251 ± 25	n.d.	n.d.
D302A	n.d.	n.d.	n.d.	n.d.
Q317A	n.d.	n.d.	n.d.	n.d.

Table 7. K_D and B_{max} values for [^{125}I]-hPrRP-20 binding to membranes from HEK293 cells transiently expressing wild-type and mutant GPR10 constructs. n.d. indicates no detectable low affinity binding site (Q141A and N298A) or no specific binding at [^{125}I]-hPrRP-20 concentrations of up to 6 nM (E213A, D302A, Q317A). GPR10-E202A was not tested in the [^{125}I]-hPrRP-20 binding assay. Data represents the mean of 3 separate experiments (± s.e.m.).

A

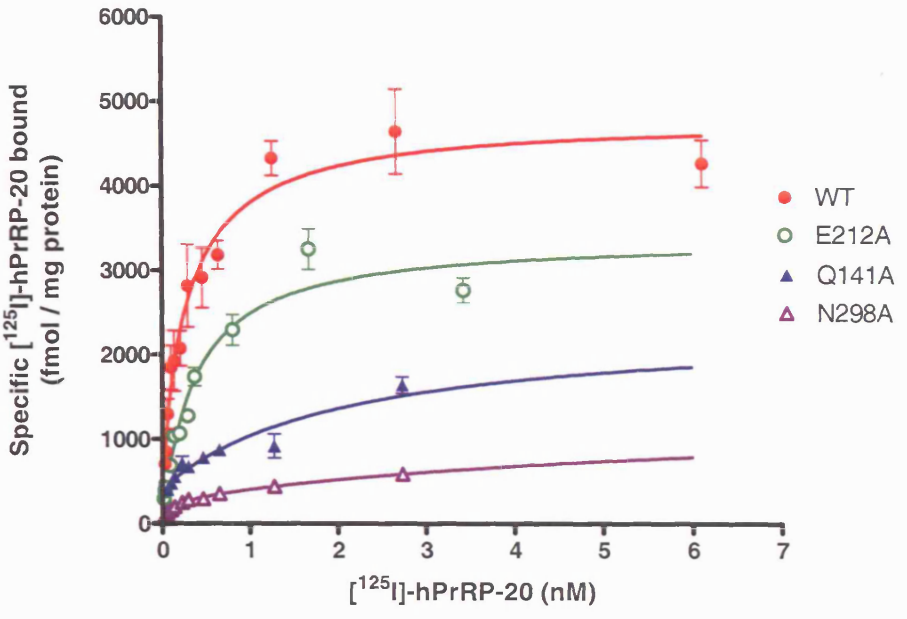

B

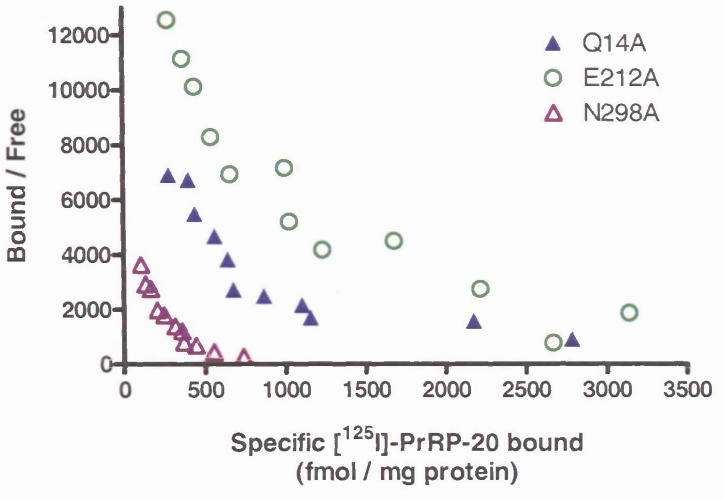

Figure 21. Saturation analyses (A) and Scatchard transformations (except wild-type) (B) of specific binding of [^{125}I]-hPrRP-20 to membranes from HEK293 cells transiently expressing GPR10-WT, GPR10-E212A, GPR10-Q141A and GPR10-N298A. Data are from a single representative experiment with each point determined in duplicate.

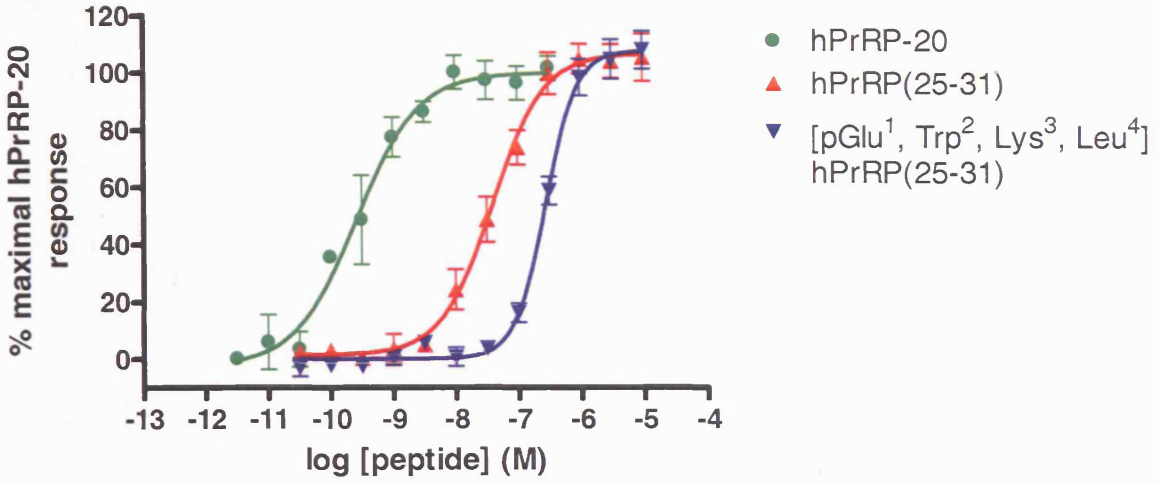

Figure 22. Concentration-dependent stimulation of intracellular Ca^{2+} mobilisation in HEK293 cells transiently expressing wild-type GPR10 by hPrRP-20, hPrRP(25-31) and [$pGlu^1$, Trp^2, Lys^3, Leu^4] hPrRP(25-31). Data are the means of 3 experiments; error bars show s.e.m..

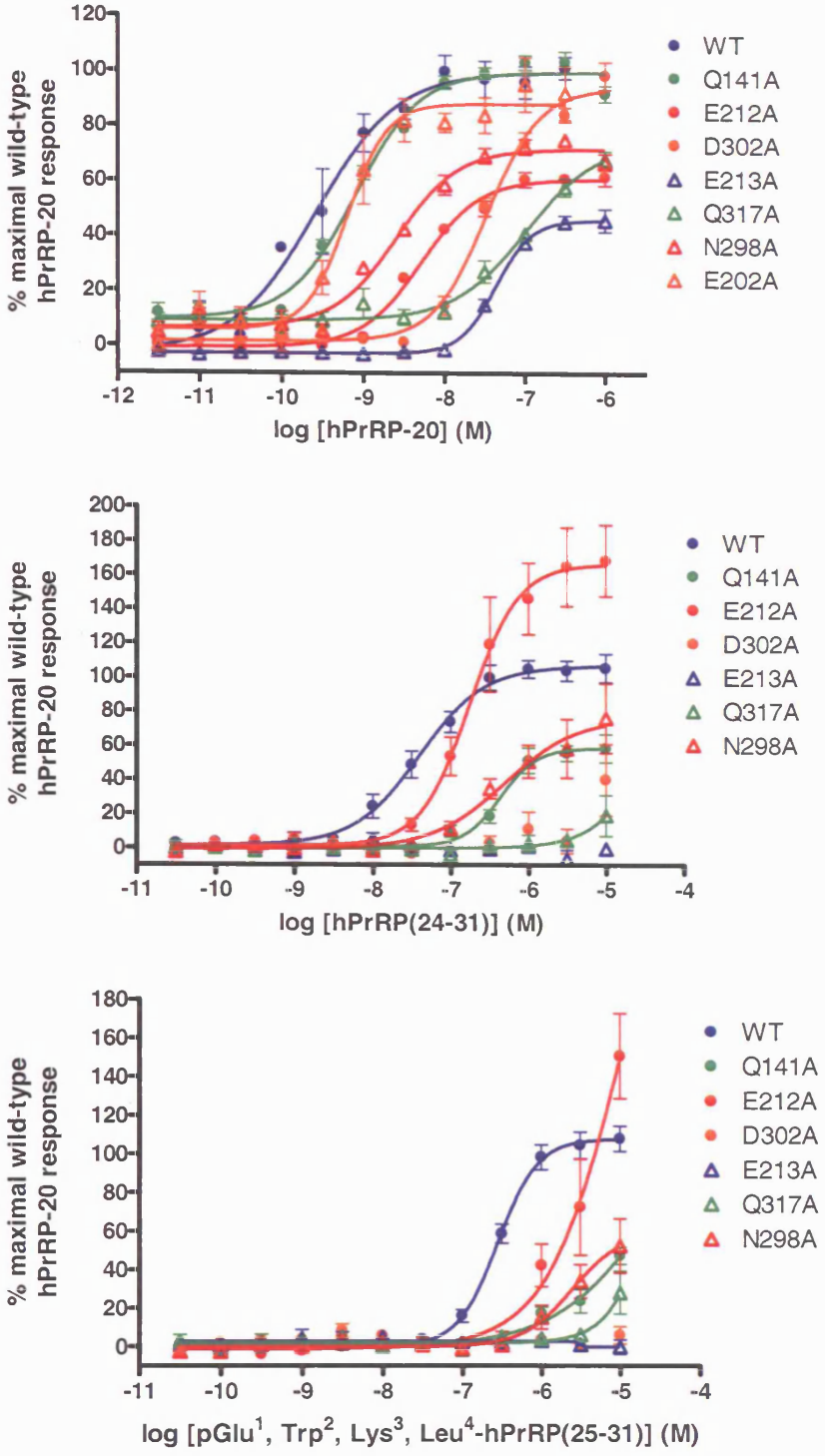

Figure 23. Concentration-dependent stimulation of Ca^{2+} mobilisation by hPrRP-20, hPrRP(25-31) and [pGlu^1, Trp^2, Lys^3, Leu^4] hPrRP(25-31) at wild type and mutant GPR10 receptor constructs transiently expressed in HEK293 cells. Data are the mean of 8 (hPrRP-20) or 3 (heptapeptides) experiments; error bars show s.e.m..

Receptor / Ligand	h-PrRP-20	h-PrRP(25-31)	[pGlu^1, Trp^2, Lys^3, Leu^4] hPrRP(25-31)
wild-type	9.54 ± 0.12	7.39 ± 0.08	6.55 ± 0.02
Q141A	9.09 ± 0.04**	6.44 ± 0.22*	5.36 ± 0.16**
E202A	9.29 ± 0.03	-	-
E212A	8.27 ± 0.05***	6.68 ± 0.10**	5.43 ± 0.16**
E213A	7.39 ± 0.05***	< 5***	< 5***
N298A	8.59 ± 0.07***	6.47 ± 0.16**	5.63 ± 0.19**
D302A	7.44 ± 0.08***	< 5***	< 5***
Q317A	7.07 ± 0.04***	< 5***	< 5***

Table 8. pEC_{50} values (± s.e.m.) for Ca^{2+} mobilisation by hPrRP-20, hPrRP(25-31) and [pGlu^1, Trp^2, Lys^3, Leu^4] hPrRP(25-31) at wild type and mutant GPR10 constructs transiently expressed in HEK293 cells. Data are the means of 8 (hPrRP-20) or 3 (heptapeptides) experiments. The heptapeptide fragments were not tested at GPR10-E202A.

* $p < 0.05$; ** $p < 0.01$; *** $p < 0.001$ significantly different from wild-type response (Student's T-test).

due to the minimal effect on potency the heptapeptide fragments were not tested against this construct.

(v) HEK293-GPR10 SDM [^{125}I]-PrRP-20 inhibition binding assays

[^{125}I]-PrRP-20 inhibition binding assays were performed to determine whether the effects observed in the functional studies were reflected in the binding affinities of the three test peptides. Human PrRP-20, h-PrRP(25-31) and [pGlu^1, Trp^2, Lys^3, Leu^4] hPrRP(25-31) inhibited [^{125}I]-hPrRP-20 specific binding in membranes from HEK293 cells transiently expressing wild-type GPR10 or GPR10-E212A in a concentration-dependent manner. Peptide affinities at both GPR10-WT and GPR10-E212A are shown in Table 9. Of the SDM constructs, only GPR10-E212A displayed sufficient levels of specific binding to yield robust inhibition curves.

(vi) Discussion

GPR10 is a relatively novel GPCR which has been characterised by a number of groups (Hinuma *et al.*, 1998; Satoh *et al.*, 2000; Langmead *et al.*, 2000). It has two endogenous ligands, known as the prolactin releasing peptides, PrRP-20 and PrRP-31. Both are high affinity, equipotent, full agonists at GPR10 (Chapter 3; Langmead *et al.*, 2000). Specific binding of [^{125}I]-hPrRP-20 to membranes from HEK293 cells transiently transfected with wild-type GPR10 displayed similar high and low affinity K_D and B_{max} values to those of the stable cell line (Chapter 3; Langmead *et al.*, 2000). Analysis of binding data revealed that [^{125}I]-hPrRP-20 bound to two sites on the HEK293-GPR10 membranes with K_D values of 0.05 ± 0.01 nM and 1.55 ± 0.52 nM, with respective B_{max} values of 2605 ± 1072 fmol mg protein^{-1} and 6275 ± 800 fmol mg protein^{-1}. Human PrRP-20 was a potent agonist at wild-type GPR10 transiently expressed in HEK293 cells, with a pEC_{50} value of 9.54 ± 0.12. This value agrees well

Ligand / Receptor	GPR10-WT	GPR10-E212A
hPrRP-20	10.09 ± 0.17	9.68 ± 0.08
hPrRP(25-31)	7.28 ± 0.04	7.21 ± 0.06
[pGlu^1, Trp^2, Lys^3, Leu^4] hPrRP(25-31)	6.33 ± 0.09	6.24 ± 0.11

Table 9. pK_i (± s.e.m.) values of hPrRP-20, hPrRP(25-31) and [pGlu^1, Trp^2, Lys^3, Leu^4] hPrRP(25-31) to inhibit binding of [^{125}I]-hPrRP-20 from membranes of HEK293 cells transiently expressing GPR10-WT and GPR10-E212A. Data are the mean of 3 experiments.

with previously reported potencies of hPrRP-20 at GPR10 (Langmead *et al.*, 2000; Roland *et al.*, 1999; Wilson *et al*, 1998). A C-terminal heptapeptide fragment of hPrRP-20, hPrRP(25-31), and a similar heptapeptide analogue, [pGlu^1, Trp^2, Lys^3, Leu^4] hPrRP(25-31) (Figure 17), retained significant functional agonist activity at GPR10, with pEC_{50} values of 7.39 ± 0.08 and 6.55 ± 0.02, respectively. Furthermore, hPrRP-20 (pK_i = 10.09 ± 0.17), hPrRP(25-31) (7.28 ± 0.04) and [pGlu^1, Trp^2, Lys^3, Leu^4] hPrRP(25-31) (6.33 ± 0.09) displayed affinities to inhibit [^{125}I]-hPrRP-20 binding from membranes of HEK293 cells transiently expressing GPR10 that were in extremely good agreement with their respective functional potencies.

These data suggest that the C-terminal portion of PrRP-20 is sufficient for binding and receptor activation. These observations are consistent with previous studies, which demonstrated that substantial functional activity and binding affinity were retained in C-terminal hexapeptide and heptapeptide fragments of hPrRP-20 (Roland *et al.*, 1999; Danho *et al.*, 2003) and confirm the tolerance of Lys in place of Arg^2 in the C-terminal heptapeptide (Boyle *et al.*, 2005). However, the potency of hPrRP(25-31) was reduced over 100-fold compared to hPrRP-20, suggesting that the N-terminal portion of hPrRP-20 must contribute to the higher potency of the longer peptide - either by stabilising the C-terminal portion of the peptide in its binding pocket or by a direct interaction with the receptor.

In this study molecular modelling has been used to predict the key residues of GPR10 for binding hPrRP-20. This involved the construction of an homology model of the GPR10 receptor, based on the crystal structure of bovine rhodopsin, followed by manual docking of the two heptapeptide ligands into potential binding sites. Site directed mutagenesis (SDM) to alanine was then performed to determine the involvement of specific amino acid residues, identified by modelling, in [^{125}I]-hPrRP-20 radioligand binding and functional calcium mobilisation assays. Point mutations of

residues to alanine is a commonly used technique as this simple residue contains no polar or aromatic side chains, yet maintains the α-helical structure of the transmembrane domains to minimise any gross changes to receptor conformation. Mutations of residues to alanine can help identify specific side-chains that are involved in ligand – receptor interactions. However, changes to the amino acid sequence of a receptor can also result in indirect conformational effects on ligand binding, hence SDM data needs to be considered carefully. A similar modelling - SDM approach has been used in the past for a number of 7TM receptors including the CCR2 (Berkhout *et al.*, 2003) and 5-HT_6 receptors (Hirst *et al.*, 2003).

Both hPrRP(25-31) and hPrRP-20 contain two basic side chains (arginine residues in positions 2 and 6) for which acidic partners were sought. Prior to the publication of the X-ray crystal structure of bovine rhodopsin, an earlier model of GPR10 had been built. This was based on a 6Å low resolution density map of bovine rhodopsin as determined by cryoelectron diffraction (Unger *et al.*, 1997). Models based on this information (Blaney *et al.*, 2001) had good alignment of the helical axes but were not able to accurately place the amino acid residues. Docking of hPrRP(25-31) into this model, which did not contain the extracellular loops, predicted the interactions of Arg^2 with E202 (located at the extracellular end of TM4) and Arg^6 with D302. The new crystal-based model, however, suggested that TM4 was twisted around its axis relative to the earlier model and therefore, that E202 was no longer accessible to ligands. D302 was still accessible but now all acceptable docking solutions proposed a salt bridge between Arg^2 of hPrRP(25-31) and this TM6 aspartate (Figure 18). In accordance with this prediction, studies showed that mutation of D302 abolished specific binding of [^{125}I]-hPrRP-20 and drastically reduced the potencies of the agonist peptides to stimulate calcium mobilisation. Despite the absence of specific radioligand binding, functional responses were observed with this construct due to the wider range of peptide concentrations tested in this functional assay format i.e.

up to 1 μM. The EC_{50} of hPrRP-20 at D302A was approximately 30 nM. Assuming that the K_D of hPrRP-20 is equal to (or greater than) the EC_{50} value determined in the functional assay, it is not surprising not to detect any specific binding at [^{125}I]-hPrRP-20 concentrations of up to only 6 nM.

In contrast to the effect upon loss of D302, E202A had little effect on the potency of hPrRP-20 to stimulate calcium mobilisation compared to wild-type GPR10. These data confirm the anticipated lack of role for E202 in the binding of hPrRP-20 and also the expected crucial role of D302.

In the latest model containing the extracellular loops, Arg^6 of hPrRP(25-31) was consistently predicted to form a salt bridge with E213 in the second extracellular loop (ECL2). In accordance with this prediction, the mutation E213A abolished the specific binding of [^{125}I]-hPrRP-20 and reduced the potency of hPrRP-20 to stimulate calcium mobilisation by more than 100-fold. As with D302A, this construct appeared functional despite a lack of specific [^{125}I]-hPrRP-20 binding. Again, this observation is probably a reflection of the much higher peptide concentrations tested in the functional assay compared to the binding assay. Furthermore, the agonist activity of hPrRP(25-31) and [pGlu^1, Trp^2, Lys^3, Leu^4] hPrRP(25-31) was abolished, suggesting that this second salt bridge is very important for agonist binding.

In previous studies, alanine substitution of Arg^2 or Arg^6 of hPrRP(25-31), or longer C-terminal peptide fragments resulted in a profound reduction in either PrRP affinity (Roland *et al.*, 1999) or potency (Boyle *et al.*, 2005) at GPR10. The data presented here correlate well with previous observations of the importance of Arg^2 and Arg^6 to the function of hPrRP(25-31) (Roland *et al.*, 1999; Boyle *et al.*, 2005). Of the two arginine residues, Arg^6 appears to be especially important to peptide binding as even a conservative substitution to Lys abolishes both binding affinity and functional

potency at GPR10 (Boyle *et al.*, 2005). However, substitution of Arg^2 for Lys is well tolerated, with only a six-fold reduction in potency and little change in affinity (Boyle *et al.*, 2005). Furthermore, an arginine residue in neuropeptide-Y (NPY; Arg^{35}) that aligns with Arg^{30} of hPrRP-31 (Arg^6 of hPrRP(25-31)) is crucial to NPY binding affinity at all cloned NPY receptor subtypes (Cabrele & Beck-Sickinger, 2000).

It is interesting to note the predicted interaction between E213 and Arg^6 of hPrRP(25-31) and the dramatic effect of the mutation of this residue. Given the importance of the penultimate arginine residue to hPrRP-20, hPrRP(25-31) and [$pGlu^1$, Trp^2, Lys^3, Leu^4] hPrRP(25-31) activity and the conservation of this residue amongst other RF-amide peptides (Han *et al.*, 2002), it is not surprising that the corresponding glutamate residue of GPR10 appears to be conserved in the RF-amide peptide receptors NPFF-1, NPFF-2 and GPR54.

Assuming that the Arg^6 - E213 interaction was correct, this gave further credence to the placement of the C-terminal phenylalanine (Phe^7) carboxamide. In the receptor model the terminal carboxamide of hPrRP(25-31) was predicted to form a series of hydrogen bonds with Q141 (TM3), E212 (ECL2) and H321 (TM7; Figure 18a). The point mutations E212A and Q141A both caused a reduction in the maximal binding capacity of, but did not abolish, the specific binding of [^{125}I]-hPrRP-20. E212A actually displays a slightly lower K_D for both the high and low affinity [^{125}I]-hPrRP-20 binding sites, but this observation is not reflected in the agonist potencies in the calcium mobilisation assay where E212A caused a 10 - 20-fold reduction in the potency of hPrRP-20 and [$pGlu^1$, Trp^2, Lys^3, Leu^4] hPrRP(25-31) and a 5-fold reduction in potency of hPrRP(25-31). Radioligand binding studies showed that loss of this glutamate residue did not significantly alter the affinity of hPrRP-20 (pK_i = 9.68 ± 0.08), hPrRP(25-31) (7.21 ± 0.06) or [$pGlu^1$, Trp^2, Lys^3, Leu^4] hPrRP(25-31) (6.24 ± 0.11) to inhibit [^{125}I]-hPrRP-20 binding to membranes of HEK293 cells transiently

expressing GPR10-E212A compared to wild-type GPR10. It is possible that these observed effects could reflect a role for E212 in the conformational change involved in receptor activation and signalling, rather than in the binding of the peptide. In the light of these somewhat mixed observations with E212A, it would be interesting to model the this construct to see how loss of this glutamate residue might be predicted to affect the interaction of hPrRP-20 with GPR10.

Q141A did not affect the K_D for the high affinity [^{125}I]-hPrRP-20 binding site, although the B_{max} was markedly reduced and the low affinity binding site was difficult to quantify and was effectively abolished. Q141A caused only 3-fold reduction in the potency of hPrRP-20 to stimulate calcium mobilisation and reduced the potency of hPrRP(25-31) and [pGlu^1, Trp^2, Lys^3, Leu^4] hPrRP(25-31) by 10-fold. These data suggest that the interactions between Q141 and E212 and the terminal carboxamide of hPrRP-20 play a role in the binding of the ligand, but neither is in itself essential to it.

A peptide ligand such as hPrRP-20 can be expected to form many interactions between its individual amino acids and the receptor. The overall binding energy will be composed of the sum of these many individual terms. Q141 and E212 were each believed to form a single hydrogen bond to the ligand. The model suggested, however, that the C-terminal phenyl ring of the peptides is tightly held in the hydrophobic pocket defined by W291, L294 (TM6) and L323 (TM7), with little conformational freedom. The removal of a single hydrogen bond to/from the carboxamide, particularly when the other is maintained, will have little entropic effect on the free energy of binding. Thus its overall effect would be expected to be much less than disruption of one of the essential interactions between E213 / D302 and the basic arginine residues of the peptide. In order to probe these theories, further studies could examine the effect of mutation of the hydrophobic residues thought to

form the binding pocket for the phenyl ring. It would also be interesting to examine GPR10 constructs containing H321A (which was not examined in this study) and both double (Q141A/E212A, Q141A/H321A, E212A/H321A) and triple (Q141A/E212A/H321A) mutants. The effect of these mutations may give greater understanding of the relative contributions of the carboxamide hydrogen bonding network and the hydrophobic interactions of Phe^7 in hPrRP-20 binding to GPR10.

This second generation receptor model, containing the extracellular loops, highlighted interactions between the ligands and two residues in ECL2, E212 and E213. It was therefore interesting to see whether these predictions, based on the inclusion in the theoretical model of extracellular loops, would be verified by the SDM studies. The successful prediction of these interactions was particularly exciting because this is the first instance of a theoretically derived loop structure for a GPCR suggesting critical interactions in the receptor model. The data for E212A and E213A, therefore, support the loop construction methodology.

The current receptor model also suggested a number of potential hydrogen bonds between the receptor and the peptide backbones of hPrRP(25-31) and [$pGlu^1$, Trp^2, Lys^3, Leu^4] hPrRP(25-31). N298 (TM6) was predicted to form a hydrogen bond with the backbone NH of Arg^6 in hPrRP(25-31). N298A, like Q141A, had little effect on the K_D of [^{125}I]-hPrRP-20 for the high affinity binding site, although it reduced the B_{max}. As for Q141A, with N298A the low affinity binding site was extremely difficult to discern and was effectively abolished. Furthermore, only a 10-fold reduction in potency was observed in the agonist responses of hPrRP-20, hPrRP(25-31) and [$pGlu^1$, Trp^2, Lys^3, Leu^4] hPrRP(25-31) in FLIPR studies. These data suggest that like Q141, N298 is involved in a single hydrogen bonding interaction which has a small but significant effect on ligand binding and receptor activation.

The ligand backbone region of Gly^3 and Val^4 (Leu^4 in [$pGlu^1$, Trp^2, Lys^3, Leu^4] hPrRP(25-31)) is a potentially flexible stretch that will define the relative interactions of the Arg^2 and Arg^6 residues and other peptide residues with the receptor. Q317 (TM7) was predicted to form a double hydrogen bond with both the backbone carbonyl and amide NH of Val^4 of hPrRP(25-31), completely locking the orientation of the heptapeptide in this region of the pocket. The loss of this double hydrogen bond in an essential part of the binding pocket would be predicted to lead to a large increase in the entropic freedom of the ligands. Unsurprisingly, Q317A abolished specific binding of [^{125}I]-hPrRP-20 and dramatically reduced the potencies of the agonist peptides, supporting previous studies that suggested that the free NH on the backbone was one of the main reasons that a valine residue was preferred in this position of hPrRP-20 (Boyle *et al.*, 2005).

Taken together, the [^{125}I]-hPrRP-20 binding and functional calcium mobilisation data with the SDM constructs largely validate the constructed theoretical model of GPR10. The model predicted strong interactions of the peptides with E213, D302 and Q317 and the mutations of these residues have dramatic effects on both peptide binding and receptor activation. The lack of specific binding of [^{125}I]-hPrRP-20 with mutation of these residues is likely to be a result of a greatly reduced affinity for the peptide (as well as any additional effects on B_{max}) as these constructs are functionally responsive to hPrRP-20 in the calcium mobilisation assay but with greatly reduced potencies compared to wild-type GPR10.

These results provide compelling evidence to implicate D302, E213 and Q317 in peptide binding and receptor activation. An exciting aspect of the modelling-SDM studies was that, based on a novel loop building algorithm, predictions were made about potential binding sites in the second extracellular loop of GPR10. SDM

experiments have strongly supported these hypotheses which gives added validity to this new methodology.

However, further credence to the predicted molecular nature of the interactions could be gained from complementary mutation studies. Given the predicted interaction between D302 and Arg^2 of hPrRP(25-31), a mutant receptor construct containing D302R would be predicted to be unresponsive to hPrRP(25-31), but should be activated by an analogue of hPrRP(25-31) in which Asp was substituted for Arg^2 and an analogue of [$pGlu^1$, Trp^2, Lys^3, Leu^4] hPrRP(25-31) in which Lys^3 was replaced by Asp. Similarly, a construct containing E213R would be expected to be activated by an analogue of hPrRP(25-31) in which Arg^6 was substituted by Glu. Additionally, if Q317A abolished [^{125}I]-hPrRP-20 binding due to the loss of a carboxamide side-chain, then a construct containing Q317N may be expected to retain some degree of ligand affinity. However, these studies would be somewhat ambitious as one of the perceived drawbacks of SDM studies is that effects observed may not be due to alteration in specific ligand-residue interactions, but rather due to a local or global change in the receptor conformation. In complementary mutation studies, these issues would be exacerbated due to changes in both the receptor and agonist peptide sequences that would render results potentially more difficult to interpret.

E212, Q141 and N298 all also form interactions with the C-terminal heptapeptide of PrRP-20, although these do not appear to have as great an effect, as their mutation has more limited effects on [^{125}I]-hPrRP-20 binding, reducing the B_{max} of the high affinity site (E212A, Q141A and N298A) with little effect on K_D. Furthermore, for Q141A and N298A, despite non-linear Scatchard plots, the low affinity binding site was extremely difficult to quantify and for the purposes of data analysis was considered to be effectively abolished. In keeping with these observations, the effect of these mutations on the potency of the agonist peptides was limited to

approximately a 10-fold or less reduction. It is possible that these reductions in potency are a result of reduced receptor expression (as exemplified by a reduced B_{max}), possibly due to enhanced agonist-induced receptor internalisation. This would result in a reduced functional receptor reserve in the calcium mobilisation assay compared to the wild-type receptor. However, intuitively it would be expected that the greater the signal amplification, the more potent an agonist may appear to be in a given assay system (Kenakin, 1997). A calcium mobilisation assay would be expected to be subject to much greater signal amplification than an inositol phosphate accumulation assay, yet hPrRP-20 is approximately 5-fold more potent in stimulating the latter compared to the former (Chapter 3). This suggests that there is actually relatively little, if any, signal amplification in the transiently expressed GPR10 calcium mobilisation assays and that any apparent reduction in potency may be a genuine consequence of impaired ligand binding or receptor activation.

This study has led to the identification of a number residues essential to both [^{125}I]-hPrRP-20 binding and receptor function (E213, D302 and Q317). However, SDM and modelling studies cannot possibly predict all ligand – receptor interactions so it is likely that there are as yet unidentified residues that contribute towards both peptide binding and receptor signalling. Hopefully the combined knowledge of these studies, together with the existing data on the structural features of hPrRP-20 required for potency and affinity at GPR10 (Boyle *et al.*, 2005) may lead to a greater understanding of the molecular nature of PrRP binding and receptor activation.

One aspect of the binding of [^{125}I]-hPrRP-20 that was not resolved by the SDM studies was the existence of both high and low affinity binding sites. As discussed in Chapter 3 this could be a result of either high and low agonist affinity states or two topographically distinct binding sites for hPrRP-20. Both transiently expressed GPR10 wild-type and E212A constructs retained two site binding, but it was

impossible to accurately define the low affinity binding site for both Q141A and N298A, even though Scatchard plots were still apparently curvilinear. It is possible that the apparent 'loss' of these binding sites was due to the limitations of the assay conditions (if the K_D for the low affinity site was increased at Q141A or N298A then it may fall outside the [^{125}I]-hPrRP-20 concentration range of the assay). It is possible, therefore, that given a larger concentration range it may have been feasible to resolve two binding sites for all the SDM constructs that displayed specific [^{125}I]-hPrRP-20 binding.

The identification of residues for SDM was based on docking of the two C-terminal heptapeptides, hPrRP(25-31) and [pGlu^1, Trp^2, Lys^3, Leu^4] hPrRP(25-31), rather than hPrRP-20 itself. Thus, the model does not take into account any additional interactions that may be made by the N-terminal 13 amino acids of hPrRP-20. It has already been noted that the full length peptide is 100-fold more potent than the C-terminal heptapeptide truncate at GPR10, implying that there is a substantial role for the N-terminal residues of hPrRP-20 in either stabilising the C-terminus in its binding pocket or in making their own interactions with the receptor. Any additional interactions of hPrRP-20 could explain both the two-site profile observed with [^{125}I]-hPrRP-20 and also why SDM studies based only on the C-terminal portion of the peptide failed to delineate the two sites. Unfortunately, it is not possible to accurately model the docking of hPrRP-20 itself – whilst the C-terminus of the peptide is thought to form a regular α-helical structure, the N-terminal region is much more flexible (D'Ursi *et al.*, 2002) and difficult to dock into the model with great accuracy. In this context, a very useful tool would be a radiolabelled form of the truncate, hPrRP(25-31). Despite its lower affinity, it would be interesting to observe the saturation binding profile of such a ligand to GPR10. If such a ligand were to display single site binding it would by virtue implicate the N-terminal region of hPrRP-20 in binding to a second site. Clearly there are numerous further studies suggested both here and in Chapter

3 that may help to elucidate the cause of the two-site nature of [^{125}I]-hPrRP-20 binding to GPR10.

Chapter 5

Pharmacological characterisation of muscarinic M_1 receptor ectopic agonists

(i) Introduction

(a) Allosterism at muscarinic receptors

As discussed in the Introduction, allosteric ligands acting at muscarinic receptors provide some of the best characterised examples of allosterism at GPCRs. Ligands such as gallamine, alcuronium, C_7/3-phth, brucine and closely related analogues have all been shown to have varying allosteric effects on muscarinic receptors. Analogues of brucine have been shown to be positive modulators of ACh with varying degrees of selectivity at muscarinic receptors. Brucine and brucine *N*-oxide are selective enhancers of M_1 and M_4 receptor subtypes, whereas NCMB selectively enhanced the actions of ACh at the M_2 and M_3 receptor subtypes, while remaining neutrally co-operative at the M_4 receptor subtype (Birdsall *et al.*, 1999). More recent data has identified thiochrome as a selective enhancer of the M_4 receptor subtype whilst remaining neutrally co-operative at the remaining muscarinic receptor subtypes (Lazareno *et al.*, 2004).

The best characterised of the negatively co-operative ligands is gallamine, whose allosteric properties were first described by Clark & Mitchelson (1976) and Stockton *et al.* (1983). Gallamine has been shown to be negatively co-operative with respect to [^{3}H]NMS at all muscarinic receptor subtypes (Gnagey *et al.*, 1999), as has C_7/3-phth (Christopoulos *et al.*, 1999). Gallamine is also negatively co-operative with respect to [^{3}H]QNB in cardiac and smooth muscle membranes (representing populations largely composed of M_2 and M_3 receptors, respectively; Nedoma *et al.*, 1986). Alcuronium is similarly negatively co-operative with respect to [^{3}H]QNB (Nedoma *et al.*, 1986). However, alcuronium is positively co-operative with respect to [^{3}H]NMS binding in rat atrial, ileal and cerebellar membranes (Tucek *et al.*, 1990) and CHO cells stably expressing the human M_2 receptor (Christopoulos, 2000), but negatively co-operative

with respect to [^{3}H]NMS in cortical and salivary gland membranes (Tucek *et al.*, 1990). These results underline the importance of interpreting results with allosteric ligands with reference to the orthosteric ligand. The phenomenon is known as 'probe-dependence', hence for therapeutic targets allosteric ligands should always be tested versus the endogenous agonist where possible.

Despite alcuronium and gallamine and C_7/3-phth having opposing effects on equilibrium binding of [^{3}H]NMS (Christopoulos *et al.*, 1999; Avlani *et al.*, 2004), all three ligands retard [^{3}H]NMS dissociation from CHO-M_2 receptor cell membranes (Avlani *et al.*, 2004). This seems counter-intuitive with their supposed opposing effects on the affinity of [^{3}H]NMS for the receptor. This is thought to be due to location of the binding site for these ligands, which is believed to lie extracellular to the orthosteric binding site (see below). It may well be that there is a component of steric hindrance with the binding of these modulators that precludes orthosteric ligand access to its binding site as well as (in the case of gallamine and C_7/3-phth) or opposed to (in the case of alcuronium) the effect of the modulator on the receptor affinity for the orthosteric ligand (Tucek & Proska, 1995).

Despite circumstantial evidence that the gallamine binding site is near, but extracellular to, the orthosteric site, the last few years has seen an increased interest in trying to identify residues involved in the interaction with these ligands. In general, gallamine-like allosteric ligands have highest affinity for the M_2 receptor subtype, with an approximate order of affinity as follows: $M_2 > M_1 = M_4 > M_3 = M_5$ (Gnagey *et al.*, 1999). Studies have identified a number of residues that may play a role in the binding of gallamine. The asparagine residue at position 419 (in the third outer loop) of the M_2 receptor has been identified as a key contact point, as mutation of the equivalent residue, valine, in the M_5 receptor subtype to asparagine, increases the affinity to that seen in the M_2 receptor subtype (Gnagey *et al.*, 1999). The equivalent

residue in the M_1 receptor is glutamate 397 (E397). Of similar importance appears to be the Glu-Asp-Gly-Glu motif (EDGE motif) in ECL2 of the M_2 receptor; replacement of this motif with the equivalent residues found in the M_1 receptor (LAGQ) reduced the affinity of gallamine (Gnagey *et al.*, 1999). Conversely, replacement of the LAGQ motif with the EDGE motif in the M_1 receptor increased the affinity for gallamine (Gnagey *et al.*, 1999). Other studies have implicated the tryptophan residues in positions 101 and 400 in the binding of gallamine to the M_1 receptor (Matsui *et al.*, 1995) and also suggest that the gallamine binding site is very close to the orthosteric site.

More recent studies have identified a second allosteric site on muscarinic receptors (Lazareno *et al.*, 2000). These studies identified staurosporine analogues and particularly KT5720 ((9S,10S,12R)-2,3,9,10,11,12-hexahydro-10-hydroxy-9-methyl-1-oxo-9,12-epoxy-1H-diindolo[1,2,3,-fg:3',2',1'-kl]pyrrolo[3,4-i][1,6]benzodiazocine-10-carboxylic acid hexyl ester) as allosteric ligands at muscarinic receptors, especially at the M_1 receptor subtype. These ligands enhanced the binding affinity of [^{3}H]NMS at the M_1 and M_2 receptor subtypes, with no effect on the equilibrium binding at the M_3 and M_4 receptor subtypes (Lazareno *et al.*, 2000; Birdsall *et al.*, 2001). Unlike a number of conventional allosteric ligands to muscarinic receptors, these analogues had more limited effects on the dissociation rate of [^{3}H]NMS. This interesting phenomenon allowed the authors to investigate whether KT5720 was capable of reversing the large inhibition of [^{3}H]NMS dissociation observed with conventional allosteric ligands. This reversal effect has been seen with another, weak, muscarinic receptor allosteric ligand, obidoxime, which also has a limited effect on [^{3}H]NMS dissociation (Ellis & Seidenberg, 1992). Surprisingly, KT5720 failed to alter the effects of gallamine at the M_1 receptor (Lazareno *et al.*, 2000; Birdsall *et al.*, 2001). These data suggested that KT5720 and gallamine do not bind to the same site, but that both bind to different sites and can be simultaneously bound to a [^{3}H]NMS

occupied receptor, with neutral co-operativity ($\alpha = 1$) with respect to each other. Clearly further studies are required to define the molecular nature of this second allosteric site on muscarinic receptors.

A number of snake venom toxins have also been shown to be highly selective antagonists of muscarinic receptors (Potter, 2001). One of the most well characterised of these polypeptide ligands is termed MT-7 (or m1-Toxin1), which displays > 10,000-fold selectivity for the M_1 receptor over the other muscarinic receptor subtypes (Mourier *et al.*, 2003). As a consequence of its size (65 aa) and its retardation of [^{3}H]NMS dissociation, this peptide is thought to interact allosterically with the extracellular loops and / or N-terminus of the M_1 receptor (Krajewski *et al.*, 2001). Of the 65 residues that make up MT-7, only 7 are not conserved amongst the other six snake venom toxins, suggesting that these must account for the selectivity of this peptide. By mutation of the C-terminal Lys^{65} residue, the authors conclude that this residue interacts with an acidic residue on the extracellular face of the M_1 receptor, possibly E170 in outer loop 2, D393 in outer loop 3 or E401 at the top of TM7, all of which are unique to the M_1 receptor (Krajewski *et al.*, 2001). This is a very interesting observation, since the tryptophan in position 400 is strongly implicated in the binding of gallamine and Y404 and Y408 are likewise involved in the binding of NMS (Matsui *et al.*, 1995).

(b) Identification of AC-42 as a selective M_1 receptor agonist

Allosteric ligands seem to offer the greatest hope of developing subtype selective reagents amongst the muscarinic receptor family. Given the high degree of conservation of the orthosteric ligand binding across the receptor subtypes, it is perhaps unsurprising that selective agonists and antagonists have proved difficult to develop (Christopoulos *et al.*, 2001). Recently, Spalding and colleagues (2002) have

described a compound, AC-42, which acts as an agonist at the human M_1 receptor and exhibits a high degree of selectivity over the human M_2 – M_5 subtypes. AC-42 activates the M_1 receptor transiently expressed in NIH 3T3 cells with a pEC_{50} of 6.7 as measured using the receptor selection and amplification technology (R-SAT) cell-based functional reporter gene assay, with an intrinsic activity of approximately 0.7 compared to carbachol. However, AC-42 displays no agonist activity at the M_2, M_3, M_4 and M_5 receptors at up to 1 μM (Spalding *et al.*, 2002). AC-42 displays a similarly selective, agonist profile for M_1 against M_3 and M_5 receptors when tested in assays of phosphoinositide hydrolysis in tSA cells (a HEK293 cell line stably transfected with the SV40 T-antigen) transiently expressing these receptor subtypes (Spalding *et al.*, 2002). This response was sensitive to concentrations of atropine that blocked carbachol stimulated PI hydrolysis, suggesting that the effect was mediated *via* muscarinic receptors. AC-42 did, however, act as a low affinity antagonist at both the M_3 and M_5 receptor subtypes, with pIC_{50} values of ~ 5.

A similar selectivity profile was observed in CHO cells stably expressing either the M_2 or M_4 receptor subtypes, where AC-42 failed to significantly inhibit forskolin stimulated cAMP levels (Spalding *et al.*, 2002). AC-42 inhibited [^{3}H]NMS binding with low affinity ($pIC_{50} \approx 5$) across all five muscarinic receptor subtypes.

Subsequently, an analogue of AC-42, AC-260984 (structure undisclosed), has been shown to have similar selective agonist properties. AC-260984 also stimulates MAP kinase activity in the CA1 region of the mouse hippocampus, an area where the muscarinic receptor population is thought to be largely of the M_1 subtype (Veinbergs *et al.*, 2003). This activity was shown to be both abolished by scopolamine and absent in the M_1 receptor knockout mouse, confirming the M_1 receptor selectivity of AC-260584.

Using chimeric receptors with regions from both the M_1 and M_5 muscarinic receptor subtypes, Spalding *et al.* (2002) demonstrated that AC-42 interacted with a site distinct from the orthosteric binding site for acetylcholine. The binding site for AC-42 seemed to be formed by epitopes in the N-terminus, TM1 and the exofacial region of TM7. The molecular nature of the binding site for AC-42 is examined further in Chapter 6. In the absence of definitive proof that AC-42 was an allosteric ligand, these data prompted the authors to term AC-42 an 'ectopic' agonist, due to its interaction with a site on the M_1 receptor distinct from that recognised by carbachol.

However, much remains to be determined in respect to the mode of action of AC-42 as an agonist at the muscarinic M_1 receptor. The studies in this chapter were designed to characterise fully the pharmacology of AC-42, its closely related analogue, 77-LH-28-1, and two novel, unrelated compounds which also purport to be selective, 'ectopic' M_1 receptor agonists, compound A and compound B (Figure 24).

These compounds have been assessed functionally using both inositol phosphate accumulation and calcium mobilisation studies in CHO cells stably expressing the muscarinic M_1 receptor. The effect of signal transduction inhibitors on the intracellular calcium response to these compounds has also been assessed and compared to that for the orthosteric agonist, carbachol. Furthermore, the interaction of carbachol, AC-42 and compound A with the orthosteric muscarinic receptor antagonists atropine and pirenzepine has been determined in order to delineate any allosteric mechanism of action of AC-42 and compound A at the M_1 receptor.

Radioligand binding studies have also been used to characterise the allosteric properties of these novel agonists. Specifically, their effects on [^{3}H]NMS dissociation rate from the M_1 receptor and their profiles of inhibition of two different concentrations of [^{3}H]NMS have been assessed.

To determine whether native tissue affinities reflect those observed in recombinant assays, inhibition binding profiles against muscarinic receptor agonist ([^{3}H]oxotremorine-M) and antagonist ([^{3}H]QNB) radioligands have been determined for both orthosteric and non-orthosteric compounds in rat cortical membranes. Finally, the functional activity of 77-LH-28-1, has also been assessed in an *in vitro* gamma frequency network oscillations model in rat cortex and this compared to that of the non-selective agonist, carbachol, to determine whether functional agonist activity in recombinant cell assays translates to a native tissue receptor population.

Carbachol

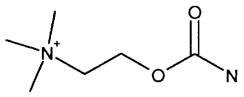

Atropine

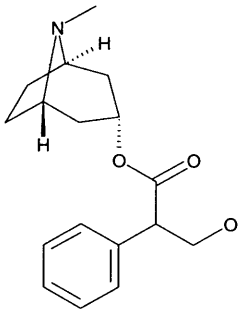

N-methyl scopolamine

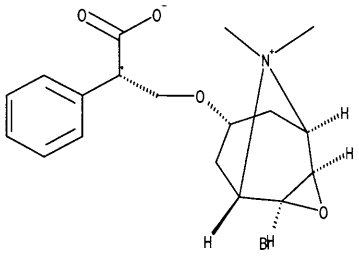

Pirenzepine

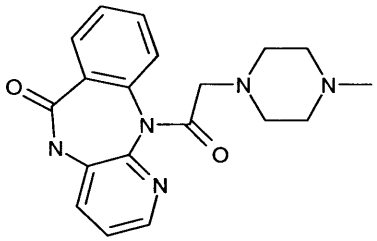

AC-42

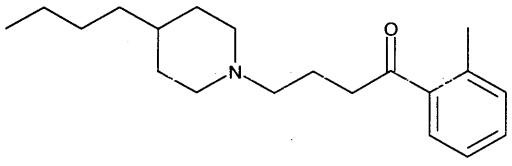

77-LH-28-1

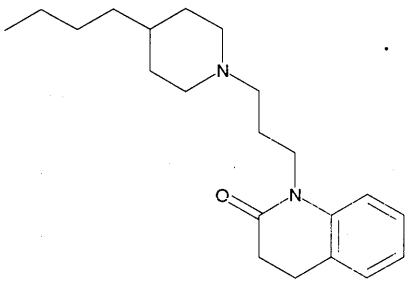

Figure 24. Structures of carbachol, atropine, *N*-methyl scopolamine, pirenzepine, AC-42 and 77-LH-28-1.

(ii) CHO-hM_1 Ca^{2+} mobilisation – signal transduction studies

FLIPR-based calcium mobilisation studies were performed to determine the agonist profile of AC-42, compound A and the reference orthosteric agonist, carbachol, at the hM_1 receptor. Furthermore, signal transduction studies were carried out on the calcium mobilisation mediated *via* the hM_1 receptor to determine whether the responses to the agonists were consistent with coupling to the $G_{q/11}$-phospholipase-C-IP_3 pathway. Carbachol, AC-42 and compound A stimulated calcium mobilisation in CHO-hM_1 cells in a concentration-dependent manner (Figure 25). AC-42 appeared as a high efficacy partial agonist, with a pEC_{50} value of 7.15 ± 0.12 and an intrinsic activity of 0.9 compared to carbachol ($p < 0.001$, F-test). The pEC_{50} value of carbachol was 8.38 ± 0.11 (Figure 25). Compound A appeared as a weaker partial agonist, with a pEC_{50} value of 7.37 ± 0.11 and an intrinsic activity of 0.4 compared to carbachol ($p < 0.0001$, F-test; Figure 25). An example trace of the temporal calcium response to carbachol (10 μM) is shown in Figure 26.

The phospholipase-C inhibitor, U73122 (10 μM), inhibited carbachol and AC-42 stimulated calcium mobilisation, producing a 20 to 30-fold parallel rightward shift in the concentration-response curves to both of these compounds (Figure 27). Furthermore, U73122 completely abolished the calcium mobilisation response induced by compound A.

The non-competitive inhibitor of the inositol triphosphate (IP_3) receptor, 2-APB (100 μM), almost abolished the calcium mobilisation response to both carbachol and AC-42 and did abolish the response to compound A (Figure 27). The Ca^{2+}-ATPase inhibitor, thapsigargin (1 μM), abolished the calcium mobilisation response to all three agonists (Figure 27).

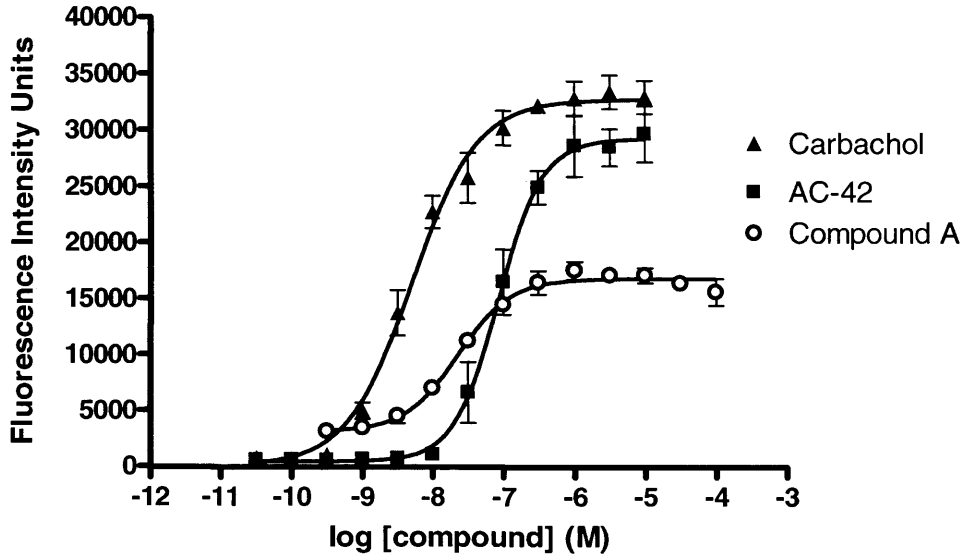

Figure 25. Concentration-dependent stimulation of intracellular calcium mobilisation by carbachol, AC-42 and compound A in CHO-hM_1 cells. Data are the mean of 3 experiments; error bars show s.e.m..

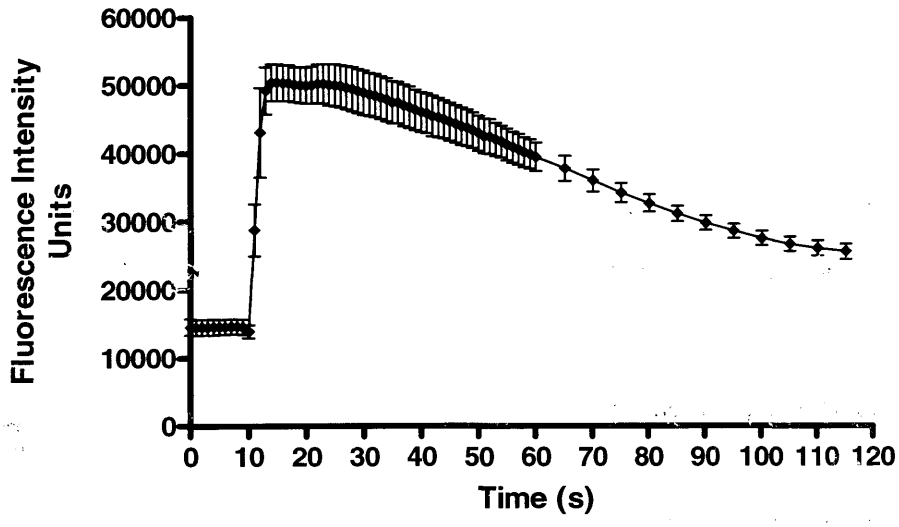

Figure 26. Temporal calcium response to carbachol (10 μM) in CHO-hM_1 cells. Carbachol was added at t = 10 s. Data represents the mean of 2 independent calcium measurements; error bars represent s.e.m..

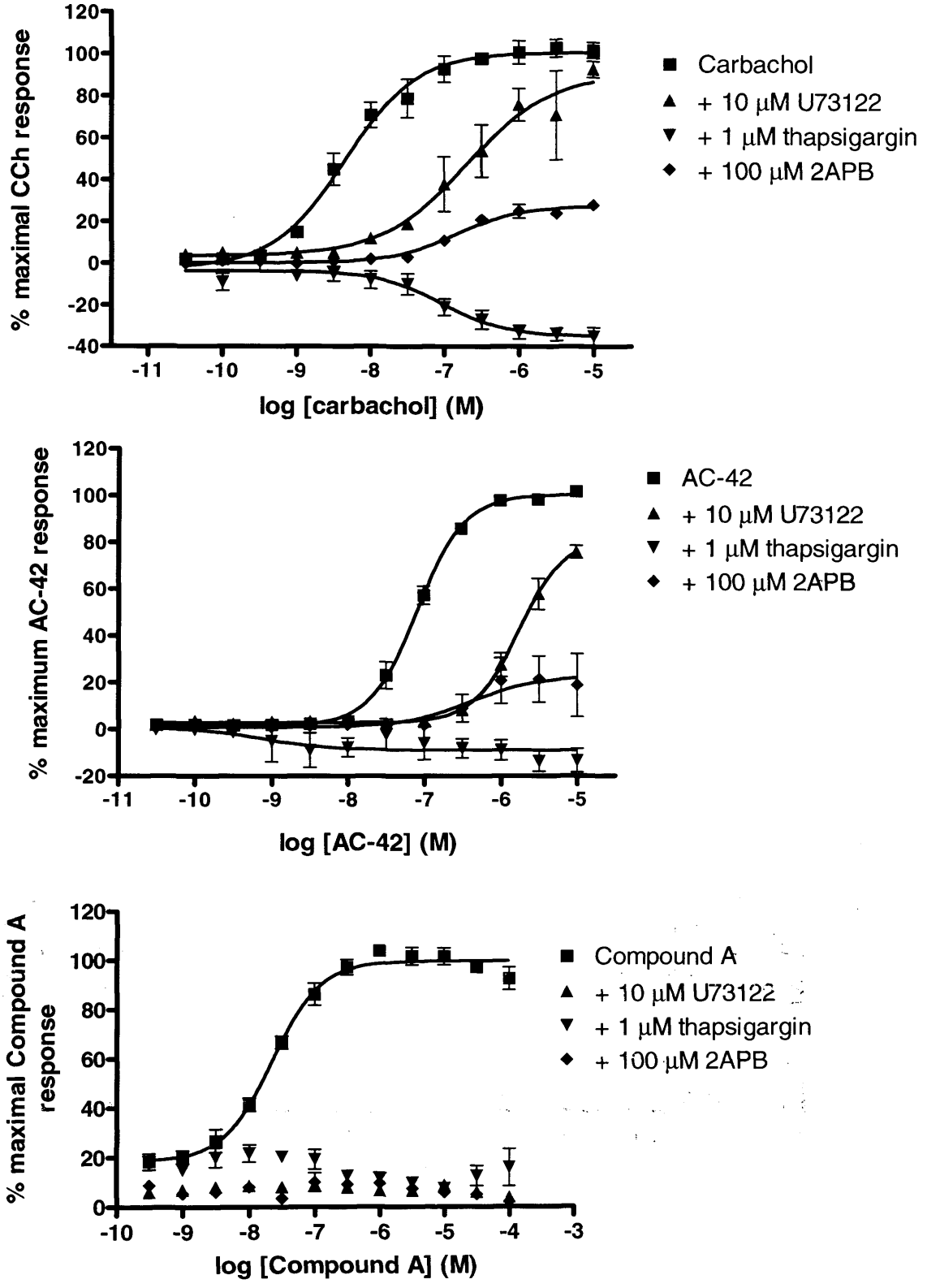

Figure 27. Effect of signal transduction inhibitors on carbachol, AC-42 and compound A stimulated calcium mobilisation in CHO-hM_1 cells. Data are the mean of 3 experiments; error bars show s.e.m..

	Carbachol		AC-42	
	Atropine	**Pirenzepine**	**Atropine**	**Pirenzepine**
Ca^{2+} mobilisation pK_B / pA_2 †	9.39 ± 0.03	8.31 ± 0.16	9.20 ± 0.33	8.44 ± 0.05
Slope ††	1.09 ± 0.03	0.96 ± 0.06	0.75 ± 0.05 *	0.58 ± 0.06 *
log α ‡	n/a	n/a	-2.30 ± 0.09	-2.58 ± 0.25
IP accumulation pK_B / pA_2 †	9.33 ± 0.05	7.97 ± 0.05	9.82 ± 0.13	8.52 ± 0.30
Slope ††	1.12 ± 0.04	1.05 ± 0.03	0.63 ± 0.06 **	0.58 ± 0.09 *
log α ‡	n/a	n/a	-2.16 ± 0.21	-2.08 ± 0.33

Table 10. Parameters describing the functional interaction between the orthosteric antagonists, atropine or pirenzepine, and the agonists, carbachol or AC-42, at the muscarinic M_1 receptor expressed in CHO cells. Data are the mean of 3 experiments (± s.e.m.).

* $p < 0.05$, ** $p < 0.01$ significantly different from hypothetical value of 1 (Student's T-test)

† Negative logarithm of antagonist dissociation constant as estimated by linear Schild regression (Appendix 1).

†† Slope value of Schild regression (Appendix 1).

‡ Logarithm of the co-operativity factor, estimated by nonlinear regression according to an allosteric ternary complex model (equation 7 of the Methods; Appendix 1).

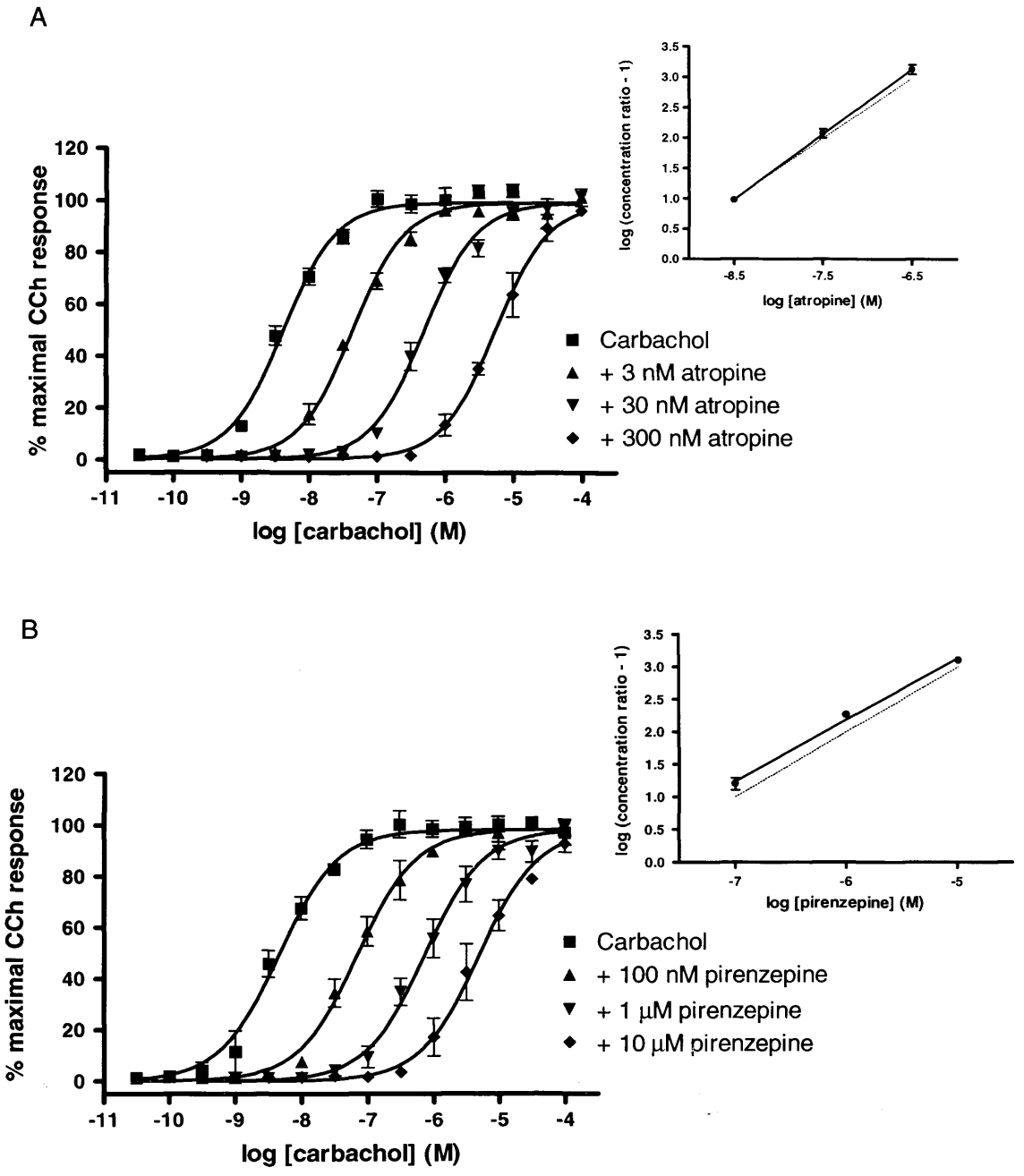

Figure 28. Concentration-dependent antagonism of carbachol-stimulated calcium mobilisation in CHO-hM_1 cells by (A) atropine (3 nM – 300 nM) and (B) pirenzepine (100 nM – 10 µM) with inset Schild regressions. Dotted lines on Schild plots indicate a theoretical slope of 1. Data are the mean of 3 independent experiments; error bars show s.e.m..

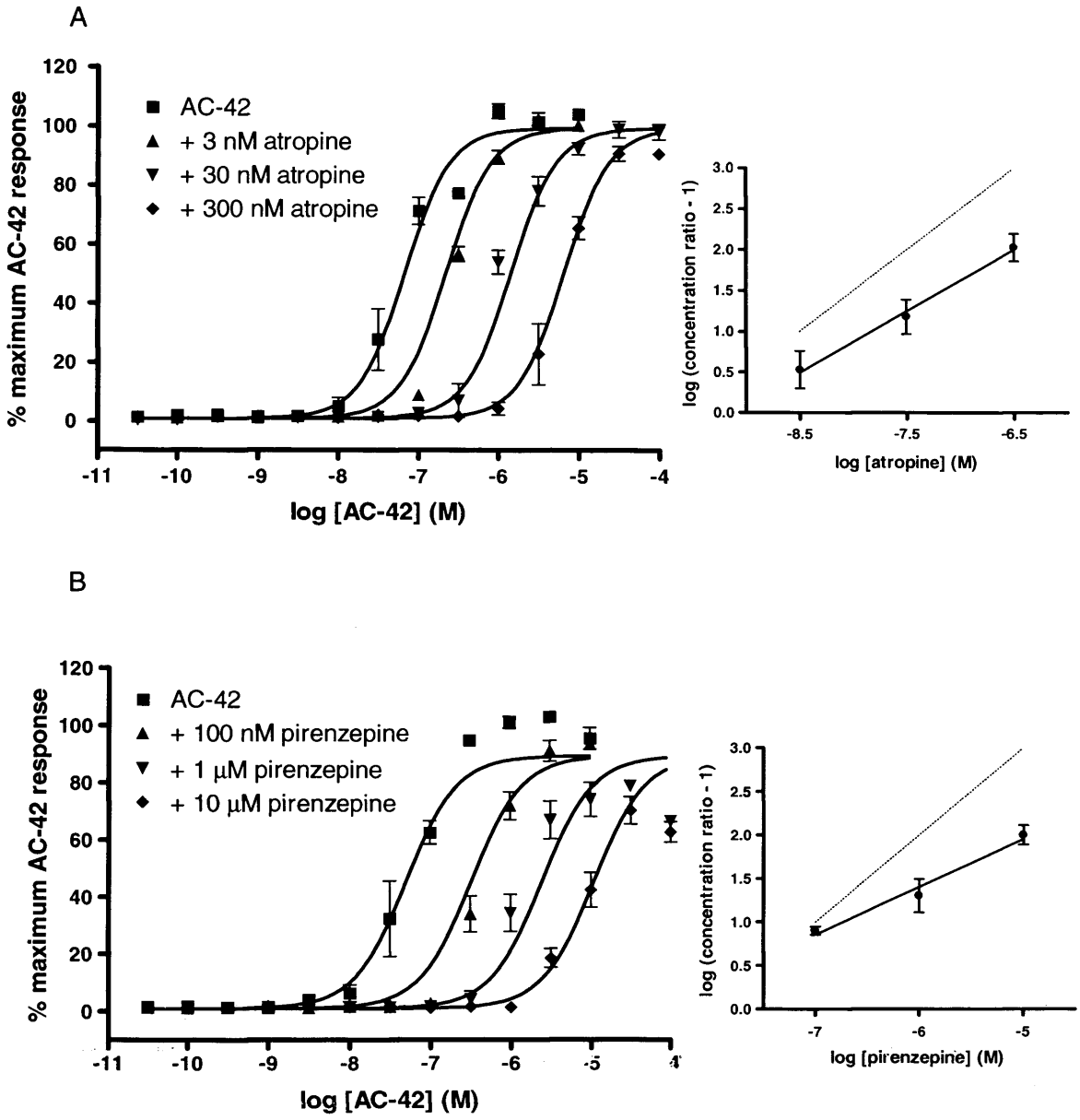

Figure 29. Concentration-dependent antagonism of AC-42-stimulated calcium mobilisation in CHO-hM_1 cells by (A) atropine (3 nM – 300 nM) and (B) pirenzepine (100 nM – 10 μM) with inset Schild regressions. Dotted lines on Schild plots indicate a theoretical slope of 1. Data are the mean of 3 independent experiments; error bars show s.e.m..

(iii) CHO-hM$_1$ Ca^{2+} mobilisation – antagonist studies

In order to further understand the nature of the interaction between the hM$_1$ receptor and AC-42 / compound A, the effects of the orthosteric antagonists atropine and pirenzepine on the calcium responses elicited by AC-42,compound A and carbachol were determined. All responses in the presence of antagonist are normalised to the % maximal asymptotic response of the control agonist.

(a) Atropine / pirenzepine-mediated antagonism of carbachol response

Increasing concentrations of the muscarinic receptor antagonist, atropine (3 – 300 nM) caused a parallel rightward shift in the concentration response curve to carbachol. Schild analysis of the data set yielded an estimated pK_B value of 9.39 ± 0.03 and a slope of 1.09 ± 0.03 (Figure 28a; Table 10; Appendix 1). Increasing concentrations of another muscarinic receptor antagonist, pirenzepine (100 nM – 10 μM), produced a similar profile, with a pK_B value of 8.31 ± 0.16 and a slope of 0.96 ± 0.06 (Figure 28b; Table 10; Appendix 1). The affinity estimates for both atropine and pirenzepine at the M$_1$ receptor are consistent with previous studies (Ellis, 2002).

(b) Atropine / pirenzepine-mediated antagonism of AC-42 response

Increasing concentrations of atropine (3 – 300 nM) also caused a parallel rightward shift in the concentration response curve to AC-42, with no depression in the maximal response and a pA_2 value of 9.20 ± 0.33 and a slope of 0.75 ± 0.05 (Figure 29a; Table 10). The shallow slope was shown to be significantly less than unity ($p < 0.05$; Student's T-test) and so it was not possible to estimate a pK_B value for the antagonist. A similar profile was observed with increasing concentrations of pirenzepine, yielding a pA_2 value of 8.44 ± 0.05 and slope of 0.58 ± 0.06 which was

significantly less than 1 ($p < 0.05$, Student's T-test; Figure 29b; Table 10). Both sets of data with AC-42 could be described by an allosteric model (equation 1) to determine a log α value for the interaction between AC-42 and atropine / pirenzepine (Table 10).

(c) Atropine-mediated antagonism of carbachol / AC-42 response – 6 point Schild analysis

An increase in the concentration range of atropine tested (3 nM – 300 μM) resulted in further rightward shifts of the concentration response curve to carbachol, with a calculated pK_B value of 9.59 ± 0.05 and a slope of 1.01 ± 0.01 (Figure 30a). However, a similar range of concentrations of atropine, when tested against AC-42, produced a shallow, non-linear Schild plot that tended to plateau at the highest concentrations of atropine (Figure 30b). Global shared analysis of the data set (equation 1) provides an estimate of log α of -3.75 ± 0.23 characterising the interaction between AC-42 and atropine (different from the log α value for atropine and AC-42 estimated from the 3 point Schild analysis – see later).

(d) Atropine / pirenzepine-mediated antagonism of compound A response

Increasing concentrations of atropine (3 – 300 nM) caused a rightward shift in the concentration response curve to compound A, with an approximate 50 % depression in the maximal response at 3 nM atropine and further reductions in the maximum asymptote at 30 nM and 300 nM (Figure 31a). Due to the non-parallel nature of the concentration response curves, it was not possible to determine a pA_2 value for atropine-mediated antagonism of compound A. Pirenzepine (100 nM) caused a 10-fold rightward shift in the concentration response curve to compound A, with an approximate 50 % depression in the maximal response (Figure 31b). No significant

A

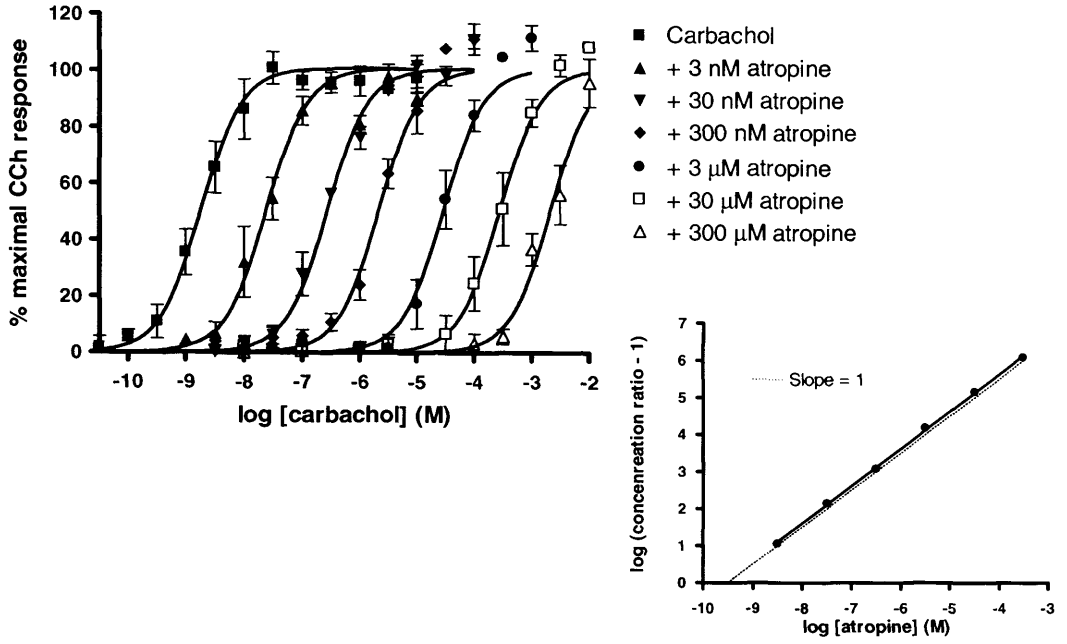

B

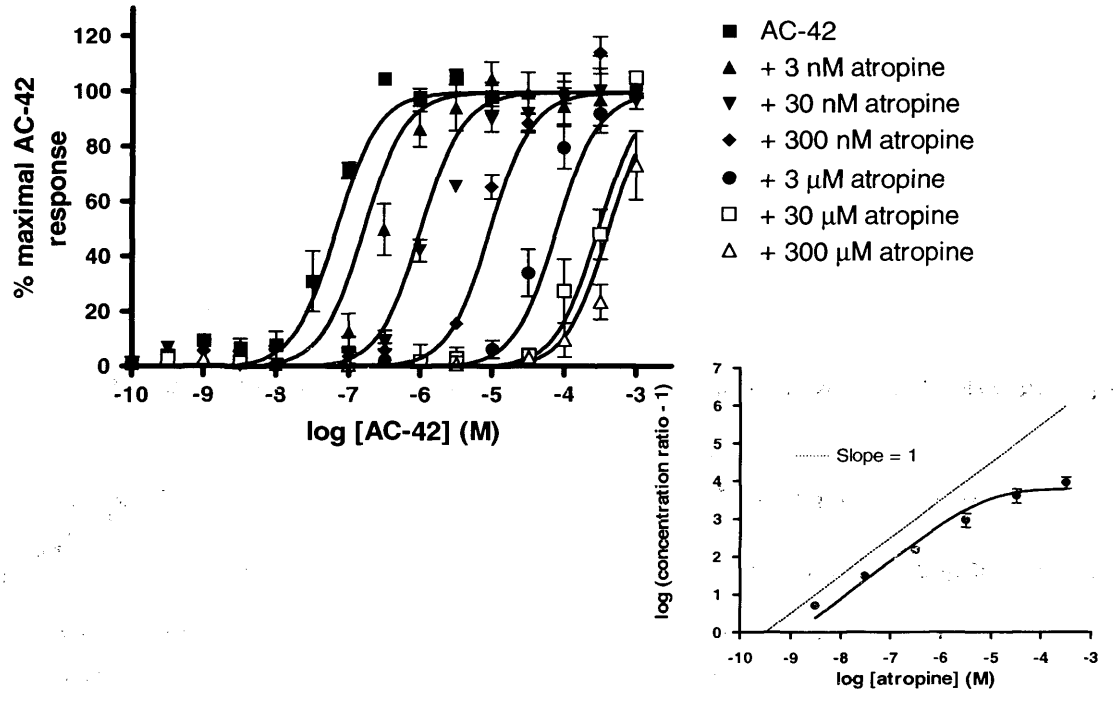

Figure 30. Concentration-dependent antagonism of (A) carbachol or (B) AC-42-stimulated calcium mobilisation in CHO-hM_1 cells by atropine (3 nM – 300 μM) with inset Schild regressions. Dotted lines on Schild plots indicate a theoretical slope of 1. Data are the mean of 3 experiments; error bars show s.e.m..

A

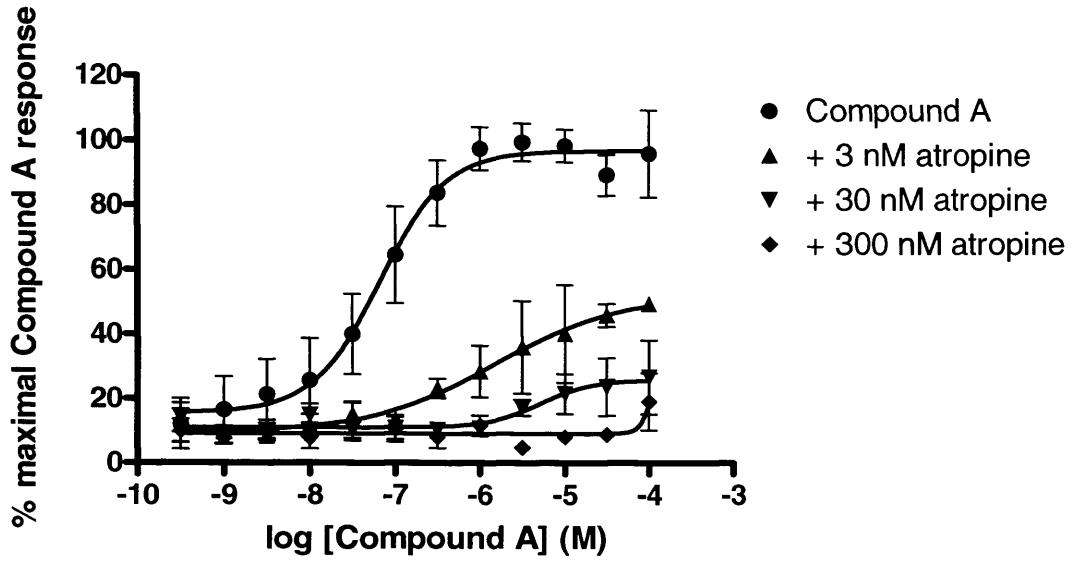

B

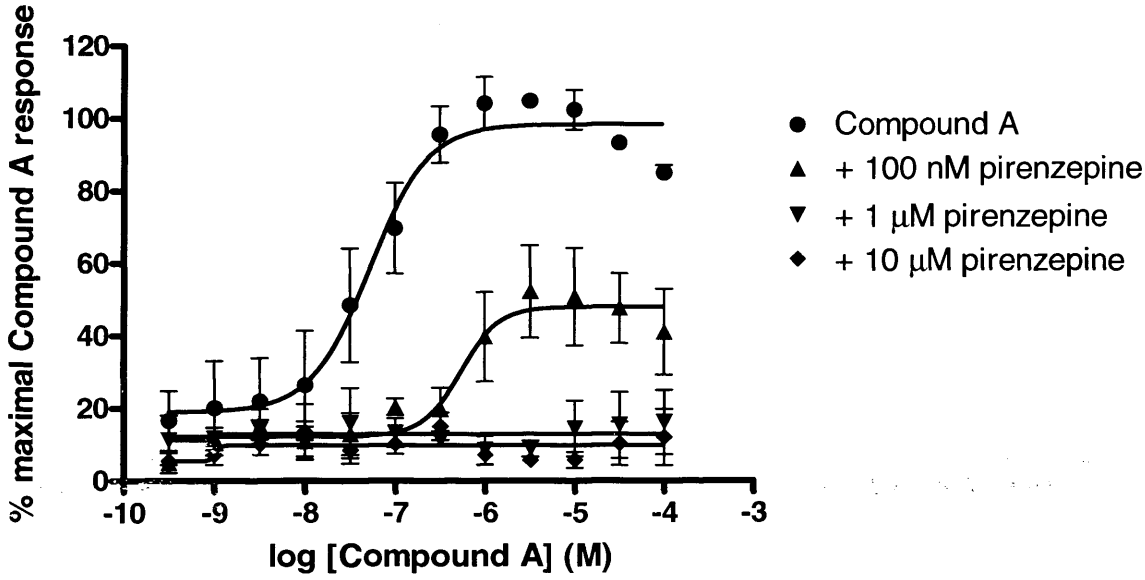

Figure 31. Concentration-dependent antagonism of compound A-stimulated calcium mobilisation in CHO-hM_1 cells by (A) atropine (3 nM – 300 nM) or (B) pirenzepine (100 nM – 10 μM). Data are the mean of 3 experiments; error bars show s.e.m..

calcium response was observed with in the presence of higher concentrations of pirenzepine (1 μM – 10 μM). As with the atropine study, it was not possible to determine a pA_2 value for pirenzepine-mediated antagonism of the compound A response. The reduction in the maximum responses to compound A by atropine and pirenzepine is likely to reflect the partial agonist properties of compound A, rather than any non-competitive interaction between this agonist and atropine and pirenzepine. As a partial agonist, compound A requires full M_1 receptor occupancy to elicit a maximal response. Any blockade of this receptor population with atropine or pirenzepine would reduce the occupancy by compound A and hence reduce the maximum response observed.

(iv) CHO-hM_1 inositol phosphate accumulation – agonist studies

Both carbachol and AC-42 stimulated inositol phosphate (IP) accumulation in CHO-hM_1 cells, with pEC_{50} values of 6.35 ± 0.02 and 6.21 ± 0.10, respectively (Figure 32). These values are in good agreement with previous estimates of both carbachol and AC-42 potency in IP studies (Lee *et al.*, 1996; Spalding *et al.*, 2002). AC-42 appeared as a partial agonist with respect to carbachol ($p < 0.0001$, F-test), with an intrinsic activity of 0.85. The AC-42 analogue 77-LH-28-1 also stimulated IP accumulation with a pEC_{50} of 7.24 ± 0.02 and appeared as a partial agonist with an intrinsic activity of 0.8 compared to carbachol ($p < 0.0001$, F-test).

Compound A and compound B only weakly stimulated IP accumulation in CHO-hM_1 cells, with pEC_{50} values of less than 5 and intrinsic activities compared to carbachol of 0.2 and 0.1, respectively (Figure 32).

(v) CHO-hM$_1$ inositol phosphate accumulation – antagonist studies

A similar profile for atropine and pirenzepine-mediated antagonism of carbachol and AC-42 was observed in IP accumulation studies in CHO-hM$_1$ cells. Both atropine and pirenzepine produced concentration-dependent rightward shifts in the concentration response curve to carbachol, with Schild analysis yielding pK_B values of 9.33 ± 0.05 and 7.97 ± 0.05, respectively and Schild slopes not significantly different from unity (Figure 33; Table 10).

Atropine and pirenzepine also produced parallel rightward shifts in the concentration response curve to AC-42 (Figure 34, Table 10). As in the calcium mobilisation studies, antagonism of the AC-42 response by atropine or pirenzepine resulted in pA_2 values similar to those observed by antagonism of the carbachol responses, but with slope values significantly lower than unity (Table 10; $p < 0.05$, Student's T-test).

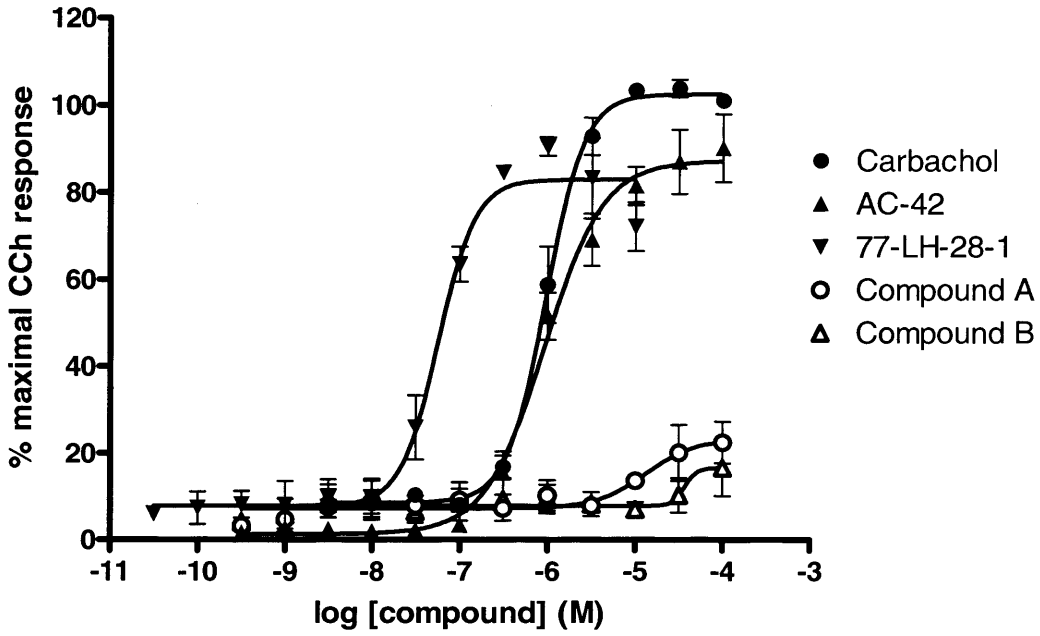

Figure 32. Concentration-dependent stimulation of IP accumulation in CHO-hM_1 cells by carbachol, AC-42, 77-LH-28-1, compound A and compound B. Data represent the mean of 3 independent experiments; error bars represent s.e.m..

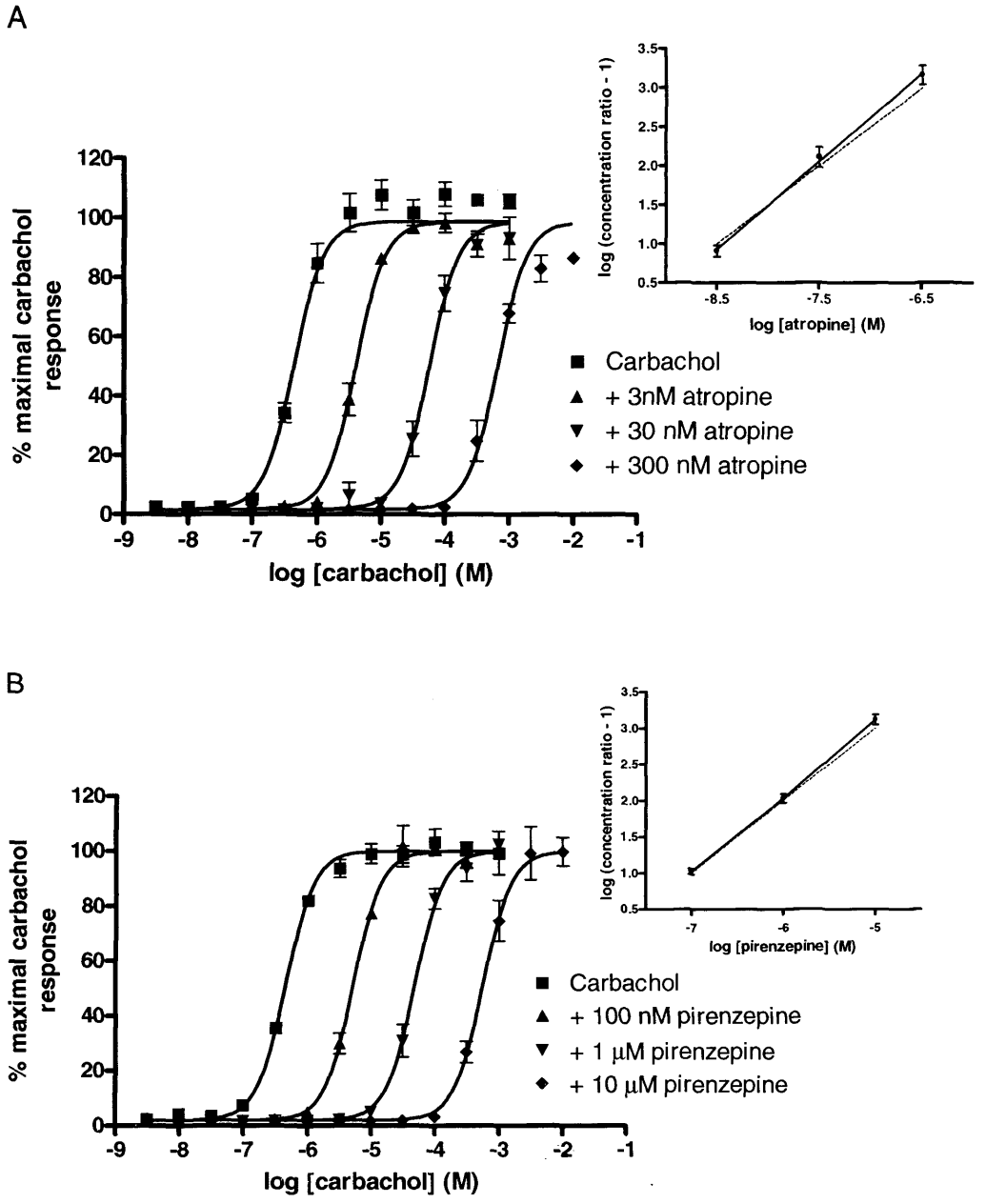

Figure 33. Concentration-dependent antagonism of carbachol-stimulated IP accumulation in CHO-hM_1 cells by (A) atropine (3 nM – 300 nM) and (B) pirenzepine (100 nM – 10 μM). Data shown are the mean of 3 experiments; error bars represent s.e.m..

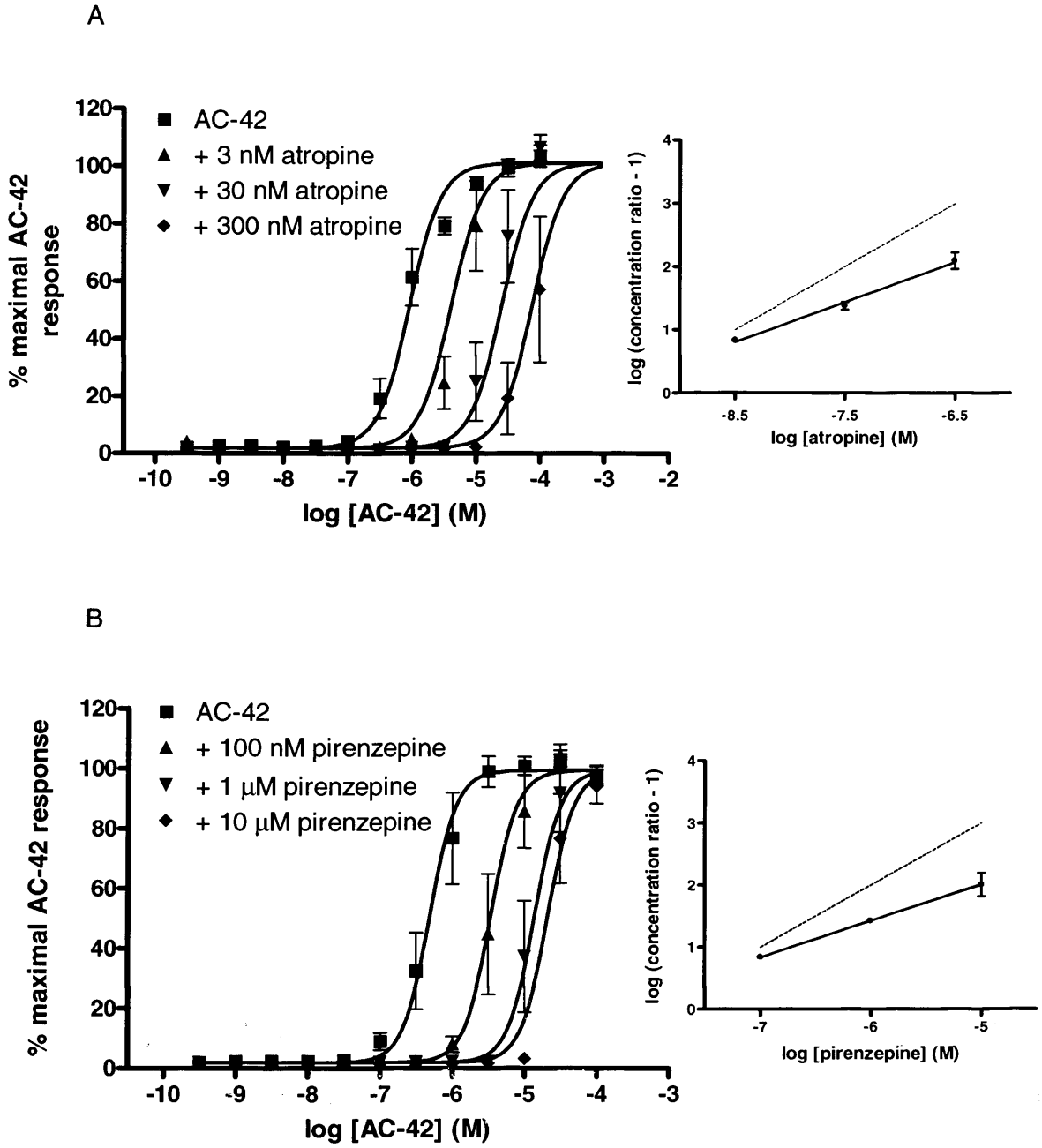

Figure 34. Concentration-dependent antagonism of AC-42-stimulated IP accumulation in CHO-hM_1 cells by (A) atropine (3 nM – 300 nM) and (B) pirenzepine (100 nM – 10 µM). Data shown are the mean of 3 experiments; error bars represent s.e.m..

(vi) CHO-hM$_1$ [^{3}H]NMS saturation binding

Specific binding of [^{3}H]NMS to CHO-hM$_1$ cell membranes was saturable and represented more than 90% of total binding (Figure 35). Non-linear regression revealed that [^{3}H]NMS bound to a single site with a K_D value of 0.27 ± 0.03 nM and a B_{max} of 1.05 ± 0.09 pmol mg protein^{-1}.

(vii) CHO-hM$_1$ [^{3}H]NMS inhibition binding

AC-42 inhibited [^{3}H]NMS binding in a concentration-dependent manner, but did not fully inhibit specific binding at a radioligand concentration of 0.2 nM (minimum asymptote greater than zero; $p < 0.05$, F-test), an effect that was more marked at 2 nM ($p < 0.01$, F-test; Table 11, Figure 36). A simultaneous analysis of each pair of inhibition curves, according to an allosteric ternary complex model of interaction (equation 3), yielded an estimate of 6.18 ± 0.18 for the negative logarithm of the affinity constant (K_B) of AC-42 for the unoccupied M$_1$ receptor and a value of –1.77 ± 0.17 for the logarithm of the degree of co-operativity (α) characterising the interaction between AC-42 and [^{3}H]NMS.

A similar profile of incomplete inhibition of specific [^{3}H]NMS binding at both 0.2 and 2 nM radioligand was observed for both 77-LH-28-1 and compound A (Figure 36; Table 11). Allosteric modelling of the inhibition curves yielded estimates of affinity for the unoccupied M$_1$ receptor (- log K_B) of 7.08 ± 0.02 and 5.38 ± 0.08 for 77-LH-28-1 and compound A respectively, with log α values of –1.76 ± 0.04 and –1.70 ± 0.23 characterising the interaction between these compounds and [^{3}H]NMS. Compound B fully inhibited the specific binding of [^{3}H]NMS at both 0.2 and 2 nM in a concentration-dependent manner.

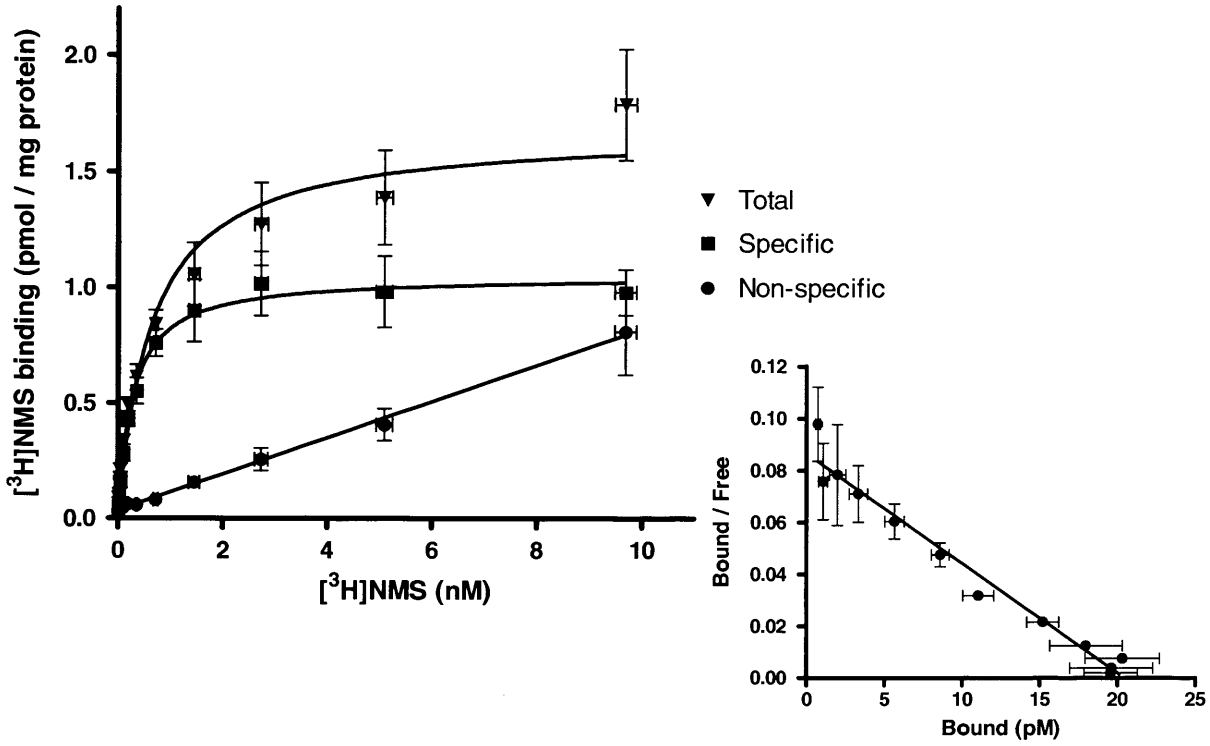

Figure 35. Saturation analysis and Scatchard transformation (inset) of binding of [^{3}H]NMS to membranes from CHO-hM_1 cells. Non-specific binding was defined with atropine (1 μM). Data are from 3 experiments; error bars represent s.e.m..

Figure 36. Inhibition of [^{3}H]NMS binding from CHO-hM_1 cell membranes at two different radioligand concentrations: 0.2 nM (■) and 2 nM (▲). Inhibition curves for atropine, pirenzepine, AC-42, compound A, compound B, 77-LH-28-1 and gallamine are shown. Data are the mean of 3 independent experiments; error bars represent s.e.m..

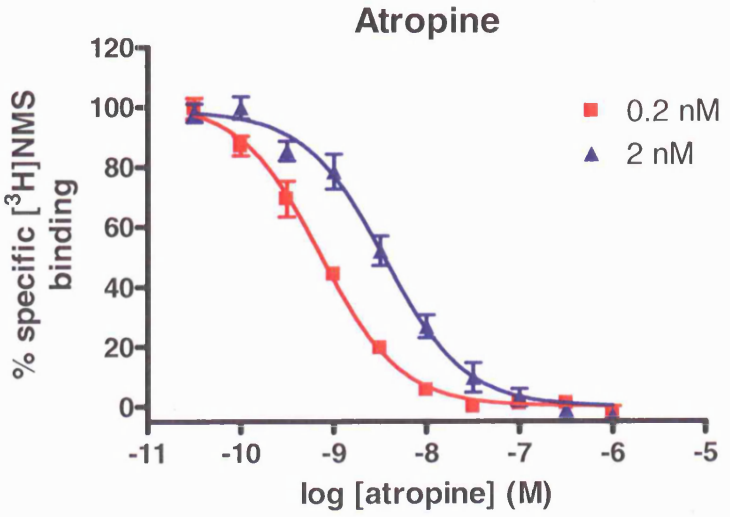

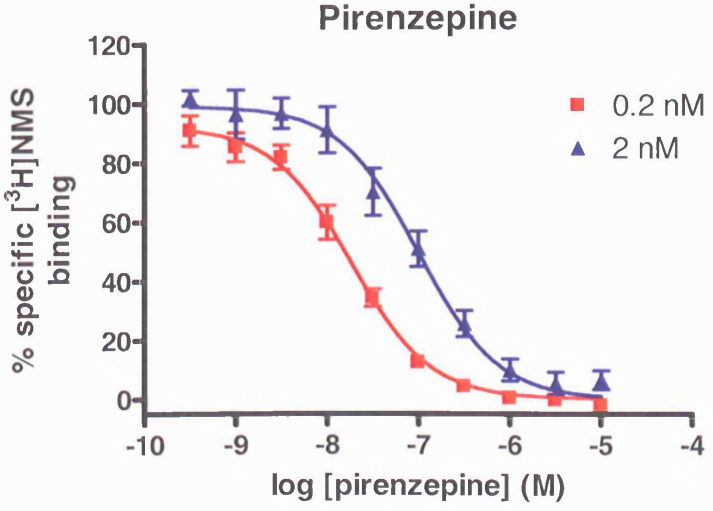

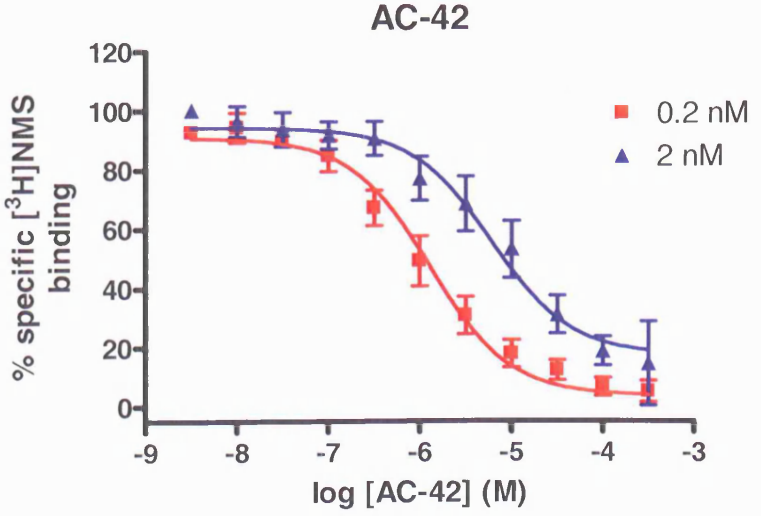

Figure 36 *cont.*

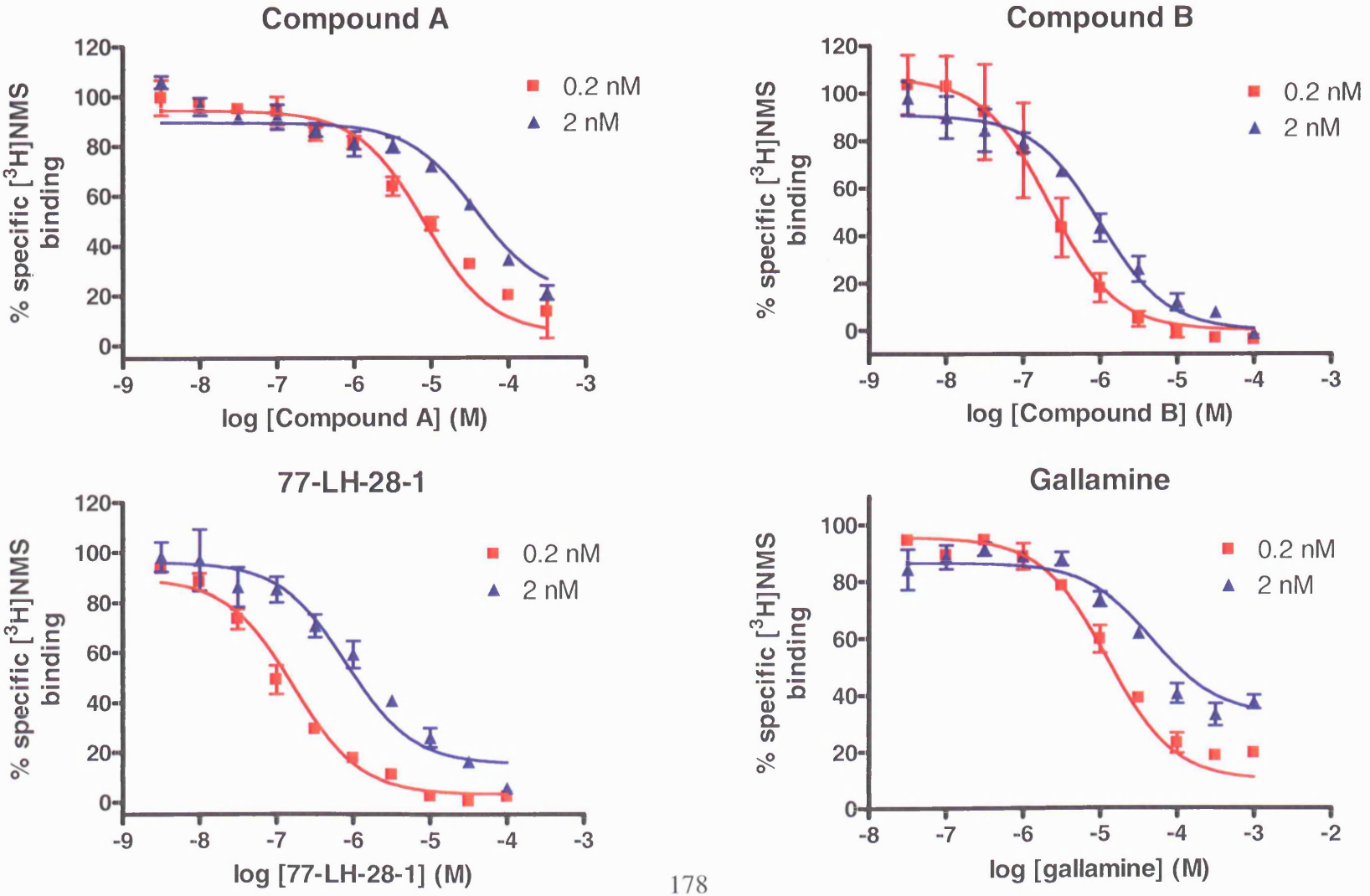

However, despite the full inhibition of specific [^{3}H]NMS binding, the meaned dataset could be fitted to the allosteric model (equation 7), yielding estimates of - log K_B = 7.00 and log α = -3.14. Given the full inhibition of [^{3}H]NMS binding, data was also analysed according to a simple competitive interaction, yielding a pK_i value 7.04 ± 0.11, though statistical comparison of the two fits by F-test yielded a clear preference for the former.

Gallamine also displayed concentration-dependent inhibition of [^{3}H]NMS binding accompanied by an inability to inhibit fully the specific binding of the radioligand (Figure 36). As with AC-42, 77-LH-28-1 and Compound A, this effect was manifest at both radioligand concentrations, being more marked at the higher concentration (2 nM). Simultaneous analysis of the two curves yielded estimates of – log K_B = 5.20 ± 0.04 and log α = -1.28 ± 0.01.

Both atropine and pirenzepine fully inhibited specific [^{3}H]NMS binding in membranes from CHO-hM$_1$ cells at radioligand concentrations of 0.2 nM and 2 nM (Figure 36) with pK_i values of 9.47 ± 0.04 and 8.06 ± 0.05, respectively. Neither atropine nor pirenzepine-mediated inhibition of [^{3}H]NMS binding fitted the allosteric model.

Calculated affinities of compounds for the [^{3}H]NMS occupied receptor (- log K_B/α) are also shown in Table 11.

(viii) CHO-hM$_1$ [^{3}H]NMS kinetic binding

The association of [^{3}H]NMS to CHO-hM$_1$ cell membranes was rapid and monophasic, with equilibrium reached within 10 min (Figure 37a). Single site analysis of these results produced a k_{obs} value of 0.257 ± 0.002 min^{-1}. Atropine (1 μM) induced dissociation of [^{3}H]NMS from CHO-hM$_1$ cell membranes under control conditions was rapid and monophasic, with a calculated k_{off} value of 0.189 ± 0.022 min^{-1}.

Compound	- log K_B	log α	- log K_B/α[‡]	Minimum asymptote significantly > 0 (F-test) ?	
				0.2 nM	2 nM
Atropine	9.47 ± 0.04[†]	n/a	n/a	No	No
Pirenzepine	8.06 ± 0.05[†]	n/a	n/a	No	No
AC-42	6.19 ± 0.18	-1.77 ± 0.17	4.50	Yes*	Yes**
77-LH-28-1	7.08 ± 0.02	-1.76 ± 0.04	5.32	Yes*	Yes*
Compound A	5.38 ± 0.08	-1.70 ± 0.23	3.16	Yes***	Yes*
Compound B	7.00[††]	-3.14[††]	2.23	No	No
Gallamine	5.20 ± 0.04	-1.28 ± 0.01	4.06	Yes***	Yes***

[†] - log K_i (pK_i) values (derived from Cheng-Prussoff correction of IC_{50} values; equation 2; Appendix 1) quoted where data could not be described by allosteric model according to equation 7 (Methods).

[††] - log K_B and log α estimate derived from meaned data.

[‡] Theoretical affinity of antagonist for [^{3}H]NMS occupied receptor derived from estimates of K_B and α (Christopoulos *et al.*, 1999).

* $p < 0.05$; ** $p < 0.01$; *** $p < 0.001$; F-test.

Table 11. Equilibrium [^{3}H]NMS inhibition binding parameters for atropine, pirenzepine, AC-42, 77-LH-28-1, compound A, compound B and gallamine in CHO-hM_1 cell membranes (Appendix 1). Data are the mean of 3 experiments (± s.e.m.).

These values led to calculated k_{on} value of 311 ± 115 min^{-1} μM^{-1}. The K_D value calculated from these estimates was 0.61 nM (Appendix 1).

The presence of gallamine (1 mM) produced a marked retardation of [^{3}H]NMS dissociation from CHO-hM_1 cell membranes, with a significantly lower k_{offobs} = 0.0170 ± 0.0008 min^{-1} compared to control conditions (Figure 37b; $p < 0.01$, T-test).

AC-42 (100 μM) also significantly slowed the rate of [^{3}H]NMS dissociation, yielding a k_{offobs} value of 0.122 ± 0.005 min^{-1} (Figure 37b; $p < 0.05$, T-test), although this effect was much less marked than that for gallamine. Compound A (100 μM) did not alter the rate of [^{3}H]NMS dissociation compared to control, yielding a k_{offobs} value of 0.176 ± 0.002 min^{-1}.

Analysis of the dissociation curves in the presence of gallamine according to equation 4 (with k_{offB} constrained to a value of zero) yielded an estimate of the affinity of gallamine for the [^{3}H]NMS occupied receptor (-log K_B/α) of -3.86 ± 0.12. Due to the relatively small effect of AC-42, it was not possible to obtain an accurate estimate of --log K_B/α.

(ix) Rat cortex [^{3}H]QNB and [^{3}H]oxotremorine-M inhibition binding

Affinities of a range of test compounds to inhibit [^{3}H]QNB and [^{3}H]oxotremorine-M binding in rat cortical membranes are shown in Table 12 and Figure 38. Atropine, scopolamine and pirenzepine displayed affinities for rat cortical membranes in line with their known affinities for the muscarinic M_1 receptor, with [^{3}H]oxotremorine-M / [^{3}H]QNB affinity ratios of approximately 1, consistent with previous studies using agonist and antagonist radioligands (Loudon *et al.*, 1997).

A

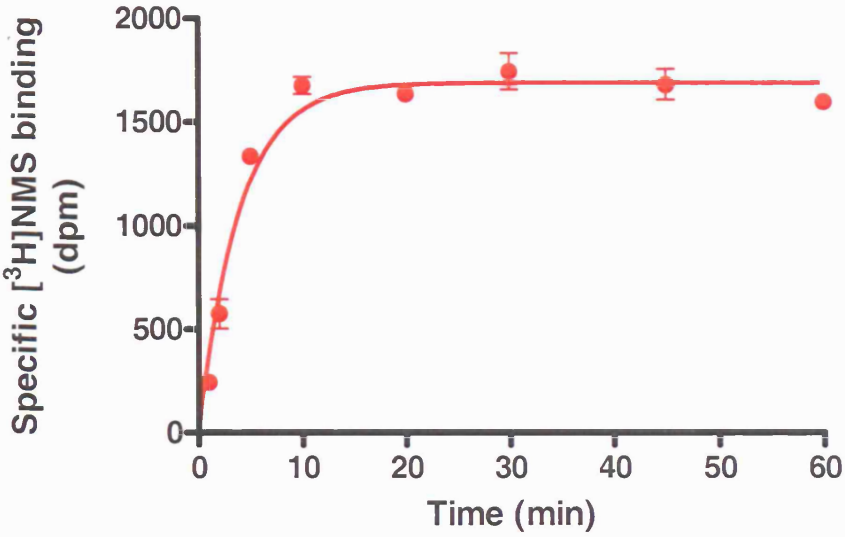

B

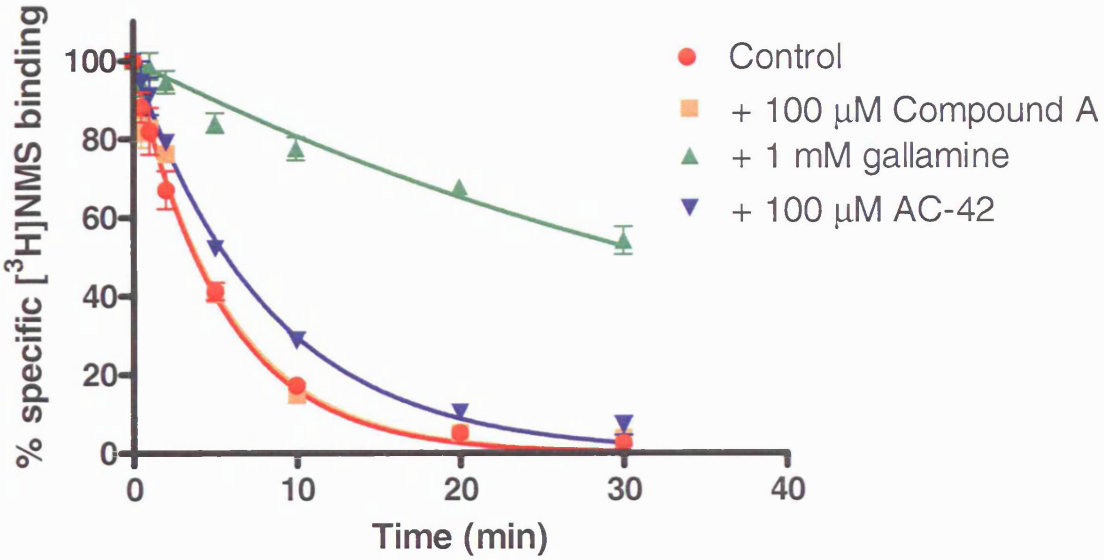

Figure 37. Time course of (A) association and (B) dissociation of [^{3}H]NMS to and from CHO-hM_1 cell membranes. Dissociation studies were carried out in the presence and absence of gallamine, AC-42 and compound A. Data represent the mean of 3 experiments; error bars represent s.e.m..

The muscarinic receptor partial agonists, xanomeline and pilocarpine display approximately 10-fold and 50-fold higher affinity, respectively, against [^{3}H]oxotremorine-M compared to [^{3}H]QNB. Muscarinic receptor agonists such as milameline, oxotremorine, muscarine, carbachol and oxotremorine-M displayed much higher affinity against [^{3}H]oxotremorine-M binding compared to [^{3}H]QNB binding, with affinity ratios ranging from approximately 500 to greater than 4000 (Table 12; Figure 38). These ratios are consistent with previous estimates using [^{3}H]oxotremorine-M and [^{3}H]QNB in rat cortex (Loudon *et al.*, 1997), but higher than estimates that have used [^{3}H]oxotremorine-M / [^{3}H]NMS affinity ratios in a mixed tissue population (Sharif *et al.*, 1995). The M_1 receptor selective agonists, AC-42, 77-LH-28-1, compound A and compound B displayed [^{3}H]oxotremorine-M / [^{3}H]QNB affinity ratios ranging between 4 and 25 (Table 12).

Figure 38. Inhibition of [^{3}H]QNB (■) and [^{3}H]oxotremorine-M (▲) binding by a range of muscarinic receptor ligands in rat cortical membranes. Data are the mean of 3 independent experiments; error bars show s.e.m..

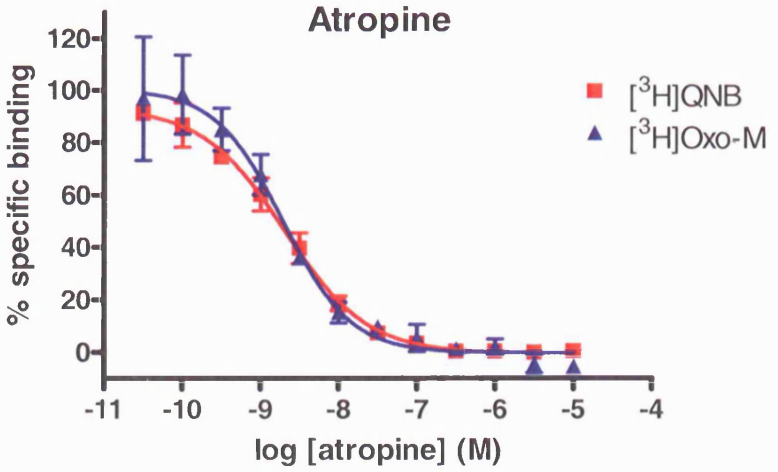

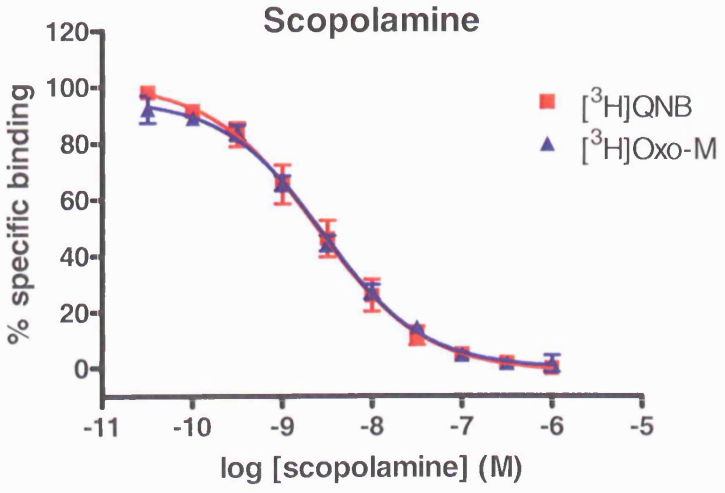

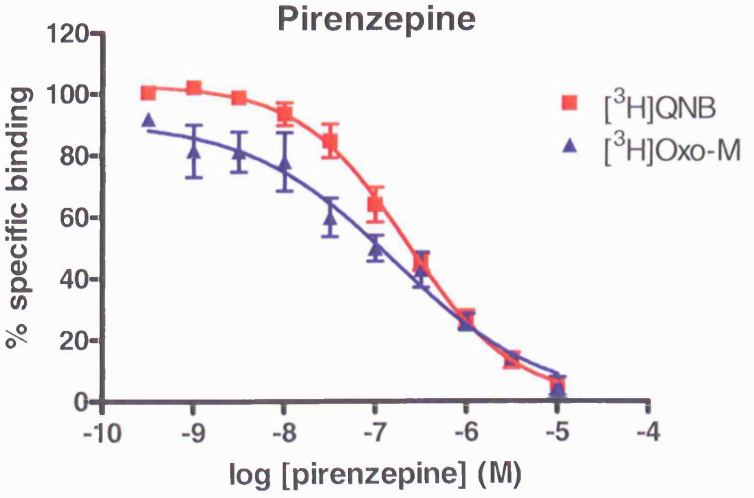

Figure 38 *cont.*

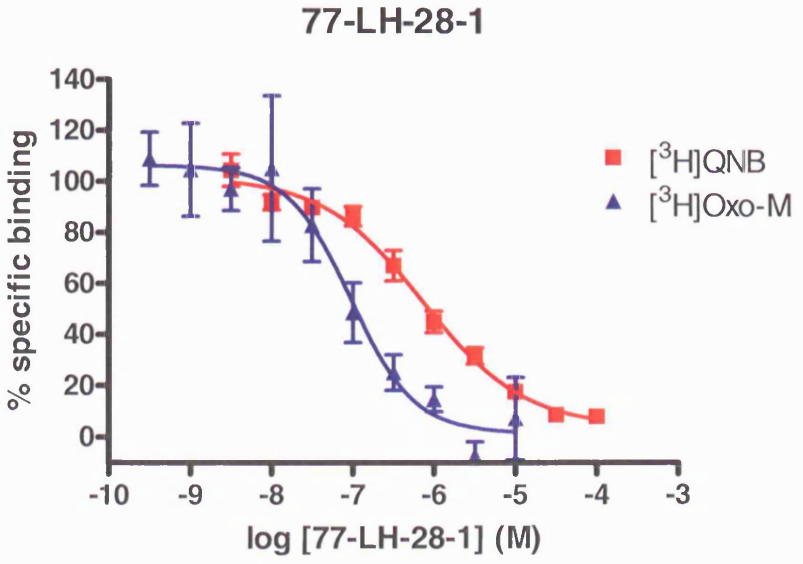

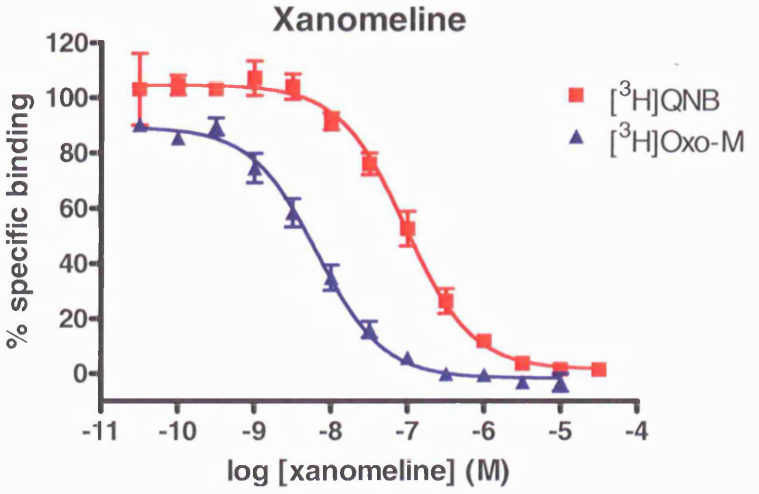

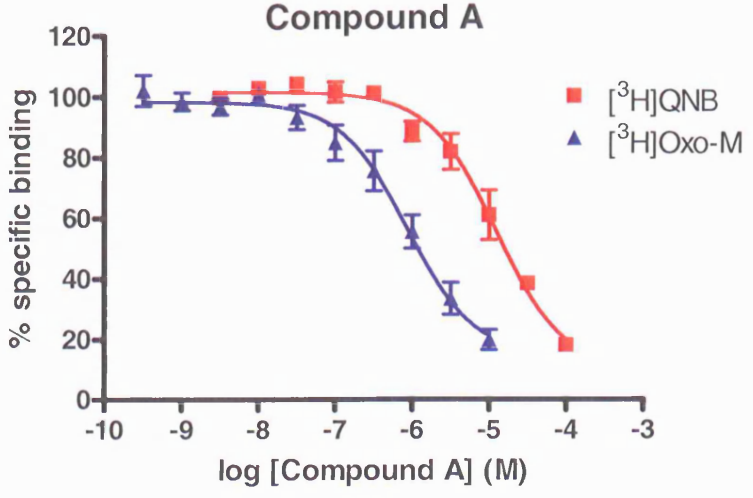

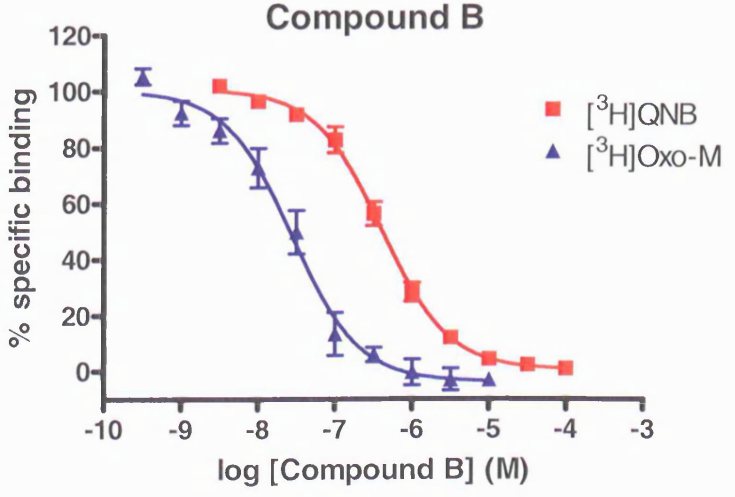

Figure 38 *cont.*

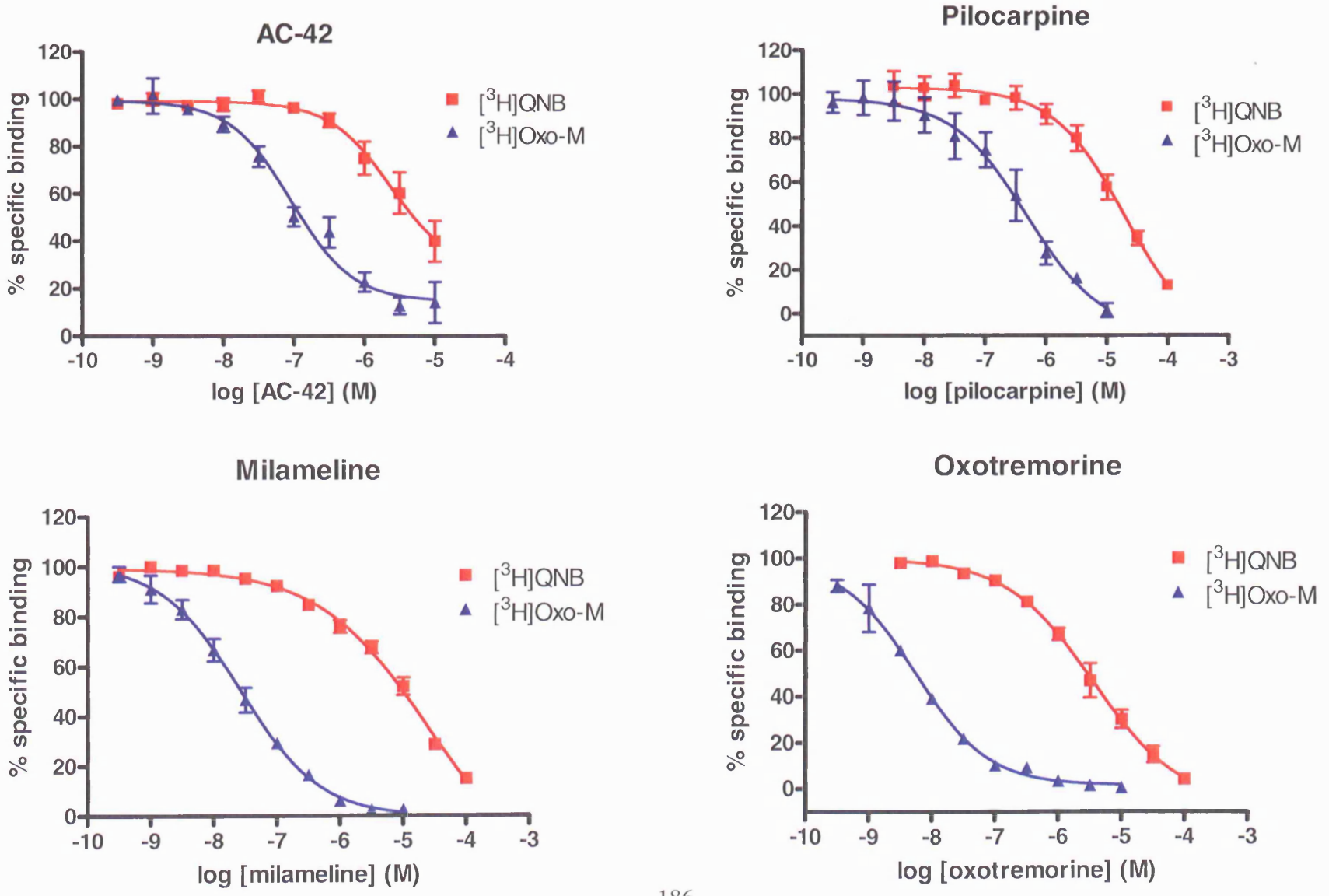

Figure 38 *cont.*

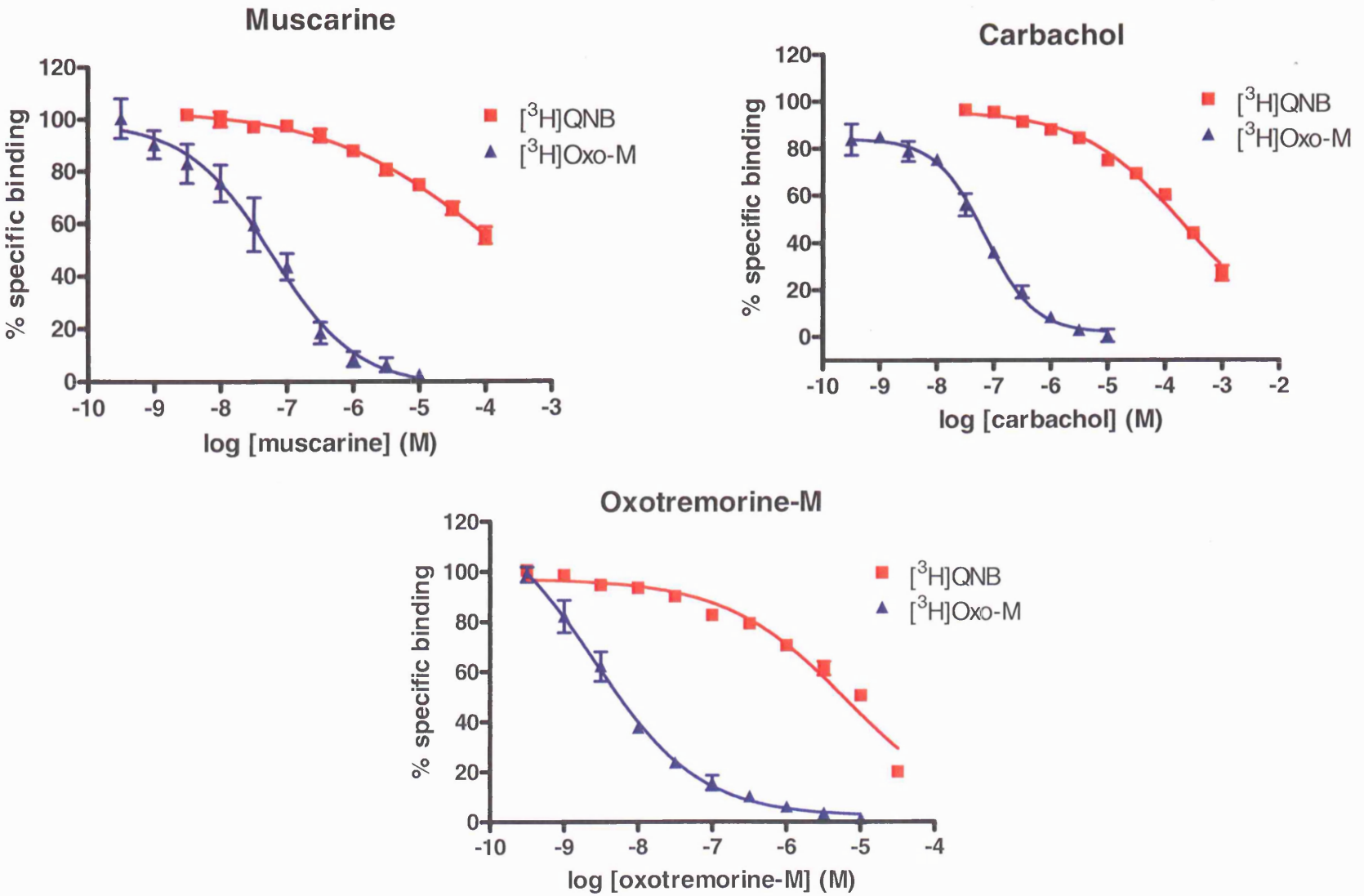

Compound	[^{3}H]QNB pK_i	[^{3}H]Oxo-M pK_i	Affinity ratio
Atropine	9.25 ± 0.21	8.98 ± 0.08	0.5
Scopolamine	8.90 ± 0.17	8.75 ± 0.05	0.7
Pirenzepine	6.93 ± 0.10	6.84 ± 0.03	0.8
77-LH-28-1	6.59 ± 0.15	7.23 ± 0.08	4
Xanomeline	7.31 ± 0.08	8.33 ± 0.07	10
Compound A	5.13 ± 0.12	6.16 ± 0.09	11
Compound B	6.70 ± 0.08	7.96 ± 0.04	18
AC-42	5.63 ± 0.14	7.01 ± 0.24	24
Pilocarpine	5.10 ± 0.02	6.84 ± 0.38	55
Milameline	5.17 ± 0.18	7.87 ± 0.10	501
Oxotremorine	5.81 ± 0.15	8.53 ± 0.04	523
Muscarine	4.48 ± 0.15	7.63 ± 0.14	1413
Carbachol	3.97 ± 0.06	7.34 ± 0.07	2301
Oxotremorine-M	4.92 ± 0.08	8.54 ± 0.16	4148

Table 12. Affinities of a range of muscarinic receptor ligands generated for inhibition of [^{3}H]QNB and [^{3}H]oxotremorine-M binding to rat cortical membranes. Data are the mean of 3 independent experiments (± s.e.m.).

(x) Cortical network oscillations

In order to determine whether the M_1 receptor allosteric agonist, 77-LH-28-1, exhibited agonist properties in a native tissue preparation, this compound, along with the non-selective cholinergic receptor agonist carbachol, was examined in an *in vitro* network oscillations model in the rat cortex. The non-selective agonist carbachol (15 μM) reversibly stimulated both beta (20 – 30 Hz) and gamma (30 – 80 Hz) frequency network oscillations in layer IV of the temporal cortex of rat brain slices (Figure 39). The muscarinic M_1 receptor selective agonist, 77-LH-28-1, at both 1 μM and 3 μM, stimulated gamma, but not beta frequency oscillations in layer IV of the temporal cortex at a mean frequency of 42.1 ± 2.0 Hz (Figure 40). The power of the gamma oscillations at 3 μM 77-LH-28-1, described by the area under the curve over the 30 – 80 Hz range, was 1.294 ± 0.119 μV^2 / Hz.kHz, compared to 0.044 ± 0.019 μV^2 / Hz.kHz for control (Figure 40). 77-LH-28-1-stimulated oscillations were abolished by atropine (10 μM; power = 0.0329 ± 0.015 μV^2 / Hz.kHz; Figure 40).

(xi) Discussion

AC-42 is a novel, functionally selective agonist of the muscarinic M_1 receptor that has been described as binding to an 'ectopic' site on the M_1 receptor (Spalding *et al.*, 2002). This site, not conserved amongst the other muscarinic receptor subtypes, is thought to confer the unprecedented selectivity for the M_1 receptor displayed by this compound. The studies in this chapter have extensively characterised the pharmacology of the interaction between the M_1 receptor and AC-42, and, to a lesser extent, an analogue of AC-42, 77-LH-28-1 and two novel, unrelated compounds, compound A and compound B that are also purported to act as selective M_1 receptor 'ectopic' agonists.

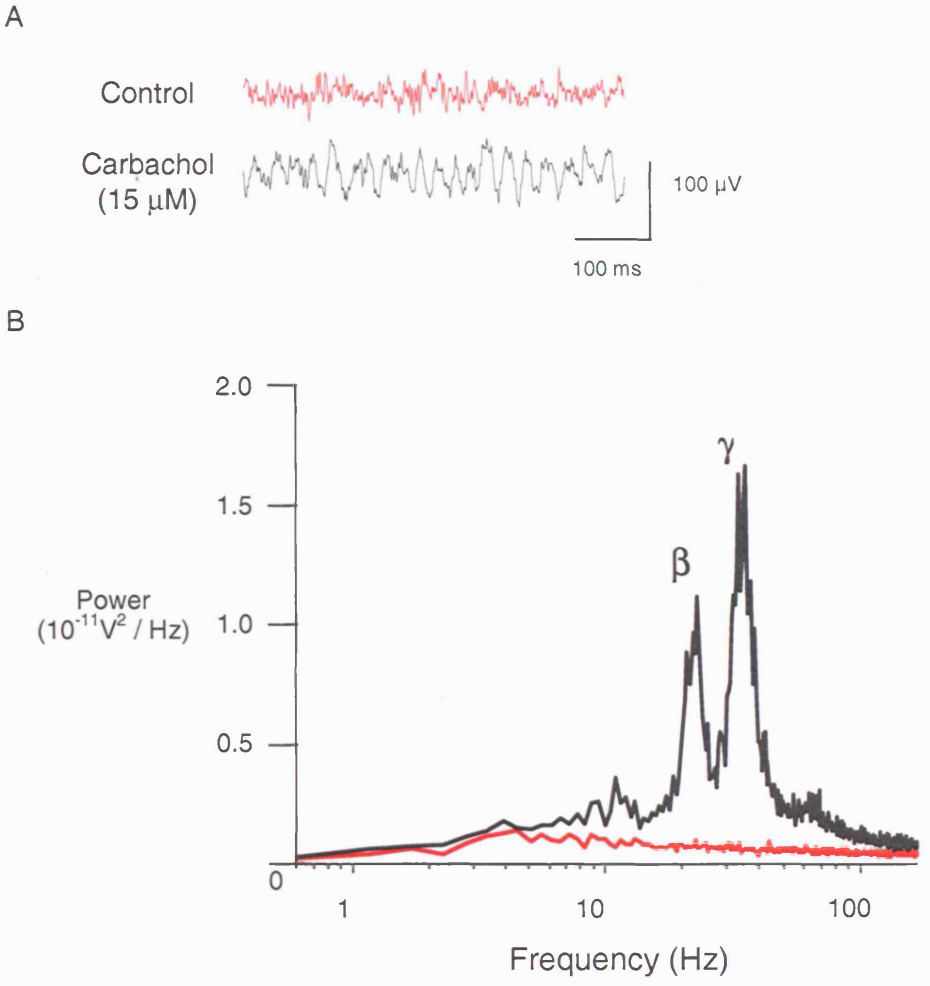

Figure 39. Carbachol-induced beta (β) and gamma (γ) network oscillations. (A) 500 ms recording of extracellular activity from layer IV of the rat temporal cortex in the presence and absence of carbachol. (B) A power spectra from a 60 s epoch of extracellular activity before and after addition of carbachol. Data are from a single representative experiment that was replicated 5 times with similar results.

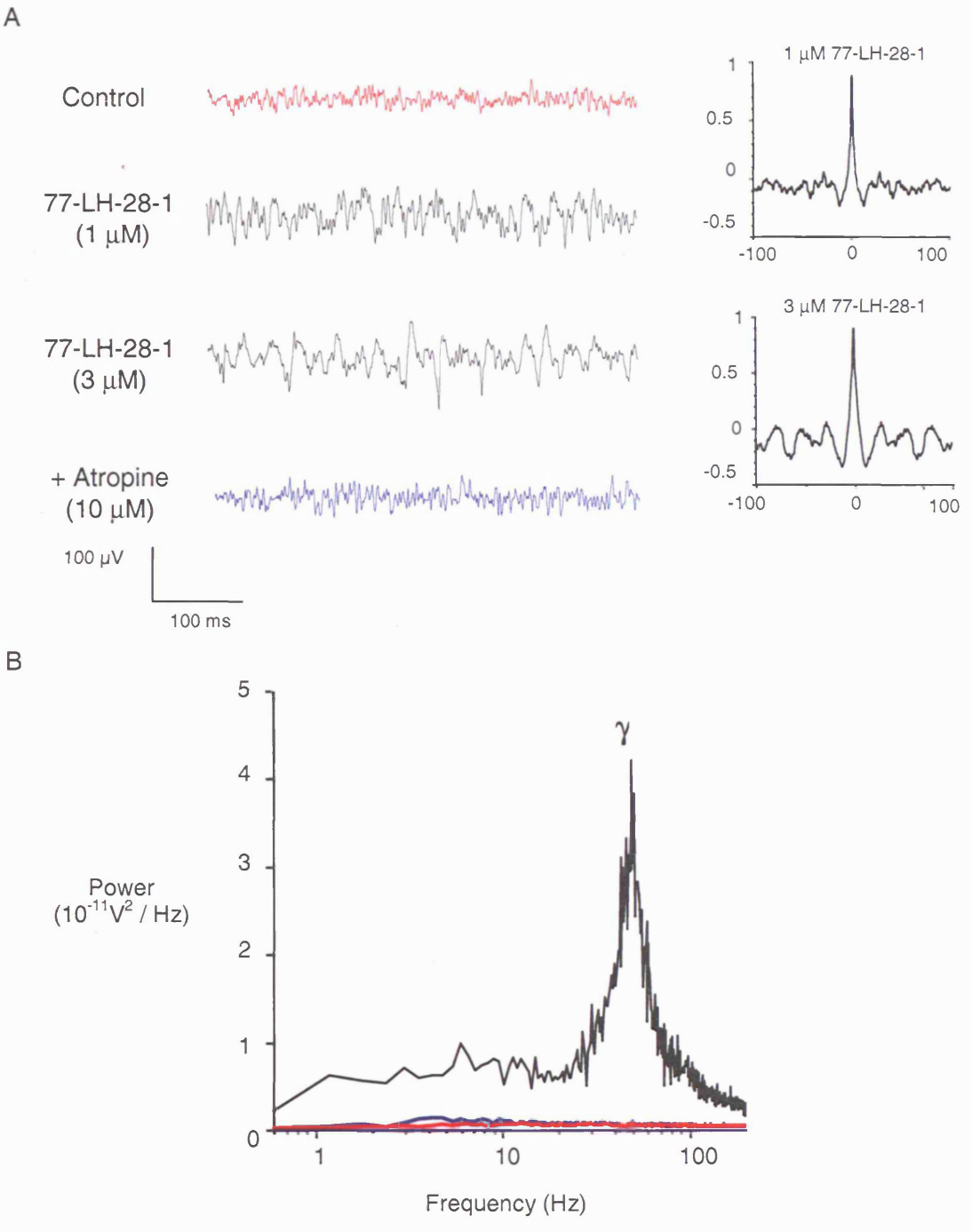

Figure 40. (A) 500 ms recording of extracellular activity from layer IV of the rat temporal cortex during (i) control conditions (red trace), (ii) after application of 77-LH-28-1 (black traces with corresponding autocorrelations from a 1 s epoch of activity) and (iii) after application of atropine (blue trace). (B) A power spectra from a 60 s epoch of extracellular activity (77-LH-28-1, 3 μM). Data are from a single representative experiment that was replicated 5 times with similar results.

Calcium mobilisation studies in CHO cells stably expressing the human muscarinic M_1 receptor suggested that the non-selective orthosteric ligand carbachol, as well as AC-42 and compound A, were agonists at the M_1 receptor, with pEC_{50} values of approximately 8.4, 7.1 and 7.4, respectively. AC-42 appeared as a high efficacy partial agonist with intrinsic activity of 0.9 compared to carbachol, whereas compound A was a much weaker partial agonist (intrinsic activity = 0.4). All three agonists displayed qualitatively similar sensitivities to a range of signal transduction inhibitors. Agonist responses were abolished by pre-incubation with the Ca^{2+}-ATPase inhibitor, thapsigargin. The phospholipase-C inhibitor, U73122, reduced the potency of both carbachol and AC-42 approximately 30-fold and abolished the response to compound A. The non-competitive inhibitor of the IP_3 receptor, 2-APB, greatly reduced the calcium response generated by carbachol and AC-42 and abolished that to compound A. The sensitivity of the calcium responses to inhibitors of phospholipase-C, the IP_3 receptor and the endoplasmic reticulum Ca^{2+}-ATPase is entirely consistent with carbachol, AC-42 and compound A stimulating the muscarinic M_1 receptor to signal through the $G_{q/11}$ pathway. These data suggest that any alternative mode of receptor activation by the 'ectopic' agonists compared to that of carbachol does not alter the predominant signal transduction pathway utilised by the M_1 receptor. However, more extensive studies looking at other G protein mediated signal transduction including more downstream pathways, such as modulation of intracellular cAMP signalling, the MAP kinase cascade or arachidonic acid release, in both recombinant systems and native tissue, are required in order to determine whether 'ectopic' agonists exert any subtle differences in signal transduction compared to orthosteric agonists. Carbachol has been shown to stimulate cAMP accumulation, arachidonic acid release (Gurwitz *et al.*, 1994) and MAP kinase (Wotta *et al.*, 1998) in CHO cells expressing the muscarinic M_1 receptor. Indeed, in the former study, the muscarinic M_1 receptor agonist AF102B (cis-2-methylspiro(1,3-oxathiolane-5,3')quinuclidine) displayed a different profile to carbachol in cAMP

studies. Clearly further studies to examine the signalling pathways stimulated by AC-42 are required.

Carbachol and AC-42 also stimulated inositol phosphate (IP) accumulation in CHO-hM_1 cells, although AC-42 appeared as a partial agonist with respect to carbachol, consistent with the calcium mobilisation studies and previous reports (Spalding *et al.*, 2002). The analogue of AC-42, 77-LH-28-1 also stimulated IP accumulation and was approximately 10-fold more potent than AC-42. 77-LH-28-1, like AC-42, appeared to be a high efficacy partial agonist with respect to carbachol. Compound A and compound B only weakly stimulated IP accumulation, with pEC_{50} values of less than 5 and intrinsic activity values of 0.2 and 0.1, respectively. These data suggest that compound A and compound B are very weak partial agonists at the M_1 receptor. The difference in the response generated by compound A in the calcium mobilisation assay compared to the IP accumulation assay may, therefore, be as a result of the much higher degree of signal amplification in the downstream calcium assay compared to the relatively proximal IP accumulation readout (Kenakin, 1997).

In functional assays, the best-characterised methods for investigating the mechanism of interaction between agonists and antagonists are the procedures underlying Schild analysis and its variants (Arunlakshana & Schild, 1959; Kenakin, 1997; Motulsky & Christopoulos, 2004). In this chapter, functional calcium mobilisation and IP accumulation studies were designed to examine the interaction between carbachol, AC-42 and compound A and the well-characterised orthosteric antagonists, atropine and pirenzepine.

In the calcium mobilisation assay, increasing concentrations of both atropine and pirenzepine cause a rightward shift in the concentration-response curve to compound A accompanied by a substantial depression in the maximal response. Indeed, in the

presence of atropine (300 nM) and pirenzepine (1 – 10 μM), the compound A response was abolished. It is possible that if compound A were acting at a site on the receptor distinct from the orthosteric site, then the effect of an orthosteric antagonist could appear to be non-competitive and yield a depression in the maximal response with increasing antagonist concentration. If this were to be the case, the apparent rightward shift in the concentration response curve that was observed could be due to the receptor reserve in the CHO-hM_1 cells. It is also possible that any depression in the maximal agonist response could be due to the hemi-equilibrium kinetics of the FLIPR assay, (whereby the measurement of the agonist – antagonist interaction takes place under non-equilibrium conditions due to the short agonist incubation and read time; Hall & Parsons, 2001). However, both calcium mobilisation and IP accumulation studies with compound A have already shown it to be a very weak partial agonist in CHO-hM_1 cells. To generate a functional response, such a compound would be required to occupy fully the hM_1 receptor population. However, the subsequent presence of an antagonist would prevent compound A from fully occupying the receptors and hence reduce the maximal response observed. It seems this is the most likely cause of the antagonist profile observed with compound A.

The interaction between carbachol or AC-42 and atropine or pirenzepine was examined in both calcium and IP accumulation assay formats. In both assays, atropine and pirenzepine antagonised the effects of carbachol in a manner that was consistent with the expectations of competition for a common (orthosteric) binding site, yielding Schild slopes not significantly different from unity. This was most evident with atropine in the calcium mobilisation assay, where a Schild slope of unity was maintained over atropine concentrations spanning six orders of magnitude (Figure 30). The resulting pK_B estimates (Table 10) were consistent with previously reported values in the literature for the binding of atropine or pirenzepine to the orthosteric site on the muscarinic M_1 receptor (Ellis, 2002).

In contrast, the rightward shift of the AC-42 concentration-response curve by either atropine or pirenzepine in either assay format led to Schild slopes significantly less than unity (Table 10), indicating that the antagonism was less than expected for a simple orthosteric interaction. Schild slopes of less than unity can arise due to a number of reasons (Kenakin, 1997), one possibility being an allosteric interaction. Negative allosteric interactions have previously been demonstrated in functional assays by a progressive inability of the antagonist to cause a rightward shift of the agonist concentration-response curve with increasing antagonist concentrations (Clark & Mitchelson, 1976; Lanzafame *et al.*, 1996), yielding a characteristic curvilinear Schild regression. Such Schild regressions, over a more limited range of antagonist concentrations, appear linear but shallow.

Accordingly, extension of the Schild analysis with AC-42 and atropine in the calcium mobilisation assay to cover atropine concentrations over six orders of magnitude, revealed a Schild plot that deviated from a slope of unity and tended to plateau at the highest atropine concentrations. Subsequent analysis of the data according to an allosteric ternary complex model yielded a pK_B estimate for atropine that was in good agreement with its known affinity for the orthosteric site (Ellis, 2002), but also provided an estimate of the co-operativity between atropine and AC-42 (α value of 0.0002). However, the conclusion from these studies is that AC-42 must be the allosteric ligand, since atropine is the best-characterised orthosteric antagonist of the muscarinic receptors. Thus, it may be concluded that the iow Schild slopes associated with the interaction between atropine or pirenzepine and AC-42 actually reflect the saturability (governed by α in the ternary complex model) of an allosteric interaction between antagonist and agonist.

Due to the solubility maxima of the compounds involved relative to their affinity, it was not possible to extend the Schild regression for pirenzepine in the calcium assay

or either antagonist in the IP accumulation assay. However, despite the lack of saturation in the allosteric effect, it was possible to generate estimates of the co-operativity governing the interaction between AC-42 and atropine or pirenzepine. These estimates also suggest negative co-operativity governing the interaction between AC-42 and pirenzepine or atropine. The estimate of log α for the interaction between AC-42 and atropine in the IP accumulation assay and also that determined in the calcium assay using three antagonist concentrations is 10-fold higher than the estimate from the calcium assay that utilised a six log unit range of antagonist. These differences probably represent the limitations of estimating log α values where the range of antagonist concentrations tested is not saturating and results in a Schild regression that is still apparently linear (as in the IP accumulation assays and the calcium mobilisation assay with pirenzepine).

More direct evidence of an allosteric mode of action for AC-42, 77-LH-28-1, compound A and compound B was obtained using radioligand binding. [^{3}H]*N*-methyl scopolamine (NMS) is an extremely well characterised radioligand used to study muscarinic receptors. These studies confirmed that [^{3}H]NMS bound with rapid kinetics to membranes from CHO cells stably expressing the human M_1 receptor with sub-nanomolar affinity, in agreement with previous studies (Christopoulos *et al.*, 1999). It is well established that allosteric modulators can have characteristic effects on the binding of orthosteric ligands (Christopoulos & Kenakin, 2002). For example, binding studies using two or more radioligand concentrations can reveal differences in the binding isotherm of the allosteric modulator because the saturability in the allosteric event becomes more evident as the concentration of orthosteric radioligand is increased (Figure 8; Christopoulos & Kenakin, 2002). Consistent with this, AC-42, 77-LH-28-1 and compound A were unable to fully inhibit the specific binding of [^{3}H]NMS at either 0.2 nM or, more strikingly (with the exception of compound A), at the higher concentration of 2 nM radioligand (Figure 36). This was a property shared

by the prototypical modulator, gallamine (Figure 36), suggesting that these compounds act as negatively co-operative allosteric ligands at the M_1 receptor. The values of affinity and co-operativity derived for gallamine from the application of an allosteric model are in excellent agreement with similar values determined previously (Matsui *et al.*, 1995), whereas this study is the first to apply such a model to the M_1 receptor 'ectopic' agonists.

These data contrasted strikingly with the profile observed with both atropine and pirenzepine, which fully inhibited [^{3}H]NMS binding at radioligand concentrations of 0.2 nM and 2 nM and whose inhibition isotherms were entirely consistent with a simple, competitive interaction.

Compound B fully inhibited the binding of [^{3}H]NMS, yet the pair of inhibition curves derived from meaned data could be fitted to an allosteric model. In fact, statistical comparison of both the allosteric and a competitive model yielded a clear preference for the former. Full inhibition of orthosteric radioligand binding does not preclude a compound from acting allosterically, but would then suggest a high degree of negative co-operativity with the radioligand (Christopoulos & Kenakin, 2002). Unsurprisingly, given the full inhibition of [^{3}H]NMS binding, the estimate of log α for compound B suggested a much higher degree of negative co-operativity with respect to [^{3}H]NMS than was determined for AC-42, 77-LH-28-1 and compound A.

In contrast to the calcium mobilisation assays, it has already been observed that both AC-42 and 77-LH-28-1 appear as partial agonists in the IP accumulation assay. As such, they require full receptor occupancy to generate their maximal responses and the pEC_{50} value of a partial agonist is a useful approximate measure of its affinity for the receptor (Kenakin, 1997). In this respect it is noteworthy that the pK_B values estimated for the binding of AC-42 and 77-LH-28-1 according to an allosteric model

(6.19 ± 0.18 and 7.08 ± 0.02, respectively) are in excellent agreement with the potency values in the IP accumulation assay (6.21 ± 0.10 and 7.24 ± 0.02, respectively).

Additionally, the estimated α value for the interaction between AC-42 and [^{3}H]NMS was markedly different from the value describing the interaction between AC-42 and atropine. This highlights a second characteristic of allosteric interactions (in addition to saturability), namely, that the degree of co-operativity between orthosteric and allosteric sites depends on the chemical nature of the ligands occupying each site. This 'probe-dependence' of allosterism can explain why in some studies, an allosteric interaction may be missed altogether if it is characterised by either neutral co-operativity (i.e. appears as if there is no interaction) or by very high negative co-operativity (i.e. appears as if the interaction is competitive).

One of the most definitive methods used to validate an allosteric mechanism of action is to monitor the effects of a putative modulator on the dissociation of a pre-formed orthosteric ligand-receptor complex; any alteration in the dissociation of such a complex must be indicative of a conformational change mediated *via* a topographically distinct site (Kostenis & Mohr, 1996). Indeed, prototypical allosteric modulators of muscarinic receptors, such as C_7/3-phth (Christopoulos *et al.*, 1999), strychnine (Lazareno & Birdsall, 1995) and gallamine (Stockton *et al.*, 1983) have all been shown to allosterically retard the rate of [^{3}H]NMS dissociation from muscarinic receptors in a concentration-dependent fashion. Thus, the most striking confirmation of the allosteric nature of AC-42, as with gallamine, was obtained from [^{3}H]NMS dissociation kinetic assays. As illustrated in Figure 37b, both AC-42 and gallamine, but not compound A, retarded the dissociation of [^{3}H]NMS from the M_1 receptor, although the effect was much more pronounced for gallamine relative to AC-42. These results can be explained by at least two reasons: First, at the concentrations

of each modulator used in the kinetic assays (reflecting solubility maxima), it can be calculated from their relative K_B and α values that 1 mM gallamine would occupy approximately 98% of the [^{3}H]NMS-bound receptors, whereas 100 μM AC-42 would only occupy approximately 77% of the [^{3}H]NMS-bound receptors and 100 μM compound A would only occupy approximately 13% of [^{3}H]NMS-bound receptors. Therefore, it is not surprising that gallamine is able to exert a larger effect on [^{3}H]NMS dissociation than AC-42 and that compound A does not alter the dissociation rate. Second, it is possible that AC-42 and compound A simply cannot exert the same maximal effect on radioligand kinetics as gallamine. Indeed, other prototypical modulators of muscarinic receptors such as obidoxime have been shown to have limited effects on radioligand dissociation (Ellis & Seidenberg, 1992).

Collectively, the data presented herein provide unambiguous evidence that the 'ectopic' agonist, AC-42, is an allosteric ligand. As such, it is more appropriate to re-class this ligand as an allosteric, rather than ectopic, agonist. The prevalence of other confirmed allosteric agonists of G protein-coupled receptors remains relatively limited in the current literature. There is some evidence that the adenosine A_1 receptor enhancer, PD 81,723 ((2-amino-4,5-dimethyl-3-thienyl)-[3-(trifluoromethyl)phenyl] methanone), is able to promote a modest degree of receptor G protein-coupling in its own right (Bhattacharya & Linden, 1995). Similarly, the peptide, ASLW, has been shown to activate the chemokine CXCR4 receptor in a manner that is likely to be allosteric (Sachpatzidis *et al.*, 2003). For the muscarinic receptor family, Jakubik *et al.* (1996) showed that gallamine and alcuronium could promote receptor activation, but these results have not been consistently reproduced (Lazareno & Birdsall, 1995; May *et al.*, 2005), and may reflect the requirement of particular stoichiometries of receptor to G protein (Jakubik *et al.*, 1998). Earlier radioligand binding studies suggested that the partial agonist, McN-A-343 (N-[3-chlorophenyl] carbamoyloxy)-2-butynyl-trimethylammonium chloride), was also an

allosteric modulator of M_2 muscarinic receptors (Birdsall *et al.*, 1983), although a subsequent functional study was unable to conclude whether this compound interacted allosterically with very high negative co-operativity or *via* simple orthosteric competition when tested against carbachol (Christopoulos & Mitchelson, 1997).

This chapter has shown, using functional, equilibrium binding and dissociation kinetic assays, that the mechanism of action of AC-42 at the M_1 muscarinic receptor is qualitatively and quantitatively consistent with an allosteric model. Equilibrium binding has also provided evidence to suggest that that 77-LH-28-1, compound A and compound B act allosterically at the M_1 receptor. Clearly further studies on the mechanism of interaction of these compounds with the M_1 receptor are warranted.

These findings have important ramifications for muscarinic receptor-based drug discovery, but also raise additional considerations. For instance, is the allosteric site recognised by AC-42 and 77-LH-28-1 the same site as that recognised by gallamine, or a second allosteric site recognised by certain staurosporine derivatives (Lazareno *et al.*, 2000), or even a third topographically distinct allosteric site? Given that AC-42 has approximately the same affinity for all the muscarinic receptor subtypes (Spalding *et al.*, 2002), what is it about the nature of the AC-42 binding site that allows almost exclusive activation of the M_1 receptor relative to other muscarinic receptor subtypes? Clearly further studies are warranted to elucidate the molecular nature of this allosteric site. In this context it would be interesting to examine using dissociation kinetic studies whether AC-42 and 77-LH-28-1 compete for the same binding site as gallamine and C_7/3-phth, as has been tested with other allosteric ligands such as obidoxime (Ellis & Seidenberg, 1992). Furthermore, studies of the interactions and affinity of AC-42 and 77-LH-28-1 at the other muscarinic receptors may shed light on why these agonists display such a selective profile.

Given that the characterisation of AC-42 and other M_1 receptor agonists was performed in recombinant systems, native tissue radioligand binding and functional assays were performed to see if this class of compounds was able to interact with native muscarinic receptors.

The ratio of affinities of a muscarinic receptor ligand to inhibit agonist (usually [^{3}H]oxotremorine-M) and antagonist ([^{3}H]NMS or [^{3}H]QNB) radioligand binding is a well established method used to qualitatively approximate efficacy at muscarinic receptors (Freedman *et al.*, 1988; Loudon *et al.*, 1997; Watson *et al.*, 1999; Tayebati *et al.*, 1999). In agreement with previous studies, the muscarinic receptor antagonists atropine, scopolamine and pirenzepine displayed approximately equal affinity in inhibiting the binding of either [^{3}H]oxotremorine-M or [^{3}H]QNB to rat cortical membranes, generating affinity ratios close to unity (Loudon *et al.*, 1997). Conversely, muscarinic receptor agonists such as carbachol, muscarine and oxotremorine-M display much greater affinity to inhibit [^{3}H]oxotremorine-M binding compared to [^{3}H]QNB binding, yielding oxotremorine-M / QNB affinity ratios in excess of 1000. These values are consistent with previously reported studies in rat cortex with muscarinic receptor agonists (Loudon *et al.*, 1997; Watson *et al.*, 1999).

It has been suggested that intermediate agonist / antagonist affinity ratios, greater than 1 but less than 500 represent ligands that possess partial agonist activity at the muscarinic receptor population being examined (Tayebati *et al.*, 1999; Watson *et al.*, 1999). Accordingly, the muscarinic receptor partial agonists, xanomeline and pilocarpine, displayed oxotremorine-M / QNB affinity ratios of 10 and 55, respectively, whilst milameline and oxotremorine displayed ratios of approximately 500. These data are consistent with these compounds acting as partial agonists in this tissue. Interestingly, despite the allosteric mode of action described earlier, AC-42, 77-LH-28-1, compound A and compound B all displayed higher affinity to inhibit

[^{3}H]oxotremorine-M binding compared to [^{3}H]QNB binding, with affinity ratios similar to xanomeline. If the same conclusions can be applied to allosteric, as well as orthosteric muscarinic receptor ligands, these data predict that AC-42, 77-LH-28-1, compound A and compound B are all partial agonists at cortical muscarinic receptors. However, this method does not seem to provide an accurate estimate of intrinsic activity. In the CHO-hM_1 IP accumulation assay, 77-LH-28-1 displayed much higher efficacy than compound A and compound B and was approximately as efficacious as AC-42. However, 77-LH-28-1 displayed the lowest oxotremorine-M / QNB affinity ratio of all the allosteric M_1 receptor agonists. This comparison of [^{3}H]oxotremorine-M / [^{3}H]QNB binding and CHO-hM_1 IP accumulation assays does make the assumptions that the muscarinic receptor population in cortical tissue is predominantly of the M_1 receptor subtype and that there are no significant differences between the rank order of efficacies at rat and human receptor subtypes. However, the affinity ratio assay appears to be limited to qualitative resolution of full agonists, partial agonists and antagonists rather than an accurate determination of intrinsic activity.

To conclude the characterisation of this novel class of selective M_1 receptor agonists, 77-LH-28-1 was examined in an *in vitro* neuronal network oscillations model in the rat temporal cortex. The non-selective cholinergic agonist, carbachol, has been shown to induce persistent rhythmical oscillatory activity in the 30 – 80 Hz (gamma) range in both rodent hippocampal (Fisahn *et al.*, 1998) and cortical (Buhl *et al.*, 1998) slices. Furthermore, muscarine induced gamma oscillations in CA3 neurons of the hippocampus are absent in mice lacking the muscarinic M_1 receptor (Fisahn *et al.*, 2002), clearly implicating this receptor subtype in the induction of the gamma frequency oscillations. In the studies described in this chapter, carbachol (15 μM) induced persistent rhythmical oscillatory activity in both the beta (20 – 30 Hz) and gamma (30 - 80 Hz) frequency ranges in layer IV of the rat temporal cortex.

Application of 77-LH-28-1 (3 μM) induced robust gamma network activity in the same region at a mean frequency of 42.1 ± 2.0 Hz. These oscillations were abolished in the presence of the muscarinic receptor antagonist, atropine, confirming that the response was muscarinic receptor mediated. However, 77-LH-28-1 did not induce oscillations in the beta frequency range. These results show that 77-LH-28-1 acts as a muscarinic receptor agonist in native cortical tissue, mimicking the gamma frequency oscillations induced by carbachol. Furthermore, these results suggest that given the selectivity profile of 77-LH-28-1, carbachol induced gamma frequency oscillations in layer IV of the temporal cortex are probably mediated entirely *via* activation of the muscarinic M_1 receptor subtype. In contrast, 77-LH-28-1 was unable to induce the beta oscillatory activity that was observed with carbachol, suggesting that activation of other muscarinic receptor subtypes or nicotinic acetylcholine receptors, either alone or in combination with the M_1 receptor subtype, are required to stimulate this oscillatory behaviour.

The studies in this chapter have extensively characterised the pharmacology of the M_1 receptor selective agonist, AC-42. Furthermore, they have examined a related analogue, 77-LH-28-1 and two novel M_1 receptor selective agonists in compound A and compound B. Both AC-42 and compound A were shown to signal through similar signal transduction pathways to carbachol at the M_1 receptor. Antagonist studies also provided direct evidence that the functionally selective M_1 receptor agonist, AC-42, is an allosteric modulator. An investigation of the mode of interaction of this agonist with various orthosteric ligands confirmed that AC-42 exhibited characteristics associated with prototypical allosteric ligands, including (i) a saturability to its allosteric effects (a property that was also shown to be shared with 77-LH-28-1 and compound A), (ii) a dependence of these effects on the nature of the orthosteric ligand with which it interacted and (iii) the ability to significantly retard the dissociation of [^{3}H]NMS from the muscarinic M_1 receptor. These results reveal that the M_1

receptor possesses an allosteric site capable of mediating receptor activation in its own right, and further reinforce the utility of allosteric binding sites for achieving selectivity at G protein-coupled receptors. Finally, these compounds were shown to interact with cortical muscarinic receptors in both radioligand binding and electrophysiological assays in a manner that suggests they possess agonist activity in a native tissue system. The discovery of an allosteric agonist site on the muscarinic M_1 receptor provides a great opportunity for future drug discovery in this area. The increasing awareness of allosteric ligands and their uses has the potential to lead to more selective drugs that target GPCRs in the future – the only currently marketed allosteric drug that acts at a GPCR is cinacalcet, an allosteric enhancer of the calcium-sensing receptor (Wess, 2005).

Chapter 6

Characterisation of the ectopic agonist – muscarinic M_1 receptor interaction

(i) Introduction

As discussed extensively in Chapter 1, the orthosteric binding site of the muscarinic M_1 receptor, deep within the TM bundle, has been extensively studied by means of homology modelling and SDM. Many interactions for both agonist (eg. ACh, carbachol) and antagonist (eg. NMS, atropine) binding have been identified. As such the M_1 receptor orthosteric site probably remains one of the best characterised amongst the GPCR superfamily. Furthermore, as shown in Chapter 5, the interaction of a number of allosteric ligands with muscarinic receptor subtypes has also been probed by SDM. Generally, ligands such as gallamine and C_7/3-phth have been shown to bind to the exofacial region of the receptor, making contacts with epitopes at the top of the TM domains and with the extracellular loops.

As discussed in Chapter 5, AC-42 has recently been identified as an ectopic agonist of the muscarinic M_1 receptor (Spalding *et al.*, 2002). This compound displays a highly selective profile, activating the M_1 receptor alone amongst the muscarinic receptor family (Spalding *et al.*, 2002). The studies in Chapter 5 have clearly demonstrated that AC-42 (and possibly other ectopic agonists) are actually allosteric ligands, a property that is likely to account for their unprecedented selectivity profile.

However, the molecular recognition site for AC-42 remains unknown. In order to understand this selective agonist activity at the M_1 receptor Spalding *et al.* (2002) constructed chimeric M_1/M_5 receptors to identify the regions of the M_1 receptor involved in the binding of AC-42. A chimera in which only 45 aa in the N-terminus and TM1 were replaced by those in the M_5 receptor was still responsive to carbachol, but failed to be stimulated by AC-42, suggesting that this region is key to the activity of AC-42 (Spalding *et al.*, 2002). However, a chimera with only the first 50 aa of the M_1 receptor and the remainder from the M_5 receptor was similarly unresponsive to

AC-42, indicating that whilst the N-terminal-TM1 region is necessary, it is not sufficient for AC-42 activity (Spalding *et al.*, 2002).

A chimera with the region from the N-terminus to the end of TM6 from the M_1 receptor (residues 1 – 388) and the remainder from the M_5 receptor was also unresponsive to AC-42. However a further chimera with the 'M_1-like' region stretching from the N-terminus to the middle of TM7, incorporating residues 1 – 418 of the hM_1 receptor, was responsive to AC-42, albeit with lower efficacy than the wild-type M_1 receptor. These data suggest that residues within the third extracellular loop (ECL3) and the top of TM7 of the M_1 receptor may also be key to AC-42 activity (Spalding *et al.*, 2002).

Studies with chimeras in which the middle of the M_1 receptor was replaced with the M_5 receptor sequence, but retained the M_1 receptor sequence in the N-terminus-TM1 and ECL3-TM7 regions (M_1-like residues 1 – 45 and 388 – 418; M_5-like residues 46 – 387 and 418 – 460), confirmed that both these regions are required and act synergistically to play a role in the activation of the M_1 receptor by AC-42 (Spalding *et al.*, 2002).

Clearly these regions that have been identified are not consistent with AC-42 binding to the orthosteric site of the M_1 receptor. In an elegant conclusion to their study, Spalding *et al.* (2002) demonstrated that the potency of AC-42 was not attenuated by the mutations Y381A or N382A in TM6, which abolish the agonist activity of carbachol (Spalding *et al.*, 2002; Ward *et al.*, 1999). In the absence of definitive proof that this ligand was allosteric (which has now been resolved as described in Chapter 5), these data prompted the authors to term AC-42 an 'ectopic' agonist, due to its interaction with a site on the M_1 receptor distinct from that recognised by carbachol.

Despite the identification of the gross regions involved in AC-42 binding, the precise molecular nature of the binding site for AC-42 and related analogues at the M_1 receptor remains unknown. In the studies described in this chapter this question has been addressed through homology modelling of the M_1 receptor based on the crystal structure of rhodopsin. This model has allowed the prediction of some of the possible molecular interactions of AC-42, 77-LH-28-1, compound A and compound B with the M_1 receptor. These predictions have been assessed by both [^{3}H]NMS saturation and inhibition binding and functional calcium mobilisation studies with M_1 receptors containing appropriate point mutations.

(ii) Ligand docking and site directed mutagenesis

The initial placement of AC-42 within the muscarinic M_1 receptor was guided by the M_1/M_5 chimeric receptor studies (Spalding *et al.*, 2002; Figure 41) and the fact that AC-42 contained a basic nitrogen for which acidic residues within the essential portion of the M_1 receptor sequence were sought. The studies by Spalding *et al.* (2002) clearly defined residues 1 – 45 and 388 – 418 of the M_1 receptor as being crucial to AC-42 agonist activity (Figure 41). Therefore, it was within these regions that candidate acidic residues to partner the basic nitrogen were identified.

Following the various initial placements of the ligand, the complex was minimised with CHARMm (using NOE distance helical constraints in the TM bundle, distance dependent dielectric, 2000 steps SD and 5000 steps ABNR).

All reasonable docking solutions suggested that the E401 on TM7 was forming a charge-charge interaction with the protonated nitrogen of AC-42 (Figure 42). This placed the aromatic benzoyl portion of AC-42 down between helices 1, 2 and 7, with the phenyl ring sitting directly above Y408 and encircled by a number of other aromatic residues: Y82, W101, Y404 and W405.

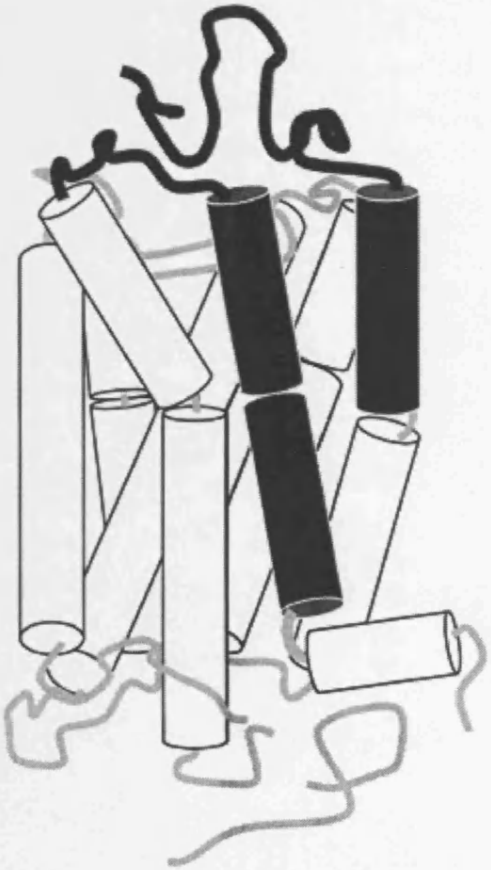

Figure 41. Representation of the 3-dimensional structure of the muscarinic receptor, modelled after the crystal structure of rhodopsin (Palczewski *et al.*, 2000). Cylinders represent helices. Lines represent connecting intracellular and extracellular loops. The extracellular surface is at the top of the page. TM1 is on the right, and the helices proceed in a counter-clockwise direction. Filled cylinders and lines represent muscarinic M_1 receptor-like sequence (residues 1 – 45 and 388 – 418); open cylinders and lines represent muscarinic M_5 receptor-like sequence (residues 46 – 387 and 418 – 460).

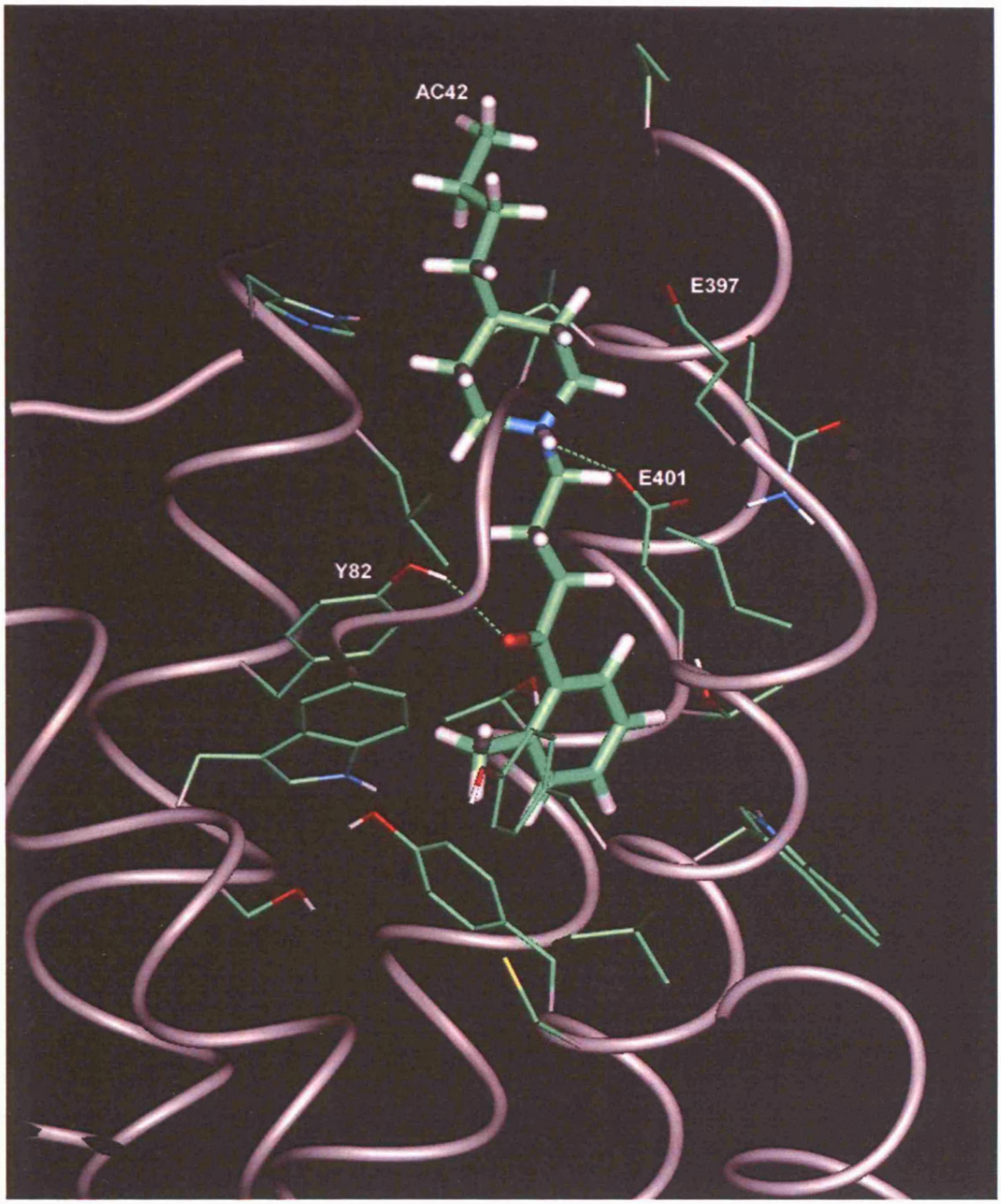

Figure 42. Predicted interactions of AC-42 with the muscarinic M_1 receptor. Charge-charge interactions of the protonated nitrogen with E397/E401 and carbonyl oxygen with Y82 are shown.

Additionally, it appeared that the hydroxyl hydrogen on T34 was forming a hydrogen bond to the π system of the phenyl ring (Meyer *et al.*, 2003). The carbonyl oxygen of the benzoyl portion was proposed to hydrogen bond to the hydroxyl portion of Y82 (Figure 42). The butyl linker between the aromatic ring and the piperidine ring was transversing a hydrophobic pocket defined by I28 and L86, and the piperidine ring and the aliphatic butyl tail of AC-42 are located at the top of this pocket forming hydrophobic interactions with L86, V25 and A175.

The docking of AC-42 was used as a basis for the docking of compound A and compound B. As with AC-42, both of these compounds contain a basic nitrogen that was predicted to form charge-charge interactions with E397 and E401. Similarly, a carbonyl oxygen of compound A and compound B was predicted to form a hydrogen bond with Y82 in TM2 and, as with AC-42, the hydroxyl hydrogen on T34 was predicted to be forming a hydrogen bond to the π system of a phenyl ring.

On the basis of these docking studies, the acidic residues E397 & E401 and the proposed hydrogen bonding residue Y82 were identified as targets for SDM studies and the mutations E397A, E401A, E397A/E401A and Y82F were made using the QuikChange PCR method. To compare and contrast this proposed binding mode with the orthosteric mode, the Y381A orthosteric mutation (Ward *et al.*, 1999) was also selected for studies and made using the method of PCR SOEing (Horton *et al.*, 1990). The location of the chosen residues is shown in Figure 43. Mutations to alanine were employed in order to remove the amino acid side-chains beyond the β-carbon whilst maintaining the α-helical structure of the transmembrane domains to minimise any gross changes to receptor conformation. The Y82F mutation was chosen to investigate the proposed role of the phenolic hydroxyl group of the tyrosine residue.

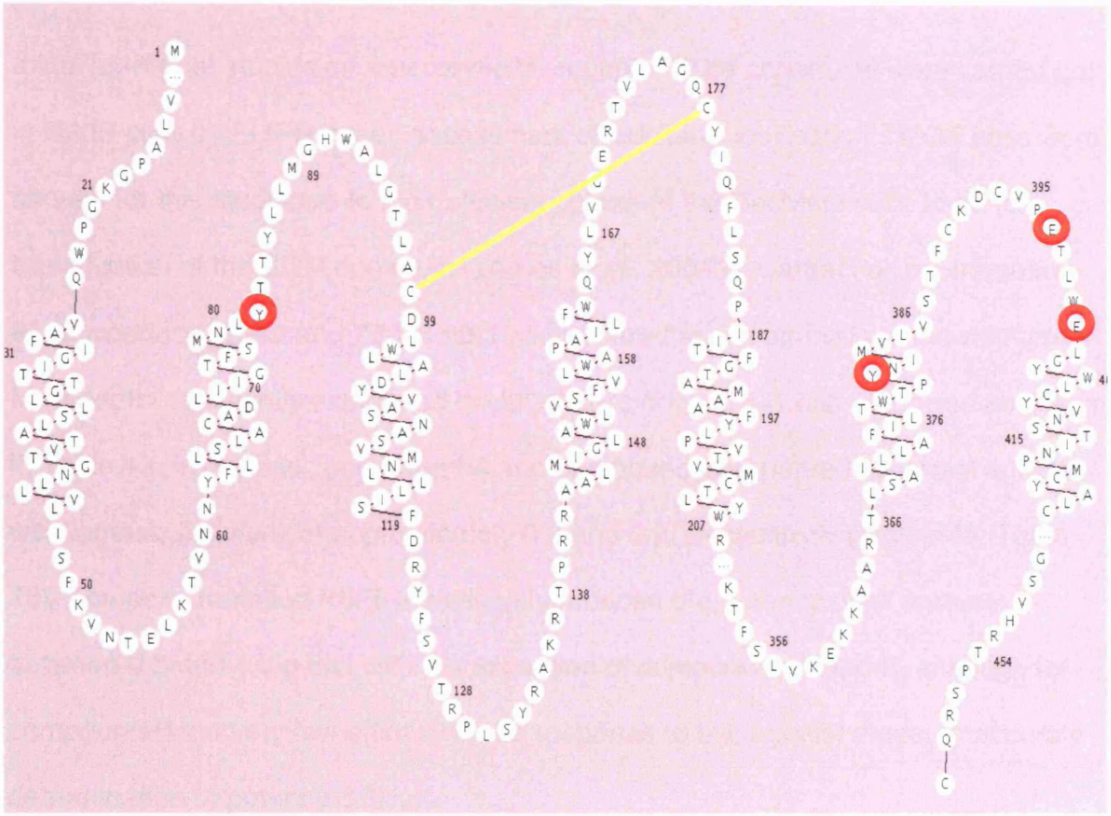

Figure 43. Schematic representation of the human muscarinic M_1 receptor highlighting key residues which were predicted to be involved in interactions with AC-42; the residues circled in red were mutated. The yellow bar represents a disulphide bond. For reasons of clarity both the C- and N-termini as well a portion of the third intracellular loop have been truncated.

(iii) U2OS and CHO-K1 SDM calcium mobilisation studies

Initial functional studies on muscarinic M_1 receptor SDM constructs were carried out in U20S cells by FLIPR based assessment of calcium mobilisation. U2OS cells were chosen for this study due to their efficient uptake of the BacMam virus used for transduction of the SDM constructs (Ames *et al.*, 2004a). Carbachol, oxotremorine-M, muscarine, AC-42 and 77-LH-28-1 all appeared as full agonists at the wild-type M_1 receptor transiently expressed in U2OS cells (Figure 44) with potencies as shown in Table 13. In contrast, compound A and compound B appeared as partial agonists with intrinsic activities of approximately 0.8 and 0.3, respectively (Figure 44; Table 13). The point mutation Y82F significantly reduced the potency of all agonists by between 0.5 and 1 log unit with the exception of compounds A and B, although for compound B the very low efficacy of the response to this agonist made an accurate determination of potency difficult.

Mutation of E397 at the top of TM7 did not significantly affect the potency of either orthosteric or ectopic agonists (Figure 44; Table 13). Similarly, loss of E401 did not significantly alter the potency of any of the agonists tested. The double mutation, E397A/E401A, did not significantly alter the potency of orthosteric agonists (with the exception of a 2-fold reduction in oxotremorine-M potency) or that of AC-42 and 77-LH-28-1. However, this mutation caused a significant 5-fold reduction in the potency of compound A and effectively abolished any agonist activity observed with compound B.

Mutation of Y381 in TM6 abolished the agonist activity of carbachol and oxotremorine-M and caused a 300-fold reduction in the potency of muscarine that was accompanied by a marked reduction in efficacy (Table 13). This mutation also effectively abolished the agonist activity observed with AC-42 and 77-LH-28-1.

However, loss of Y381 yielded significant *increases* in the potency of compounds A and B, with 2-fold and 10-fold leftward shifts in the concentration response curves to these agonists, respectively. In the case of compound B this was accompanied by an increase in the efficacy of the response.

Calcium mobilisation studies were also performed using CHO-K1 cells as the parental cell line as a functional comparison to the [^{3}H]NMS binding studies. Agonist responses to carbachol, compound A, AC-42 and 77-LH-28-1 were determined against wild-type, E397A/E401A and Y381A constructs (Figure 45; Table 14). Mutation of Y381 reduced the potency of carbachol by greater than 1000-fold. Surprisingly in light of the previous results, this mutation did not abolish the responses to AC-42 and 77-LH-28-1 in the same way that it did for carbachol. However, the potencies of AC-42 and 77-LH-28-1 were significantly reduced 4-fold and 17-fold, respectively, with approximately a 30% reduction in the maximal response. Conversely, loss of Y381 caused a significant 10-fold increase in the potency of compound A to stimulate calcium mobilisation. The double mutation, E397A/E401A, did not affect the potency of carbachol but produced a 2-fold reduction in the potencies of AC-42, 77-LH-28-1 and compound A; only the reduction in compound A potency reached significance ($p < 0.05$; Figure 45; Table 14).

Figure 44. Concentration-dependent stimulation of Ca^{2+} mobilisation by muscarinic receptor agonists at wild type and mutant muscarinic M_1 receptor constructs transiently expressed in U2OS cells. All compounds and constructs were assesses in parallel, hence all data are normalised to the maximal wild-type carbachol response. Data are the mean of 3 experiments; error bars show s.e.m..

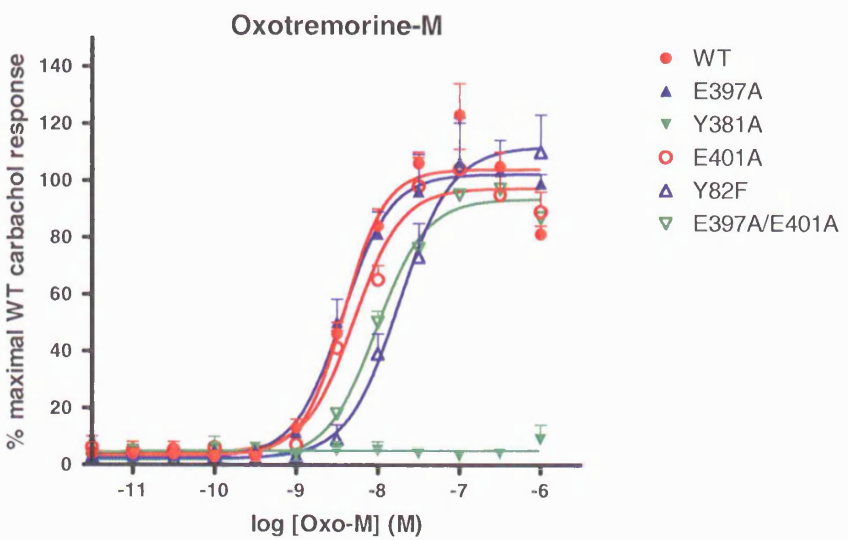

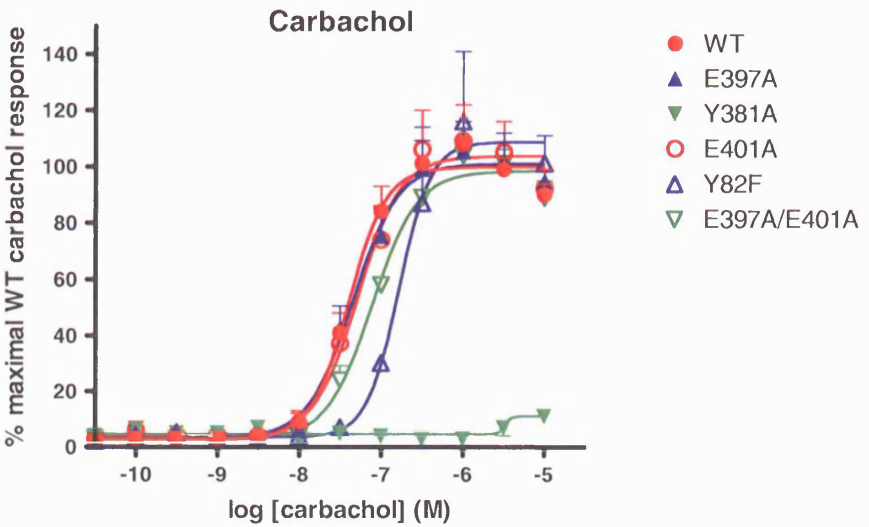

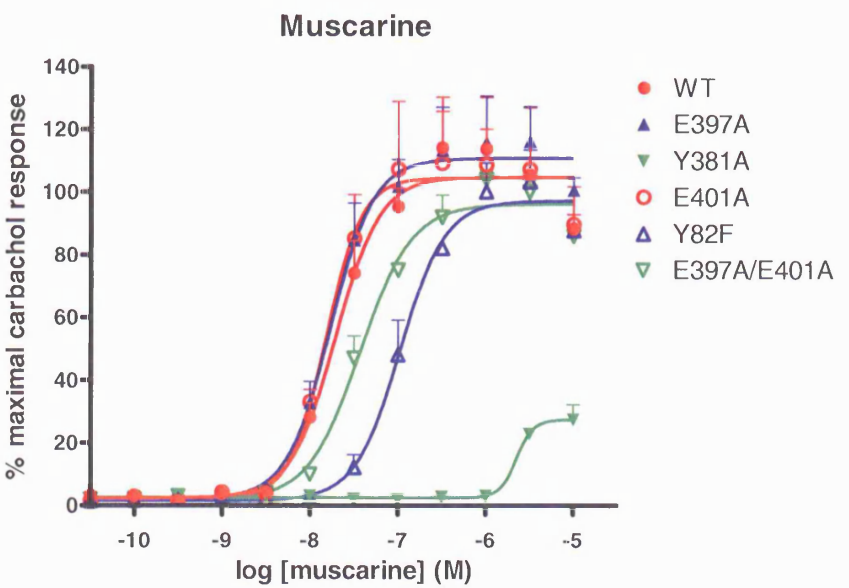

Figure 44. *cont.*

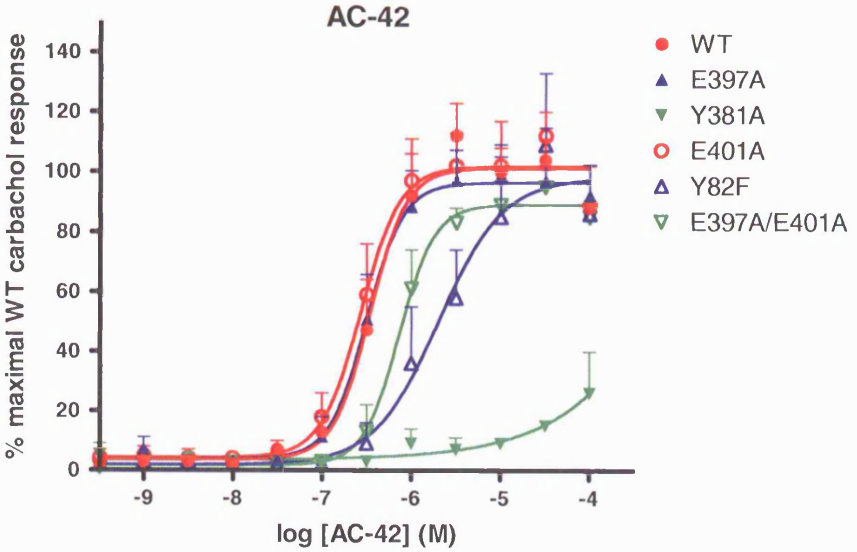

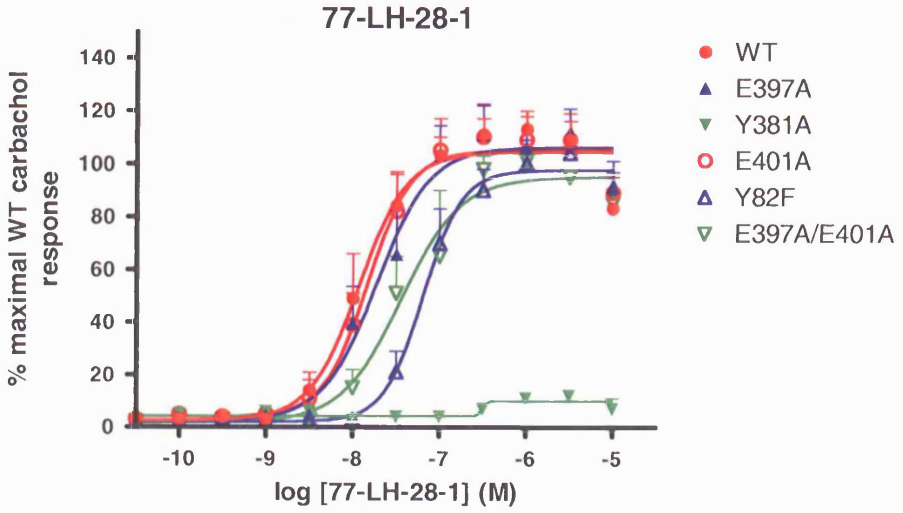

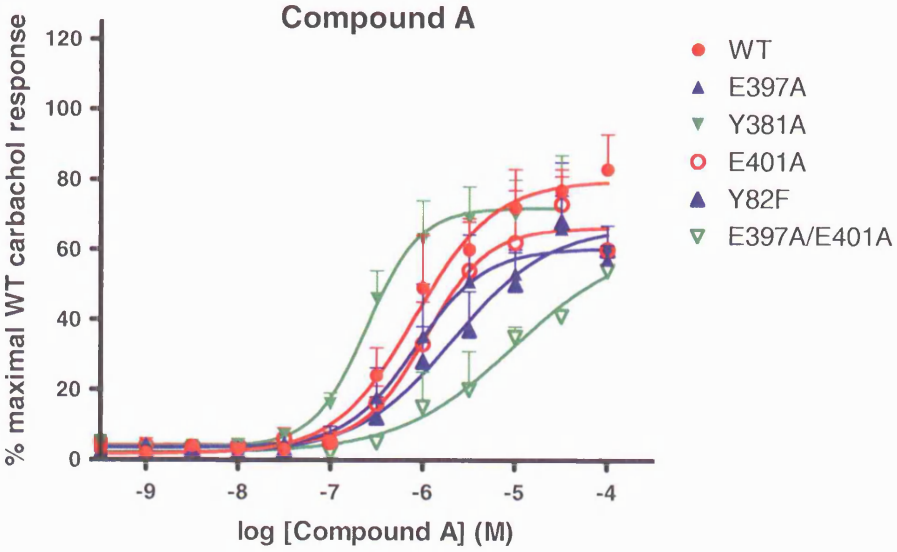

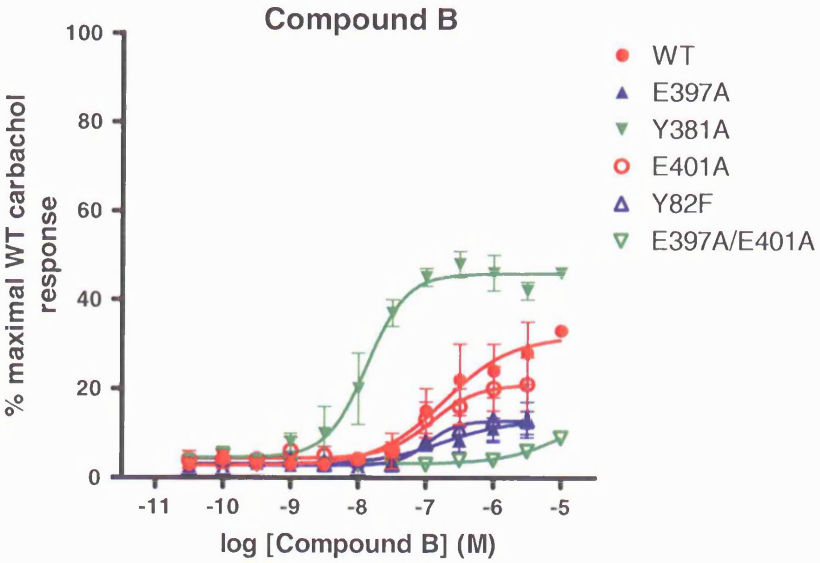

Compound	WT	Y82F	E397A	E401A	E397A/E401A	Y381A
Carbachol	7.36 ± 0.06 (1.0; *n=6*)	6.66 ± 0.07*** (1.0; *n=6*)	7.28 ± 0.10 (1.0; *n=4*)	7.28 ± 0.06 (1.0; *n=5*)	7.30 ± 0.08 (1.0; *n=6*)	< 5*** (0.1; *n=4*)
Oxotremorine-M	8.38 ± 0.08 (1.0; *n=6*)	7.69 ± 0.12*** (1.1 *n=6*)	8.34 ± 0.10 (1.0 *n=4*)	8.34 ± 0.06 (1.0; *n=5*)	8.09 ± 0.07* (1.0; *n=6*)	< 5*** (0.1; *n=4*)
Muscarine	8.04 ± 0.13 (1.0; *n=5*)	7.14 ± 0.12** (1.0; *n=4*)	7.78 ± 0.03 (1.1; *n=3*)	7.91 ± 0.09 (1.0; *n=4*)	7.75 ± 0.14 (1.0; *n=5*)	5.55 ± 0.35*** (0.3; *n=3*)
AC-42	6.78 ± 0.14 (1.0; *n=6*)	5.99 ± 0.19** (1.0; *n=6*)	6.60 ± 0.15 (1.0; *n=4*)	6.73 ± 0.18 (1.0; *n=5*)	6.60 ± 0.16 (0.9; *n=6*)	< 5*** (0.3; *n=4*)
77-LH-28-1	7.93 ± 0.08 (1.0; *n=6*)	7.22 ± 0.05*** (1.0; *n=5*)	7.72 ± 0.16 (1.1; *n=4*)	7.85 ± 0.09 (1.0; *n=5*)	7.62 ± 0.12 (0.9; *n=6*)	< 5*** (0.1; *n=4*)
Compound A	6.26 ± 0.08 (0.8; *n=7*)	5.95 ± 0.22 (0.7; *n=5*)	6.13 ± 0.22 (0.6; *n=4*)	5.99 ± 0.11 (0.7; *n=5*)	5.69 ± 0.17* (0.6; *n=7*)	6.62 ± 0.04† (0.7; *n=4*)
Compound B	6.86 ± 0.22 (0.3; *n=6*)	6.98‡ (0.1; *n=8*)	6.74‡ (0.1; *n=5*)	6.92‡ (0.2; *n=6*)	n.r.*** (*n=6*)	7.86 ± 0.20†† (0.5; *n=5*)

Table 13. pEC_{50} and intrinsic activity values for intracellular Ca^{2+} mobilisation induced by muscarinic receptor agonists at wild type and mutant muscarinic M_1 receptor constructs transiently expressed in U2OS cells. Data are the mean ± s.e.m. (intrinsic activity; '*n*' number); each experiment was performed on a separate viral transduction. ‡ Potency estimates derived from meaned data; n.r. = no response at concentrations up to 10 μM. * $p < 0.05$; ** $p < 0.01$; *** $p < 0.001$ significantly reduced compared to wild-type response; † $p < 0.05$; †† $p < 0.01$ significantly increased compared to wild type response (Student's T-test).

Ligand / Receptor	WT	Y381A	E397A/E401A
Carbachol	8.28 ± 0.11 (*n=5*)	< 5*** (*n=4*)	8.25 ± 0.03 (*n=4*)
AC-42	7.56 ± 0.13 (*n=5*)	6.92 ± 0.10** (*n=5*)	7.27 ± 0.10 (*n=4*)
77-LH-28-1	9.13 ± 0.12 (*n=6*)	7.89 ± 0.04*** (*n=4*)	8.84 ± 0.06# (*n=5*)
Compound A	6.93 ± 0.07 (*n=5*)	7.95 ± 0.18††† (*n=5*)	6.62 ± 0.06* (*n=4*)

Table 14. pEC_{50} (± s.e.m.) values for intracellular Ca^{2+} mobilisation induced by carbachol, compound A, AC-42 and 77-LH-28-1 at wild type and mutant muscarinic M_1 receptor constructs transiently expressed in CHO-K1 cells.

* $p < 0.05$; ** $p < 0.01$; *** $p < 0.001$ significantly reduced compared to wild-type response; † $p < 0.05$; ††† $p < 0.001$ significantly increased compared to wild type response (Student's T-test). # $p = 0.07$.

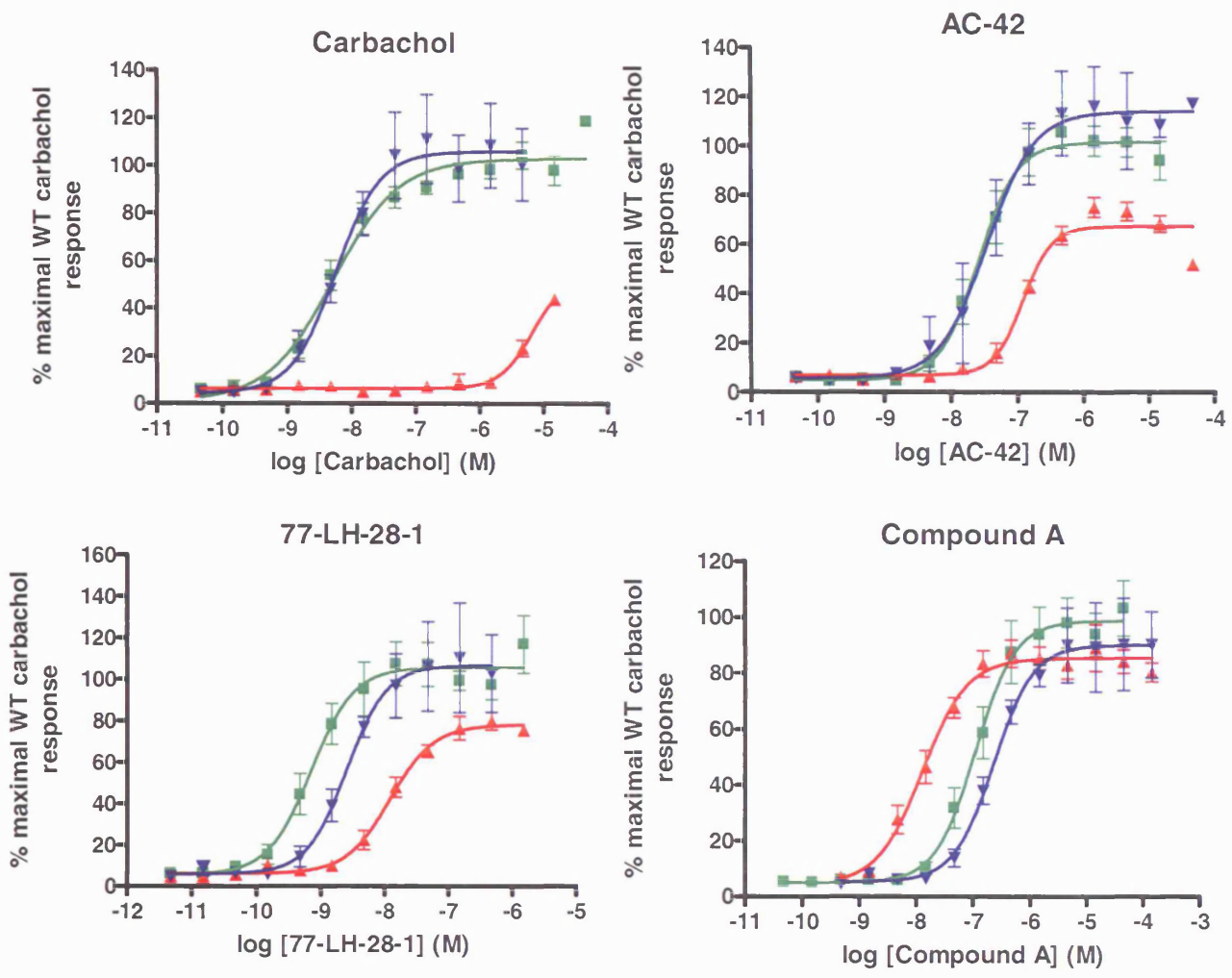

Figure 45. Concentration-dependent stimulation of Ca^{2+} mobilisation induced by carbachol, AC-42, 77-LH-28-1 and compound A at wild type (■), E397A/E401A (▼) and Y381A (▲) mutant muscarinic M_1 receptor constructs transiently expressed in CHO cells. Data are the mean of 3 experiments; error bars show s.e.m..

(iv) CHO-K1 SDM [^{3}H]NMS saturation binding

Specific binding of [^{3}H]NMS to membranes from CHO cells transiently transduced with the wild-type muscarinic M_1 receptor was saturable and represented more than 70% of total binding. Non-linear regression revealed that [^{3}H]NMS bound to a single site with a K_D value of 0.26 ± 0.04 nM and a B_{max} of 173.6 ± 29.9 fmol mg protein^{-1} (Figure 46). Specific binding of [^{3}H]NMS to membranes from CHO-M_1-E397A/E401A cells represented less than 50% of total binding. The affinity of [^{3}H]NMS binding was unaltered by the mutation of E397 and E401 (K_D = 0.34 ± 0.13 nM), although there was a significant reduction in the B_{max} compared to wild-type cell membranes (50.8 ± 3.1 fmol mg protein^{-1}; F-test; Figure 46). CHO cells transiently expressing the M_1-Y381A construct displayed no specific binding of [^{3}H]NMS up to concentrations of 2.2 nM (Figure 46).

(v) CHO-K1 SDM [^{3}H]NMS inhibition binding

The broad spectrum muscarinic receptor antagonist atropine inhibited specific [^{3}H]NMS binding to membranes from CHO-K1 cells transiently expressing the wild-type muscarinic M_1 receptor, with a pK_i value of 9.20 ± 0.05 (Table 15; Figure 47). Atropine displayed a similar affinity (9.18 ± 0.01) at the muscarinic M_1 receptor containing the double point mutation, E397A/E401A. Compound A inhibited [^{3}H]NMS binding to the wild-type M_1 receptor with a pK_i value of 5.30 ± 0.07. The affinity of compound A was not significantly altered at the double mutant receptor (Table 15, Figure 47). In contrast, AC-42 displayed a significantly reduced affinity for M_1-E397A/E401A (pK_i = 5.34 ± 0.03) compared to the wild-type receptor (5.76 ± 0.06; p < 0.01; T-test).

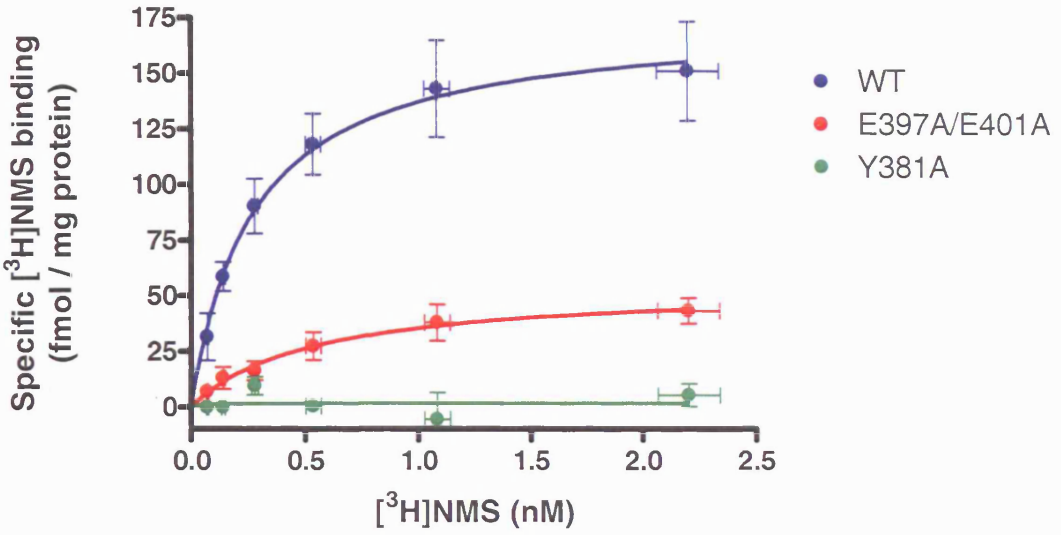

Figure 46. Saturation analysis of specific binding of [^{3}H]NMS to membranes from CHO cells transiently expressing the wild-type muscarinic M_1 receptor and constructs containing the point mutations E397A/E401A and Y381A. Data shown are the mean of 3 experiments; error bars represent s.e.m..

A

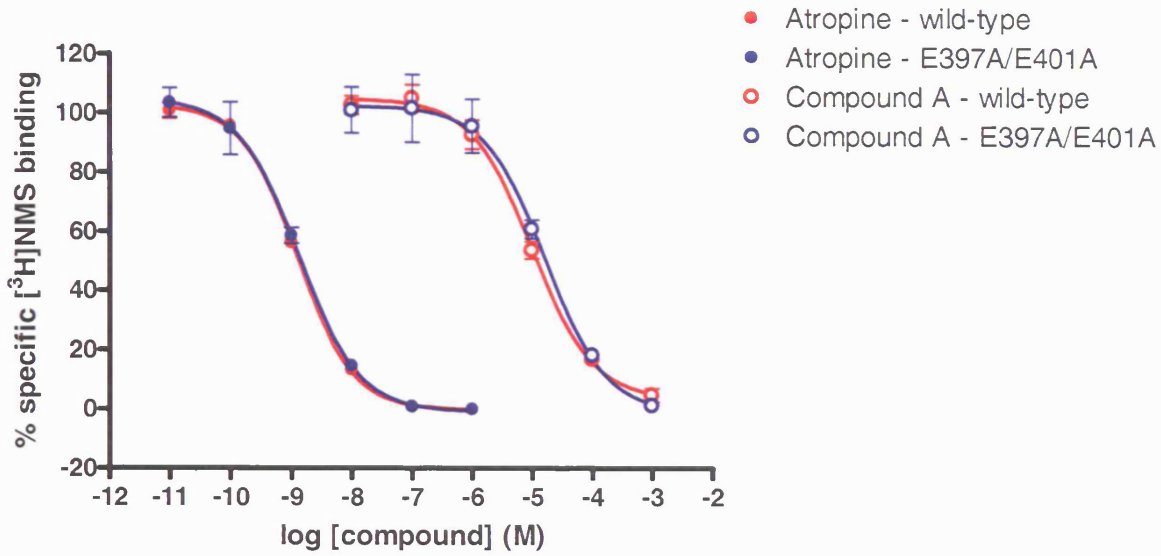

B

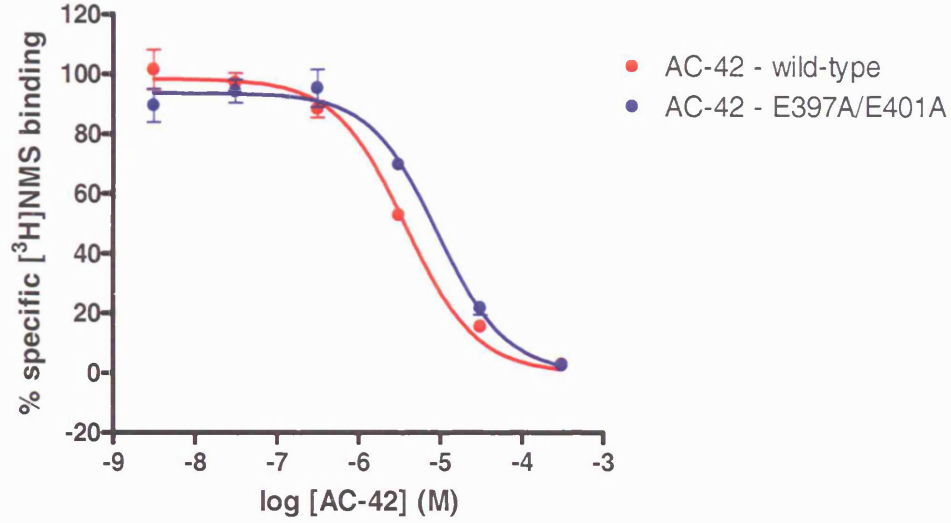

Figure 47. Concentration-dependent inhibition of specific [^{3}H]NMS binding to membranes from CHO cells transiently expressing the wild-type muscarinic M_1 receptor and a construct containing the point mutations E397A/E401A by (A) atropine and compound A and (B) AC-42. Data shown are the mean of 3 experiments; error bars represent s.e.m..

Ligand / Receptor	WT	E397A/E401A
Atropine	9.20 ± 0.05	9.18 ± 0.01
Compound A	5.30 ± 0.07	5.07 ± 0.13
AC-42	5.76 ± 0.06	5.34 ± 0.03

Table 15. pK_i values (± s.e.m.) of atropine, compound A and AC-42 to inhibit binding of [^{3}H]NMS from membranes of CHO cells transiently expressing M_1-WT and M_1-E397A/E401A. Data are the mean of 3 experiments.

(vi) Discussion

The studies in Chapter 5 have characterised the pharmacology of AC-42 and a range of other allosteric agonists at the muscarinic M_1 receptor. It is apparent from the chimeric M_1/M_5 receptor studies performed by Spalding *et al.* (2002) that the binding site for AC-42 is at least partially or wholly distinct from the well conserved orthosteric binding site of the muscarinic receptor family. However, little is known of the molecular nature of the recognition site for these selective agonists.

In this chapter, as with PrRP and GPR10 in Chapter 4, a combined molecular modelling and SDM approach has been used in order to elucidate the molecular nature of the allosteric agonist binding site. A homology model of the muscarinic M_1 receptor was constructed based on the crystal structure of bovine rhodopsin (Palczewski *et al.*, 2000) followed by manual docking of both AC-42 and compound A. Site directed mutagenesis was then carried out on various amino acid residues identified as possible attachment points for AC-42 and compound A. Mutant constructs were assessed using a combination of functional calcium mobilisation studies and [^{3}H]NMS binding.

Using the results from the chimera studies (Spalding *et al.*, 2002) as a basis, acidic residues within the essential portion of the M_1 receptor sequence were sought to complement the protonated nitrogen of AC-42. All acceptable solutions placed the protonated nitrogen in close proximity to E401 and also near E397. This orientation suggested that the carbonyl oxygen of AC-42 formed a hydrogen bond with the phenolic hydroxyl group of Y82. In light of these predictions, constructs containing the single point mutations E397A and E401A, as well as a double mutation, E397A/E401A were made. Furthermore, a construct containing the point mutation Y82F, which lacks the hydroxyl moiety, was made to test the predicted interaction with the carbonyl oxygen. Finally, a construct containing the well characterised

mutation of the orthosteric site, Y381A, was made. This mutation has been shown to reduce the potency of carbachol and acetylcholine by greater than 1000-fold (Ward *et al.*, 1999). However, this mutation leaves responses to AC-42 and *N*-desmethylclozapine (a metabolite of the anti-psychotic drug, clozapine, that purports to be an allosteric agonist of the muscarinic M_1 receptor) relatively unaffected (Spalding *et al.*, 2002; Sur *et al.*, 2003). Whilst not defining the recognition site of the allosteric M_1 receptor agonists, this mutation was key to determining whether this class of compounds interacted at a site that was non-orthosteric.

The loss of the hydroxyl group of Y82 caused an approximate 5-fold reduction in potency of all the muscarinic receptor agonists to stimulate calcium mobilisation in U2OS cells. The mutation Y82F has previously been demonstrated to reduce both the affinity and potency of carbachol (the latter approximately 3.5-fold) at the rat muscarinic M_1 receptor (Lee *et al.*, 1996). The authors were unable to conclude whether Y82 played a direct role in the binding of carbachol, or rather associated with important residues in other TM domains to maintain proper receptor conformation.

The model presented in this chapter predicts that Y82 is positioned far removed from the conserved aspartate residue in TM3 (D105) to rule out any role in the direct binding of orthosteric agonists. Given the universal effect of Y82F on agonist potencies, it is possible that its effects are due to a global disruption in the receptor conformation that mediates agonist activation. Alternatively, this mutation could be directly affecting the binding of the allosteric agonists (by disruption of the carbonyl oxygen hydrogen bond) and indirectly affecting the binding of orthosteric agonists by disrupting the conformation of the receptor deeper in the TM bundle. However, given the relatively small effects of this mutation on the potencies of the allosteric agonists, it is unlikely that Y82 is the main attachment point for this class of compounds at the M_1 receptor.

The results with the individual point mutations E397A and E401A were largely disappointing. Neither individual mutation had any significant effect on the potency of either orthosteric or allosteric agonists to stimulate calcium mobilisation in U2OS cells. However, when AC-42 was docked into the homology model it did appear that it could adopt conformations in which the protonated nitrogen could interact with either of the glutamate residues. If so, then single mutation of either of the glutamate residues could feasibly still leave an acidic residue with which AC-42 could interact. Accordingly, a construct containing both the E397A and E401A mutations was made. This double mutation did not significantly affect the potencies of the orthosteric agonists, carbachol, oxotremorine-M or muscarine, or those of AC-42 or 77-LH-28-1. However, the potency of compound A was reduced 4-fold and the weak partial agonist activity of compound B was abolished. It is possible that E397 and E401 may play a role in the binding, or receptor activation, mediated by compound A and compound B. However, it may also be that as partial agonists, the responses to these compounds may be more sensitive to reductions in levels of receptor expression. This was indeed demonstrated for the E397A/E401A mutant using [^{3}H]NMS binding.

It should, however, be noted that in similar calcium mobilisation studies in CHO cells (designed to complement the [^{3}H]NMS binding studies that were also carried out in the CHO cell background), the effect of the E397A/E401A mutation on compound A was more limited, causing only a 2-fold reduction in potency. A similar level of effect was observed with AC-42 and 77-LH-28-1. As in the U2OS cells, there was no effect of E397A/E401A on the potency of carbachol to induce calcium mobilisation.

[^{3}H]NMS binding studies were also performed in order to investigate further the role of E397 and E401. [^{3}H]NMS bound to the E397A/E401A mutant with an unchanged K_D (re-affirming the lack of role for these residues in the binding of orthosteric

ligands), but with a reduced B_{max} compared to wild-type. Furthermore, the affinity of atropine and compound A to inhibit [^{3}H]NMS binding was unchanged compared to wild-type, although the affinity of AC-42 was reduced 2.5-fold.

Taken together, these data, whilst suggesting that E397 and E401 may have a role in the binding of the allosteric agonists, are clearly not consistent with these residues mediating the major charge-charge interaction associated with ligand binding and M_1 receptor activation. The consequences of these results in delineating the nature of the allosteric agonist binding site(s) are discussed later.

Probably the most interesting findings were generated with the construct in which Y381 in TM6 was mutated. As discussed earlier, this residue has been extensively implicated in both orthosteric agonist and antagonist binding of the muscarinic M_1 receptor (Nordvall & Hacksell, 1993; Ward *et al.*, 1999; Spalding *et al.*, 2002; Sur *et al.*, 2003). Accordingly, mutation of this residue to alanine in the human muscarinic M_1 receptor caused an approximately 1000-fold reduction in the potency of carbachol to stimulate calcium mobilisation in both U2OS and CHO cells. Similar effects were seen in respect to the responses to the orthosteric agonists oxotremorine-M and muscarine in U2OS cells. Furthermore, the Y381A construct displayed no specific binding of [^{3}H]NMS.

Somewhat surprisingly, the calcium mobilisation responses to AC-42 and 77-LH-28-1 were abolished by Y381A in the U2OS cell line. This is in marked contrast to the results of previous studies, which have shown that loss of Y381 has only minimal effects on the potency of AC-42 to activate the M_1 receptor, although with a reduction in the maximal response observed (Spalding *et al.*, 2002; Sur *et al.*, 2003). However, when tested in the CHO cell background, Y381A caused only a 4-fold reduction in the potency of AC-42 compared to wild-type, with a slightly more marked effect on

77-LH-28-1 (17-fold reduction). These results are qualitatively similar to the observations of Spalding *et al.* (2002) and Sur *et al.* (2003).

Compound A and compound B both stimulated calcium mobilisation at the wild-type M_1 receptor expressed in U2OS cells. Interestingly, both compounds appeared as partial agonists in this assay, with intrinsic activities of 0.8 and 0.3, respectively. These data complement the calcium mobilisation and IP accumulation data in the CHO-hM_1 stable cell line (Chapter 5), which suggested that these compounds were partial agonists at the M_1 receptor. Mutation of Y381 actually increased the potencies of compound A and compound B 2-fold and 10-fold, respectively, to stimulate calcium mobilisation in the U2OS cell line, coupled with an increased maximal response for compound B. Furthermore, when tested in the CHO cell background, the potency of compound A was increased 10-fold. These results are very similar to those observed by Sur *et al.* (2003) with *N*-desmethylclozapine at the Y381A construct. The lack of deleterious effect of Y381A on compound A and compound B stimulated calcium mobilisation reinforces the concept that these compounds do not bind to the orthosteric site in the same fashion as carbachol. However, the increase in potencies suggests that compound A and compound B may interact with a site in very close proximity to the orthosteric site such that its alteration in Y381A is able to positively affect the binding and potency of these compounds.

The difference in the responses observed at the Y381A construct in the two cell lines with AC-42 and 77-LH-28-1 is puzzling. It is unlikely to be due to the Y381A being non-functional in the U2OS cell line, as both compound A and compound B were agonists at this construct in the same background. The lower potencies of the agonists in the U2OS cell line compared to the CHO background, coupled with the resolution of partial agonism in the U2OS assay, suggests that M_1 receptor expression and / or level of G protein coupling may well be lower in the U2OS cell

background. Unfortunately, due to the very slow growth of the U2OS cells, it was not possible to carry out radioligand binding studies to determine the level of receptor expression in comparison with the CHO cell background. Thus it is possible that the lack of response to AC-42 in this cell line may be due to the reduced receptor expression, coupled with a reduction in the intrinsic efficacy due to the mutation. Alternatively, the lack of response to AC-42 and 77-LH-28-1 may represent an example of agonist-dependent signalling at this construct whereby these two compounds, unlike other agonists, do not activate the necessary signal transduction pathways to stimulate the mobilisation of intracellular calcium. This phenomenon of agonist trafficking has previously been described for the muscarinic receptor family with pilocarpine and methacholine (Akam *et al.*, 2001).

Overall, the calcium mobilisation data supports the notion that neither the aromatic portion nor the phenolic hydroxyl group of Y381 is required for the agonist activity of the allosteric agonists presented here. In this context, it would be extremely interesting to investigate the effect of mutation of other key residues thought to comprise the orthosteric site such as D105 (Hulme *et al.*, 1995; Page *et al.*, 1995; Huang *et al.*, 1999), N382 (Huang *et al.*, 1999; Ward *et al.*, 1999; Spalding *et al.*, 2002) and Y404 / Y408 (Lu *et al.*, 2001). N382 may be a key residue as it lies adjacent to Y381. It will be very interesting to see whether mutation of this residue distinguishes between orthosteric and allosteric agonists in a similar fashion to Y381A. Additionally, it would be interesting to examine the role of D105, the aspartate residue in TM3 that mediates the main charge – charge interaction for classical orthosteric agonists. Given the essential nature of D105 in M_1 receptor function, it seems highly likely that that this aspartate residue will prove to be required for receptor activation by AC-42 and other allosteric agonists. These studies may help elucidate the nature of the allosteric binding site and its relationship with the orthosteric site.

Unfortunately, the results of the calcium mobilisation studies largely do not support the current modelling of the binding site for AC-42 and compound A to the M_1 receptor. Whilst both Y82 and the E397/E401 doublet appear to play a role in the binding of the allosteric agonists, mutation of these residues does not alter the response in a manner consistent with these residues forming the main attachment point on the receptor for these agonists. Therefore, it remains to be seen which residues of the M_1 receptor form the key interaction(s) with AC-42. There has been a recent report suggesting that F77 in TM2 plays a key role in the binding of, and receptor activation by, AC-42 (Jacobson *et al.*, 2004). However, the effect of the mutation F77I is limited to a 10-fold reduction in potency, again not consistent with F77 being the main point of ligand interaction. Furthermore, in the homology model described here, F77 appears on the outside face of TM2, suggesting that it is unlikely to play a direct role in the binding of AC-42.

As discussed earlier, it appears that two glutamate residues at the top of TM7 probably do not form a major charge – charge interaction with AC-42 and compound A. However, it is possible that these compounds still form a hydrogen bond donor – acceptor interaction with E397/E401. If this is the case, then the predicted orientation of AC-42 and compound A becomes more extracellular, located in a similar pocket to that thought to accommodate gallamine and other prototypical allosteric modulators. In this context, it is interesting to note that alcuronium and gallamine have both been shown to possess modest degrees of agonist activity at the muscarinic M_1 receptor (Jakubik *et al.*, 1996).

A further complication in trying to identify the binding site for agonist ligands in this way is that homology models such as the one described here are based on the crystal structure of the inactive form of rhodopsin. It is now well known that the activation of GPCRs (such as rhodopsin and the β_2 adrenoceptor) causes

conformational changes in the TM domains, involving rotation of TM4, the displacement of TM6 away from TM3 and an increased flexibility of the intracellular portion of TM7 (Gouldson *et al.*, 2004). A model of the muscarinic M_1 receptor based on the active state does not currently exist, but may help in the future identification of the allosteric agonist binding site.

The results in this chapter have combined molecular modelling and SDM techniques in an attempt to identify the molecular nature of the allosteric agonist binding site on the muscarinic M_1 receptor. Whilst not fully establishing the key interactions of AC-42 and compound A with the receptor, these studies have clearly demonstrated the independence of their agonist activity from Y381, a key component of the orthosteric site. This observation further reinforces the evidence from Chapter 5 that suggests that this class of compounds are allosteric agonists at the muscarinic M_1 receptor.

Chapter 7

General Discussion

These studies have used a combination of pharmacological techniques, homology modelling and site-directed mutagenesis to characterise the interaction between a novel GPCR, GPR10 and its recently identified peptide ligand, PrRP. Similar techniques have been applied to characterise the interaction between a well established GPCR, the muscarinic M_1 receptor and a novel class of selective agonists.

In Chapter 3, the binding of [^{125}I]-hPrRP-20 to GPR10 has been characterised. [^{125}I]-hPrRP-20 has been shown to be high affinity radioligand that displayed binding to both high and low affinity binding sites. The existence of both low and high affinity binding sites for [^{125}I]-hPrRP-20 is described for the first time here, although their aetiology is still unclear. Furthermore, [^{125}I]-hPrRP-20 was shown to possess association and dissociation kinetics consistent with its high affinity as measured using saturation binding. Both rat and human PrRP-31, along with the C-terminal 20 amino acid truncates, PrRP-20, inhibit [^{125}I]-hPrRP-20 binding to GPR10 with sub-nanomolar affinity, in agreement with previous studies (Roland *et al.*, 1999).

Both rat and human PrRP-31 and PrRP-20 stimulated intracellular calcium mobilisation in HEK293 cells expressing GPR10 as full agonists and displayed sensitivity to inhibitors of phospholipase-C, the IP_3 receptor and the endoplasmic reticulum Ca^{2+}-ATPase. Furthermore, hPrRP-20 potently stimulated IP accumulation in HEK293-GPR10 cells, but did not alter intracellular cAMP levels. These data strongly suggest that GPR10 couples predominantly *via* the $G_{q/11}$ pathway to stimulate the mobilisation of intracellular calcium. Similar studies in Chapter 5 clearly demonstrated that despite any alternative mode of action at the muscarinic M_1 receptor, the agonist activity of compounds such as AC-42 and compound A display similar sensitivities to inhibitors of phospholipase-C, the IP_3 receptor and the endoplasmic reticulum Ca^{2+}-ATPase as does the orthosteric agonist carbachol. This

suggests that AC-42 and compound A cause the M_1 receptor to signal primarily *via* the $G_{q/11}$ pathway.

Unfortunately, a lack of pharmacological tools has prevented a more thorough characterisation of GPR10; at present only the native PrRPs and truncates thereof have been shown to activate GPR10 and there are no known antagonists of this receptor. In contrast, the muscarinic M_1 receptor is an extremely well studied GPCR with many well characterised pharmacological tools. The availability of a range of radioligands, agonists and antagonists for the M_1 receptor has enabled a thorough characterisation of the interaction of a novel class of 'ectopic' agonists with this receptor. AC-42 has been shown to stimulate both calcium mobilisation and IP accumulation in CHO cells expressing the human muscarinic M_1 receptor. Blockade of these responses with orthosteric antagonists such as atropine and pirenzepine resulted in parallel rightward shifts of the agonist response curve, but yielded non-linear Schild regressions characteristic of a negatively co-operative allosteric interaction. Analysis of the data according to the simple allosteric ternary complex (Ehlert *et al.*, 1988; Christopoulos & Motulsky, 2004) has generated estimates of the co-operativity (α) governing the interaction between AC-42 and atropine or pirenzepine. Most notably, the antagonist effect of atropine on AC-42 stimulated calcium mobilisation in CHO-hM_1 cells was clearly shown to be saturable, a hallmark of an allosteric interaction (Christopoulos & Kenakin, 2002). It was concluded that AC-42 must be the allosteric ligand since atropine and pirenzepine are two of the best characterised orthosteric antagonists of the muscarinic receptor family.

Such saturability to an allosteric effect was also demonstrated using equilibrium binding assays in CHO-hM_1 cells with the orthosteric radioligand, [^{3}H]NMS. AC-42, 77-LH-28-1 and gallamine, a prototypical allosteric modulator of muscarinic receptors, displayed an inability to inhibit fully the specific binding of [^{3}H]NMS, an

effect that was more profound at a higher radioligand concentration. Compound A also shared this property, although its low affinity made it difficult to estimate accurately the minimum asymptotes of the inhibition isotherms. In contrast, both atropine and pirenzepine both fully inhibited [^{3}H]NMS binding, consistent with a simple competitive interaction. Analysis of the data according to the allosteric ternary complex model generated estimates of the co-operativity factor, α, governing the interaction between AC-42, 77-LH-28-1, gallamine and compound A and NMS. Interestingly, the estimate of co-operativity between AC-42 and NMS is markedly different to that between AC-42 and atropine. This is an example of another hallmark of allosteric interactions, namely a probe dependence of the co-operativity on the orthosteric ligand used (Christopoulos, 2000).

In addition to saturability of effect and orthosteric probe-dependence, another key property of allosteric ligands is the ability to alter the dissociation rate of orthosteric ligands (Christopoulos *et al.*, 1999; Lazareno & Birdsall, 1995). In these studies it has been shown that the prototypical allosteric modulator, gallamine, markedly retards the dissociation of [^{3}H]NMS from CHO-hM_1 cell membranes. In addition, AC-42 significantly slowed the rate of [^{3}H]NMS dissociation, although not to the same extent as gallamine. Compound A did not alter the dissociation rate, however this probably reflects a combination of the solubility maximum and the low predicted affinity of compound A for the [^{3}H]NMS occupied receptor. Collectively, these studies provide unambiguous evidence that the 'ectopic' agonist, AC-42, is an allosteric ligand. As such, it is more appropriate to re-class this ligand as an allosteric, rather than ectopic, agonist. There is also evidence to suggest that the other 'ectopic' agonists share this property.

The final studies in Chapter 5 were designed to determine whether the agonist activity of these compounds was evident at native muscarinic receptors. AC-42, 77-

LH-28-1, compound A and compound B all displayed a higher affinity to inhibit [^{3}H]oxotremorine-M binding than [^{3}H]QNB binding in rat cortical membranes. The ratio of affinities against agonist and antagonist radioligands has often been used as a predictor of ligand efficacy (Loudon *et al.*, 1997; Watson *et al.*, 1999) and the data presented here are consistent with these compounds possessing agonist activity in rat cortex. This was emphatically demonstrated with the selective muscarinic M_1 receptor agonist, 77-LH-28-1, which evoked cortical gamma network oscillations in layer IV of the rat temporal cortex *in vitro*. These oscillations mimicked the gamma oscillations elicited by the non-selective cholinergic agonist, carbachol, suggesting (a) that the gamma oscillations produced by carbachol are mediated *via* the muscarinic M_1 receptor and (b) 77-LH-28-1 is an agonist at native tissue muscarinic receptors.

Having characterised the pharmacology of both the PrRPs at GPR10 and AC-42 (plus other allosteric agonists) at the muscarinic M_1 receptor, Chapters 4 and 6 sought to establish the molecular nature of their respective binding sites for these compounds at their receptors. These studies utilised homology modelling of both GPR10 and the muscarinic M_1 receptor based on the crystal structure of bovine rhodopsin. Manual docking of the C-terminal heptapeptide of hPrRP-20, hPrRP(25-31) and AC-42 / compound A, respectively, led to predictions of key amino acid residues involved in the binding of these ligands. These predictions were tested using site-directed mutagenesis (SDM) in conjunction with functional calcium mobilisation and radioligand binding approaches.

For GPR10, acidic residues were sought for the two basic arginine residues in positions 2 and 6 of hPrRP(25-31). All acceptable docking solutions suggested the formation of a salt bridge between D302 (TM6) and Arg^2 and E213 (ECL2) and Arg^6. Accordingly, mutation of either of these residues to alanine resulted in a loss of

specific [^{125}I]-hPrRP-20 binding and a markedly reduced potency of hPrRP-20 to stimulate calcium mobilisation. The successful prediction of these interactions was particularly exciting because this was the first instance of a theoretically derived loop structure for a GPCR suggesting critical interactions in the receptor model.

The docking of the hPrRP(25-31) into GPR10 suggested that a double hydrogen bond would be formed between Val^4 of hPrRP(25-31) and Q317 (TM7) – this interaction was predicted to be key in defining the position of the two arginine residues of the heptapeptide relative to E213 and D302. As anticipated, the mutant Q317A abolished specific [^{125}I]-hPrRP-20 binding and vastly reduced the potency of hPrRP-20 to stimulate calcium mobilisation.

Q141, E212 and N298 were also thought to form hydrogen bonds with either Arg^6 or the terminal carboxamide of hPrRP(25-31). These interactions were not predicted to be as crucial to the binding of the heptapeptide as those for E213, D302 and Q317 and, accordingly, their mutation had more limited effects on [^{125}I]-hPrRP-20 binding and hPrRP-20 stimulated calcium mobilisation. These observations have clearly validated the homology model of GPR10 and may aid the future rational design of agonists or antagonists of this receptor.

In contrast, the effort to identify the molecular nature of the allosteric agonist site on the muscarinic M_1 receptor was less successful. Based on the essential portion of the muscarinic M_1 receptor sequence required for AC-42 agonist activity (Spalding *et al.*, 2002), manual docking of AC-42 predicted a clear interaction between the protonated nitrogen of this compound and either of the glutamate residues, E397 or E401, at the top of TM7. Additionally, a hydrogen bond was predicted between the carbonyl oxygen of AC-42 and Y82 in TM2. Unfortunately, none of these residues, when mutated, selectively affected the agonist activity of AC-42 or any other allosteric

agonist. AC-42 displayed a small reduction in affinity for a construct containing point mutations of both E397 and E401; compound A also displayed a slightly reduced potency at this construct. However, whilst these results suggested that there may be a small role for E397 and E401 in the binding of allosteric agonists, these results are not consistent with these amino acid residues forming the major charge-charge interaction with AC-42.

It is possible that further refinement of the homology model may yield a better understanding of the allosteric binding site. There are several amino acid residues, which were highlighted in the ligand docking, which may play a greater role in the binding of AC-42 than first anticipated. These include T34 in TM1, which was predicted to form a hydrogen bond with the π system of the phenyl ring (Meyer *et al.*, 2003) and D393, which may also form an interaction with the protonated nitrogen of AC-42 and compound A as well as, or instead of, E397/E401. Furthermore, W101, a turn above D105 in TM3, was also predicted to be very close to the carbonyl oxygen atoms of AC-42 and compound A, so it is possible that this residue, rather than Y82, forms a hydrogen bond with the carbonyl oxygen. This would be of further interest if AC-42 and gallamine were to be occupying the same site as W101 which has previously been implicated in the binding of gallamine to the muscarinic M_1 receptor (Matsui *et al.*, 1995). Thus, these three amino acid residues would be strong candidates for future SDM work.

However, substantial evidence that these compounds interact at a non-orthosteric site was obtained with a M_1 receptor construct containing the Y381A mutation (Ward *et al.*, 1999). In contrast to the large deleterious effect on the potency of carbachol, this mutation left the agonist response to the allosteric agonists relatively unaffected, and even potentiated the response to compound A and compound B. However, the relationship between the orthosteric site and the binding site for the allosteric

agonists still remains largely unclear. Further refinement of the homology model, together with more SDM work, is required in order to elucidate the precise nature of the allosteric agonist binding site.

The studies within this thesis have offered the first example of functional characterisation of the signal transduction pathways activated by GPR10 and also an extensive characterisation of the binding of [^{125}I]-hPrRP-20 to GPR10. Furthermore the results generated have revealed the existence of high and low affinity binding sites and molecular modelling in combination with SDM studies have also identified for the first time the molecular nature of the peptide binding site for this receptor.

With respect to the muscarinic M_1 receptor extensive pharmacological characterisation has also shown that AC-42 displays a unique allosteric mode of agonist action at the receptor. Homology modelling and SDM of the muscarinic M_1 receptor has also clearly identified a non-orthosteric molecular mechanism of action for this class of muscarinic receptor agonists.

Bibliography

Aarnisalo AA, Tuominen RK, Nieminen M, Vainio P, and Panula P (1997) Evidence for prolactin releasing activity of neuropeptide FF in rats. *Neuroendocrinology Letters* **18**:191-196.

Ames R, Nuthulaganti P, Fornwald J, Shabon U, van der Keyl H, and Elshourbagy N (2004a) Heterologous expression of G protein-coupled receptors in U-2 OS osteosarcoma cells. *Receptors & Channels* **10**:117-124.

Ames R, Fornwald J, Nuthulaganti P, Trill J, Foley J, Buckley P, Kost T, Wu Z, and Romanos M (2004b) BacMam recombinant baculoviruses in G protein-coupled receptor drug discovery. *Receptors & Channels* **10**:99-107.

Akam EC, Challiss RA, and Nahorski SR (2001) $G_{q/11}$ and $G_{i/o}$ activation profiles in CHO cells expressing muscarinic acetylcholine receptors: dependence on agonist as well as receptor-subtype. *British Journal of Pharmacology* **132**:950-958

Anagnostaras SG, Murphy GG, Hamilton SE, Mitchell SL, Rahnama NP, Nathanson NM, and Silva AJ (2003) Selective cognitive dysfunction in acetylcholine M_1 muscarinic receptor mutant mice. *Nature Neuroscience* **6**:51-58.

Arunlakshana O and Schild HO (1959) Some quantitative uses of drug antagonists. *British Journal of Pharmacology.* **14**:48-58

Avlani V, May LT, Sexton PM, and Christopoulos A (2004) Application of a kinetic model to the apparently complex behavior of negative and positive allosteric modulators of muscarinic acetylcholine receptors. *Journal of Pharmacology & Experimental Therapeutics* **308**:1062-1072.

Baldwin JM, Schertler GF, and Unger VM (1997) An alpha-carbon template for the transmembrane helices in the rhodopsin family of G-protein-coupled receptors. *Journal of Molecular Biology* **272**:144-164.

Barlow RB, Berry KJ, Glenton PA, Nilolaou NM, and Soh KS (1976) A comparison of affinity constants for muscarine-sensitive acetylcholine receptors in guinea-pig atrial pacemaker cells at 29 degrees C and in ileum at 29 degrees C and 37 degrees C. *British Journal of Pharmacology* **58**:613-620.

Befort K, Tabbara L, Kling D, Maigret B, and Kieffer BL (1996) Role of aromatic transmembrane residues of the delta-opioid receptor in ligand recognition. *Journal of Biological Chemistry* **271**:10161-10168.

Berkeley JL, Gomeza J, Wess J, Hamilton SE, Nathanson NM, and Levey AI (2001) M1 muscarinic acetylcholine receptors activate extracellular signal-regulated kinase in CA1 pyramidal neurons in mouse hippocampal slices. *Molecular & Cellular Neurosciences* **18**:512-524.

Berkhout TA, Blaney FE, Bridges AM, Cooper DG, Forbes IT, Gribble AD, Groot PH, Hardy A, Ife RJ, Kaur R, Moores KE, Shillito H, Willetts J, and Witherington J (2003) CCR2: characterization of the antagonist binding site from a combined receptor modeling/mutagenesis approach. *Journal of Medicinal Chemistry* **46**:4070-4086.

Bernheim L, Mathie A, and Hille B (1992) Characterization of muscarinic receptor subtypes inhibiting Ca^{2+} current and M current in rat sympathetic neurons. *Proceedings of the National Academy of Sciences of the United States of America* **89**:9544-9548.

Bhattacharya S and Linden J (1995) The allosteric enhancer, PD 81,723, stabilizes human A1 adenosine receptor coupling to G proteins. *Biochimica et Biophysica Acta* **1265**:15-21.

Bhattacharyya S, Luan J, Challis B, Schmitz C, Clarkson P, Franks PW, Middelberg R, Keogh J, Farooqi IS, Montague C, Brennand J, Wareham NJ, and O'Rahilly S (2003) Association of polymorphisms in GPR10, the gene encoding the prolactin-releasing peptide receptor with blood pressure, but not obesity, in a U.K. Caucasian population. *Diabetes* **52**:1296-1299.

Bikker JA, Trumpp-Kallmeyer S, and Humblet C (1998) G-Protein coupled receptors: models, mutagenesis, and drug design. *Journal of Medicinal Chemistry* **41**:2911-2927.

Birdsall NJ and Hulme EC (1983) Muscarinic receptor subtypes. *Trends in Pharmacological Sciences* **4**:459-463

Birdsall NJ, Burgen AS, Hulme EC, Stockton JM, and Zigmond MJ (1983) The effect of McN-A-343 on muscarinic receptors in the cerebral cortex and heart. *British Journal of Pharmacology* **78**:257-259.

Birdsall NJ, Farries T, Gharagozloo P, Kobayashi S, Lazareno S, and Sugimoto M (1999) Subtype-selective positive cooperative interactions between brucine analogs and acetylcholine at muscarinic receptors: functional studies. *Molecular Pharmacology* **55**:778-786.

Birdsall NJ, Lazareno S, Popham A, and Saldanha J (2001) Multiple allosteric sites on muscarinic receptors. *Life Sciences* **68**:2517-2524.

Blaney FE, Raveglia LF, Artico M, Cavagnera S, Dartois C, Farina C, Grugni M, Gagliardi S, Luttmann MA, Martinelli M, Nadler GM, Parini C, Petrillo P, Sarau HM, Scheideler MA, Hay DW, and Giardina GA (2001) Stepwise modulation of neurokinin-3 and neurokinin-2 receptor affinity and selectivity in quinoline tachykinin receptor antagonists. *Journal of Medicinal Chemistry* **44**:1675-1689.

Bonner TI, Buckley NJ, Young AC, and Brann MR (1987) Identification of a family of muscarinic acetylcholine receptor genes. *Science* **237**:527-532.

Bonner TI, Young AC, Brann MR, and Buckley NJ (1988) Cloning and expression of the human and rat m5 muscarinic acetylcholine receptor genes. *Neuron* **1**:403-410.

Bowen WP and Jerman JC (1995) Nonlinear regression using spreadsheets. *Trends in Pharmacological Sciences* **16**:413-417.

Boyle RG, Downham R, Ganguly T, Humphries J, Smith J, and Travers S (2005) Structure-activity studies on prolactin-releasing peptide (PrRP). Analogues of PrRP-(19-31)-peptide. *Journal of Peptide Science* **11**:161-165.

Bradford MM (1976) A rapid and sensitive method for the quantitation of microgram quantities of protein utilizing the principle of protein-dye binding. *Analytical Biochemistry* **72** :248-254.

Brandish PE, Hill LA, Zheng W, and Scolnick EM (2003) Scintillation proximity assay of inositol phosphates in cell extracts: high-throughput measurement of G-protein-coupled receptor activation. *Analytical Biochemistry* **313**:311-318.

Brown DA, Forward A, and Marsh S (1980) Antagonist discrimination between ganglionic and ileal muscarinic receptors. *British Journal of Pharmacology* **71**:362-364.

Brown DA and Adams PR (1980) Muscarinic suppression of a novel voltage-sensitive K+ current in a vertebrate neurone. *Nature* **283**:673-676.

Bruns RF and Fergus JH (1990) Allosteric enhancement of adenosine A_1 receptor binding and function by 2-amino-3-benzoylthiophenes. *Molecular Pharmacology* **38**:939-949.

Buhl EH, Tamas G, and Fisahn A (1998) Cholinergic activation and tonic excitation induce persistent gamma oscillations in mouse somatosensory cortex in vitro. *Journal of Physiology* **513**:117-126.

Bunemann M and Hosey MM (1999). G protein - coupled receptor kinases as modulators of G protein signalling. *Journal of Physiology* **517**:5-23

Cabrele C and Beck-Sickinger AG (2000) Molecular characterization of the ligand-receptor interaction of the neuropeptide Y family. *Journal of Peptide Science* **6**:97-122.

Cabrera-Vera TM, Vanhauwe J, Thomas TO, Medkova M, Preininger A, Mazzoni MR, and Hamm HE (2003) Insights into G protein structure, function, and regulation. *Endocrine Reviews* **24**:765-781.

Cassel D and Selinger Z (1977) Mechanism of adenylate cyclase activation by cholera toxin: inhibition of GTP hydrolysis at the regulatory site. *Proc. Natl. Acad. Sci. U.S.A.* 74:3307-3311

Caulfield MP (1993) Muscarinic receptors - characterization, coupling and function. *Pharmacology & Therapeutics* **58**:319-379.

Caulfield MP and Birdsall NJ (1998) International Union of Pharmacology. XVII. Classification of muscarinic acetylcholine receptors. *Pharmacological Reviews* **50**:279-290.

Challiss RAJ and Nahorski SR (2002) GPCR signalling through enzymatic cascades, in: Understanding G Protein-coupled receptors and their role in the CNS (Pangalos MN and Davies CH eds) pp. 87 - 107, Oxford University Press

Chen C, Dun SL, Dun NJ, and Chang JK (1999) Prolactin-releasing peptide-immunoreactivity in A1 and A2 noradrenergic neurons of the rat medulla. *Brain Research* **822**:276-279.

Cheng Y and Prussoff WH (1973) Relationship between the inhibition constant (K_i) and the concentration of inhibitor which causes 50 per cent inhibition (I_{50}) of an enzymatic reaction. *Biochemical Pharmacology* **22**:3099-3108.

Christopoulos A and Mitchelson F (1997) Pharmacological analysis of the mode of interaction of McN-A-343 at atrial muscarinic M_2 receptors. *European Journal of Pharmacology* **339**:153-156.

Christopoulos A, Lanzafame A, and Mitchelson F (1998) Allosteric interactions at muscarinic cholinoceptors. *Clinical & Experimental Pharmacology & Physiology* **25**:185-194.

Christopoulos A, Sorman JL, Mitchelson F, and el Fakahany EE (1999) Characterization of the subtype selectivity of the allosteric modulator heptane-1,7-bis-(dimethyl-3'-phthalimidopropyl) ammonium bromide (C_7/3-phth) at cloned muscarinic acetylcholine receptors. *Biochemical Pharmacology* **57**:171-179.

Christopoulos A (2000) Overview of receptor allosterism. *Current Protocols in Pharmacology* 1.21.1 – 1.21.45

Christopoulos A, Grant MK, and el Fakahany EE (2000) Transducer abstraction: a novel approach to the detection of partial agonist efficacy in radioligand binding studies. *Journal of Pharmacological & Toxicological Methods* **43**:55-67.

Christopoulos A, Grant MK, Ayoubzadeh N, Kim ON, Sauerberg P, Jeppesen L, and el Fakahany EE (2001) Synthesis and pharmacological evaluation of dimeric muscarinic acetylcholine receptor agonists. *Journal of Pharmacology & Experimental Therapeutics* **298**:1260-1268.

Christopoulos A and Kenakin T (2002) G protein-coupled receptor allosterism and complexing. *Pharmacological Reviews* **54**:323-374.

Christopoulos A (2002) Allosteric binding sites on cell-surface receptors: novel targets for drug discovery. *Nature Reviews Drug Discovery.* **1**:198-210.

Clark AL and Mitchelson F (1976) The inhibitory effect of gallamine on muscarinic receptors. *British Journal of Pharmacology* **58**:323-331.

Colquhoun D, Ogden DC, and Mathie A (1987) Nicotinic acetylcholine receptors of nerve and muscle: functional aspects. *Trends in Pharmacological Sciences* **8**:465-472

Conklin BR, Brann MR, Buckley NJ, Ma AL, Bonner TI, and Axelrod J (1988) Stimulation of arachidonic acid release and inhibition of mitogenesis by cloned genes for muscarinic receptor subtypes stably expressed in A9 L cells. *Proceedings of the National Academy of Sciences of the United States of America* **85**:8698-8702.

Conklin BR, Farfel Z, Lustig KD, Julius D and Bourne HR (1993). Substitution of three amino acids switches receptor specificity of $G_{q\alpha}$ to that of $G_{i\alpha}$. *Nature* **363**:274-

Conklin BR, Herzmark P, Ishida S, Voyno-Yasenetskaya TA, Sun Y, Farfel Z, and Bourne HR (1996). Carboxyl-terminal mutations of $G_q\alpha$ and $G_s\alpha$ that alter the fidelity of receptor activation. *Molecular Pharmacology* **50**:885-890.

Curlewis JD, Kusters DH, Barclay JL, and Anderson ST (2002) Prolactin-releasing peptide in the ewe: cDNA cloning, mRNA distribution and effects on prolactin secretion in vitro and in vivo. *Journal of Endocrinology* **174**:45-53.

Danho W, Swistok J, Khan W, Truitt T, Kurylko G, Fry D, Greeley D, Sun H, Dvorozniak M, Machie G, Spence C, and Goodnow R (2003) Structure-activity relationships and bioactive conformations of prolactin releasing peptides. Ligands for a potential obesity target. *American Peptide Symposium, Boston* P284

D'Ursi AM, Albrizio S, Di Fenza A, Crescenzi O, Carotenuto A, Picone D, Novellino E, and Rovero P (2002) Structural studies on Hgr3 orphan receptor ligand prolactin-releasing peptide. *Journal of Medicinal Chemistry* **45**:5483-5491.

Dockray GJ, Reeve JR, Jr., Shively J, Gayton RJ, and Barnard CS (1983) A novel active pentapeptide from chicken brain identified by antibodies to FMRFamide. *Nature* **305**:328-330.

Dunbrack RL, Jr. and Karplus M (1993) Backbone-dependent rotamer library for proteins. Application to side-chain prediction. *Journal of Molecular Biology* **230**:543-574.

Ehlert FJ (1988) Estimation of the affinities of allosteric ligands using radioligand binding and pharmacological null methods. *Molecular Pharmacology* **33**:187-194.

Ellacott KL, Lawrence CB, Rothwell NJ, and Luckman SM (2002) PRL-releasing peptide interacts with leptin to reduce food intake and body weight. *Endocrinology* **143**:368-374.

Ellacott KL, Lawrence CB, Pritchard LE, and Luckman SM (2003) Repeated administration of the anorectic factor prolactin-releasing peptide leads to tolerance to its effects on energy homeostasis. *American Journal of Physiology - Regulatory Integrative & Comparative Physiology* **285**:R1005-R1010.

Ellis J and Seidenberg M (1992) Two allosteric modulators interact at a common site on cardiac muscarinic receptors. *Molecular Pharmacology* **42**:638-641.

Ellis J (2002) Muscarinic receptors, in: Understanding G Protein-coupled receptors and their role in the CNS (Pangalos MN and Davies CH eds) pp. 349 - 371, Oxford University Press

Elshourbagy NA, Ames RS, Fitzgerald LR, Foley JJ, Chambers JK, Szekeres PG, Evans NA, Schmidt DB, Buckley PT, Dytko GM, Murdock PR, Milligan G, Groarke DA, Tan KB, Shabon U, Nuthulaganti P, Wang DY, Wilson S, Bergsma DJ, and Sarau HM (2000) Receptor for the pain modulatory neuropeptides FF and AF is an orphan G protein-coupled receptor. *Journal of Biological Chemistry* **275**:25965-25971.

Engstrom M, Brandt A, Wurster S, Savola JM, and Panula P (2003) Prolactin releasing peptide has high affinity and efficacy at neuropeptide FF2 receptors. *Journal of Pharmacology & Experimental Therapeutics* **305**:825-832.

Fanelli F, Menziani C, Scheer A, Cotecchia S, and de Benedetti PG (1998) Ab initio modeling and molecular dynamics simulation of the alpha 1b-adrenergic receptor activation. *Methods (Duluth)* **14**:302-317.

Fanelli F, Barbier P, Zanchetta D, de Benedetti PG, and Chini B (1999) Activation mechanism of human oxytocin receptor: a combined study of experimental and computer-simulated mutagenesis. *Molecular Pharmacology* **56**:214-225.

Fisahn A, Pike FG, Buhl EH, and Paulsen O (1998) Cholinergic induction of network oscillations at 40 Hz in the hippocampus in vitro. *Nature* **394**:186-189.

Fisahn A, Yamada M, Duttaroy A, Gan JW, Deng CX, McBain CJ, and Wess J (2002) Muscarinic induction of hippocampal gamma oscillations requires coupling of the M_1 receptor to two mixed cation currents. *Neuron* **33**:615-624.

Foord SM, Jupe S, and Holbrook J (2002) Bioinformatics and type II G-protein-coupled receptors. *Biochemical Society Transactions* **30**:473-479.

Fraser CM, Wang CD, Robinson DA, Gocayne JD, and Venter JC (1989) Site-directed mutagenesis of m1 muscarinic acetylcholine receptors: conserved aspartic acids play important roles in receptor function. *Molecular Pharmacology* **36**:840-847.

Fredriksson R, Gloriam DE, Hoglund PJ, Lagerstrom MC, and Schioth HB (2003) There exist at least 30 human G-protein-coupled receptors with long Ser/Thr-rich N-termini. *Biochemical & Biophysical Research Communications* **301**:725-734.

Freedman SB, Harley EA, and Iversen LL (1988) Relative affinities of drugs acting at cholinoceptors in displacing agonist and antagonist radioligands: the NMS/Oxo-M ratio as an index of efficacy at cortical muscarinic receptors. *British Journal of Pharmacology* **93**:437-445.

Fujii R, Fukusumi S, Hosoya M, Kawamata Y, Habata Y, Hinuma S, Sekiguchi M, Kitada C, Kurokawa T, Nishimura O, Onda H, Sumino Y, and Fujino M (1999) Tissue distribution of prolactin-releasing peptide (PrRP) and its receptor. *Regulatory Peptides* **83**:1-10.

Gantz I, DelValle J, Wang LD, Tashiro T, Munzert G, Guo YJ, Konda Y, and Yamada T (1992) Molecular basis for the interaction of histamine with the histamine H_2 receptor. *Journal of Biological Chemistry* **267**:20840-20843.

Gether U (2000) Uncovering molecular mechanisms involved in activation of G protein-coupled receptors. *Endocrine Reviews* **21**:90-113.

Gether U, Asmar F, Meinild AK, and Rasmussen SG (2002) Structural basis for activation of G-protein-coupled receptors. *Pharmacology & Toxicology* **91**:304-312.

Gouldson PR, Kidley NJ, Bywater RP, Psaroudakis G, Brooks HD, Diaz C, Shire D, and Reynolds CA (2004) *Proteins: Structure, Function and Bioinformatics* **56**:67 – 84.

Gnagey AL, Seidenberg M, and Ellis J (1999) Site-directed mutagenesis reveals two epitopes involved in the subtype selectivity of the allosteric interactions of gallamine at muscarinic acetylcholine receptors. *Molecular Pharmacology* **56**:1245-1253.

Greasley PJ, Fanelli F, Scheer A, Abuin L, Nenniger-Tosato M, DeBenedetti PG, and Cotecchia S (2001) Mutational and computational analysis of the alpha(1b)-adrenergic receptor. Involvement of basic and hydrophobic residues in receptor activation and G protein coupling. *Journal of Biological Chemistry* **276**:46485-46494.

Greasley PJ, Fanelli F, Rossier O, Abuin L, and Cotecchia S (2002) Mutagenesis and modelling of the alpha(1b)-adrenergic receptor highlight the role of the helix 3/helix 6 interface in receptor activation. *Molecular Pharmacology* **61**:1025-1032.

Gregory RB and Barritt GJ (2003) Evidence that Ca^{2+}-release-activated Ca^{2+} channels in rat hepatocytes are required for the maintenance of hormone-induced Ca^{2+} oscillations. *Biochemical Journal* **370**:695-702.

Gu W, Geddes BJ, Zhang C, Foley KP, and Stricker-Krongrad A (2004) The prolactin-releasing peptide receptor (GPR10) regulates body weight homeostasis in mice. *Journal of Molecular Neuroscience* **22**:93-103.

Gurwitz D, Haring R, Heldman E, Fraser CM, Manor D, and Fisher A (1994) Discrete activation of transduction pathways associated with acetylcholine m1 receptor by several muscarinic ligands. *European Journal of Pharmacology* **267**:21-31.

Haga K and Haga T (1983) Affinity chromatography of the muscarinic acetylcholine receptor. *Journal of Biological Chemistry* **258**:13575-13579.

Hall D and Parsons S (2001) Non-surmountable antagonism: a general drawback of pre-steady state measurement? *Trends in Pharmacological Sciences* **22**:63-65

Hamilton SE, Loose MD, Qi M, Levey AI, Hille B, McKnight GS, Idzerda RL, and Nathanson NM (1997) Disruption of the m1 receptor gene ablates muscarinic receptor-dependent M current regulation and seizure activity in mice. *Proceedings of the National Academy of Sciences of the United States of America* **94**:13311-13316.

Hammer R, Berrie CP, Birdsall NJ, Burgen AS, and Hulme EC (1980) Pirenzepine distinguishes between different subclasses of muscarinic receptors. *Nature* **283**:90-92.

Han SK, Dong X, Hwang JI, Zylka MJ, Anderson DJ, and Simon MI (2002) Orphan G protein-coupled receptors MrgA1 and MrgC11 are distinctively activated by RF-

amide-related peptides through the Galpha q/11 pathway. *Proceedings of the National Academy of Sciences of the United States of America* **99**:14740-14745.

Hepler JR and Saugstad JA (2002) Protein regulators of GPCR function, in: Understanding G Protein-coupled receptors and their role in the CNS (Pangalos MN and Davies CH eds) pp. 124-140, Oxford University Press

Hinuma S, Habata Y, Fujii R, Kawamata Y, Hosoya M, Fukusumi S, Kitada C, Masuo Y, Asano T, Matsumoto H, Sekiguchi M, Kurokawa T, Nishimura O, Onda H, and Fujino M (1998) A prolactin-releasing peptide in the brain. *Nature* **393**:272-276.

Hinuma S, Onda H, and Fujino M (1999) The quest for novel bioactive peptides utilizing orphan seven-transmembrane-domain receptors. *Journal of Molecular Medicine* **77**:495-504.

Hinuma S, Shintani Y, Fukusumi S, Iijima N, Matsumoto Y, Hosoya M, Fujii R, Watanabe T, Kikuchi K, Terao Y, Yano T, Yamamoto T, Kawamata Y, Habata Y, Asada M, Kitada C, Kurokawa T, Onda H, Nishimura O, Tanaka M, Ibata Y, and Fujino M (2000) New neuropeptides containing carboxy-terminal RFamide and their receptor in mammals. *Nature Cell Biology* **2**:703-708.

Hirst WD, Abrahamsen B, Blaney FE, Calver AR, Aloj L, Price GW, and Medhurst AD (2003) Differences in the central nervous system distribution and pharmacology of the mouse 5-hydroxytryptamine-6 receptor compared with rat and human receptors investigated by radioligand binding, site-directed mutagenesis, and molecular modeling. *Molecular Pharmacology* **64**:1295-1308.

Hizume T, Watanobe H, Yoneda M, Suda T, and Schioth HB (2000) Involvement of prolactin-releasing peptide in the preovulatory luteinizing hormone and prolactin surges in the rat. *Biochemical & Biophysical Research Communications* **279**:35-39.

Ho MKC and Wong YH (2002) G protein structure diversity, in: Understanding G Protein-coupled receptors and their role in the CNS (Pangalos MN and Davies CH eds) pp. 63 - 86, Oxford University Press

Hoare SR and Strange PG (1996) Regulation of D_2 dopamine receptors by amiloride and amiloride analogs. *Molecular Pharmacology* **50**:1295-1308.

Horiuchi J, Saigusa T, Sugiyama N, Kanba S, Nishida Y, Sato Y, Hinuma S, and Arita J (2002) Effects of prolactin-releasing peptide microinjection into the ventrolateral medulla on arterial pressure and sympathetic activity in rats. *Brain Research* **958**:201-209.

Horton RM, Cai ZL, Ho SN, and Pease LR (1990) Gene splicing by overlap extension: tailor-made genes using the polymerase chain reaction. *Biotechniques* **8**:528-535.

Huang XP, Nagy PI, Williams FE, Peseckis SM, and Messer WS, Jr. (1999) Roles of threonine 192 and asparagine 382 in agonist and antagonist interactions with M_1 muscarinic receptors. *British Journal of Pharmacology* **126**:735-745.

Hulme EC, Birdsall NJ, and Buckley NJ (1990) Muscarinic receptor subtypes. *Annual Review of Pharmacology & Toxicology* **30**:633-673.

Hulme EC, Curtis CA, Page KM, and Jones PG (1995) The role of charge interactions in muscarinic agonist binding, and receptor-response coupling. *Life Sciences* **56**:891-898.

Hulme EC, Lu ZL, Saldanha JW, and Bee MS (2003) Structure and activation of muscarinic acetylcholine receptors. *Biochemical Society Transactions* **31**:29-34.

Ibata Y, Iijima N, Kataoka Y, Kakihara K, Tanaka M, Hosoya M, and Hinuma S (2000) Morphological survey of prolactin-releasing peptide and its receptor with special reference to their functional roles in the brain. *Neuroscience Research* **38** :223-230.

Iijima N, Matsumoto Y, Yano T, Tanaka M, Yamamoto T, Kakihara K, Kataoka Y, Tamada Y, Matsumoto H, Suzuki N, Hinuma S, and Ibata Y (2001) A novel function of prolactin-releasing peptide in the control of growth hormone *via* secretion of somatostatin from the hypothalamus. *Endocrinology* **142**:3239-3243.

Jacobson MA, O'Brien JA, Pascarella D, Mallorga PJ, Scolnick EM, Sur C. Mapping the interaction site of M_1 muscarinic receptor allosteric agonists (2004) *Abstract Viewer/Itinerary Planner: Society for Neuroscience*

Jakubik J, Bacakova L, Lisa V, el Fakahany EE, and Tucek S (1996) Activation of muscarinic acetylcholine receptors *via* their allosteric binding sites. *Proceedings of the National Academy of Sciences of the United States of America* **93**:8705-8709.

Jakubik J, Haga T, and Tucek S (1998) Effects of an agonist, allosteric modulator, and antagonist on guanosine-gamma-[^{35}S]thiotriphosphate binding to liposomes with varying muscarinic receptor/G_o protein stoichiometry. *Molecular Pharmacology* **54**:899-906.

Jarry H, Heuer H, Schomburg L, and Bauer K (2000) Prolactin-releasing peptides do not stimulate prolactin release in vivo. *Neuroendocrinology* **71**:262-267.

Kenakin TP (1997) *Pharmacologic Analysis of Drug-Receptor Interaction.* Lippincott-Raven, Philadelphia, PA.

Kenakin T (2004) Allosteric Modulators: The New Generation of Receptor Antagonist. *Molecular Interventions* **4**:222-229

Kim J, Jiang Q, Glashofer M, Yehle S, Wess J, and Jacobson KA (1996) Glutamate residues in the second extracellular loop of the human A_{2a} adenosine receptor are required for ligand recognition. *Molecular Pharmacology* **49**:683-691.

Kimura A, Ohmichi M, Tasaka K, Kanda Y, Ikegami H, Hayakawa J, Hisamoto K, Morishige K, Hinuma S, Kurachi H, and Murata Y (2000) Prolactin-releasing peptide activation of the prolactin promoter is differentially mediated by extracellular signal-regulated protein kinase and c-Jun N-terminal protein kinase. *Journal of Biological Chemistry* **275**:3667-3674.

Kolakowski LF, Jr. (1994) GCRDb: a G-protein-coupled receptor database. *Receptors & Channels* **2**:1-7.

Kostenis E and Mohr K (1996) Two-point kinetic experiments to quantify allosteric effects on radioligand dissociation. *Trends in Pharmacological Sciences* **17**:280-283.

Kotani M, Mollereau C, Detheux M, Le Poul E, Brezillon S, Vakili J, Mazarguil H, Vassart G, Zajac JM, and Parmentier M (2001a) Functional characterization of a human receptor for neuropeptide FF and related peptides. *British Journal of Pharmacology* **133**:138-144.

Kotani M, Detheux M, Vandenbogaerde A, Communi D, Vanderwinden JM, Le Poul E, Brezillon S, Tyldesley R, Suarez-Huerta N, Vandeput F, Blanpain C, Schiffmann SN, Vassart G, and Parmentier M (2001b) The metastasis suppressor gene KiSS-1

encodes kisspeptins, the natural ligands of the orphan G protein-coupled receptor GPR54. *Journal of Biological Chemistry* **276**:34631-34636.

Krajewski JL, Dickerson IM, and Potter LT (2001) Site-directed mutagenesis of m1-toxin1: two amino acids responsible for stable toxin binding to M_1 muscarinic receptors. *Molecular Pharmacology* **60**:725-731.

Kristiansen K (2004) Molecular mechanisms of ligand binding, signaling, and regulation within the superfamily of G-protein-coupled receptors: molecular modeling and mutagenesis approaches to receptor structure and function. *Pharmacology & Therapeutics* **103**:21-80.

Kubo T, Maeda A, Sugimoto K, Akiba I, Mikami A, Takahashi H, Haga T, Haga K, Ichiyama A, and Kangawa K (1986a) Primary structure of porcine cardiac muscarinic acetylcholine receptor deduced from the cDNA sequence. *FEBS Letters* **209**:367-372.

Kubo T, Fukuda K, Mikami A, Maeda A, Takahashi H, Mishina M, Haga T, Haga K, Ichiyama A, and Kangawa K (1986b) Cloning, sequencing and expression of complementary DNA encoding the muscarinic acetylcholine receptor. *Nature* **323**:411-416.

Lahti RA, Figur LM, Piercey MF, Ruppel PL, and Evans DL (1992) Intrinsic activity determinations at the dopamine D_2 guanine nucleotide-binding protein-coupled receptor: utilization of receptor state binding affinities. *Molecular Pharmacology* **42**:432-438.

Lamberts SW and Macleod RM (1990) Regulation of prolactin secretion at the level of the lactotroph. *Physiological Reviews* **70**:279-318.

Landry Y, Niederhoffer N, Sick E, and Gies JP (2006) Heptahelical and Other G-protein-Coupled Receptors (GPCRs) Signaling. *Current Medicinal Chemistry* **13**:51-63.

Langmead CJ, Szekeres PG, Chambers JK, Ratcliffe SJ, Jones DN, Hirst WD, Price GW, and Herdon HJ (2000) Characterization of the binding of [(125)I]-human prolactin releasing peptide (PrRP) to GPR10, a novel G protein coupled receptor. *British Journal of Pharmacology* **131**:683-688.

Lanzafame A, Christopoulos A, and Mitchelson F (1996) Interactions of agonists with an allosteric antagonist at muscarinic acetylcholine M_2 receptors. *European Journal of Pharmacology* **316**:27-32.

Lanzafame A, Christopoulos A, and Mitchelson F (1997) Three allosteric modulators act at a common site, distinct from that of competitive antagonists, at muscarinic acetylcholine M2 receptors. *Journal of Pharmacology & Experimental Therapeutics* **282**:278-285.

Lanzafame A and Christopoulos A (2004) Investigation of the interaction of a putative allosteric modulator, N-(2,3-dipheny!-1,2,4-thiadiazole-5-(2H)-ylidene) methanamine hydrobromide (SCH-202676), with M_1 muscarinic acetylcholine receptors. *Journal of Pharmacology & Experimental Therapeutics* **308**:830-837.

Lawrence CB, Celsi F, Brennand J, and Luckman SM (2000) Alternative role for prolactin-releasing peptide in the regulation of food intake. *Nature Neuroscience* **3**:645-646.

Lawrence CB, Liu YL, Stock MJ, and Luckman SM (2004) Anorectic actions of prolactin-releasing peptide are mediated by corticotropin-releasing hormone

receptors. *American Journal of Physiology - Regulatory Integrative & Comparative Physiology* **286**:R101-R107.

Lazareno S, Buckley NJ, and Roberts FF (1990) Characterization of muscarinic M_4 binding sites in rabbit lung, chicken heart, and NG108-15 cells. *Molecular Pharmacology* **38**:805-815.

Lazareno S and Birdsall NJ (1995) Detection, quantitation, and verification of allosteric interactions of agents with labeled and unlabeled ligands at G protein-coupled receptors: interactions of strychnine and acetylcholine at muscarinic receptors. *Molecular Pharmacology* **48**:362-378.

Lazareno S, Birdsall B, Fukazawa T, Gharagozloo P, Hashimoto T, Kuwano H, Popham A, Sugimoto M, and Birdsall NJ (1999) Allosteric effects of four stereoisomers of a fused indole ring system with ^{3}H-*N*-methylscopolamine and acetylcholine at M_1-M_4 muscarinic receptors. *Life Sciences* **64**:519-526.

Lazareno S, Popham A, and Birdsall NJ (2000) Allosteric interactions of staurosporine and other indolocarbazoles with N-[methyl-(3)H]scopolamine and acetylcholine at muscarinic receptor subtypes: identification of a second allosteric site. *Molecular Pharmacology* **58**:194-207.

Lazareno S, Dolezal V, Popham A, and Birdsall NJ (2004) Thiochrome enhances acetylcholine affinity at muscarinic M_4 receptors: receptor subtype selectivity *via* cooperativity rather than affinity. *Molecular Pharmacology* **65**:257-266.

Lazareno S and Birdsall NJM (2005) Allosterism at Muscarinic Receptors: Ligands and Mechanisms. *Mini Reviews in Medicinal Chemistry* **5**:523-543

Lee JH, Miele ME, Hicks DJ, Phillips KK, Trent JM, Weissman BE, and Welch DR (1996) KiSS-1, a novel human malignant melanoma metastasis-suppressor gene. *Journal of the National Cancer Institute* **88**:1731-1737.

Lee SY, Zhu SZ, and el Fakahany EE (1996) Role of two highly conserved tyrosine residues in the m1 muscarinic receptor second transmembrane domain in ligand binding and receptor function. *Receptors & Signal Transduction* **6**:43-52.

Lee SY, Zhu SZ, and el Fakahany EE (1996) Role of two highly conserved tyrosine residues in the m1 muscarinic receptor second transmembrane domain in ligand binding and receptor function. *Receptors & Signal Transduction* **6**:43-52.

Lee Y, Yang SP, Soares MJ, and Voogt JL (2000) Distribution of prolactin-releasing peptide mRNA in the rat brain. *Brain Research Bulletin* **51**:171-176.

Leppik RA, Mynett A, Lazareno S, and Birdsall NJ (2000) Allosteric interactions between the antagonist prazosin and amiloride analogs at the human alpha$_{1A}$-adrenergic receptor. *Molecular Pharmacology* **57**:436-445.

Litschig S, Gasparini F, Rueegg D, Stoehr N, Flor PJ, Vranesic I, Prezeau L, Pin JP, Thomsen C, and Kuhn R (1999) CPCCOEt, a noncompetitive metabotropic glutamate receptor 1 antagonist, inhibits receptor signaling without affecting glutamate binding. *Molecular Pharmacology* **55**:453-461.

Loudon JM, Bromidge SM, Brown F, Clark MS, Hatcher JP, Hawkins J, Riley GJ, Noy G, and Orlek BS (1997) SB 202026: a novel muscarinic partial agonist with functional selectivity for M1 receptors. *Journal of Pharmacology & Experimental Therapeutics* **283**:1059-1068.

Lu ZL and Hulme EC (1999) The functional topography of transmembrane domain 3 of the M_1 muscarinic acetylcholine receptor, revealed by scanning mutagenesis. *Journal of Biological Chemistry* **274**:7309-7315.

Lu ZL, Saldanha JW, and Hulme EC (2001) Transmembrane domains 4 and 7 of the M_1 muscarinic acetylcholine receptor are critical for ligand binding and the receptor activation switch. *Journal of Biological Chemistry* **276**:34098-34104.

Lu ZL, Saldanha JW, and Hulme EC (2002) Seven-transmembrane receptors: crystals clarify. *Trends in Pharmacological Sciences* **23**:140-146.

Ma HT, Venkatachalam K, Li HS, Montell C, Kurosaki T, Patterson RL, and Gill DL (2001) Assessment of the role of the inositol 1,4,5-trisphosphate receptor in the activation of transient receptor potential channels and store-operated Ca^{2+} entry channels. *Journal of Biological Chemistry* **276**:18888-18896.

Mansour A, Meng F, Meador-Woodruff JH, Taylor LP, Civelli O, and Akil H (1992) Site-directed mutagenesis of the human dopamine D_2 receptor. *European Journal of Pharmacology* **227**:205-214.

Marchese A, Heiber M, Nguyen T, Heng HH, Saldivia VR, Cheng R, Murphy PM, Tsui LC, Shi X, and Gregor P (1995) Cloning and chromosomal mapping of three novel genes, GPR9, GPR10, and GPR14, encoding receptors related to interleukin 8, neuropeptide Y, and somatostatin receptors. *Genomics* **29**:335-344.

Marshall IC, Owen DE, Cripps TV, Davis JB, McNulty S, and Smart D (2003) Activation of vanilloid receptor 1 by resiniferatoxin mobilizes calcium from inositol 1,4,5-trisphosphate-sensitive stores. *British Journal of Pharmacology* **138**:172-176.

Maruyama M, Matsumoto H, Fujiwara K, Kitada C, Hinuma S, Onda H, Fujino M, and Inoue K (1999) Immunocytochemical localization of prolactin-releasing peptide in the rat brain. *Endocrinology* **140**:2326-2333.

Maruyama T, Kanaji T, Nakade S, Kanno T, and Mikoshiba K (1997) 2APB, 2-aminoethoxydiphenyl borate, a membrane-penetrable modulator of Ins(1,4,5)P3-induced Ca^{2+} release. *Journal of Biochemistry* **122**:498-505.

Matsui H, Lazareno S, and Birdsall NJ (1995) Probing of the location of the allosteric site on m1 muscarinic receptors by site-directed mutagenesis. *Molecular Pharmacology* **47**:88-98.

Matsumoto H, Murakami Y, Horikoshi Y, Noguchi J, Habata Y, Kitada C, Hinuma S, Onda H, and Fujino M (1999) Distribution and characterization of immunoreactive prolactin-releasing peptide (PrRP) in rat tissue and plasma. *Biochemical & Biophysical Research Communications* **257**:264-268.

Monod J, Changeux J-P, and Jacob F (1963) Allosteric proteins and cellular control systems. *Journal of Molecular Biology* **6**:306-329.

Matsumoto H, Maruyama M, Noguchi J, Horikoshi Y, Fujiwara K, Kitada C, Hinuma S, Onda H, Nishimura O, Inoue K, and Fujino M (2000) Stimulation of corticotropin-releasing hormone-mediated adrenocorticotropin secretion by central administration of prolactin-releasing peptide in rats. *Neuroscience Letters* **285**:234-238.

May LT, Avlani VA, Sexton PM, and Christopoulos A (2004) Allosteric modulation of G protein-coupled receptors. *Current Pharmaceutical Design* **10**:2003-2013.

May LT, Lin Y, Sexton PM, and Christopoulos A (2005) Regulation of M_2 muscarinic acetylcholine receptor expression and signaling by prolonged exposure to allosteric modulators. *Journal of Pharmacology & Experimental Therapeutics* **312**:382-390.

McGehee DS and Role LW (1995) Physiological diversity of nicotinic acetylcholine receptors expressed by vertebrate neurons. *Annual Review of Physiology* **57**:521-546.

Meyer EA, Castellano RK, and Diederich F (2003) Interactions with aromatic rings in chemical and biological recognition. *Angewandte Chemie* **42**:1210-1250.

Minami S, Nakata T, Tokita R, Onodera H, and Imaki J (1999) Cellular localization of prolactin-releasing peptide messenger RNA in the rat brain. *Neuroscience Letters* **266**:73-75.

Miyamoto Y, Habata Y, Ohtaki T, Masuda Y, Ogi K, Onda H, and Fujino M (1994) Cloning and expression of a complementary DNA encoding the bovine receptor for pituitary adenylate cyclase-activating polypeptide (PACAP). *Biochimica et Biophysica Acta* **1218**:297-307.

Morales T and Sawchenko PE (2003) Brainstem prolactin-releasing peptide neurons are sensitive to stress and lactation. *Neuroscience* **121**:771-778.

Motulsky HJ and Christopoulos A (2004) *Fitting models to biological data using linear and nonlinear regression. A practical guide to curve fitting.* Oxford University Press, New York.

Mourier G, Dutertre S, Fruchart-Gaillard C, Menez A, and Servent D (2003) Chemical synthesis of MT1 and MT7 muscarinic toxins: critical role of Arg-34 in their interaction with M_1 muscarinic receptor. *Molecular Pharmacology* **63**:26-35.

Muir AI, Chamberlain L, Elshourbagy NA, Michalovich D, Moore DJ, Calamari A, Szekeres PG, Sarau HM, Chambers JK, Murdock P, Steplewski K, Shabon U, Miller JE, Middleton SE, Darker JG, Larminie CG, Wilson S, Bergsma DJ, Emson P, Faull R, Philpott KL, and Harrison DC (2001) AXOR12, a novel human G protein-coupled receptor, activated by the peptide KiSS-1. *Journal of Biological Chemistry* **276**:28969-28975.

Nedoma J, Tucek S, Danilov AF, and Shelkovnikov SA (1986) Stabilization of antagonist binding to cardiac muscarinic acetylcholine receptors by gallamine and other neuromuscular blocking drugs. *Journal of Pharmacology & Experimental Therapeutics* **236**:219-223.

Newman-Tancredi A, Verriele L, Chaput C, and Millan MJ (1998) Labelling of recombinant human and native rat serotonin 5-HT_{1A} receptors by a novel, selective radioligand, [^{3}H]-S 15535: definition of its binding profile using agonists, antagonists and inverse agonists. *Naunyn-Schmiedebergs Archives of Pharmacology* **357**:205-217.

Nielsen SM, Elling CE, and Schwartz TW (1998). Split receptors in the tacykinin neurokinin-1 system – mutational analysis of intracellular loop 3. *European Journal of Biochemistry* **251**:217-226.

Nieminen ML, Nystedt J, and Panula P (2003) Expression of neuropeptide FF, prolactin-releasing peptide, and the receptor UHR1/GPR10 genes during embryogenesis in the rat. *Developmental Dynamics* **226**:561-569.

Nishimura O, Moriya T, Suenaga M, Tanaka Y, Itoh T, Koyama N, Fujii R, Hinuma S, Kitada C, and Fujino M (1998) Synthesis of new peptides with prolactin-releasing

activity by a combination of recombinant DNA technology and a cysteine-specific cyanylation reaction. *Chemical & Pharmaceutical Bulletin* **46**:1490-1492.

Nordvall G and Hacksell U (1993) Binding-site modeling of the muscarinic m1 receptor: a combination of homology-based and indirect approaches. *Journal of Medicinal Chemistry* **36**:967-976.

Ohtaki T, Shintani Y, Honda S, Matsumoto H, Hori A, Kanehashi K, Terao Y, Kumano S, Takatsu Y, Masuda Y, Ishibashi Y, Watanabe T, Asada M, Yamada T, Suenaga M, Kitada C, Usuki S, Kurokawa T, Onda H, Nishimura O, and Fujino M (2001) Metastasis suppressor gene KiSS-1 encodes peptide ligand of a G-protein-coupled receptor. *Nature* **411**:613-617.

Page KM, Curtis CA, Jones PG, and Hulme EC (1995) The functional role of the binding site aspartate in muscarinic acetylcholine receptors, probed by site-directed mutagenesis. *European Journal of Pharmacology* **289**:429-437.

Paton WDM and Rang HP (1965) The uptake of atropine and related drugs by intestinal smooth muscle of guinea-pig in relation to acetylcholine receptors. *Proceedings of the Royal Society of London* **163**:1-44

Palczewski K, Kumasaka T, Hori T, Behnke CA, Motoshima H, Fox BA, Le Trong I, Teller DC, Okada T, Stenkamp RE, Yamamoto M, and Miyano M (2000) Crystal structure of rhodopsin: A G protein-coupled receptor. *Science* **289**:739-745.

Perlman JH, Thaw CN, Laakkonen L, Bowers CY, Osman R, and Gershengorn MC (1994) Hydrogen bonding interaction of thyrotropin-releasing hormone (TRH) with transmembrane tyrosine 106 of the TRH receptor. *Journal of Biological Chemistry* **269**:1610-1613.

Perlman JH, Wang W, Nussenzveig DR, and Gershengorn MC (1995) A disulphide bond between conserved extracellular cysteines in the thyrotropin-releasing hormone receptor is critical for binding. *Journal of Biological Chemistry* 270:682-685.

Peterson GL, Herron GS, Yamaki M, Fullerton DS, and Schimerlik MI (1984) Purification of the muscarinic acetylcholine receptor from porcine atria. *Proceedings of the National Academy of Sciences of the United States of America* **81**:4993-4997.

Pierce KL, Premont RT, and Lefkowitz RJ (2002) Seven-transmembrane receptors. *Nature Reviews Molecular Cell Biology* **3**:639-650.

Pin JP, Galvez T, and Prezeau L (2003) Evolution, structure, and activation mechanism of family 3/C G-protein-coupled receptors. *Pharmacology & Therapeutics* **98**:325-354.

Potter LT (2001) Snake toxins that bind specifically to individual subtypes of muscarinic receptors. *Life Sciences* **68**:2541-2547.

Ramachandran GN, Ramakrishnan C, Sasisekharan V. (1963) Stereochemistry of polypeptide chain configurations. *Journal of Molecular Biology* **7**:95-99.

Rang HP, Dale MM, and Ritter JM (1999). Pharmacology. Churchill Liviingstone.

Rasmussen SGF and Gether U (2002) Structural mechanics of GPCR activation, in: Understanding G Protein-coupled receptors and their role in the CNS (Pangalos MN and Davies CH eds) pp. 43 - 62, Oxford University Press

Riker WF and Wescoe WC (1951) The pharmacology of flaxedil with observations on certain analogues. *Annals of the New York Academy of Science* **54**:373-394

Robbins J, Marsh SJ, and Brown DA (1993) On the mechanism of M-current inhibition by muscarinic m1 receptors in DNA-transfected rodent neuroblastoma x glioma cells. *Journal of Physiology* **469**:153-178.

Roland BL, Sutton SW, Wilson SJ, Luo L, Pyati J, Huvar R, Erlander MG, and Lovenberg TW (1999) Anatomical distribution of prolactin-releasing peptide and its receptor suggests additional functions in the central nervous system and periphery. *Endocrinology* **140**:5736-5745.

Roumy M and Zajac JM (1998) Neuropeptide FF, pain and analgesia. *European Journal of Pharmacology* **345**:1-11.

Rubinek T, Hadani M, Barkai G, Melmed S, and Shimon I (2001) Prolactin (PRL)-releasing peptide stimulates PRL secretion from human fetal pituitary cultures and growth hormone release from cultured pituitary adenomas. *Journal of Clinical Endocrinology & Metabolism* **86**:2826-2830.

Sachpatzidis A, Benton BK, Manfredi JP, Wang H, Hamilton A, Dohlman HG, and Lolis E (2003) Identification of allosteric peptide agonists of CXCR4. *Journal of Biological Chemistry* **278**:896-907.

Samson WK, Resch ZT, Murphy TC, and Chang JK (1998) Gender-biased activity of the novel prolactin releasing peptides: comparison with thyrotropin releasing hormone reveals only pharmacologic effects. *Endocrine* **9**:289-291.

Samson WK, Resch ZT, and Murphy TC (2000) A novel action of the newly described prolactin-releasing peptides: cardiovascular regulation. *Brain Research* **858**:19-25.

Samson WK, Keown C, Samson CK, Samson HW, Lane B, Baker JR, and Taylor MM (2003) Prolactin-releasing peptide and its homolog RFRP-1 act in hypothalamus but not in anterior pituitary gland to stimulate stress hormone secretion. *Endocrine* **20**:59-66.

Satoh F, Smith DM, Gardiner JV, Mahmoodi M, Murphy KG, Ghatei MA, and Bloom SR (2000) Characterization and distribution of prolactin releasing peptide (PrRP) binding sites in the rat - evidence for a novel binding site subtype in cardiac and skeletal muscle. *British Journal of Pharmacology* **129**:1787-1793.

Schoneberg T, Liu J, and Wess J (1995) Plasma membrane localization and functional rescue of truncated forms of a G protein coupled receptor. *Journal of Biological Chemistry* **270**:18000-18006.

Schoneberg T, Schultz G, and Gudermann T (1999) Structural basis of G protein-coupled receptor function. *Molecular & Cellular Endocrinology* **151**:181-193.

Schoneberg T (2002) GPCR superfamily and its structural characterization, in: Understanding G Protein-coupled receptors and their role in the CNS (Pangalos MN and Davies CH eds) pp. 3 - 27, Oxford University Press

Seal LJ, Small CJ, Dhillo WS, Stanley SA, Abbott CR, Ghatei MA, and Bloom SR (2001) PRL-releasing peptide inhibits food intake in male rats *via* the dorsomedial hypothalamic nucleus and not the paraventricular hypothalamic nucleus. *Endocrinology* **142**:4236-4243.

Seal LJ, Small CJ, Dhillo WS, Kennedy AR, Ghatei MA, and Bloom SR (2002) Prolactin-releasing peptide releases corticotropin-releasing hormone and increases

plasma adrenocorticotropin *via* the paraventricular nucleus of the hypothalamus. *Neuroendocrinology* **76**:70-78.

Shapiro MS, Gomeza J, Hamilton SE, Hille B, Loose MD, Nathanson NM *et al* (2001) Identification of subtypes of muscarinic receptors that regulate Ca2+ and K+ channel activity in sympathetic neurons. *Life Sciences* **68**:2481-2487.

Shin N, Coates E, Murgolo NJ, Morse KL, Bayne M, Strader CD, and Monsma FJ, Jr. (2002) Molecular modeling and site-specific mutagenesis of the histamine-binding site of the histamine H_4 receptor. *Molecular Pharmacology* **62**:38-47.

Spalding TA, Birdsall NJ, Curtis CA, and Hulme EC (1994) Acetylcholine mustard labels the binding site aspartate in muscarinic acetylcholine receptors. *Journal of Biological Chemistry* **269**:4092-4097.

Spalding TA, Trotter C, Skjaerbaek N, Messier TL, Currier EA, Burstein ES, Li D, Hacksell U, and Brann MR (2002) Discovery of an ectopic activation site on the M_1 muscarinic receptor. *Molecular Pharmacology* **61**:1297-1302.

Spiegel AM (1995). Defects in G protein-coupled signal transduction in human disease. *Annual Review of Physiology* **58**:143-170.

Spooren WP, Gasparini F, Salt TE, and Kuhn R (2001) Novel allosteric antagonists shed light on mglu(5) receptors and CNS disorders. *Trends in Pharmacological Sciences* **22**:331-337.

Stockton JM, Birdsall NJ, Burgen AS, and Hulme EC (1983) Modification of the binding properties of muscarinic receptors by gallamine. *Molecular Pharmacology* **23**:551-557.

Strader CD, Sigal IS, Register RB, Candelore MR, Rands E, and Dixon RA (1987) Identification of residues required for ligand binding to the beta-adrenergic receptor. *Proceedings of the National Academy of Sciences of the United States of America* **84**:4384-4388.

Strader CD, Candelore MR, Hill WS, Sigal IS, and Dixon RA (1989) Identification of two serine residues involved in agonist activation of the beta-adrenergic receptor. *Journal of Biological Chemistry* **264**:13572-13578.

Suh BC and Hille B (2002) Recovery from muscarinic modulation of M current channels requires phosphatidylinositol 4,5-bisphosphate synthesis. *Neuron* **35**:507–520.

Sur C, Mallorga PJ, Wittmann M, Jacobson MA, Pascarella D, Williams JB, Brandish PE, Pettibone DJ, Scolnick EM, and Conn PJ (2003) *N*-desmethylclozapine, an allosteric agonist at muscarinic 1 receptor, potentiates *N*-methyl-D-aspartate receptor activity. *Proceedings of the National Academy of Sciences of the United States of America* **100**:13674-13679.

Takahashi K, Yoshinoya A, Arihara Z, Murakami O, Totsune K, Sone M, Sasano H, and Shibahara S (2000) Regional distribution of immunoreactive prolactin-releasing peptide in the human brain. *Peptides* **21**:1551-1555.

Takasaki J, Saito T, Taniguchi M, Kawasaki T, Moritani Y, Hayashi K, and Kobori M (2004) A novel Galphaq/11-selective inhibitor. *Journal of Biological Chemistry* **279**:47438-47445.

Tayebati SK, Piergentili A, Natale D, and Amenta F (1999) Evaluation of an agonist index: affinity ratio for compounds active on muscarinic cholinergic M_2 receptors. *Journal of Autonomic Pharmacology* **19**:77-84.

Taylor MM and Samson WK (2001) The prolactin releasing peptides: RF-amide peptides. *Cellular & Molecular Life Sciences* **58**:1206-1215.

Thompson AK, Mostafapour SP, Denlinger LC, Bleasdale JE, and Fisher SK (1991) The aminosteroid U-73122 inhibits muscarinic receptor sequestration and phosphoinositide hydrolysis in SK-N-SH neuroblastoma cells. A role for Gp in receptor compartmentation. *Journal of Biological Chemistry* **266**:23856-23862.

Tucek S, Musilkova J, Nedoma J, Proska J, Shelkovnikov S, and Vorlicek J (1990) Positive cooperativity in the binding of alcuronium and N-methylscopolamine to muscarinic acetylcholine receptors. *Molecular Pharmacology* **38**:674-680.

Tucek S and Proska J (1995) Allosteric modulation of muscarinic acetylcholine receptors. *Trends in Pharmacological Sciences* **16**:205-212.

Unger VM, Hargrave PA, Baldwin JM, and Schertler GF (1997) Arrangement of rhodopsin transmembrane alpha-helices. *Nature* **389**:203-206.

Veinbergs I, Friberg M, Schurb K, Hansen L, Kock K, Spalding TA, Bradley SR, Lameh J, Tolf B-R, Hacksell U, Brann MR, Davis RE, and Vanover KE (2003). Antipsychotic-like efficacy of a muscarinic M_1 receptor selective agonist in animal models. *Abstract Viewer/Itinerary Planner. Society for Neuroscience.*

Venter JC, Adams MD, Myers EW, Li PW, Mural RJ, Sutton GG, Smith HO, Yandell M, Evans CA, Holt RA *et al.* The Sequence of the Human Genome (2001) *Science* 291, 1304-1351

Wang CD, Gallaher TK, and Shih JC (1993) Site-directed mutagenesis of the serotonin 5-hydroxytrypamine2 receptor: identification of amino acids necessary for ligand binding and receptor activation. *Molecular Pharmacology* **43**:931-940.

Ward SD, Curtis CA, and Hulme EC (1999) Alanine-scanning mutagenesis of transmembrane domain 6 of the M_1 muscarinic acetylcholine receptor suggests that Tyr381 plays key roles in receptor function. *Molecular Pharmacology* **56**:1031-1041.

Watanobe H (2001) In vivo release of prolactin-releasing peptide in rat hypothalamus in association with luteinizing hormone and prolactin surges. *Neuroendocrinology* **74**:359-366.

Watson J (1998). In Vitro Measurement of the Second Messenger cAMP: RIA vs. FlashPlate. *FlashPlate File #7, http://las.perkinelmer.com/ApplicationsSummary/ Applications/Flashplate-flashplate.htm*

Watson JM, Hunter AJ, Brown AM, and Middlemiss DN (1999) In vitro characterisation of the muscarinic receptor partial agonist, sabcomeline, in rat cortical and heart membranes. *European Journal of Pharmacology* **370**:69-77.

Welch SK, O'Hara BF, Kilduff TS, and Heller HC (1995) Sequence and tissue distribution of a candidate G-coupled receptor cloned from rat hypothalamus. *Biochemical & Biophysical Research Communications* **209**:606-613.

Wess J (2005) Allosteric Binding Sites on Muscarinic Acetylcholine Receptors. *Molecular Pharmacology* **68**:1506-1509.

Wilson S, Bergsma DJ, Chambers JK, Muir AI, Fantom KG, Ellis C, Murdock PR, Herrity NC, and Stadel JM (1998) Orphan G-protein-coupled receptors: the next generation of drug targets? *British Journal of Pharmacology* **125**:1387-1392.

Wotta DR, Wattenberg EV, Langason RB, and el Fakahany EE (1998) M_1, M_3 and M_5 muscarinic receptors stimulate mitogen-activated protein kinase. *Pharmacology* **56**:175-186.

Yamakawa K, Kudo K, Kanba S, and Arita J (1999) Distribution of prolactin-releasing peptide-immunoreactive neurons in the rat hypothalamus. *Neuroscience Letters* **267**:113-116.

Yamano Y, Ohyama K, Kikyo M, Sano T, Nakagomi Y, Inoue Y, Nakamura N, Morishima I, Guo DF, and Hamakubo T (1995) Mutagenesis and the molecular modeling of the rat angiotensin II receptor (AT_1). *Journal of Biological Chemistry* **270**:14024-14030.

Yang HY, Fratta W, Majane EA, and Costa E (1985) Isolation, sequencing, synthesis, and pharmacological characterization of two brain neuropeptides that modulate the action of morphine. *Proceedings of the National Academy of Sciences of the United States of America* **82**:7757-7761.

Zaagsma J, Roffel AF, and Meurs H (1997) Muscarinic control of airway function. *Life Sciences* **60**:1061-1068.

Zhang H, Craciun LC, Mirshahi T, Rohacs T, Lopes CM, Jin T, and Logothetis DE. 2003. PIP_2 activates KCNQ channels, and its hydrolysis underlies receptor- mediated inhibition of M currents. *Neuron.* **37**:963–975

Zhang SQ, Kimura M, and Inoue S (2000) Effects of prolactin-releasing peptide (PrRP) on sleep regulation in rats. *Psychiatry & Clinical Neurosciences* **54**:262-264.

Zhao MM, Hwa J, and Perez DM (1996) Identification of critical extracellular loop residues involved in alpha 1-adrenergic receptor subtype-selective antagonist binding. *Molecular Pharmacology* **50**:1118-1126.

Zhu LL and Onaka T (2003) Facilitative role of prolactin-releasing peptide neurons in oxytocin cell activation after conditioned-fear stimuli. *Neuroscience* **118**:1045-1053.

Appendix 1 – Definitions and Example Calculations

(i) Definition of EC_{50} and IC_{50}

Effective concentration $(EC)_{50}$ represents the molar concentration of agonist required to produce 50% of the maximal possible response. In a radioligand binding assay, inhibitory concentration $(IC)_{50}$ represents the molar concentration of ligand to inhibit 50% of the specific binding of the radioligand. For a functional assay, IC_{50} represents the molar concentration of antagonist which reduces the response to a fixed concentration of agonist by 50%. Both EC_{50} and IC_{50} values are calculated using a four-parameter logistic fit (equations 1 and 6 in Methods).

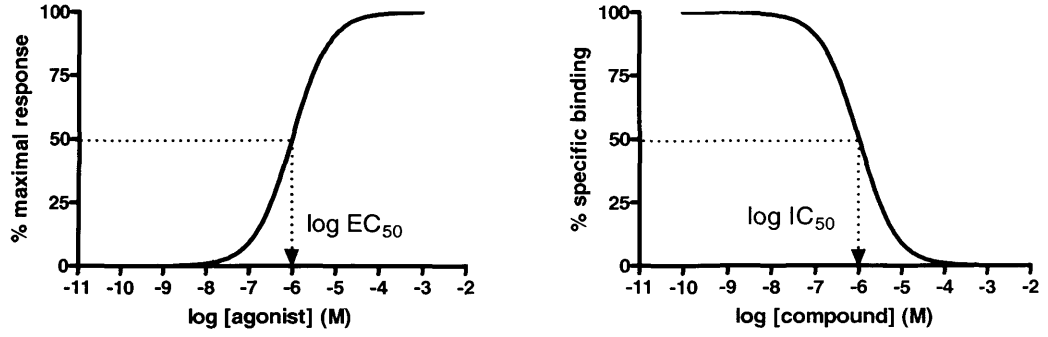

(ii) Definition of K_D and B_{max}

The equilibrium dissociation constant (K_D) is the molar concentration of ligand required to occupy 50% of the receptor population. The maximal binding capacity (B_{max}) for a ligand represents the amount of ligand, usually expressed in pmol / mg protein, which can bind specifically to a receptor population in a membrane preparation. Both terms are usually estimated by non-linear regression of saturation analysis data.

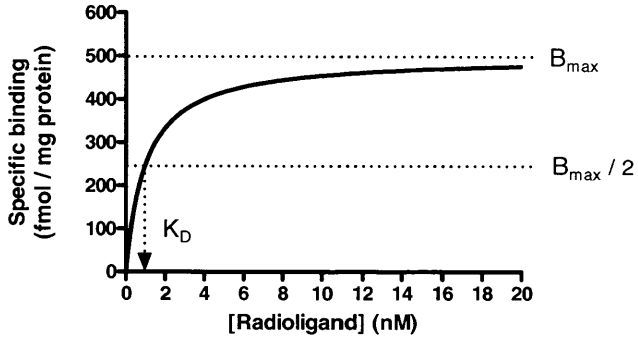

(iii) Conversion of IC_{50} to K_i

An IC_{50} value from a radioligand binding assay is converted to yield the equilibrium dissociation constant for the inhibitor (K_i) using the Cheng-Prussoff equation (equation 2 in Methods):

$$K_i = \frac{IC_{50}}{1+\frac{[L]}{K_D}}$$

Assuming the equilibrium dissociation constant for the radioligand, K_D = 0.2 nM and the radioligand concentration, $[L]$ = 0.2 nM, then:

$$K_i = \frac{5x10^{-8}}{1+\frac{2x10^{-10}}{2x10^{-10}}}$$

$$K_i = 2.5 \times 10^{-8} \text{ M}$$

(iv) Calculation of pEC_{50} / pK_I

pEC_{50} and pK_i values are the negative logarithm of EC_{50} and K_i values, respectively eg.

$$K_i = 2.5 \times 10^{-8} \text{ M}$$

$$pK_i = - \log (2.5 \times 10^{-8})$$

$$pK_i = 7.60$$

(v) Calculation of K_{on} from K_{off} and K_{obs}

The association rate constant, K_{on} is calculated from the dissociation rate constant, K_{off} and the *observed* association rate constant, K_{obs} and the radioligand concentration [*L*].

$$K_{on} = \frac{K_{obs} - K_{off}}{[L]}$$

$$K_{on} = \frac{0.24\text{min}^{-1} - 0.2\text{min}^{-1}}{2x10^{-10}M}$$

$$K_{on} = 200 \text{ min}^{-1} \mu\text{M}^{-1}$$

(vi) Calculation of K_D from K_{off} and K_{on}

The equilibrium dissociation constant, K_D, is the ratio of the dissociation rate constant, K_{off} and the association constant, K_{on}.

$$K_D = \frac{K_{off}}{K_{on}}$$

$$K_D = \frac{0.2\text{min}^{-1}}{200\text{min}^{-1}\mu M^{-1}}$$

$$K_D = 1 \text{ x } 10^{-9} \text{ M}$$

$$K_D = 1 \text{ nM}$$

(vii) Calculation of pK_B for competitive antagonists

In a functional assay where agonist concentration-response curves are measured in the presence and absence of multiple fixed concentrations of a test antagonist,

Schild analysis is used to determine the antagonist affinity, pK_B. A Schild regression of the logarithm of the concentration ratio – 1 (where the concentration ratio is the ratio of equi-effective agonist concentrations in the presence and absence of antagonist) against the logarithm of the molar antagonist concentration that yields a straight line with a slope value not significantly different from 1 suggests that the antagonist is competitive. The intercept on the X-axis is then equal to the pK_B value for the antagonist.

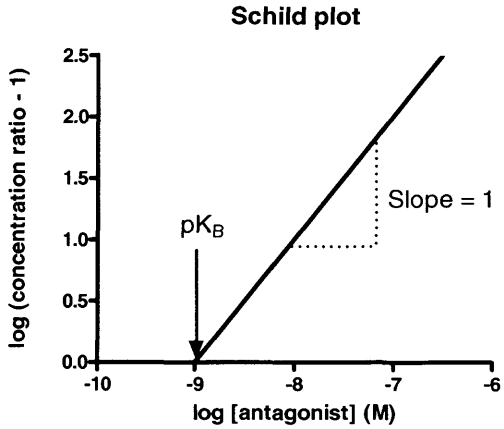

(viii) Calculation of pA_2 and co-operativity values (α) for allosteric interactions

In a functional assay where agonist concentration-response curves are measured in the presence and absence of multiple fixed concentrations of a test antagonist, Schild analysis is used to determine an empirical estimate of antagonist affinity, pA_2. A Schild regression of the logarithm of the concentration ratio – 1 (where the concentration ratio is the ratio of equi-effective agonist concentrations in the presence and absence of antagonist) against the logarithm of the molar antagonist concentration is often used to examine negatively co-operative interactions. Schild regressions for such interactions yield either a straight line with a slope value significantly less than 1, or a curve that eventually reaches an asymptotic value. The intercept on the X-axis can be taken as an estimate of the antagonist affinity (pA_2), whereas the asymptote of the curve is approximately equal to the negative logarithm

of the co-operativity (α) between the two ligands. This value is usually estimated by non-linear regression according to equation 7 in Methods.

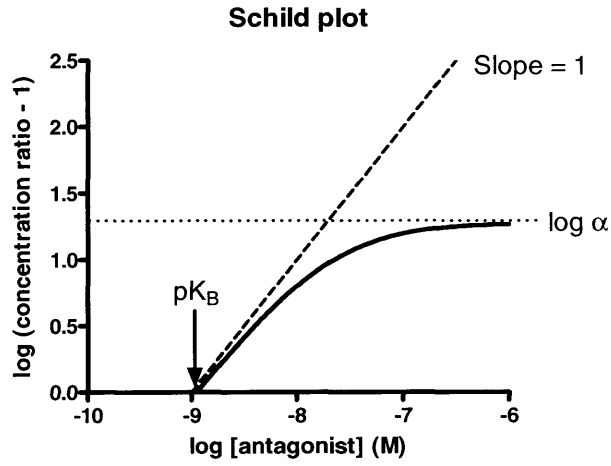

Appendix 2 - List of Publications

Langmead CJ, Szekeres PG, Chambers JK, Ratcliffe SJ, Jones DN, Hirst WD, Price GW, and Herdon HJ (2000) Characterization of the binding of [^{125}I]-human prolactin releasing peptide (PrRP) to GPR10, a novel G protein coupled receptor. *British Journal of Pharmacology* **131**:683-688.

Langmead CJ, Fry VAH, Forbes IT, Branch CA, Christopoulos A, Wood MD, and Herdon HJ (2006) Probing the molecular mechanism of interaction between AC-42 and the muscarinic M_1 receptor: Direct evidence that AC-42 is an allosteric agonist. *Molecular Pharmacology* **69**:236-246

Langmead CJ*, Blaney FE*, Bridges A, Evans N, Herdon HJ, Jones DNC, Ratcliffe SJ, and Szekeres PG (2005) Molecular modelling and site directed mutagenesis of the human prolactin releasing peptide (h-PrRP-20) binding site of GPR10, a novel G protein-coupled receptor. *Molecular Pharmacology* (*submitted).*

* contributed equally to work